

**The Effects of Electron-Withdrawing Ring Substituents  
on the Reactivity of Cyclopentadienyl Ruthenium  
Complexes**

**Mairéad Crushell, M.Sc.**

**Thesis for the Degree of Ph.D.**

**Submitted to**

**The National University of Ireland, Galway**



**School of Chemistry,**

**National University of Ireland, Galway**

**September 2011**

**Head of School: Professor Paul V. Murphy**

**Supervisor: Professor Patrick McArdle**

## Contents

Abstract	i
Abbreviations	ii
<b><u>Chapter 1 Introduction</u></b>	<b>1</b>
<u>1.1 Cyclopentadiene</u>	1
<u>1.2 Substituted Cyclopentadienes</u>	2
<u>1.3 Ring Substituted Metal Complexes</u>	3
<u>1.3.1 Alkyl Substituted Cyclopentadienes</u>	3
<u>1.3.2 Aryl Substituted Cyclopentadienes</u>	8
<u>1.4 Cyclopentadienes with Electron Withdrawing Substituents</u>	14
<u>1.5 Organolithium Reagents</u>	19
<u>1.6 Ortholithiation</u>	21
<u>1.7 Acid Chlorides</u>	23
<u>1.8 Lithium Reagents and Carbonyl Compounds</u>	26
<u>1.9 1,2-Diaroylcyclopentadiene and its Compounds</u>	30
<u>1.9.1 The History of 1,2-Dibenzoylcyclopentadiene</u>	30
<u>1.9.2 Compounds containing the 1,2-dibenzoylcyclopentadienyl ligand</u>	32
<u>1.10 The Chemistry of Ferrocene</u>	35
<b><u>Chapter 2 Carbonyl Substitution Reactions</u></b>	<b>39</b>
<u>2.1 Transition Metal Carbonyls</u>	39
<u>2.1.1 The Carbonyl Ligand</u>	39
<u>2.1.2 Carbonyl Stretching Frequencies</u>	41
<u>2.2 Tertiary Phosphine Ligands</u>	46
<u>2.3 Substitution Reactions</u>	48
<u>2.3.1 The 16 and 18-Electron Rules</u>	48
<u>2.3.2 The Dissociative (D) Mechanism</u>	50
<u>2.3.3 The Associative (A) Mechanism</u>	52
<u>2.3.4 The Interchange (I<sub>a</sub> and I<sub>d</sub>) Mechanisms</u>	54
<u>2.4 Carbonyl Substitution Reactions of Cyclopentadienyl Complexes</u>	56
<u>2.4.1 Substitution Reactions of Cyclopentadienyl Iron and Ruthenium Complexes</u>	56
<u>2.4.2 Ring Slippage and the Indenyl Effect</u>	59
<u>2.4.3 [MCp(CO)<sub>2</sub>]<sub>2</sub> as a Catalyst (M = Fe, Ru)</u>	64
<u>2.4.4 17-Electron Metal-Centred Radicals</u>	68

2.4.5	<u>19-Electron Metal-Centres</u>	72
<b>Chapter 3</b>	<b><u>Experimental</u></b>	<b>76</b>
3.1	<u>Solvents and Starting Materials</u>	76
3.2	<u>Instrumentation</u>	76
3.3	<u>Synthesis of ArCOCl</u>	77
3.4	<u>Synthesis of Ligands</u>	78
3.4.1	<u>Synthesis of dibenzoylcyclopentadiene (dbzCpH)</u>	78
3.4.2	<u>Synthesis of C<sub>5</sub>H<sub>4</sub>(CO-<i>p</i>-tol)<sub>2</sub></u>	80
3.4.3	<u>Synthesis of (CH<sub>3</sub>)C<sub>5</sub>H<sub>3</sub>(CO-<i>p</i>-tol)<sub>2</sub></u>	81
3.4.4	<u>Synthesis of C<sub>5</sub>H<sub>4</sub>(CO-<i>p</i>-ClC<sub>6</sub>H<sub>4</sub>)<sub>2</sub></u>	83
3.4.5	<u>Synthesis of C<sub>5</sub>H<sub>4</sub>(CO-<i>o</i>-ClC<sub>6</sub>H<sub>4</sub>)<sub>2</sub></u>	84
3.4.6	<u>Synthesis of 1,4-diphenyl-cyclopenta[d]pyridizine</u>	85
3.4.7	<u>Synthesis of C<sub>5</sub>H<sub>5</sub>CPh<sub>3</sub></u>	86
3.4.8	<u>Synthesis of (COPh)<sub>2</sub>C<sub>5</sub>H<sub>3</sub>CPh<sub>3</sub></u>	86
3.4.9	<u>Attempted benzylation of indene</u>	88
3.5	<u>Synthesis of Parent Cyclopentadienyl Complexes</u>	89
3.5.1	<u>Synthesis of [RuCp(CO)<sub>2</sub>X]</u>	89
3.5.2	<u>Synthesis of [RuCp(CO)PPh<sub>3</sub>X]</u>	92
3.6	<u>Synthesis of dbzCp Ruthenium Dimeric Complexes</u>	93
3.6.1	<u>Synthesis of [Ru(η<sup>5</sup>-1,2-C<sub>5</sub>H<sub>3</sub>(COPh)<sub>2</sub>)(CO)<sub>2</sub>]<sub>2</sub></u>	93
3.6.2	<u>Synthesis of [Ru(η<sup>5</sup>-1,2-C<sub>5</sub>H<sub>3</sub>(CO-<i>p</i>-tol)<sub>2</sub>)(CO)<sub>2</sub>]<sub>2</sub></u>	94
3.6.3	<u>Synthesis of [Ru(η<sup>5</sup>-1,2-(CH<sub>3</sub>)C<sub>5</sub>H<sub>2</sub>(CO-<i>p</i>-tol)<sub>2</sub>)(CO)<sub>2</sub>]<sub>2</sub></u>	94
3.6.4	<u>Synthesis of [Ru(η<sup>5</sup>-1,2-C<sub>5</sub>H<sub>3</sub>(CO-<i>p</i>-ClC<sub>6</sub>H<sub>4</sub>)<sub>2</sub>)(CO)<sub>2</sub>]<sub>2</sub></u>	95
3.6.5	<u>Synthesis of [Ru(η<sup>5</sup>-1,2-C<sub>5</sub>H<sub>3</sub>(CO-<i>o</i>-ClC<sub>6</sub>H<sub>4</sub>)<sub>2</sub>)(CO)<sub>2</sub>]<sub>2</sub></u>	95
3.7	<u>Synthesis of dbzCp Ruthenium Halide Complexes</u>	96
3.7.1	<u>Synthesis of [Ru(η<sup>5</sup>-1,2-C<sub>5</sub>H<sub>3</sub>(COPh)<sub>2</sub>)(CO)<sub>2</sub>I]</u>	96
3.7.2	<u>Synthesis of [Ru(η<sup>5</sup>-1,2-C<sub>5</sub>H<sub>3</sub>(COPh)<sub>2</sub>)(CO)<sub>2</sub>Br]</u>	97
3.7.3	<u>Synthesis of [Ru(η<sup>5</sup>-1,2-C<sub>5</sub>H<sub>3</sub>(CO-<i>p</i>-tol)<sub>2</sub>)(CO)<sub>2</sub>I]</u>	97
3.7.4	<u>Synthesis of [Ru(η<sup>5</sup>-1,2-(CH<sub>3</sub>)C<sub>5</sub>H<sub>2</sub>(CO-<i>p</i>-tol)<sub>2</sub>)(CO)<sub>2</sub>I]</u>	97
3.7.5	<u>Synthesis of [Ru(η<sup>5</sup>-1,2-C<sub>5</sub>H<sub>3</sub>(CO-<i>p</i>-ClC<sub>6</sub>H<sub>4</sub>)<sub>2</sub>)(CO)<sub>2</sub>I]</u>	98
3.7.6	<u>Synthesis of [Ru(η<sup>5</sup>-1,2-C<sub>5</sub>H<sub>3</sub>(CO-<i>o</i>-ClC<sub>6</sub>H<sub>4</sub>)<sub>2</sub>)(CO)<sub>2</sub>I]</u>	98
3.8	<u>Synthesis of Triphenylphosphine Derivatives</u>	99
3.8.1	<u>Synthesis of [Ru(η<sup>5</sup>-1,2-C<sub>5</sub>H<sub>3</sub>(COPh)<sub>2</sub>)(CO)IPPh<sub>3</sub>]</u>	99
3.8.2	<u>Synthesis of [Ru(η<sup>5</sup>-1,2-C<sub>5</sub>H<sub>3</sub>(CO-<i>p</i>-tol)<sub>2</sub>)(CO)IPPh<sub>3</sub>]</u>	100

3.8.3	<a href="#">Synthesis of [Ru(<math>\eta^5</math>-1,2-(CH<sub>3</sub>)C<sub>5</sub>H<sub>2</sub>(CO-<i>p</i>-tol)<sub>2</sub>)(CO)IPPh<sub>3</sub>]</a>	100
3.8.4	<a href="#">Synthesis of [Ru(<math>\eta^5</math>-1,2-C<sub>5</sub>H<sub>3</sub>(CO-<i>p</i>-ClC<sub>6</sub>H<sub>4</sub>)<sub>2</sub>)(CO)IPPh<sub>3</sub>]</a>	100
3.9	<a href="#">Synthesis of Indenyl Complexes</a>	101
3.9.1	<a href="#">Synthesis of [RuInd(CO)<sub>2</sub>]<sub>2</sub></a>	101
3.9.2	<a href="#">Synthesis of [RuInd(CO)<sub>2</sub>I]</a>	102
3.10	<a href="#">Kinetic Studies</a>	103
3.11	<a href="#">Molecular Mass Determination of 1,4-diphenyl-2-cyclopenta[<i>d</i>]pyridazine</a>	103
<b><a href="#">Chapter 4 Theoretical Studies</a></b>		<b>105</b>
4.1	<a href="#">Introduction</a>	105
4.2	<a href="#">Quantum Mechanical Methods</a>	105
4.3	<a href="#">Density Functional Theory</a>	106
4.3.1	<a href="#">Brief Summary of Calculation Methods</a>	107
4.3.2	<a href="#">Strengths and Weakness of DFT</a>	108
4.4	<a href="#">Molecular Modelling Packages</a>	108
4.5	<a href="#">Calculation of Atom Charges</a>	109
4.5.1	<a href="#">Mulliken Population Analysis Method</a>	109
4.6	<a href="#">The Eyring Equation</a>	111
<b><a href="#">Chapter 5 Crystallographic Data</a></b>		<b>112</b>
5.1	<a href="#">Crystal Structure of C<sub>19</sub>H<sub>14</sub>N<sub>2</sub> Form I</a>	113
5.2	<a href="#">Crystal Structure of C<sub>19</sub>H<sub>14</sub>N<sub>2</sub> Form II</a>	120
5.3	<a href="#">Crystal Structure of Ph<sub>3</sub>C-C<sub>5</sub>H<sub>3</sub>(COPh)<sub>2</sub></a>	130
5.4	<a href="#">Crystal Structure for C<sub>23</sub>H<sub>16</sub>O<sub>2</sub></a>	139
5.5	<a href="#">Crystal structure of [Ru(dbzCp)(CO)IPPh<sub>3</sub>]</a>	150
5.6	<a href="#">Crystal Structure of [Ru((CO-<i>p</i>-tolyl)<sub>2</sub>C<sub>5</sub>H<sub>3</sub>)(CO)IPPh<sub>3</sub>]</a>	160
5.7	<a href="#">Crystal Structure of [Ru(indenyl)(CO)<sub>2</sub>I]</a>	171
5.8	<a href="#">Crystal structure of [Ru(indenyl)COIPPh<sub>3</sub>]</a>	178
<b><a href="#">Chapter 6 Results and Discussion</a></b>		<b>187</b>
6.1	<a href="#">Dibenzoylcyclopentadienyl Ligands</a>	187
6.1.1	<a href="#">Dibenzoylcyclopentadiene</a>	187
6.1.2	<a href="#">(CH<sub>3</sub>)C<sub>5</sub>H<sub>3</sub>(CO-<i>p</i>-tol)<sub>2</sub></a>	189
6.2	<a href="#">1,4-diphenyl-2-cyclopenta[<i>d</i>]pyridazine</a>	192
6.3	<a href="#">Carbonyl Stretching Frequencies</a>	195
6.4	<a href="#">Kinetics and Mechanism of Carbonyl Substitution on [RuCp(CO)<sub>2</sub>X] with PPh<sub>3</sub></a>	

<a href="#"><u>6.5 Kinetics and Mechanism of CO Substitution on dbzCpRu(CO)<sub>2</sub>X with Tertiary Phosphines</u></a>	201
<a href="#"><u>6.6 Ring Slippage and the Indenyl Effect</u></a>	204
<a href="#"><u>6.7 The Radical Mechanism</u></a>	209
<b><a href="#"><u>Conclusion</u></a></b>	<b>213</b>

## Abstract

This thesis describes the synthesis of ruthenium complexes which contain cyclopentadienyl ligands with electron-withdrawing ring substituents and the effects of these substituents on the reactivity of the metal centre. Two metal complexes containing the dibenzoylcyclopentadienyl ligand have been reported in the literature. However, the effects of these substituents on the reactivities of the complexes have not been investigated.

Several dibenzoylcyclopentadiene analogues react readily with triruthenium dodecacarbonyl in toluene when heated under reflux to form bridging carbonyl dimeric complexes. The metal–metal bond in the dimers is cleaved upon reaction with halogen sources. These halide complexes undergo CO substitution with tertiary phosphines. The rate constants for the CO substitution reactions of the  $(\eta^5\text{-}1,2\text{-}(\text{COPh})_2\text{C}_5\text{H}_3)\text{Ru}(\text{CO})_2\text{X}$  complexes with tertiary phosphines have been measured.

Reaction rates for the parent cyclopentadienyl complexes,  $[\text{RuCp}(\text{CO})_2\text{X}]$ , have been repeated and the rates of the related indenyl complexes,  $[\text{Ru}(\text{indenyl})(\text{CO})_2\text{X}]$ , have been measured for comparison. The electron withdrawing ring substituents activate the complexes for CO substitution. The reaction mechanism is dissociative in all cases except the  $[\text{RuCp}(\text{CO})_{21}]$  which has an  $\text{I}_d$  mechanism.

DFT calculations for second row transition metals are limited to 3-21G\* basis sets. However, they are able to reproduce new  $\nu_{\text{MC-O}}$  stretching frequencies and atom charges for the metal atoms which reflect the electron withdrawing effects of the ring substituents.

## Abbreviations

BuLi	Butyllithium
CO	Carbonyl
Cp	Cyclopentadienyl ligand
Cp*	Pentamethylcyclopentadienyl ligand
dbzCp	1,2-Dibenzoylcyclopentadienyl ligand
DCM	Dichloromethane
Et <sub>2</sub> O	Diethyl ether
EtOH	Ethanol
Fe(CO) <sub>5</sub>	Iron pentacarbonyl
M	Metal
M–M	Metal–Metal bond
Ph	Phenyl
PhCOCl	Benzoyl chloride
PPh <sub>3</sub>	Triphenylphosphine
PhLi	Phenyllithium
Ru <sub>3</sub> (CO) <sub>12</sub>	Triruthenium dodecacarbonyl
THF	Tetrahydrofuran
TLC	Thin layer chromatography
TMEDA	N,N,N'-Trimethylethylenediamene

# Chapter 1 Introduction

## 1.1 Cyclopentadiene

The discovery of ferrocene in 1951 by Pauson and Kealy<sup>1</sup> expanded the world of organometallic chemistry to include the transition metals. This was a major advance in new and significant chemistry. Since then, an enormous number of transition metal complexes of the M–Cp type have been synthesised and characterized.<sup>2</sup> The current interest in this area lies in the synthesis and investigation of these organometallic compounds as catalysts and as stoichiometric mediators in a wide range of procedures.

The cyclopentadienyl ligand has grown to be one of the most important and useful ligands in organometallic chemistry with one source stating that in excess of 80% of all organometallic complexes of the transition metals contain this ligand.<sup>3</sup> The importance of the cyclopentadienyl ligand in transition metal chemistry arises from the strength of the metal ligand bonding interaction<sup>4</sup> and its ability to occupy three coordination sites in its  $\eta^5$ -bonding form.<sup>5</sup> Strong bonding interactions are produced from the overlap between the degenerate pair of  $e_1$   $\pi$ -bonding orbitals in the cyclopentadienyl ring and the metal  $d_{xz}$  and  $d_{yz}$  orbitals and this together with the steric protection offered by the ligand can lead to the formation of very stable metal complexes.

There are three main classes of cyclopentadienyl complexes, **(A)** sandwich or metallocene complexes, **(B)** bent metallocenes and **(C)** half-sandwich complexes.

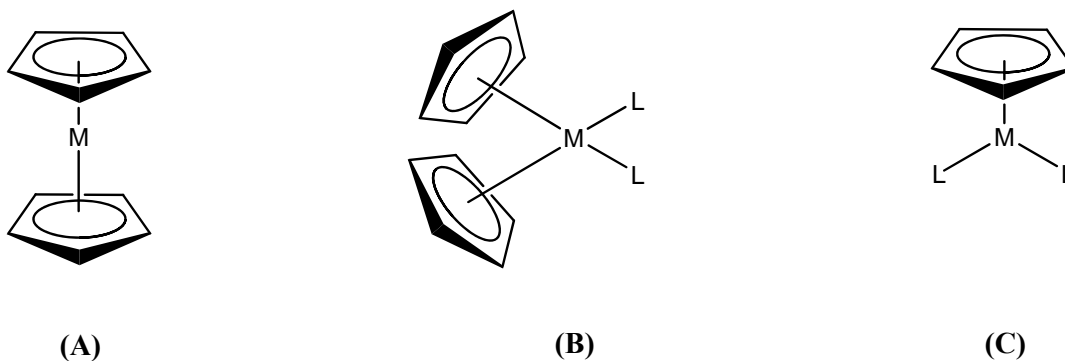


**Figure 1.1** (A) Sandwich complex, (B) Bent metallocene and (C) Half-sandwich complex.

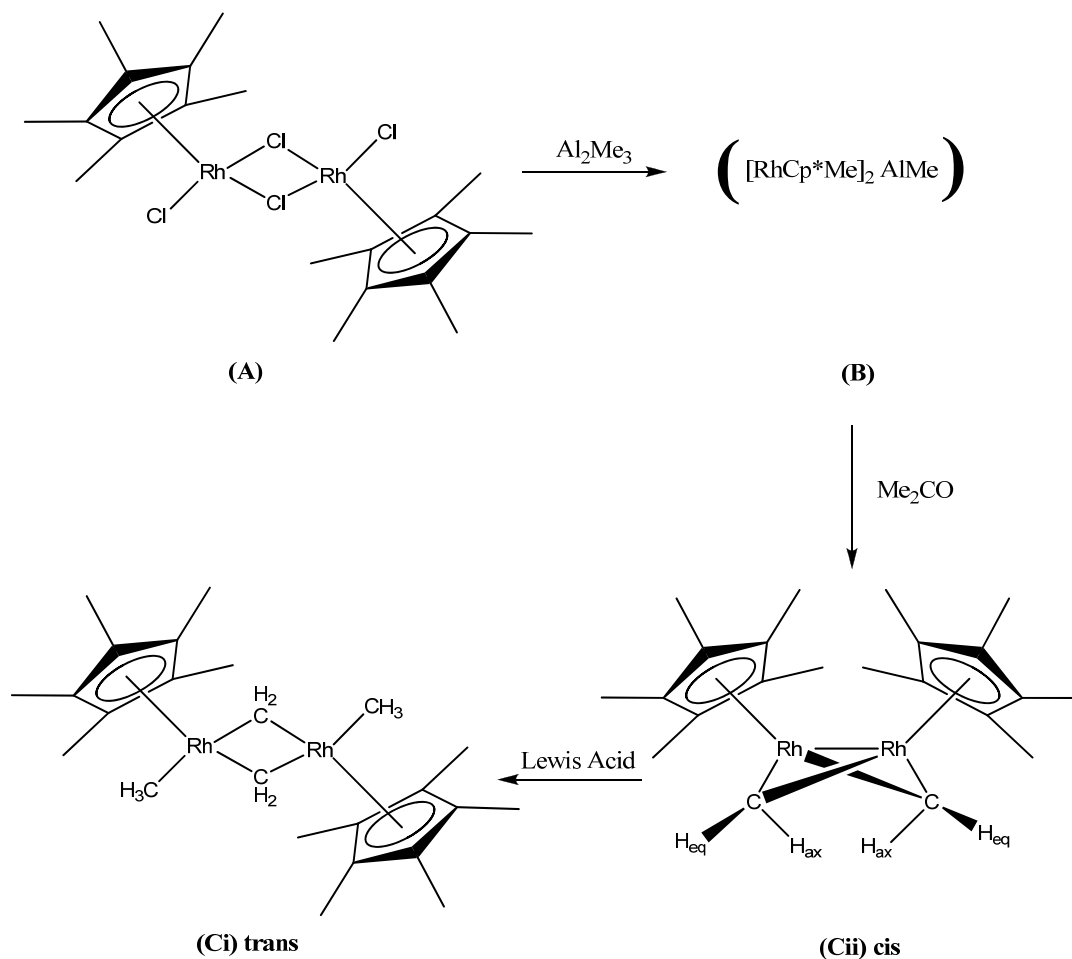
## 1.2 Substituted Cyclopentadienes

Substituted cyclopentadienes have attracted a lot of attention as they offer a far greater range of reactivity, structure and physical features than the unsubstituted parent ligands to transition metal complexes. The level and nature of substitution is virtually limitless and can provide Cp based ligands with enhanced bonding to metal atoms, catalytic activity, heteroatoms containing functional groups, increased steric bulk, chiral functionality and ring-ring bridging groups.<sup>6</sup> With these ligands, in their substituted or unsubstituted forms, metals may be stabilised in high or low oxidation states using bonding modes ranging from  $\eta^1$  to  $\eta^5$ .

Peralkyl cyclopentadienyl ligands have increased greatly in popularity since recognition of the positive effects the alkyl groups have on the solubility, electron releasing ability and steric protection of metal complexes.<sup>7</sup> The uses of these highly alkylated cyclopentadienes range from industrial lubricants to sterically bulky ligands for transition metal complexes and catalysts.<sup>8</sup>

## 1.3 Ring Substituted Metal Complexes

### 1.3.1 Alkyl Substituted Cyclopentadienes

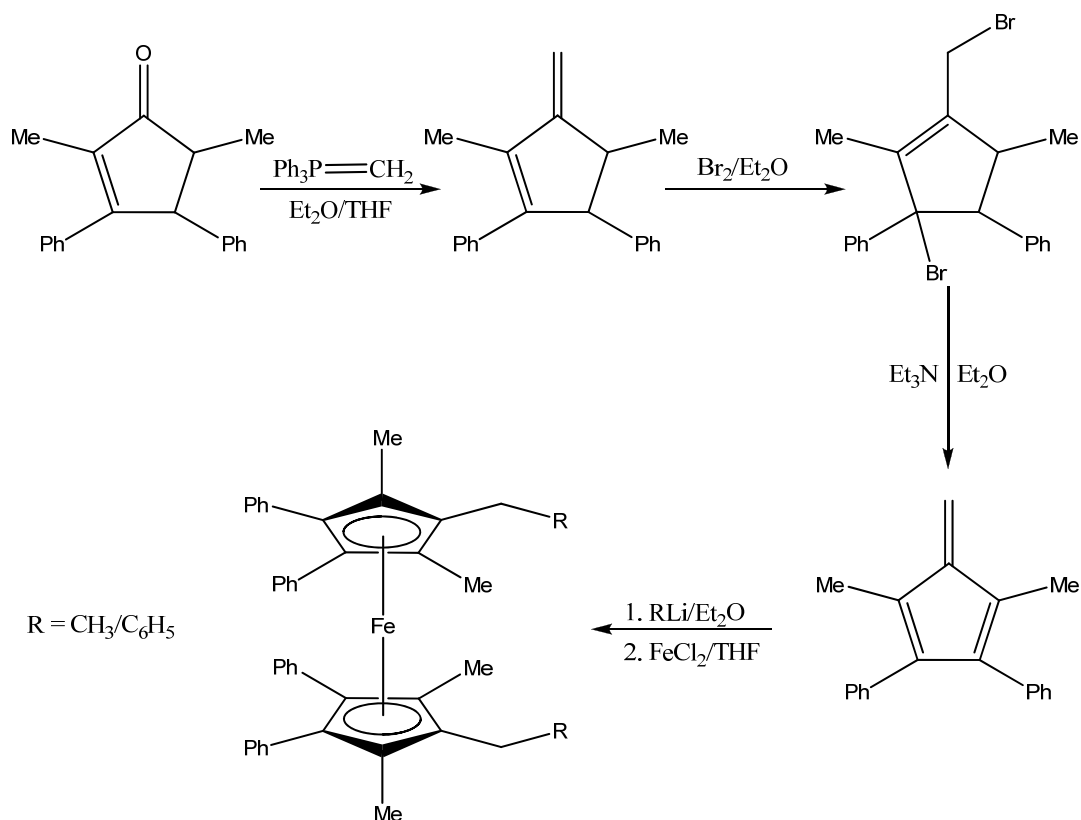


**Scheme 1.1** Reaction of  $[\text{Rh}(\eta^5\text{-C}_5\text{Me}_5)\text{Cl}_2]_2$  with  $\text{Al}_2\text{Me}_6$

The discovery of pentamethylcyclopentadienyl rhodium and iridium complexes,  $[\text{M}(\eta^5\text{-C}_5\text{Me}_5)\text{Cl}_2]_2$ , (**Scheme 1.1**), was first made by Kang and Maitlis in 1968.<sup>9</sup> These molecules were to attract a lot of attention from other researchers on account of their unique combination of the inert  $\text{Cp}^* - \text{M}$  bonds and labile anionic ligands which allow the molecules to undergo a varied range of reactions such as nucleophilic substitution, C–H activation and hydrogen transfer without loss of the  $\text{Cp}^*$  ring.<sup>10</sup>

For example, the  $[\text{RhCp}^*\text{Cl}_2]_2$  reacts with methylating agents, e.g., MeLi giving  $[\text{RhCp}^*(\mu\text{-CH}_2)_2(\text{Me})_2]_2$  in 90% yield when acetone was used as a H-acceptor before work-up. The rhodium methyls can then be removed as  $\text{CH}_4$  with acid and replaced with a huge variety of ligands to give complexes of the type  $[\text{RhCp}^*(\mu\text{-CH}_2)_2(\text{L}^1)(\text{L}^2)]^{2+}$  with  $\text{L}^1$  and  $\text{L}^2$  being ligands such as CO, pyridine and MeCN. The Rh(III) ion is paramagnetic. However, the odd electrons are paired in the metal-metal bond and the two  $\mu\text{-CH}_2$  bridges are very stable which are only converted when oxidising agents are used. One of the more successful routes for the preparation of substituted cyclopentadienes has been the addition of nucleophiles to fulvenes. However, the reactions of substituted fulvenes with heteroatom-based nucleophiles will result in deprotonation as opposed to nucleophilic attack more often and this has been a problem reported by several researchers.<sup>11</sup>

The use of tetra-substituted fulvenes was one of the measures taken to overcome this problem as they have no competing acidic protons. 1,4-dimethyl-2,3-phenylfulvene was prepared by Donovalova and co-workers from 2,5-dimethyl-3,4-diphenylcyclopent-2-enone in an 80% yield. This was then treated with both methyl and phenyl lithium prior to reaction with  $\text{FeCl}_2$  to yield 1,1'-diethyl-2,2',5,5'-tetramethyl-3,3',4,4'-tetraphenylferrocene in a 58% yield and 1,1'-dibenzyl-2,2',5,5'-tetramethyl-3,3',4,4'-tetraphenylferrocene in a 43% yield.<sup>12</sup> Moderate yields of the corresponding substituted metallocenes were also obtained using a variety of other lithiating agents, (*Scheme 1.2*).



**Scheme 1.2:** Synthesis of, 1'-diethyl-2,2',5,5'-tetramethyl-3,3',4,4'-tetraphenylferrocene and 1,1'-dibenzyl-2,2',5,5'-tetramethyl-3,3',4,4'-tetraphenylferrocene

deVries reported the synthesis of pentamethylcyclopentadiene involving a five step process with a yield of ~75% in 1960.<sup>13</sup> The procedure has since been improved to a one-pot synthesis with reasonable yields by Kohl *et al*<sup>14</sup> leading to an increased popularity of the ligand.

Röhl *et al.* reported the synthesis of  $\text{C}_{10}\text{H}_{14}\text{TiCl}_3$  by heating titanium tetrachloride with various butanes at 300°C. NMR analysis showed a single sharp proton resonance confirming the  $\eta^5$ -pentamethylcyclopentadienyl trichlorotitanium structure. The enhanced stability, high solubility and the low additional molecular weights of the added methyl substituents have promoted the use of the  $\pi$ -pentamethylcyclopentadienyl ligand to that of the most popular completely substituted cyclopentadienyl derivative.<sup>15</sup>

Compound	Colour	Melting point (°C)
[TiCp*Cl <sub>3</sub> ]	Red	225-227
[FeCp* <sub>2</sub> ]	Yellow	291-295
[FeCp*(CO) <sub>2</sub> ] <sub>2</sub>	Red/Violet	Dec. ~280
[CoCp*(CO) <sub>2</sub> ]	Red	56-58
[ReCp*(CO) <sub>3</sub> ]	White	151-153
[MoCp*(CO) <sub>3</sub> CH <sub>3</sub> ]	Orange	141-145
[MoCp*(CO) <sub>2</sub> ] <sub>2</sub>	Red	Dec. ~273

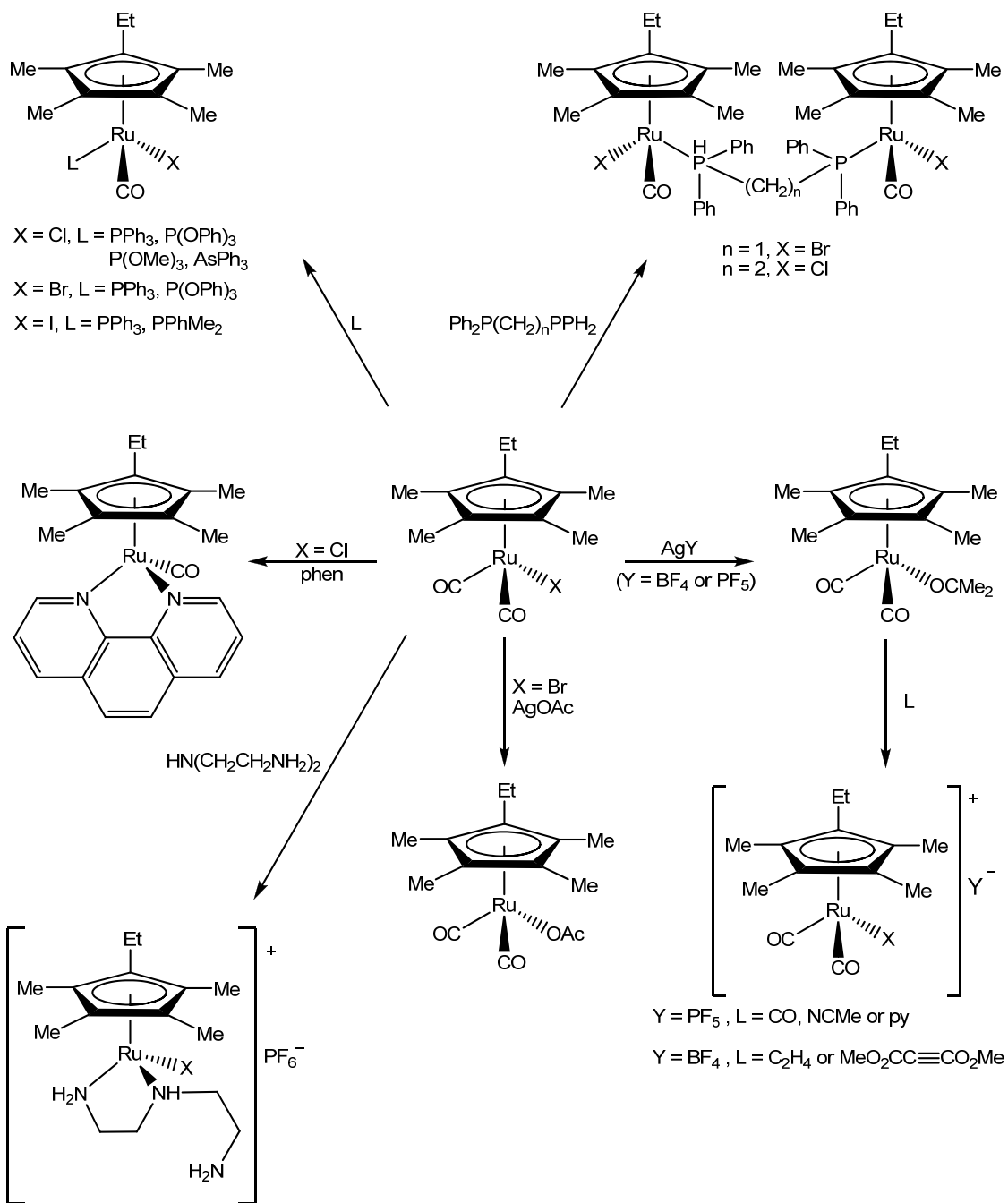
**Table 1.1:** Some  $\pi$ -pentamethylcyclopentadienyl derivatives

Following the pentamethylcyclopentadienyl ligand the tetramethylcyclopentadienyl ligand has also become popular in transition metal chemistry. It is slightly less electron donating but decidedly less sterically hindering, thus leading to an advantageous influences on the reactivity of its complexes.<sup>16</sup> The remaining unsubstituted position on tetramethylcyclopentadiene is easily alkylated allowing the preparation of functionalised tetramethylcyclopentadienes as well as bridging bis(tetramethylcyclopentadienyl) ligands.<sup>17</sup>

In recent years much effort has been expended on the synthesis of new multiply functionalized cyclopentadienyl ligands, together with their sandwich and half sandwich metal complexes.<sup>7</sup>

Fischer and his group examined substituted benzene and related substituent effects in six carbon ring ligands when they concluded that hexamethylbenzene forms far more stable  $\pi$ -complexes with various metals than benzene. The complex [Fe( $\eta^6$ -C<sub>6</sub>(CH<sub>3</sub>)<sub>6</sub>)<sub>2</sub>] was the first to be examined followed by similar complexes of cobalt and rhodium.<sup>18</sup>

The chemistry of compounds of the type [Ru( $\eta^5$ -C<sub>5</sub>Me<sub>4</sub>Et)(CO)<sub>2</sub>X] (X = Cl, Br, I) was studied by White *et al.* and reported in 1996.<sup>19</sup> These compounds were found to react with unidentate ligands, L (L = phosphorus, arsenic donor ligands), to yield the corresponding compounds of the type [Ru( $\eta^5$ -C<sub>5</sub>Me<sub>4</sub>Et)(CO)LX]. The complexes were prepared by heating the parent complexes under reflux with a slight excess of L in toluene or benzene. The time for the reaction to go to completion depended upon the halide attached with reaction times increasing along the series Cl < Br < I.



**Scheme 1.3:** The reaction of  $[\text{Ru}(\eta^5\text{-C}_3\text{Me}_4\text{Et})(\text{CO})_2\text{X}]$  with  $L$  ( $L$  = phosphine, arsenic donor ligands).

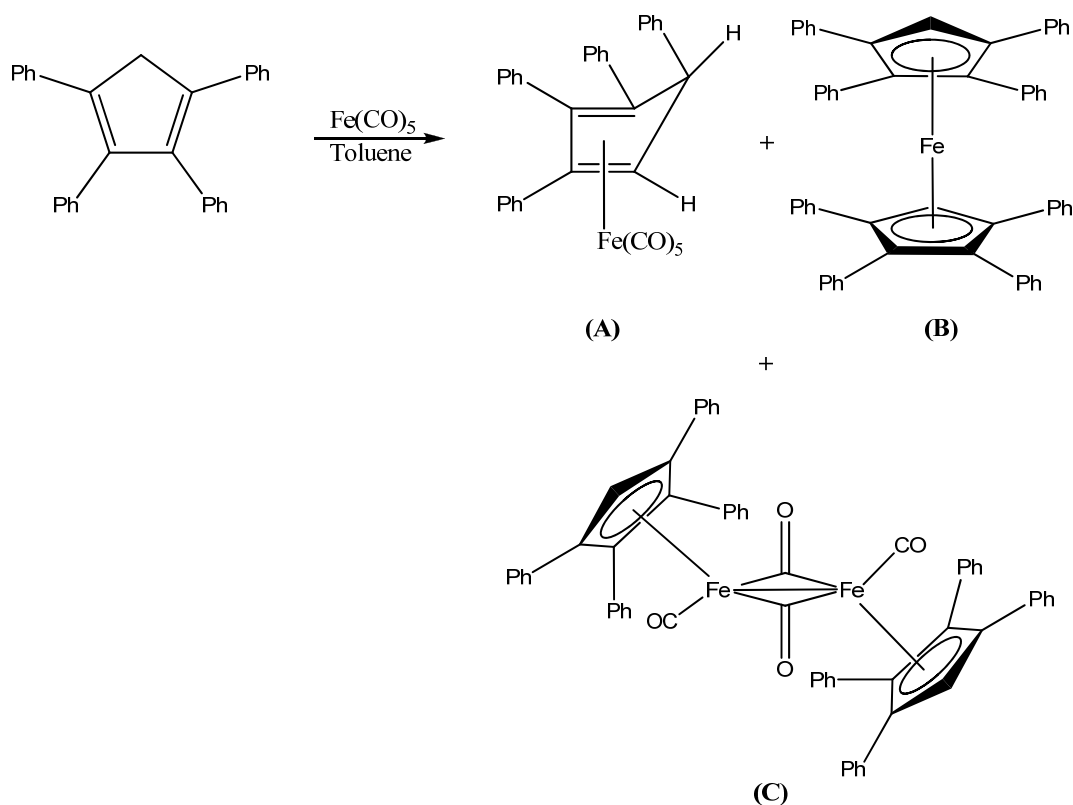
### 1.3.2 Aryl Substituted Cyclopentadienes

Metal complexes with completely substituted  $\pi$ -cyclopentadienyl groups are of specific interest, as these substituents should have the maximum effect on physical and chemical properties. Aromatic rings in close proximity tend to adopt propeller arrangements which would have the potential to direct incoming groups in catalytic processes as has been demonstrated for phenyl substituted phosphines.<sup>15</sup>

The synthesis of a series of phenyl substituted ferrocenes from their corresponding phenyl-substituted cyclopentadienes was reported by Pauson in 1954.<sup>20</sup> His previous attempts to introduce phenyl groups into ferrocene by reaction with benzoyl peroxide had failed which lead him to revise his route. He first attempted to prepare ferrocene derivatives using 1,3-diphenylcyclopentadiene with ethylmagnesium bromide forming the corresponding Grignard reagent which then yielded the desired 1,3,1,3-tetraphenylferrocene on reaction with ethereal ferric chloride. This procedure showed potential after the subsequent synthesis of 1,2,4,1',2',4'-hexaphenylferrocene from 1,2,4-triphenylcyclopentadiene.

The same procedure was then applied to 1,2,3,4-tetraphenylcyclopentadiene but no ferrocene derivative was obtained. The poor nucleophilicity of the grignard reagent was suggested to be the cause of the reaction's failure. To query this, 1,2,3,4-tetraphenylcyclopentadiene was converted to its bromide form and treated with phenyl lithium to form tetraphenylcyclopentadienyl lithium. This was then reacted with ferric chloride but yet again, the desired product eluded the researchers. After a failed attempt at converting 1,2,3,4,5-pentaphenylcyclopentadiene to the ferrocene derivatives, it was concluded that steric hindrance in the system was just too high.

Xu *et al.*, also researched the consequences of having phenyl groups attached to the cyclopentadienyl rings.<sup>6</sup> Tetraphenylcyclopentadiene<sup>21</sup> was heated under reflux in toluene with iron pentacarbonyl for 16 hours to give three products, (A) to (C), (*Scheme 1.4*).

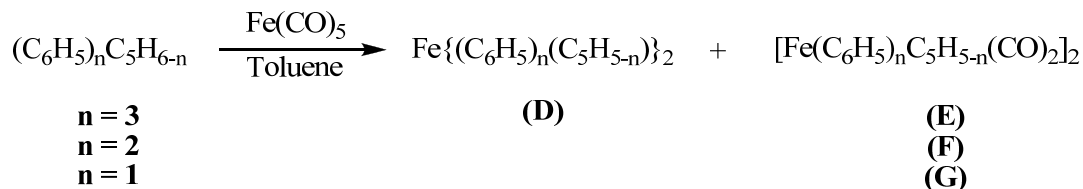


**Scheme 1.4:** Reaction of tetraphenylcyclopentadiene and iron pentacarbonyl

The products (A) - (C) were obtained in poor yields of 10, 5 and 15% respectively and their structures were assigned on the basis of analytical and spectroscopic data. Compound (A) was a light yellow crystalline solid and was assigned the  $\eta^4$ -diene structure on the basis of the three strong IR bands at 2034, 1972 and  $1964\text{cm}^{-1}$  and the two singlets present in the  $^1\text{H}$  NMR spectrum at 5.09 and 6.31ppm were assigned to the two hydrogens on the ring. This complex was thermally and air stable both in the solid state and in solution, similar to  $[\text{Fe}(\eta^4\text{-C}_5\text{Bz}_5\text{H})(\text{CO})_3]$  but unlike the unsubstituted analogue,  $[\text{Fe}(\eta^4\text{-C}_5\text{H}_6)(\text{CO})_3]$  which converts back to the dimer  $[\text{Fe}(\eta^5\text{-C}_5\text{H}_6)(\text{CO})_3]_2$  at temperatures above  $0^\circ\text{C}$ .<sup>22</sup>

Compound (B) was only obtained in a 5% yield but Castellani and co-workers reported this compound in a 58% yield in 1986, *via* direct ferrocene synthesis by treating anhydrous  $\text{FeCl}_2$  in THF with lithium tetraphenylcyclopentadienide resulting in a red, air stable crystalline solid.<sup>23</sup> The dark red crystals of (C) had an IR spectrum showing both the bridging and terminal  $\nu\text{MC-O}$  bands expected for the dimeric structure.

The effects of the number of phenyl substituents on cyclopentadiene were investigated by reacting mono-, di- and tri-phenyl cyclopentadienes with iron pentacarbonyl.



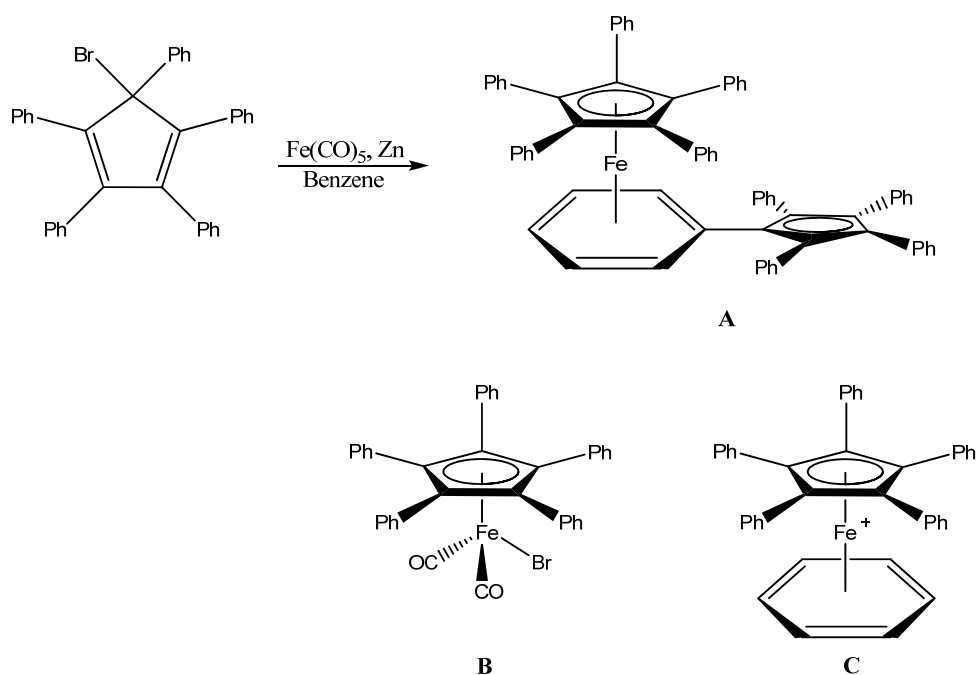
**Scheme 1.5:** Reaction of phenylsubstituted cyclopentadienes and iron pentacarbonyl

1,2,4-triphenylcyclopentadiene<sup>24</sup> was refluxed with iron pentacarbonyl in toluene for 21 hours to obtain **(D)** and **(E)** in 2% and 11% yields respectively (**Scheme 1.5**). The reaction of 1,3-diphenylcyclopentadiene with Fe(CO)<sub>5</sub> gave the diiron complex **(F)** in a 14% yield which was similar to product **(G)**, the sole product obtained in a 14% yield when phenylcyclopentadiene was refluxed with Fe(CO)<sub>5</sub> for 18 hours.

After combining their results, Xu and co-workers came to the conclusion that like unsubstituted cyclopentadiene, one and two phenyl substituted cyclopentadienes react with iron pentacarbonyl to give only the diiron complexes. However, once more than two phenyl groups were added to the cyclopentadienes a greater variety of ferrocene derivatives were obtained, most likely due to steric effects.<sup>6</sup>

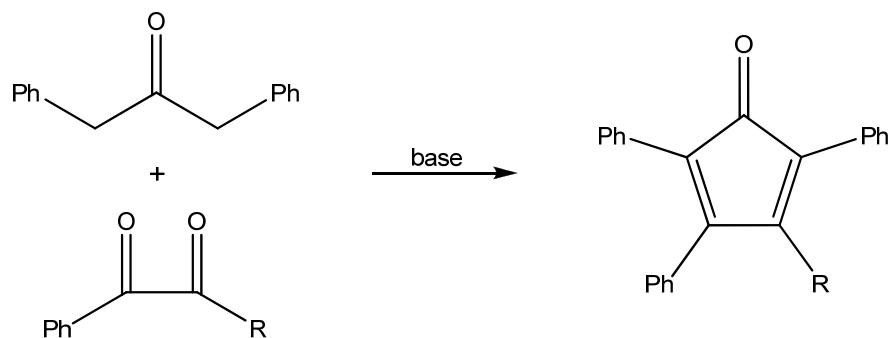
A number of decaphenylmetallocenes have been reported. However, only the tin, germanium, lead and nickel systems have been satisfactorily characterised. Brown *et al.* synthesised and characterized ( $\eta^5$ -pentaphenylcyclopentadienyl)-iron (II), a linkage isomer of decaphenylferrocene, with a zwitterionic structure, by reacting iron pentacarbonyl, zinc dust and bromopentaphenylcyclopentadiene in a 1:2:2 ration in refluxing benzene for 40 hrs yielding **(A)**, an intensely blue crystalline solid in a 53% yield. Products **(B)** and **(C)** were minor products.

Both <sup>1</sup>H and <sup>13</sup>C NMR spectra of **(A)**, (**Scheme 1.6**), show that in solution, the ( $\eta^6$ -C<sub>6</sub>H<sub>5</sub>-C<sub>5</sub>Ph<sub>4</sub>) ligand adopts a geometry with the  $\eta^6$ -ring co-planar with the five carbon atoms of the attached cyclopentadienyl ring so as the ligand has minor symmetry, allowing the ( $\eta^6$ -C<sub>6</sub>H<sub>5</sub>-C<sub>5</sub>Ph<sub>4</sub>) fragment to maximise  $\pi$ - $\pi$ -overlap and delocalise charge over the Ph<sub>5</sub>C<sub>5</sub>- and coordinating  $\eta^6$ -C<sub>6</sub>H<sub>5</sub> ring.



**Scheme 1.6:** Reaction of bromopentaphenylcyclopentadiene and iron pentacarbonyl

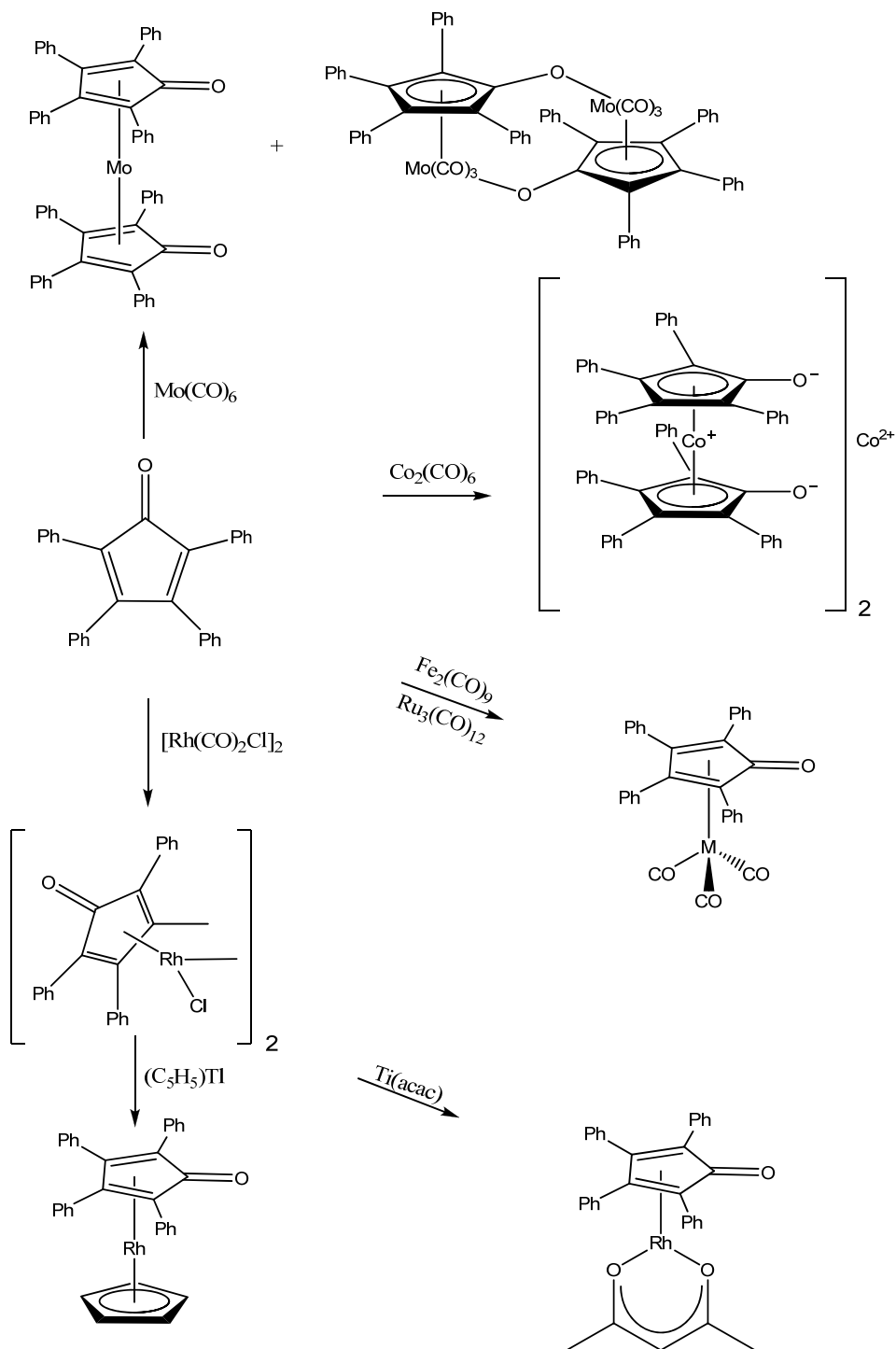
The reaction of benzyl and suitably substituted 1,3-propanones result in cyclopentadienones.<sup>25</sup>



**Scheme 1.7:** The synthetic route to cyclopentadienones

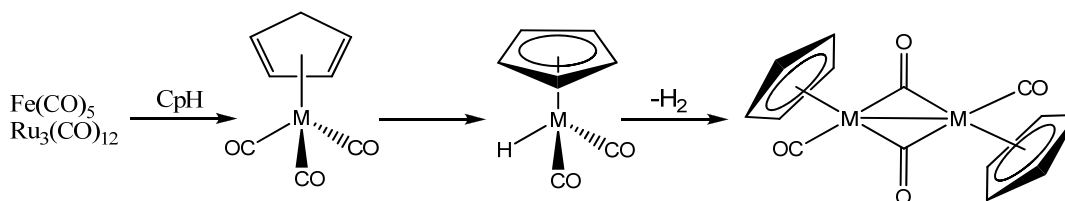
The chemistry of these compounds is controlled by the small energy separation between the HOMO and LUMO orbitals which explains their intense visible absorption. Cyclopentadienones undergo Diels-Alder dimerization readily, consequently, all attempts of isolation of monomer complexes have failed. Tri- and tetra-substituted derivatives containing at least two phenyl groups have been detected successfully.<sup>26</sup> Tetracyclone,

being readily available, continues to be used as a starting material for many organometallic reactions, as below, (**Scheme 1.8**).<sup>25</sup>



**Scheme 1.8:** Some metal complexes of tetracyclone

The reaction of triruthenium dodecacarbonyl and iron pentacarbonyl with cyclopentadiene form the dimeric complexes  $[M(\eta^5\text{-C}_5\text{H}_5)(\text{CO})_2]_2$ , (M = Fe/Ru) *via* the hydride intermediate,<sup>27</sup> (**Scheme 1.9**).



**Scheme 1.9:** Reaction of cyclopentadiene with  $\text{Ru}_3(\text{CO})_{12}$  and  $\text{Fe}(\text{CO})_5$

Kochhar and Petit prepared cyclopentadieneiron tricarbonyl by reacting di-iron nonacarbonyl with cyclopentadiene at low temperature. At temperatures above  $0^\circ\text{C}$  the reaction proceeds to the dimer.<sup>28</sup>

Humphries and Knox investigated the ruthenium analogues by refluxing triruthenium dodecacarbonyl with cyclopentadiene in heptane under nitrogen, forming the corresponding hydride  $[\text{RuCp}(\text{CO})_2\text{H}]$  after an hour. The hydride is air sensitive and its isolation is difficult. However, while in solution it is available for further reaction. The addition of triphenylphosphine to the boiling solution resulted in the formation of the stable hydride derivative  $[\text{RuCp}(\text{CO})\text{HPPH}_3]$  in a 74% yield.

Dimers of the type  $[\text{MCp}(\text{CO})_2]_2$ , where M = Ru or Fe, can form *cis* or *trans* arrangements of the Cp ligands with respect to the metal-metal bond.<sup>29</sup> The *trans* isomer is sterically favoured but orbital overlap considerations favour *cis* geometry, however, the energy difference is small and the two isomers interconvert *via* a non-bridging intermediate and an equilibrium is usually established.<sup>30</sup>

## 1.4 Cyclopentadienes with Electron Withdrawing Substituents

In 1995 Costa *et al.* reported on their development of a new multi-step procedure for the synthesis of cyclopentadiene derivatives substituted by one methoxy carbonyl group and two methoxycarbonylmethylene groups<sup>31</sup> (HMDMCp).

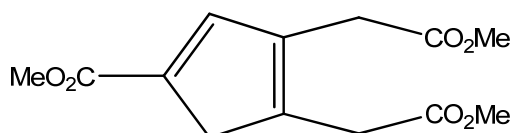


**Figure 1.2:** *1-Methoxycarbonyl-3,4-Di(methoxycarbonylmethylene)cyclopentadiene (HMDMCp)*

This substituted cyclopentadiene was subsequently reacted with  $(\text{RhCl}(\text{L})_2)_2$   $\mu$ -halo complexes ( $\text{L} = \text{CO}, \text{C}_2\text{H}_4, 1,5\text{-cyclooctadiene}$ ) yielding the corresponding  $\eta^5$ -cyclopentadienyl complexes illustrated below, (**Figure 1.3**).

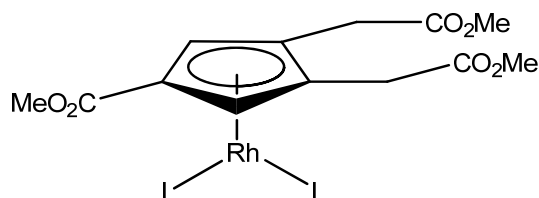


**Figure 1.3:**  $\eta^5$ -cyclopentadienyl rhodium complexes

The ligand was also used in reactions with other metal complexes. It was, for example, reacted with  $\text{CoCl}(\text{PPh}_3)_3$  in the presence of 1,5-cyclooctadiene to yield the cobalt complex below in a 39% yield.<sup>32</sup>

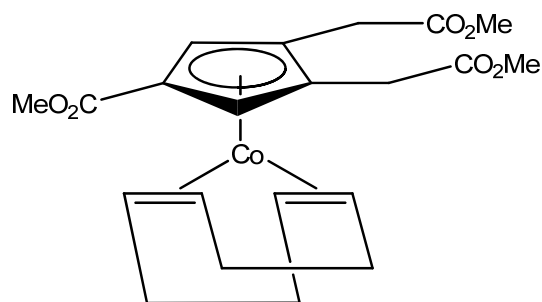
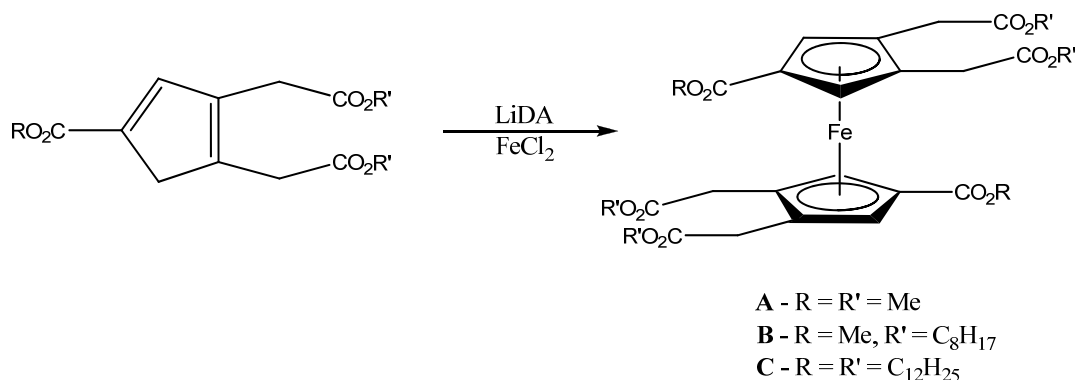


**Figure 1.4:** Monosubstituted cobalt complex

Costa *et al.* also synthesised ferrocene type complexes using the trisubstituted ligand with the procedure progressing *via* a direct reaction between transition metal complexes and the substituted Cp rings, rather than introducing the electron withdrawing substituents into the ring after preparation of the metal complex. After converting the substituted cyclopentadiene into its anion using lithium diisopropylamide it was subsequently treated with dry  $\text{FeCl}_2$  to form the substituted ferrocene.



**Scheme 1.10:** Synthesis of substituted ferrocene

The yields of these products were low (**A** = 35%, **B** = 28%, **C** = 15%), and this was attributed to losses during the purification processes. Complete rotational freedom in the two rings was indicated by the  $^1\text{H}$  NMR data. Only one signal was observed for the four hydrogen atoms on the two cyclopentadienyl rings indicating rotational averaging of ligand environments.

This ligand was also used in the synthesis of dimeric metal complexes by reaction with  $\text{Fe}_2(\text{CO})_9$  and  $\text{Ru}_3(\text{CO})_{12}$  in the presence of norbornene as a hydrogen acceptor with yields of 40% and 42% respectively.

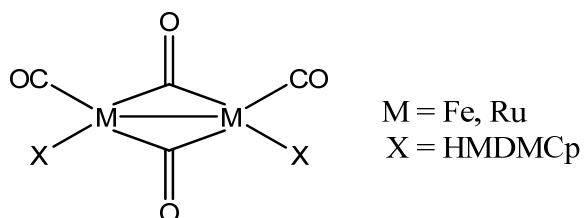


**Figure 1.5:** *Dimeric metal complexes*

The  $\nu_{\text{MC-O}}$  vibrational bands were reported in both solid state and solution. The vibrational frequencies for some typical cyclopentadienyl dimeric complexes are listed below, (*Table 1.2*).

M	Cp	Solvent	Terminal CO $\nu_{CO}(cm^{-1})$		Bridging CO	Ref.
Fe	C <sub>5</sub> H <sub>5</sub>	Hexane <sup>a</sup>	2005	1961	1794.5	33
Ru	C <sub>5</sub> H <sub>5</sub>	Heptane <sup>b</sup>	2010	1965	1794	33
Ru	C <sub>5</sub> H <sub>5</sub>	CHCl <sub>3</sub> <sup>b</sup>	2009	1968	1768	33
Ru	C <sub>5</sub> H <sub>5</sub>	CS <sub>2</sub> <sup>a</sup>	2004	1960	1785	33
Ru	MeC <sub>5</sub> H <sub>4</sub>	Heptane <sup>b</sup>	2006	1960	1790	33
Ru	MeC <sub>5</sub> H <sub>4</sub>	CHCl <sub>3</sub> <sup>b</sup>	2003	1959	1779	33
Ru	(C <sub>5</sub> H <sub>4</sub> CH(NMe <sub>2</sub> )) <sub>2</sub>	Heptane <sup>b</sup>	2002	1964	1793	33
Ru	C <sub>9</sub> H <sub>7</sub>	CHCl <sub>3</sub> <sup>b</sup>	2003	1961	1779	33
Fe	MDMCp <sup>c</sup>	KBr <sup>b</sup>	2004	1963	1779	7
Fe	MDMCp <sup>c</sup>	CH <sub>2</sub> Cl <sub>2</sub> <sup>b</sup>	2008	1970	1786	7
Ru	MDMCp <sup>c</sup>	KBr <sup>b</sup>	2005	1960	1783	7
Ru	MDMCp <sup>c</sup>	CH <sub>2</sub> Cl <sub>2</sub> <sup>b</sup>	2014	1973	1787	7

**Table 1.2:** Carbonyl stretching frequencies ( $\nu_{CO}(cm^{-1})$ ) for  $(CpM(CO)_2)_2$

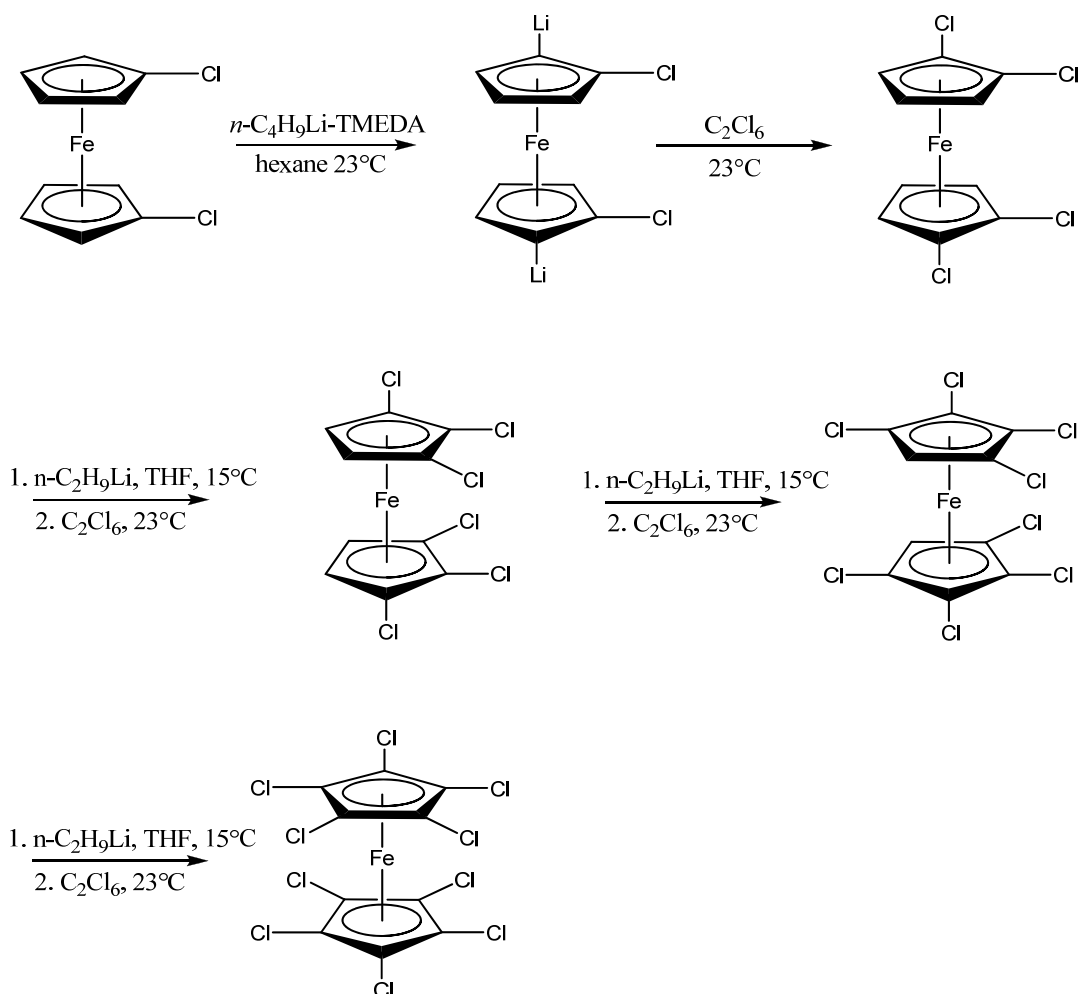
<sup>a</sup> = At low temperature

<sup>b</sup> = At room temperature

<sup>c</sup> = 1-methoxycarbonyl-3,4-di(methoxycarbonylmethylene)cyclopentadienyl

Despite appearances the MDMCp ligands do not have effective electron-withdrawing groups. The inherent electron releasing abilities of the methyl groups effectively negate the electron withdrawing abilities of the CO<sub>2</sub>Me group.

To date decachloroferrocene is the only perhalo oxidatively stable metallocene and it is also the only case to be completely substituted with what are undeniably electron withdrawing groups. This, with other polychlorinated ferrocenes, has been prepared in a four step synthesis from the easily accessible 1,1-dichloroferrocene by a series of repetitive metalation exchange halogenation reactions.<sup>34</sup> The key to the successive addition of chlorine to the ferrocene is  $\alpha$ -proton abstraction which the chloroferrocene undergoes upon reaction with n-butyllithium, (**Scheme 1.11**).



**Scheme 1.11:** Synthesis of 1,1',2,2',3,3',4,4',5,5'-decachloroferrocene from 1,1'-dichloroferrocene

The yield of the final product was very low (ca. 7%). The low yield of final product was attributed to the formation of by-products in each step in the series. This loss in final product led the authors to repeat the procedure with the initial complex being converted to the final product without purifying the intermediates. This gave a 42% yield. This direct method was used for the ruthenium analogue leading to a 14% yield.

In the past these research groups had tried to synthesise the final product by reacting ferrous chloride with pentachlorocyclopentadienyllithium but failed to produce the metallocene. Hedberg and co-workers also tried to react the pentachlorocyclopentadienyllithium with ferrous iodide and ferrous acetylacetonate as

well as attempting to react pentachlorocyclopentadiene with diethylamine and ferrous acetylacetonate, but as before they found no evidence of the desired metallocene. The low nucleophilicity of the pentachlorocyclopentadienyl anion is thought to be the reason for the failure of these reactions.

## 1.5 Organolithium Reagents

Organolithium reagents became a popular organometallic area after 1917 when Schlenk and Holtz synthesised the first analogue *via* a transmetalation reaction between diethylmercury and lithium metal.<sup>35,36</sup> In 1930 Ziegler and Colonius reported a new method for preparing organolithium compounds by a metal-halogen exchange reaction of organic halides with lithium metal<sup>37</sup>, their work being continued by Gilman *et al.*<sup>38</sup> and Wittig and Leo.<sup>39</sup>

The popularity of organolithium compounds arises from their high reactivity, even under mild conditions. This is due to the polarity of the carbon-lithium bond which presents a highly reactive carbanion, a particularly useful moiety in carbon-carbon bond forming processes. During the reactions of organolithium a new functionality may be formed at the same time, as in the case of the reaction of organolithium with a carbonyl compound. This is a very important concept in synthetic chemistry as the functionality present in the intermediate can be transferred to the electrophile, and thus poly-functionalised molecules are produced in a one pot synthesis.<sup>40</sup>

The reactivity of the intermediates depends greatly on the metal type. Very low temperatures are often employed with functionalised organolithium derivatives due to problems arising from the compatibility between different functionalities and the carbon-lithium bond, as well as from possible elimination processes. In organozinc compounds the functional group compatibility is far higher due to zinc being a less electropositive metal. However, they are not as reactive as their organolithium analogues and need either very reactive electrophiles or the aid of a transition metal catalyst.<sup>41</sup> The reactivity of organolithiums can be greatly enhanced by coordinating solvents.<sup>42</sup> The most commonly

used coordinating solvents in organolithium reactions are (in approximate empirical order of decreasing activity power):

HMPA > PMDTA > (-)-sparteine > DMPU > DME > TMEDA > THF > *t*-BuOMe > Et<sub>2</sub>O

The reactivity differences observed for organolithiums in a hydrocarbon solution vs. ether or THF can be described by deaggregation. However, there is little evidence that the differences in reactivity between organolithium species in coordinating solvents are primarily due to their ability to deaggregate the organolithiums. While the beneficial effect TMEDA has on many lithiation reactions with *s*-BuLi is evident, it is not clear if this is due to the deaggregation of the *s*-BuLi. Moreover, it is evident that THF is a superior ligand for lithium than TMEDA since alkylolithiums are deaggregated by THF to the same extent as a THF/TMEDA solution.<sup>43</sup>

Temperatures above room temperature, and in some cases even 0°C, cannot be employed with the solvents mentioned above and organolithiums due to their tendencies to react with polar bonds. However, a diethyl ether/BuLi solution is stable over a period of days at room temperature,<sup>44</sup> in contrast a THF solution will decompose at this temperature.<sup>45,46</sup> The rate of metalation and an expansion of the range of compounds capable of deprotonation can be achieved by the use of complexing and chelating reagents like DMPU, TMEDA and HMPA. The rates of S<sub>N</sub>2 reactions and changing the ratios of 1,2- to 1,4-addition by the organolithiums are effected by the polar co-solvents, however, they can also favour side reactions such as proton transfer. In order for the lithiation of a C–H bond to occur at a reasonable rate the organolithium product must display intramolecular coordination of the electron deficient lithium atom by a heteroatom and stabilization of the electron-rich C–Li bond by a nearby empty orbital of an electron-withdrawing group.<sup>42</sup>

## 1.6 Ortholithiation

Ortholithiation occurs when metalation of an aromatic ring is achieved adjacent to a donor atom containing functional group. It is a well-documented reaction since the first metalation of anisole by Gilman<sup>47</sup> and Wittig.<sup>48</sup> An extensive review of this area has been provided by Gschwend and Rodriguez.<sup>49</sup>

Ortholithiations involve deprotonating a substituted aromatic ring with a reactive organolithium, usually n-, s-, or t-butyllithium. This is thought to proceed due to the provision of an adjacent coordination site for lithium, thus increasing reactivity and directing regioselectivity.<sup>50</sup> This, however, is not the case for weaker ortholithiation directors, but it can be assumed for strong director coordination between substrate and the alkyllithium. This may lead to deaggregation of the alkyllithium and result in lithiation, whether it proves to be ortholithiation or not.

The ortholithiation of aromatics has become an important synthetic tool<sup>51</sup> and while many substituents are known activators of the *ortho* position towards deprotonation by strong bases, only one systematic examination has been carried out to assess the relative activation abilities.<sup>52</sup> Slocum and Jennings<sup>53</sup> carried out a study which showed that relative to the methoxy group, there is a range of reactivity among substituents. They illustrated this by determining the site of metalation in a series of substituted anisoles. They concluded that SO<sub>2</sub>NMe<sub>2</sub>, SO<sub>2</sub>NHMe, CONHMe and CH<sub>2</sub>NMe<sub>2</sub> were all more reactive toward metalation than the methoxy group.

The base involved in the lithiation process can also influence the relative importance of coordination and acidity. For example, alkyllithiums become less Lewis-acidic once coordinated to a basic solvent like TMEDA or THF, therefore having a decreased tendency to be directed by coordination and acidity can become the dominant factor.

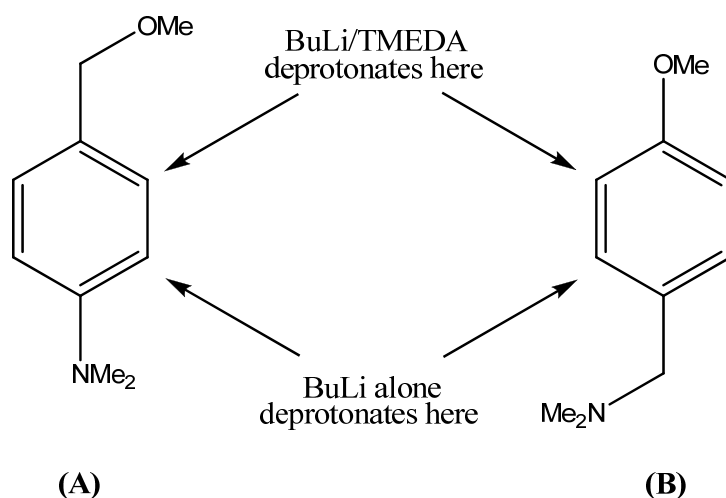


**Figure 1.6:** Deprotonation sites using BuLi or BuLi/TMEDA

This effect is illustrated by the deprotonation of **(A)** and **(B)**, (**Figure 1.6**). Deprotonation occurs *ortho* to the more Lewis-basic amino group in the absence of TMEDA, and *ortho* to the more electronegative and therefore acidic MeO group in the presence of TMEDA.<sup>53</sup>

Thus the ortholithiation reaction has two steps, complex-formation and deprotonation, in which the two key features are the rate and regioselectivity of lithiation which are controlled by the coordination by the heteroatom and the acidity of the proton which is removed.

The most effective directing groups tend to have a mixture of the basic properties required for the coordination of the lithium and the acidic properties needed for rapid and efficient deprotonation. The typical ortholithiation-directing groups were divided into classes by Snieckus, according to their ease of lithiation and the uses of their application in synthesis.<sup>54</sup> The scheme below is a guide of the favoured conditions typically required for lithiation of a particular functional group.

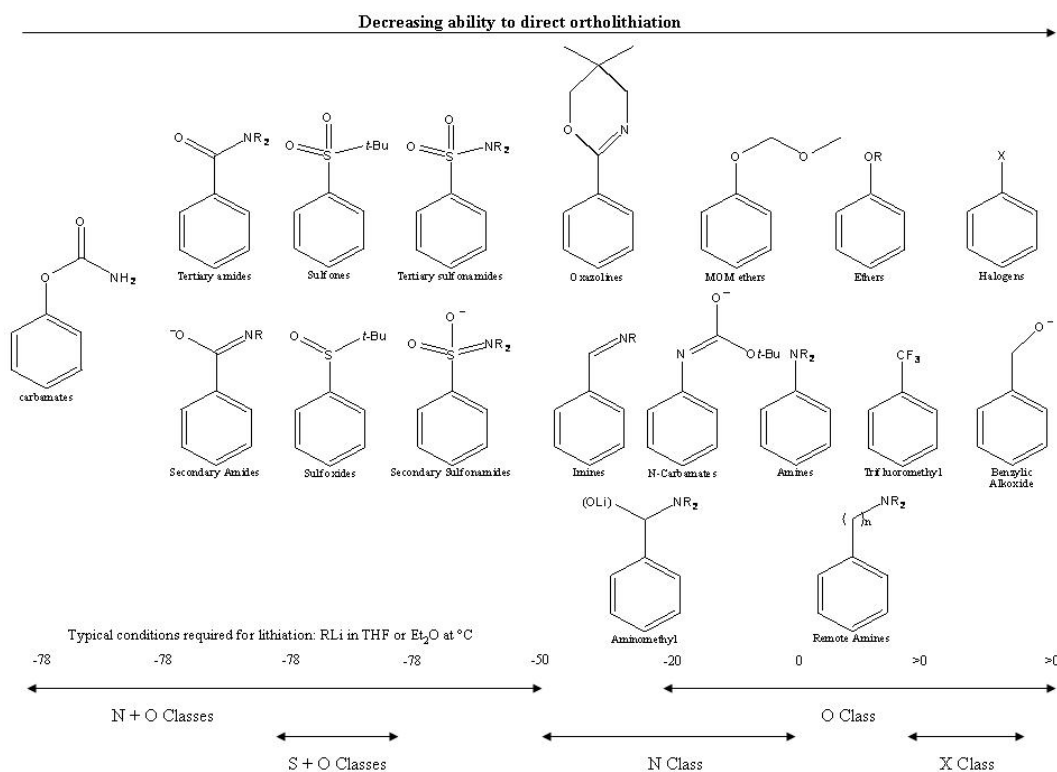


**Figure 1.7:** Ortholithiation directing groups

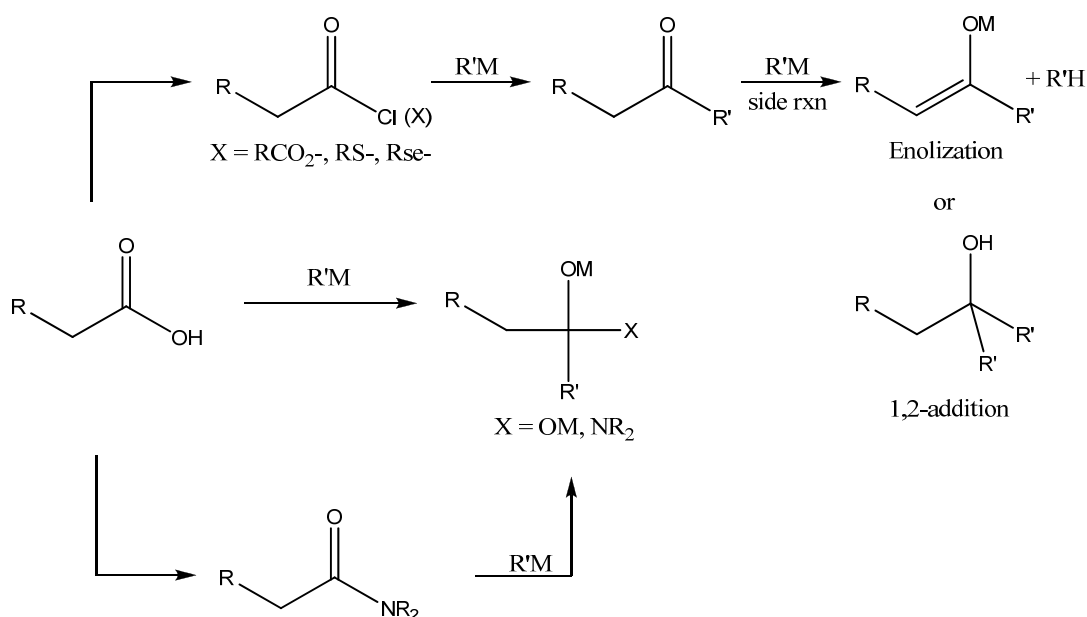
## 1.7 Acid Chlorides

The chemistry of organometallic reagents has often been examined by reaction with acid chlorides, the long history of which paralleled the development of organometallic chemistry.<sup>55</sup> The acylation of an organocopper reagent was first reported by Gilman in 1936,<sup>56</sup> this was then followed by Whitesides utilization of lithium dialkylcuprates in 1967.<sup>57</sup>

The preparation of ketones from carboxylic acids or their derivatives is a significant synthetic procedure, involving C–C bond formation and functional group interconversion. The difficulty of converting a carboxylic acid to a ketone in a single step typifies the complications arising from reactivity and chemical stability in organic synthesis. Dieter's

work illustrates two strategies exploiting the relative reactivities of the carboxylic acid derivative and ketone product toward nucleophilic attack (**Scheme 1.12**).<sup>58</sup>

1,2-Addition of hard organometallic reagents to carboxylic acids and amides produce stable tetrahedral intermediates in the reaction conditions below. The more reactive ketone is unavailable to the attacking nucleophile since the ketone is unmasked by collapse of the tetrahedral intermediate during the work-up procedure.



**Scheme 1.12:** Ketone synthesis using organometallic reagents

Acid chlorides, thiol esters, seleno esters, and anhydrides are more reactive toward many organometallic reagents than the product ketones and the influence of temperature, solvent, and modification of reagent reactivity can result in chemoselectivity.

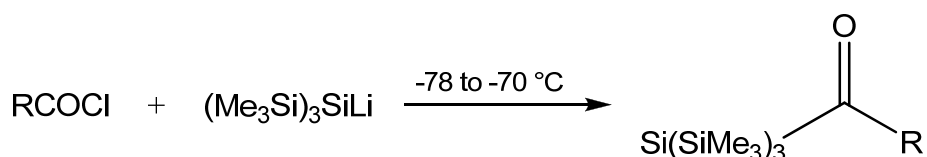
Thus the synthesis of ketones can be achieved in a quick and convenient procedure by the reaction of acid chlorides with organometallic reagents.<sup>59</sup> However, the relative reactivity of the acid chloride, the ketone product and the organometallic reagent can be problematic. These factors have led to much research in the areas of balancing the reactivity of the reactants and ketone products. The high reactivity of acyl chlorides make them ideal examples for exploring the chemistry and reactivity of organometallic reagents.

The reaction between acid chlorides and organometallic reagents, specifically those of Mg, Cd and Zn were reviewed in 1954<sup>60</sup> and many developments in this area of ketone synthesis have since been reported.<sup>61</sup>

The general consensus is that organometallic reagents of the type RNa and RLi react with acid chlorides to give ketones but in low yields. The ketone initially formed is subsequently lost *via* either enolization or 1,2-addition as shown, (**Scheme 1.13**). The formation of tertiary alcohols is the predominant product in said reactions.

Silyl ketones have however been prepared in good yields by the addition of silyllithium reagents to a three-fold excess of acid chloride in THF at low temperatures (**Table 1.3**).<sup>62-</sup>

64



**Scheme 1.13:** Synthesis of silyl ketones from acid chloride

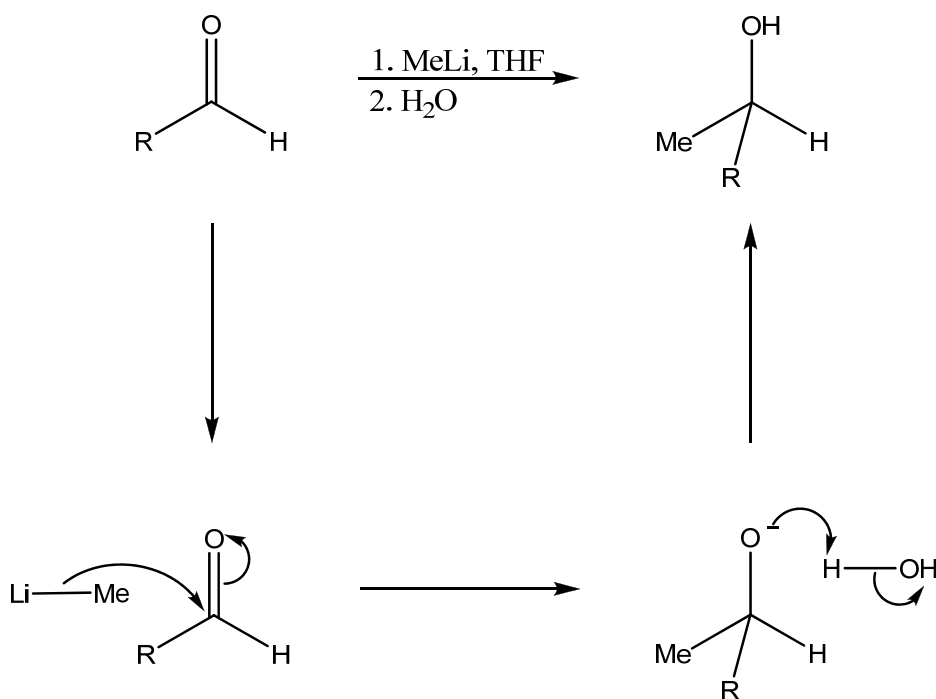
R	RCOCl:silyllithium	Solvent	% Yield
Ph, Me, Me <sub>3</sub> C	3:1	THF	60-70
Et, <sup>i</sup> Pr	1:1	Pentane	54-72

**Table 1.3:** Conditions used for the synthesis of silyl ketones

By using pentane as the solvent, a stoichiometric ratio of acid chloride to silyllithium may be used. The steric bulk of the (R<sub>3</sub>Si)<sub>3</sub>SiLi anions are thought to be the reason for the success of this reaction since zinc silylcuprate reagents are used to prepare silyl ketones.

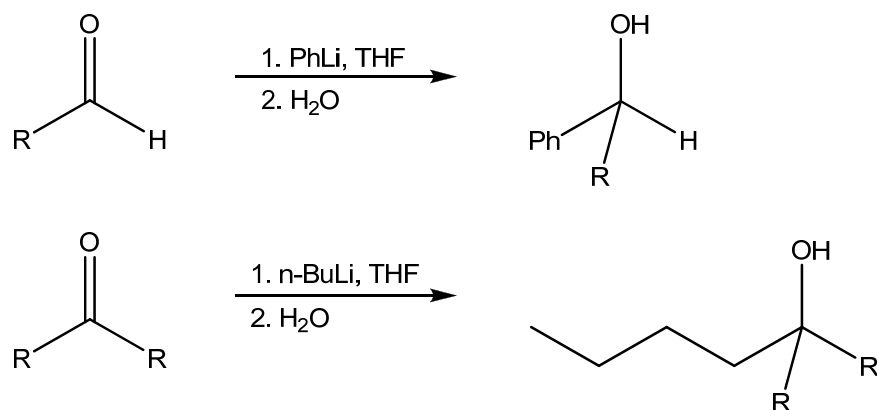
## 1.8 Lithium Reagents and Carbonyl Compounds

The formation of carbon-carbon bonds while introducing a new stereogenic centre can be easily achieved with the use of organometallic reagents.<sup>65</sup> While the reactivity of organolithium reagents may be considered outstanding as nucleophiles they are seldom used in the asymmetric alkylation of carbonyl compounds. This may be due to the large exothermicity of alkyllithium condensation on most electrophiles which tends to outweigh the influence of the relatively small energy differences between diastereomeric transition states.<sup>66</sup> The nucleophilic organometallic reagents attack the electrophilic carbonyl groups on aldehydes and ketones as below in the reaction of methyl lithium with an aldehyde forming the corresponding alcohol.



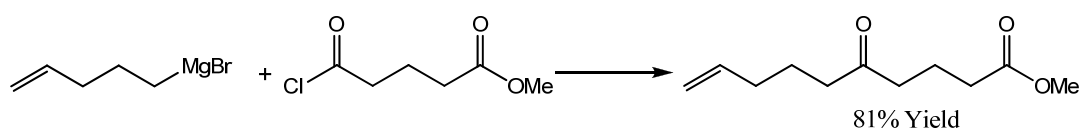
**Scheme 1.14:** Synthesis of alcohols from aldehydes using organolithium reagents

The formation of secondary and tertiary alcohols can be achieved by the reaction of aldehydes or ketones with other organolithium reagents, e.g., n-butyllithium and phenyl lithium.



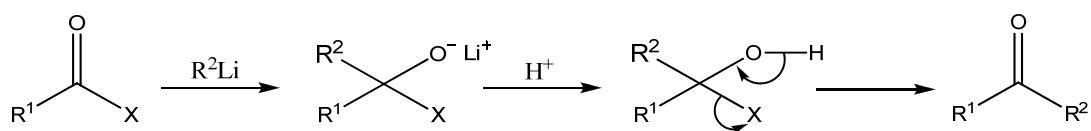
**Scheme 1.15:** Synthesis of secondary and tertiary alcohols using  $RLi$  reagents

Acyl chlorides can be reacted with Grignard reagents to form the following:



**Scheme 1.16:** Reaction of acid chloride and  $RMgX$  in ketone synthesis

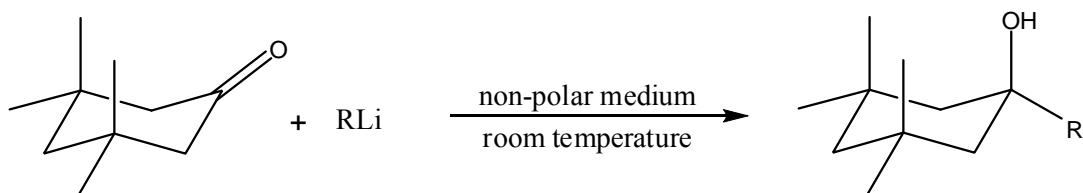
Other viable synthesis of ketones rely on choosing the correct starting material as the tetrahedral intermediate can become stable enough to avoid collapse to the ketone during reaction.<sup>42</sup>



**Scheme 1.17:** Formation of ketones

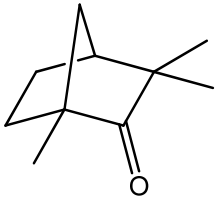
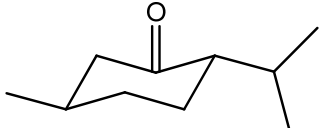
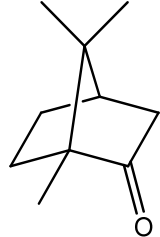
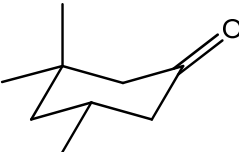
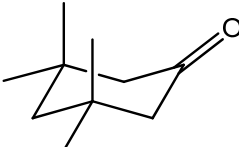
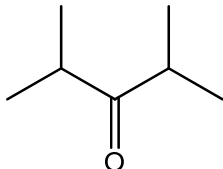
Due to the difficulty of addition of organolithiums to hindered ketones, various methods have been designed to reduce the basicity or increase the nucleophilicity of the

organometallic complex. These methods include transmetalation of the organolithiums or Grignard reagents using cerium or titanium salts.<sup>67</sup> The addition of phenyl lithium to hindered ketones by the use of non-polar media was introduced by Lecomte *et al.* Before this report previous literature described only the addition of phenyllithium to hindered ketones in ethers, diethyl ether and THF, and furthermore only moderate yields were obtained. The ketones used in this study were (-)-fenchone (**1**), (-)-methanone (**2**), (+)-camphor (**3**), 3,3,5-trimethylcyclohexanone (**4**), 3,3,5,5-tetramethylcyclohexanone (**5**) and 2,4-dimethylpentan-3-one (**6**).<sup>68</sup> The expected reaction is illustrated, (**Scheme 1.18**).



**Scheme 1.18:** Alcohol synthesis from the reaction of a ketone with an organolithium reagent

The results illustrate that a non-polar solvent at room temperature provides the best conditions for a high yield, especially in the case of ketones **1**, **2** and **6**, (**Table 1.4**).

	<b>Ketone</b>	<b>Solvent</b>	<b>%Yield</b>	<b>Solvent</b>	<b>%Yield</b>
1		Et <sub>2</sub> O	35-64	Toluene	96
2		Et <sub>2</sub> O	31	Toluene	83
3		Et <sub>2</sub> O	58	Toluene/ Et <sub>2</sub> O 6:4	45
4				Toluene	71
5				Toluene/ Et <sub>2</sub> O 6:4	63
6				Toluene	90

**Table 1.4:** Results obtained from the addition of PhLi to hindered ketones

Other factors that influence the success of the reaction between PhLi and hindered ketones are reaction time, temperature and the order of addition of the organolithium and the ketone.

## 1.9 1,2-Diaroylcyclopentadiene and its Compounds

### 1.9.1 The History of 1,2-Dibenzoylcyclopentadiene

The first reported treatment of metallic derivatives of cyclopentadiene with acid halides was the work of Linn and Sharkey in 1957.<sup>69</sup> Cyclopentadiene was reacted with phenyl lithium and then various aromatic chlorides to form 1-aryl-6-hydroxy-6-arylfulvenes. The structure in **Figure 1.8** was proposed after analysis of the orange crystalline product.

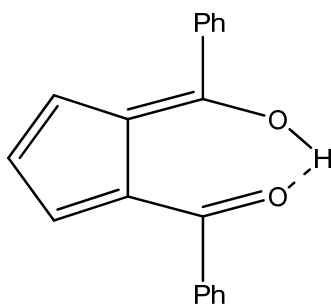
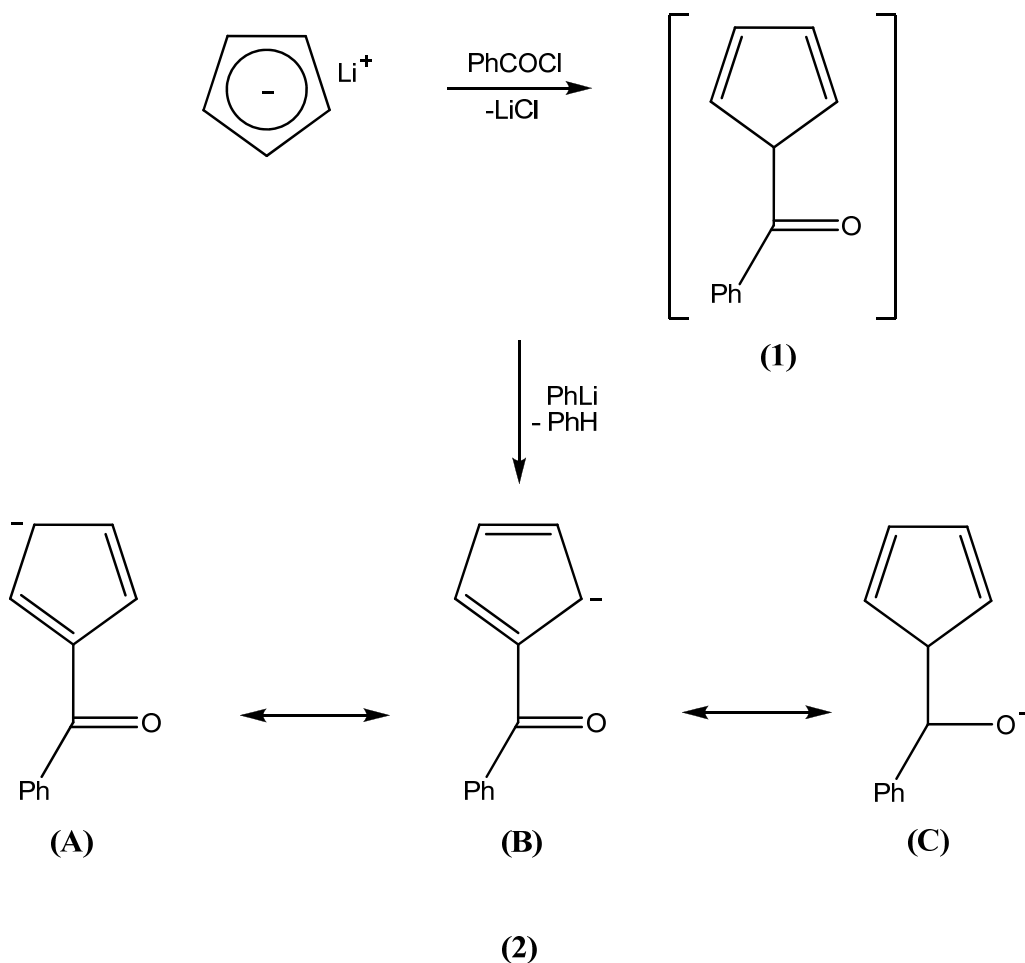


**Figure 1.8:** Structure of 1-aryl-6-hydroxy-6-arylfulvene (1,2-dibenzoylcyclopentadiene, dbzCp)

The highest yield recorded for the reaction was 37%, even after variation of temperature and solvent and inverse addition of the reagents. The reaction product was concluded to be an enol, 1-benzoyl-6-hydroxy-6-phenylfulvene (later named 2,3-dibenzoylcyclopentadiene). <sup>1</sup>H NMR data supported the presence of the chelated proton between the enol and the carbonyl of the benzoyl group. Upon examination of the infrared spectrum Linn and Sharkey observed the absence of absorption in the region usually assigned to carbonyl group. This would be expected from an intramolecularly hydrogen bonded enol structure where the H-bond leads to a large shift in the resultant carbonyl infrared bands. **Scheme 1.19** below outlines the proposed mechanism of formation of the 1,2-disubstituted cyclopentadiene.



**Scheme 1.19:** Proposed mechanism for the formation of 1,2-disubstituted cyclopentadiene

The authors proposed that one mole of cyclopentadienyllithium forms the intermediate **(1)**, which then reacted with the benzoyl chloride. The remaining hydrogen on the allylic carbon is easily removed by a second mole of cyclopentadienyllithium to form the resonance stabilized anion **(B)**. Higher substituted compounds were expected but in fact did not appear. One explanation for this is that the formation of the salt terminates the reaction, (**Figure 1.9**). This salt also explains the formation of the 1,2-substituted product, in which the coordinated lithium directs the incoming benzoyl group to the position adjacent to the first substitution.

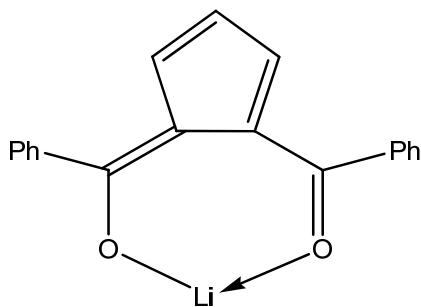
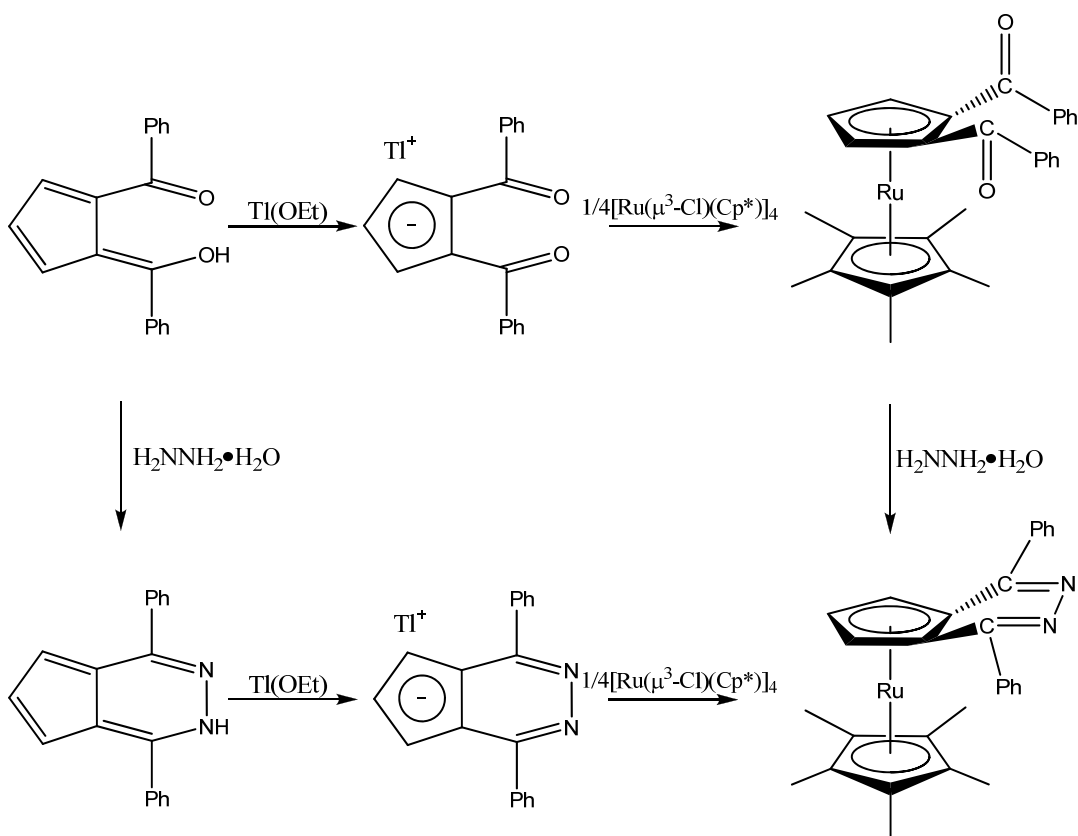


**Figure 1.9:** Proposed structure of salt formed during benzoylation of cyclopentadiene

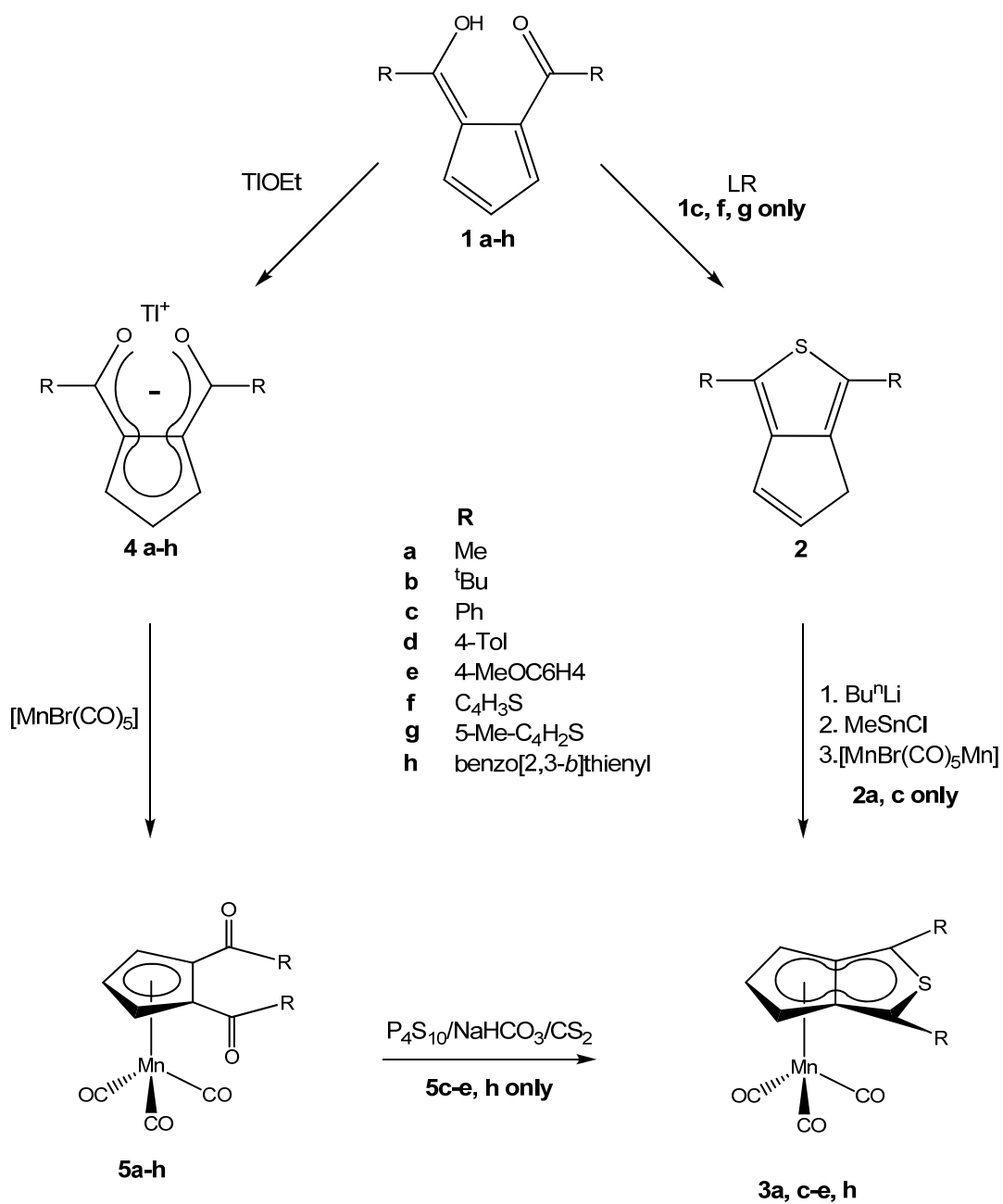
### 1.9.2 Compounds containing the 1,2-dibenzoylcyclopentadienyl ligand

While there are few examples of the use of the 1,2-dibenzoylcyclopentadienyl (dbzCp) ligand in the literature, no effort to date has been made to fully understand the impact the electron withdrawing substituents on the cyclopentadienyl ring have on the metal to which it is bound.<sup>70,71</sup> In 1998 Selegue *et al.* reported the binding of dibenzoylcyclopentadiene (dbzCpH) to ruthenium.<sup>72</sup> The authors included the pentamethylcyclopentadiene ligand to counteract the electronwithdrawing abilities of the dbzCp. This system was then converted to the pyridazine either by direct reaction with hydrazine or by converting the dbzCp to the imine with thallium ethoxide before reaction with the ruthenium complex, (**Scheme 1.20**).



**Scheme 1.20:** Synthesis of 1,2-Dibenzoylruthenocene and a Derived Pyridazine

The manganese analogue was synthesised in later work in the preparation of various manganese cyclopenta[c]thiophenyl complexes.<sup>73</sup> dbzCpH was either first converted to the thiophene and then reacted with  $[\text{MnBr}(\text{CO})_5]$  to form the manganese cyclopenta[c]thiophenyl complex, or converted to the anion with thallium ethoxide and then reacted with  $[\text{MnBr}(\text{CO})_5]$  in benzene and subsequently converted to the cyclopentathiophenyl complex, (**Scheme 1.21**).



*Scheme 1.21: The synthesis of the manganese cyclopenta[*c*]thiophenyl complexes*

## 1.10 The Chemistry of Ferrocene

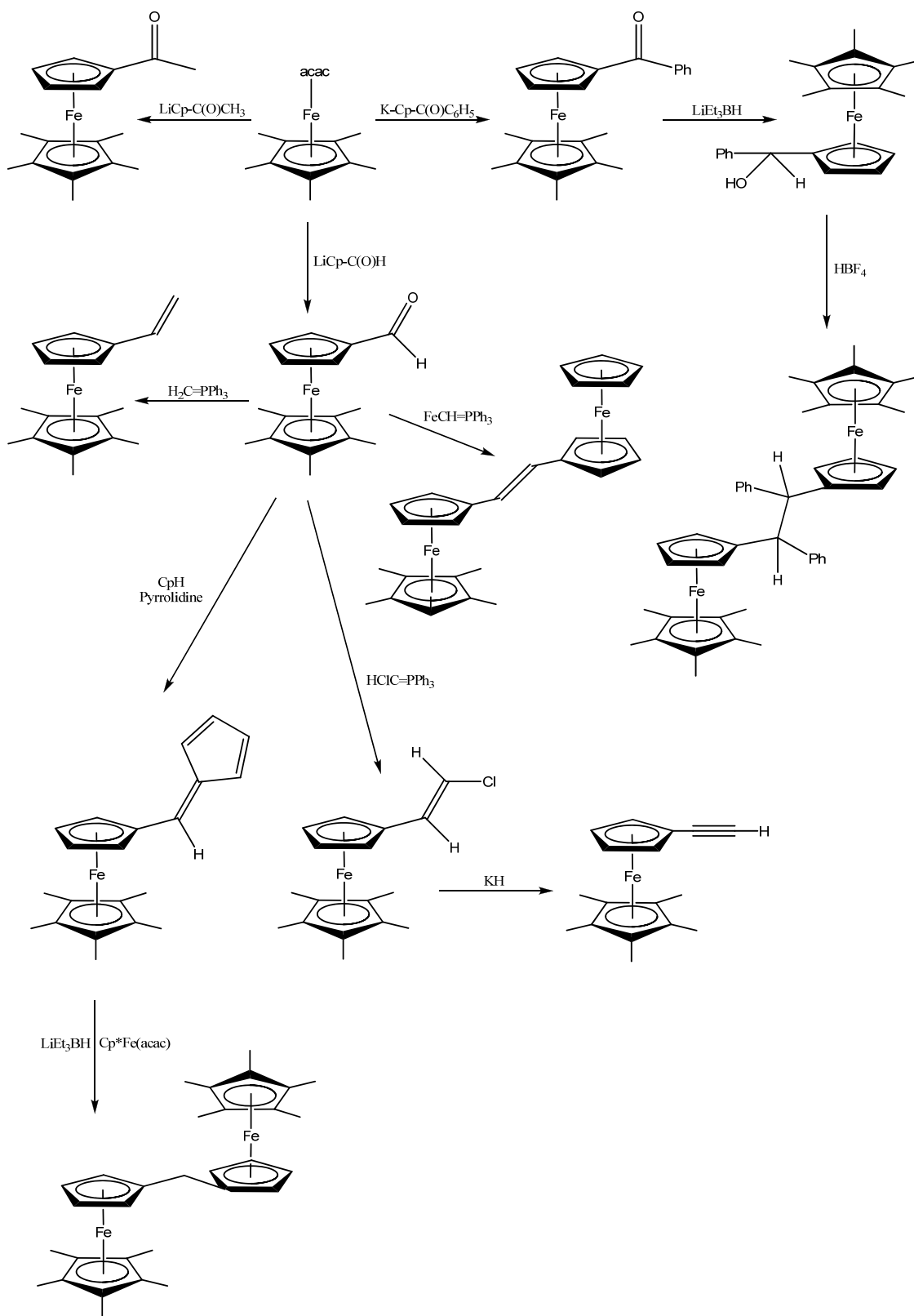
As briefly mentioned earlier, Kealy and Pauson's discovery of ferrocene and the subsequent elucidation of its structure revolutionized the field of organometallic chemistry.<sup>74</sup> There has been extensive investigation into its uses in synthetic procedures and various applications. This arises from its thermal stability and ease of synthesis as well as the strong bonding generally found between metal centers and the cyclopentadienyl ligand. These characteristics have resulted in a vast amount of published research in ferrocene chemistry.<sup>75</sup>

The conversion of ferrocene to its many derivatives is achieved by electrophilic substitution or by reactions involving metalation as the first step.<sup>76</sup> The permethylated derivative (Cp\*), has many advantages over the unsubstituted ligand, including steric bulk, increased electron donicity and solubility.<sup>77</sup> There are two methods employed in the synthesis of the peralkylated derivatives, either the indirect or direct route. In the indirect method the substituent can be introduced by either electrophilic substitution or the use of 1'-metallated pentamethylferrocenes. The direct route proceeds by the formation of the 1'-substituted pentamethylferrocene by the reaction of an appropriately substituted cyclopentadienide with a pentamethylcyclopentadienide-iron (II) complex.

The utilisation of the direct route is preferred in terms of ease of operation and accessibility to different target compounds due to the limitations associated with the indirect route. The limitation of which was illustrated in the difficulty encountered by the authors when attempting the metalation of pentamethylferrocene. Treatment with the regular deprotonating agents (MeLi, *n*-BuLi in hexane, Et<sub>2</sub>O or THF) had no effect and both HMPA and TMEDA were unsuccessful when used as metal chelating solvents.

*n*-butyllithium and potassium *t*-butoxide eventually led to the deprotonation and subsequent carboxylation of pentamethylferrocene, and the synthesis of 1,2,3,4,5-pentamethyl-1'-carboxylic acid was hereafter achieved. However, other attempted reactions failed to proceed to completion, for example, 1'-chloropentamethylferrocene could not be isolated when hexachloroethane was used as a halogenating agent.<sup>77</sup>

After the limitations incurred by employment of the indirect route, the second, direct route **(B)** was investigated. The difference in ease of reaction between the two routes can be illustrated by the formation of pentamethylferrocenyl aldehyde. Using the indirect route **(A)** a 35% yield was obtained after the reaction of pentamethylferrocene with DMF. This compound was more conveniently achieved by route **(B)** in the one pot synthesis of preformed formylcyclopentadienide with lithiated pentamethylcyclopentadiene and iron (II) bis (acetylacetonate) at  $-80^{\circ}\text{C}$ .<sup>78,79</sup>



**Scheme 1.22:** Synthesis of compounds using the direct route to substituted ferrocenes

Substituted cyclopentadienide ions, which will potentially form sandwich complexes upon reaction with ferrous chloride, may be prepared by the action of lithiating agents or sodium on fulvenes highlight the importance of fulvenes in synthetic chemistry. Acylcyclopentadienes may be considered fulvenoid compounds in that enolization of these systems produce hydroxyfulvenes. Diaroylcyclopentadienes readily form salts with strong bases thus producing a possible route to tetraaroylferrocenes upon reaction with ferrous ions. However Little *et al.* could not achieve this despite preparing salts of dbzCpH using different basic conditions.<sup>80</sup> The authors proposed that the  $\pi$ -electrons in the dibenzoylcyclopentadienide were too localized for effective sandwich bonding in order to explain their defeat.

## Chapter 2 Carbonyl Substitution Reactions

### 2.1 Transition Metal Carbonyls

#### 2.1.1 The Carbonyl Ligand

Schützenberger's synthesis of  $\text{PtCl}_2(\text{CO})_2$  in 1868 was the starting point for metal carbonyl synthesis and since then the carbonyl ligand (CO) has become ubiquitous in organometallic chemistry.<sup>81</sup> Mond's accidental synthesis of nickel tetracarbonyl was another milestone in organometallics.<sup>82</sup> Although clearly not the first transition metal carbonyl species reported, the remarkable properties and industrial importance of the discovery gained much attention. Since then transition metal carbonyl complexes have become one of the most important families of compounds in organometallic chemistry.<sup>83</sup> The importance of the CO ligand is due to its  $\pi$ -acid nature. It is capable of accepting metal  $d_\pi$  electrons by back bonding from the metal  $d_\pi$  orbitals to its empty  $\pi^*$  orbitals, (*Figure 2.1*).

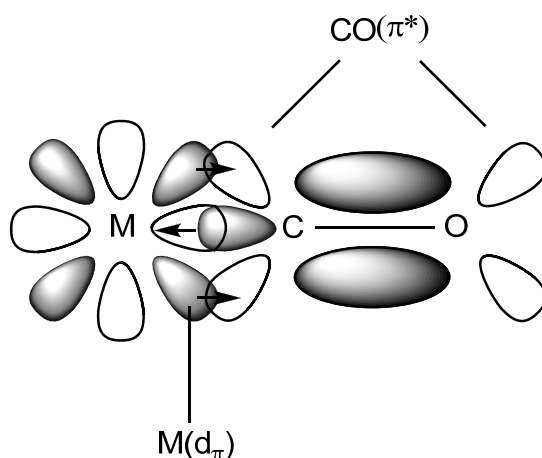


**Figure 2.1:** Back bonding in MCO fragment

Although the CO  $\pi^*$  antibonding orbitals are high energy CO orbitals, they are able to stabilize the metal  $d_\pi$  orbitals. The consequence of this is that the ligand field splitting parameter rises and also back bonding allows electron density on the metal to reduce as it makes its way back to the ligands.

Thus the CO HOMO donates electrons to an empty  $M(d_\sigma)$  orbital while the filled  $M(d_\pi)$  back donates to the CO LUMO. This synergic scheme leads to a polarization of the CO on binding as the electrons donated by the HOMO removes electron density from the

carbon and donation to the LUMO increases electron density both at C and O. This polarization, modulated by the other ligands attached to the metal and the overall charge on the complex, chemically activates the ligand and makes the carbon more susceptible to nucleophilic attack and the oxygen more susceptible to electrophilic attack. In  $L_nM(CO)$  the carbon of the CO will be acutely  $\delta^+$  in character should the ligand groups be good  $\pi$  acids or the complex cationic (e.g.,  $Mo(CO)_6$ ,  $[Fe(CO)_6]^{2+}$ ), as the CO-to-metal  $\sigma$ -donor electron transfer will be enhanced at the expense of the metal-to-CO back-donation (**Figure 2.2**).

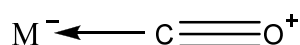


**Figure 2.2:** CO acting as a pure  $\sigma$  donor.

If the L groups are good donors or the complex is anionic (e.g.,  $[WCp_2(CO)]$ ,  $[V(CO)_6]^-$ ), back donation will be encouraged and the carbon of the CO will lose its pronounced  $\delta^+$  and instead the oxygen of the CO will become significantly  $\delta^-$  (**Figure 2.3**).

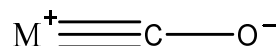


**Figure 2.3:** Both  $\pi^*_{px}$  and  $\pi^*_{py}$  involved in M–CO back bonding.

This versatile nature of the CO ligand leads to a range of bonding modes in metal carbonyl cluster chemistry, (**Figure 2.4**). The most prevalent bonding mode in metal carbonyls is the terminal mode. However bridging between two ( $\mu_2$ ) and three ( $\mu_3$ ) metals is also common. The CO bond is further weakened in these bridge bonding modes due to increased  $\pi$ -bonding resulting from back donation from more metal centers.<sup>84</sup>

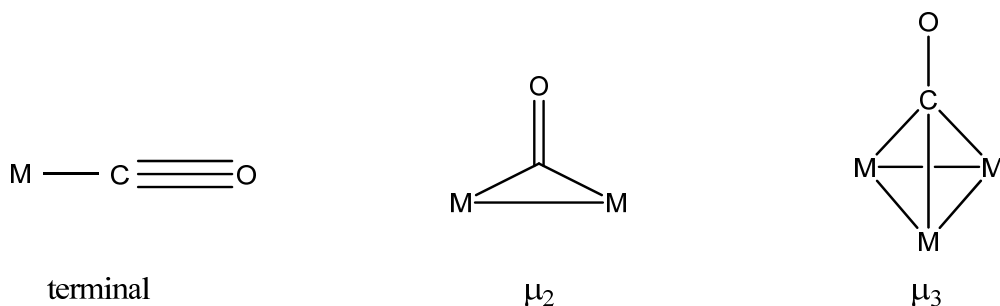
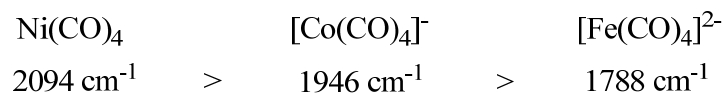


**Figure 2.4:** Most common bonding modes in metal carbonyls

### 2.1.2 Carbonyl Stretching Frequencies

Studies of the carbonyl stretching frequencies of metal carbonyl complexes provide valuable information about structure and bonding.  $\nu_{\text{MC-O}}$  is not obscured by the presence of other vibrations and is generally free from coupling with other modes. Most metal carbonyls exhibit sharp  $\nu_{\text{MC-O}}$  bands between  $\sim 2100 - 1800 \text{ cm}^{-1}$  and the  $\nu(\text{CO})$  for free CO is  $2155 \text{ cm}^{-1}$ .<sup>84</sup> The bonding mode of the CO and the electronic density on the metal dictates the position of the carbonyl bands in the IR. The number and intensity of the carbonyl bands observed depends on the multiple natures of the M-CO bond, In general, the terminal  $\nu_{\text{MC-O}}$  is higher than the bridging  $\nu_{\text{MC-O}}$  and the  $\nu_{\text{MC-O}}$  is lowered as the negative charge on the metal carbonyl increases, for example;



Equally, as the negative charge decreases on the metal,  $\nu_{\text{MC-O}}$  shifts to a higher frequency as the  $\sigma$ -bonding becomes more predominant and  $\pi$ -backbonding decreases.<sup>85-</sup>

<sup>87</sup> An extreme example of this being the increase of  $\sim 200 \text{ cm}^{-1}$  upon going from  $(\text{Pt(CO)}_4)$  ( $2054 \text{ cm}^{-1}$ ) to  $[\text{Pt(CO)}_4]^{2+}$  ( $2281, 2257$  and  $2235 \text{ cm}^{-1}$ ).<sup>88,89</sup> Vibrational spectroscopy has been widely used to study the effects of the substitution of a CO ligand for others, most notably halogens, phosphorus and cyclopentadienyl ligands (**Table 2.1**). The substitution of a halogen for a CO results in a higher  $\nu_{\text{MC-O}}$  than the parent complex due to the increased positive charge on the metal. However, if CO is replaced by a phosphine the  $\nu_{\text{MC-O}}$  decreases since phosphine ligands are strong  $\sigma$ -donors and poor  $\pi$ -acceptors.

Compound	State/Solvent	$\nu_{MC-O}$ $cm^{-1}$	Reference
[TiCp <sub>2</sub> (CO) <sub>2</sub> ]	Solid	1969, 1890	90
[TiCp* <sub>2</sub> (CO) <sub>2</sub> ]	Heptane	1940, 1860	91
[VCp(CO) <sub>4</sub> ]	<i>n</i> -heptane	2029, 1932	92
[VCp*(CO) <sub>4</sub> ]	<i>n</i> -heptane	2015, 1917	92
[VCp(CO) <sub>3</sub> PPh <sub>3</sub> ]	hexane	1960, 1865	93
[CrCp(CO) <sub>3</sub> D]	Solid	2020, 1934	90
[CrCp*(CO) <sub>3</sub> D]	Toluene	1995, 1260	94
[MoCp(CO) <sub>3</sub> H]	Solid	2028, 1934	90
[MoCp*(CO) <sub>3</sub> H]	Heptane	2015, 1936	95
[MoCp(CO) <sub>3</sub> Cl]	Solid	2062, 1992, 1965	90
[MoCp*(CO) <sub>3</sub> Cl]	Nujol	2030, 1965, 1945	96
[MoCp(CO) <sub>2</sub> ClPPh <sub>3</sub> ]	CHCl <sub>3</sub>	1975, 1885	97
[MoCp*(CO) <sub>2</sub> ClPPh <sub>3</sub> ]	DCM	1948, 1863	98
[MoCp(CO) <sub>3</sub> Br]	CHCl <sub>3</sub>	2050, 1980	97
[MoCp(CO) <sub>2</sub> BrPPh <sub>3</sub> ]	CHCl <sub>3</sub>	1980, 1890	97
[MoCp*(CO) <sub>3</sub> Br]	THF	2039, 1940	99
[MoCp(CO) <sub>3</sub> I]	CHCl <sub>3</sub>	2045, 1975	97
[MoCp(CO) <sub>2</sub> IPPh <sub>3</sub> ]	CHCl <sub>3</sub>	1972, 1890	97
[WCp(CO) <sub>3</sub> ] <sub>2</sub>	Solid	1965, 1866	90
[WCp*(CO) <sub>3</sub> ] <sub>2</sub>	<i>n</i> -tetradecane	1920, 1893	100
[WCp(CO) <sub>3</sub> H]	Solid	2024, 1927	90
[WCp*(CO) <sub>3</sub> H]	Nujol	2008, 1919	101
[WCp(CO) <sub>3</sub> I]	CHCl <sub>3</sub>	2040, 1960	97
[WCp(CO) <sub>2</sub> IPPh <sub>3</sub> ]	CHCl <sub>3</sub>	1960, 1860	97
[MnCpMn(CO) <sub>3</sub> ]	Solid	2017, 1916	102
[MnCp*(CO) <sub>3</sub> ]	Solid	2004, 1910	103
[FeCp(CO) <sub>2</sub> Cl]	DCM	2053, 2007	104
[FeCp(CO)ClPPh <sub>3</sub> ]	DCM	1959	105
[FeCp*(CO) <sub>2</sub> Cl]	CCl <sub>4</sub>	2030, 1980	106
[FeCp(CO) <sub>2</sub> I]	DCM	2041, 1996	104
[FeCp(CO) <sub>2</sub> I]	<i>n</i> -heptane	2041, 2002	107
[Fe( $\eta^5$ -C <sub>5</sub> H <sub>4</sub> Me)(CO) <sub>2</sub> I]	CCl <sub>4</sub>	2039, 2000	108
[Fe( $\eta^5$ -C <sub>5</sub> H <sub>4</sub> Me)(CO)IPPh <sub>3</sub> ]	CHCl <sub>3</sub>	1950	109
[FeCp*(CO) <sub>2</sub> I]	DCM	2019, 1971	110
[RuCp(CO) <sub>2</sub> I]	<i>n</i> -heptane	2049, 2004	107
[RuCp(CO) <sub>2</sub> I]	DCM	2048, 2000	111
[RuCp(CO)IPPh <sub>3</sub> ]	DCM	1950	112
[RuCp*(CO) <sub>2</sub> I]	DCM	2030, 1981	113
[Ru( $\eta^5$ -C <sub>5</sub> Me <sub>4</sub> Et)(CO)IPPh <sub>3</sub> ]	DCM	1940	19

**Table 2.1:**  $\nu_{MC-O}$  of some metallocene complexes demonstrating the effects of substituents on the ring or the metal

The number of CO bands observed in the  $\nu_{\text{MC-O}}$  IR spectrum depends on the local symmetry of the  $\text{M}(\text{CO})_n$  group.<sup>90</sup>  $[\text{FeCp}_2(\text{CO})_2]$  was originally thought to contain two  $\pi$ -bonded Cp rings, however upon further examination using IR and NMR it was found that one ring is  $\pi$ -bonded and the other  $\sigma$ -bonded to the metal.<sup>114,115</sup> X-ray analysis later confirmed this structure and this complex was one of the first ring whizzers to be characterised.<sup>116</sup>

The study of  $[\text{FeCp}(\text{CO})_2]_2$  proved at the time to be somewhat controversial. In the solid state it adopts either the *trans*-bridged or the *cis*-bridged structure.<sup>117-119</sup> The *cis*-isomer shows two terminal (1975 and 1933  $\text{cm}^{-1}$ ) and two bridging (1801 and 1766  $\text{cm}^{-1}$ ) bands. In solution the non-centrosymmetric *cis* structure **(A)** was argued to be the dominant species in hexane solutions along with trace amounts of the non-bridged isomer, **(B)**.<sup>33</sup> Cotton and co-workers demonstrated that the IR spectra are solvent dependant in the 1700-2100  $\text{cm}^{-1}$  regions.<sup>120</sup> However, Manning then argued that this was also true in other regions of the IR spectrum, e.g. the 500-700  $\text{cm}^{-1}$  and the 3500-4000  $\text{cm}^{-1}$  regions. He proposed an equilibrium involving the four isomers of **(A)**- **(D)** below.<sup>121</sup> This was supported by low temperature  $^1\text{H}$  NMR studies.<sup>120</sup>

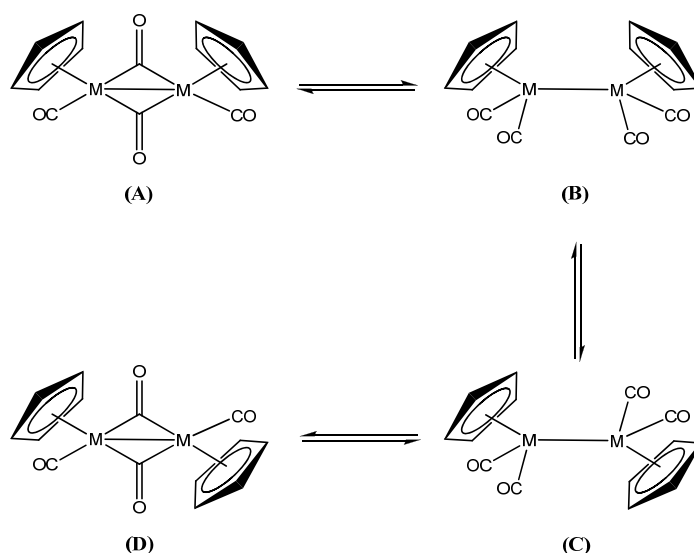


**Figure 2.5:** Behaviour of  $(\eta^5\text{-C}_5\text{H}_5)\text{M}(\text{CO})_2$  in solution

It is now accepted that the iron dimer in solution exists in a solvent dependant *cis-trans* equilibrium, the ratio of which increases with increasing polarity of solvent. The ruthenium analogue,  $[\text{RuCp}(\text{CO})_2]_2$  was also investigated by Manning and McArdle.<sup>122</sup> In

this case the proportion of the non-bridged forms **(B)** and **(C)** were much greater, especially in non-polar solvents.

The bridging CO groups of  $[\text{FeCp}(\text{CO})_2]_2$  can form an adduct with trialkylaluminium.<sup>123</sup> This would imply that the basicity of the bridging groups is greater than that of the terminal groups.

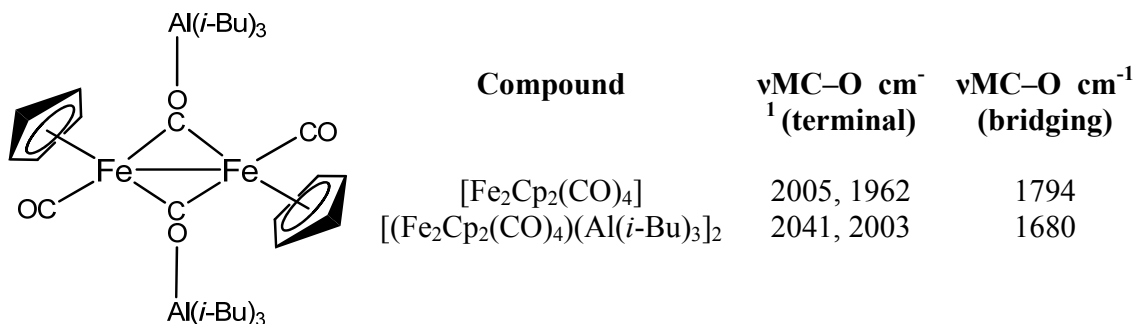


**Figure 2.6:**  $(\text{Cp}_2\text{Fe}_2(\text{CO})_4)(\text{Al}(i\text{-Bu})_3)_2$  adduct and the effects on  $\nu_{\text{MC-O}}$

Bor carried out an investigative study into solvent effects on the infrared spectra of metal carbonyls in 1961.<sup>124</sup> The results for  $\text{Co}(\text{CO})_3\text{NO}$  show that whereas there is only a slight difference in frequency compared with the value measured in *n*-hexane, the half band width values show a considerable increase in halogenated, aromatic and polar solvents, (**Table 2.2**).

Solvent	Band of the <i>A<sub>1</sub></i> vibration				Band of the <i>E</i> vibration			
	$\nu_{\text{MC-O}}$	$\nu_{\text{vap}} - \nu_{\text{sol}}$	$\nu_{\text{sol}} - \nu_{\text{hexane}}$	Half band width (found)	$\nu_{\text{MC-O}}$	$\nu_{\text{vap}} - \nu_{\text{sol}}$	$\nu_{\text{sol}} - \nu_{\text{hexane}}$	Half band width (found)
				$\Delta \nu^{(a)}_{1/2}$				$\Delta \nu^{(a)}_{1/2}$
Vapour	2108.0	-	-	-	2046.8	-	-	-
Cyclohexane	2100.4	7.6	-0.8	3.5	2034.1	12.7	-1.3	4.3
n-hexane	2101.2	6.8	-	3.7	2035.4	11.4	-	4.8
n-heptane	2101.1	6.9	-0.1	3.8	2035.1	11.7	-0.3	5.0
Cyclohexene	2100.2	7.8	-1.0	3.8	2033.4	13.4	-2.0	7.0
CS <sub>2</sub>	2098.2	9.8	-3.0	4.1	2030.8	16.0	-4.6	7.7
C <sub>2</sub> Cl <sub>4</sub>	2100.1	7.9	-1.1	4.0	2032.8	14.0	-2.6	8.5
CCl <sub>4</sub>	2100.8	7.2	-0.4	4.2	2034.1	12.7	-1.3	9.6
Et <sub>2</sub> O	2102.8	5.2	1.6	5.8	2035.7	11.1	0.3	16.6
Toluene	2100.7	7.3	-0.5	5.7	2032.1	14.7	-3.3	19.0
Acetonitrile	2104.4	3.6	3.2	7.8	2035.0	11.8	0.4	19.5
EtOH	2103.0	5.0	1.8	6.8	2035.7	11.1	0.3	19.7
Benzene	2101.1	6.9	-0.1	6.3	2032.8	14.0	-2.6	20.1
Chloroform	2101.3	6.7	0.1	6.6	2034.7	12.1	-0.7	21.9
THF	2101.9	6.1	0.7	7.9	2032.6	14.2	-2.8	23.1
Acetone	2104.2	3.8	3.0	7.8	2035.1	11.7	-0.3	23.5
C <sub>2</sub> H <sub>2</sub> Cl <sub>2</sub>	2101.3	6.7	0.1	7.4	2032.5	14.3	-2.9	23.9
2-butanone	2103.7	4.3	2.5	8.0	2035.1	11.7	-0.3	24.5

**Table 2.2:** Solvent effects on the frequency and half band width of C≡O stretching bands of Co(CO)<sub>3</sub>NO (all values in cm<sup>-1</sup>)

## 2.2 Tertiary Phosphine Ligands

Phosphines are generally spectator rather than actor ligands. The importance of tertiary phosphines,  $\text{PR}_3$ , arises from their ability to alter their electronic and steric properties in a systematic and predictable way over a wide range of varying R.

$\text{PR}_3$  ligands have a lone pair of electrons on the phosphorus atom which can be donated to a metal. The extent of their  $\pi$  acidity depends on the nature of the R groups present on the  $\text{PR}_3$  ligand. In the case of  $\text{PF}_3$  the  $\pi$  acidity is as great as that of the CO ligand. Aryl, dialkylamino and alkoxy groups are successively more  $\pi$  acidic and for alkyl phosphines the  $\pi$  acidity is weak. The order of increasing  $\pi$ -acid character is:



Unlike the CO ligand, both the  $\sigma^*$  and d-orbitals of the P–R bonds act as the acceptor in  $\text{PR}_3$ .<sup>125,126</sup>

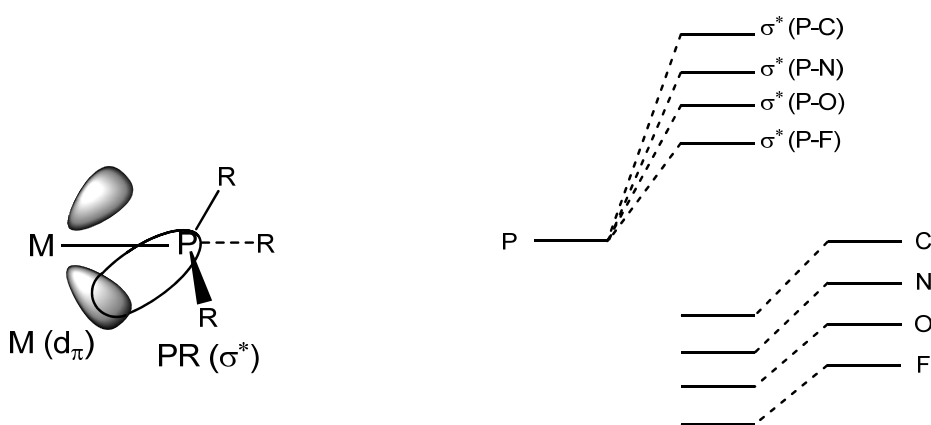


**Figure 2.7:**  $\sigma^*$  MO of a P–R ligand acting as acceptor in metal complexes of  $\text{PR}_3$

The more electronegative the R group, the more stable the orbital the R fragment uses to bond to the phosphorus becomes. This coupled with an increasing contribution of the phosphorus to the  $\sigma^*$  and the increasing size of the  $\sigma^*$  pointing towards the metal make the empty  $\sigma^*$  more accessible for back donation. This occupation of the P–R  $\sigma^*$  by back bonding from the metal would imply a shortening of the P–R upon binding. However,

this is masked by the decrease in P(lone pair)–R(bonding pair) repulsions arising from the shortening of the P–R bond due to donation of the P lone pair to the metal.

Tolman measured the effects of changing the R group on various PR<sub>3</sub> ligands, (L), by comparing the  $\nu_{\text{MC-O}}$  frequencies of a series of complexes of the type LNi(CO)<sub>3</sub>.<sup>127</sup> The  $\nu_{\text{MC-O}}$  stretching frequency is lowered on the nickel complexes containing stronger donating phosphine ligands. These ligands increase the electron density on the metal centre thus increasing electron donation to the CO *via* back bonding.

L	$\nu_{\text{MC-O}}$ (cm <sup>-1</sup> )	$\Delta\nu_{\text{MC-O}}$ (cm <sup>-1</sup> )
P( <i>p</i> -Tol) <sub>3</sub>	2066.7	
P( <i>o</i> -Tol) <sub>3</sub>	2066.6	0.1
PMe <sub>3</sub>	2064.1	2.4
Pet <sub>3</sub>	2061.7	2.5
P( <i>i</i> -Pr) <sub>3</sub>	2059.2	3.1
P( <i>t</i> -Bu) <sub>3</sub>	2056.1	

**Table 2.3:** CO stretching frequencies of compounds of Ni(CO)<sub>3</sub>PR<sub>3</sub>

The variable steric size of the R group on the PR<sub>3</sub> is also an important feature of the ligand. CO ligands are small and so can bind as necessary to form an 18-electron complex, this however is not easily accomplished with respect to phosphine ligands. The larger the R group attached to the PR<sub>3</sub> the less ligands that can attach to the metal. For example, Pt(PCy<sub>3</sub>)<sub>2</sub> and [Rh(PPh<sub>3</sub>)<sub>3</sub>]<sup>+</sup>. These complexes are both unsaturated and yet stabilized by the bulky phosphine ligands.

## 2.3 Substitution Reactions

### 2.3.1 The 16 and 18-Electron Rules

Tolman reported his 16 and 18 Electron Rules in organometallic chemistry in 1972.<sup>128</sup> This was an expansion of existing 18-electron rule concepts. He organized the various types of organometallic reactions involved in catalysis systematically. His system may be used to predict restrictions to organometallic compounds and the type of reactions they may undergo. He proposed that:

1. Diamagnetic organometallic complexes of transition metals may exist in a significant concentration at moderate temperatures if the metal's valence shell contains 16 or 18 electrons.
2. Organometallic reactions, including catalytic ones, proceed by elementary steps involving only intermediates with 16 or 18 metal valence electrons.

Reactions directly involving the transition metal were broken down into five elementary reactions, each with a microscopic reverse. He classified the reactions based upon the changes in the number of metal valence electrons ( $\Delta NVE$ ), formal oxidation state ( $\Delta OS$ ) and co-ordination number ( $\Delta N$ ), (**Table 2.4**). Reactions **1** and **2** involve dissociation and association of ligands whereas **3-5** involve reactions between co-ordinated ligands. CO is classified as a Lewis base ligand as it contributes a pair of electrons to the metal valence shell whereas Lewis acid ligands, such as  $H^+$  and  $BF_3$ , do not contribute any valence electrons. The term "oxidative addition" is used to describe a reaction in which the formal oxidation state of the metal and the co-ordination number increase by either one or two.<sup>129</sup> "Oxidative coupling" is used to denote reactions such as the one in **Figure 2.8** below in which the formal oxidation state of the metal increases by two but the co-ordination number does not change.

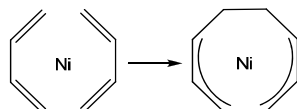
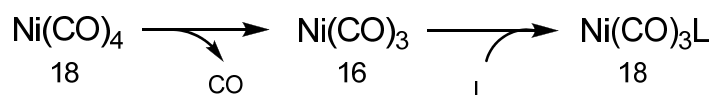


**Figure 2.8:** Oxidative addition

Reaction	$\Delta NVE$	$\Delta OS$	$\Delta N$	16/18	Example	Reverse Reaction	$\Delta NVE$	$\Delta OS$	$\Delta N$	16/18
1 Lewis acid ligand dissociation or	0	0	-1	18/16	$[\text{RhCp}(\text{C}_2\text{H}_4)_2\text{SO}_2] \rightleftharpoons \text{SO}_2 + [\text{RhCp}(\text{C}_2\text{H}_4)_2]$ $\text{HCo}(\text{CO})_4 \rightleftharpoons \text{H}^+ + \text{Co}(\text{CO})_4^-$	Lewis acid association	0	0	+1	16/18
	0	-2	-1			Lewis base association	0	+2	+1	
2 Lewis base ligand dissociation	-2	0	-1	18	$\text{NiL}_4 \rightleftharpoons \text{NiL}_3 + \text{L}$	Lewis base association	+2	0	+1	16
3 Reductive elimination	-2	-2	-2	18	$\text{H}_2\text{IrCl}(\text{CO})\text{L}_2 \rightleftharpoons \text{H}_2 + \text{IrCl}(\text{CO})\text{L}_2$	Oxidative addition	+2	+2	+2	16
4 Insertion	-2	0	-1	18	$\text{MeMn}(\text{CO})_5 \rightleftharpoons \text{MeCOMn}(\text{CO})_4$	Deinsertion	+2	0	+1	16
5 Oxidative coupling	-2	+2	0	18	$(\text{C}_2\text{F}_4)_2\text{Fe}(\text{CO})_3 \rightleftharpoons$ $\begin{array}{c} \text{F}_2 \\   \\ \text{F}_2\text{C} - \text{C} \\   \quad \diagup \\ \text{F}_2\text{C} - \text{C} \\   \\ \text{F}_2 \end{array} \text{Fe}(\text{CO})_3$	Reductive decoupling	+2	-2	0	16

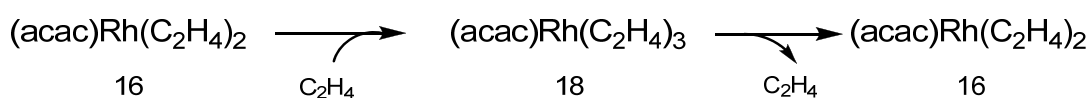
**Table 2.4:** Elementary organometallic reactions

Tolman's 16 and 18-Electron Rule restricts the types of reaction that a particular complex can undergo. It states that Lewis base ligand dissociation is restricted to 18-electron complexes and Lewis base association reactions to 16-electron complexes. Examples include exchange of CO from Ni(CO)<sub>4</sub> by L = CO or PPh<sub>3</sub>, (**Scheme 2.1**)<sup>130</sup>



**Scheme 2.1:** The dissociative pathway of CO substitution in Ni(CO)<sub>4</sub>

Cramer observed that [Rh(acac)(C<sub>2</sub>H<sub>4</sub>)<sub>2</sub>] exchanges ethylene rapidly whereas [RhCp(C<sub>2</sub>H<sub>4</sub>)<sub>2</sub>] is very inert to exchange exactly as Tolman's rule requires.<sup>131</sup> The 16-electron acetylacetonate complex exchanges *via* the associative mechanism, (**Scheme 2.2**), but for the 18-electron [RhCp(C<sub>2</sub>H<sub>4</sub>)<sub>2</sub>] complex the associative pathway is not possible.



**Scheme 2.2:** The associative pathway of CO substitution in Ni(CO)<sub>4</sub>

### 2.3.2 The Dissociative (D) Mechanism

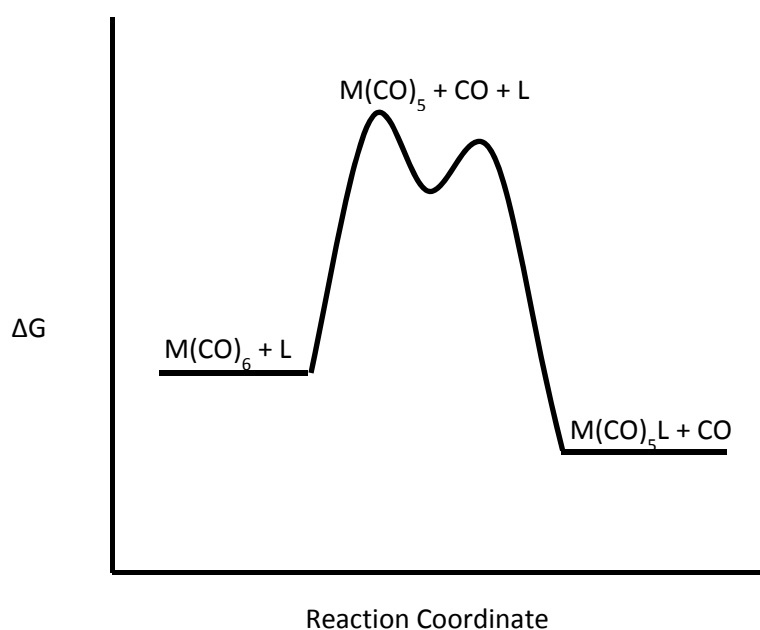
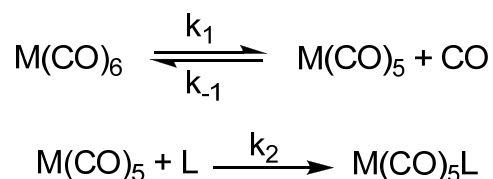


**Figure 2.9:** Free energy diagram for the dissociative mechanism

Carbonyl substitution by phosphines was one of the first organometallic substitution reactions studied.<sup>132,133</sup>

For an octahedral  $M(\text{CO})_6$  substrate:



**Scheme 2.3:** *The dissociative mechanism for  $M(\text{CO})_6$*

The rate determining step in the dissociative mechanism involves an initial loss of CO which generates a vacant site at the metal. This is then filled by the incoming ligand, L.

The rate law is:

$$\text{Rate} = \frac{k_1 k_2 [M(\text{CO})_6][\text{L}]}{k_{-1}[\text{CO}] + k_2[\text{L}]} \quad (1)$$

This reduces to when  $k_2[\text{L}] \gg k_{-1}$ :

$$\text{Rate} = k_1 [M(\text{CO})_6] \quad (2)$$

Should the reaction proceed *via* an associative mechanism the intermediate formed would be a 20-electron species. Although 20-electron transition metal species are not forbidden, nickelocene being a well-known example, the 16-electron intermediate offers a lower energy path in most cases.<sup>134</sup> These reactions are similar to the  $S_N1$  mechanism of alkyl halides and the entropy of activation for the dissociative reactions is positive.

The octahedral geometry of the complex can be retained if the intermediate adopts a square pyramidal geometry **(A)**, (**Figure 2.10**). Should the intermediate adopt a trigonal bipyramidal geometry the stereochemistry will be lost as the incoming ligand may attack at three different places in the equatorial plane as in **(B)**.

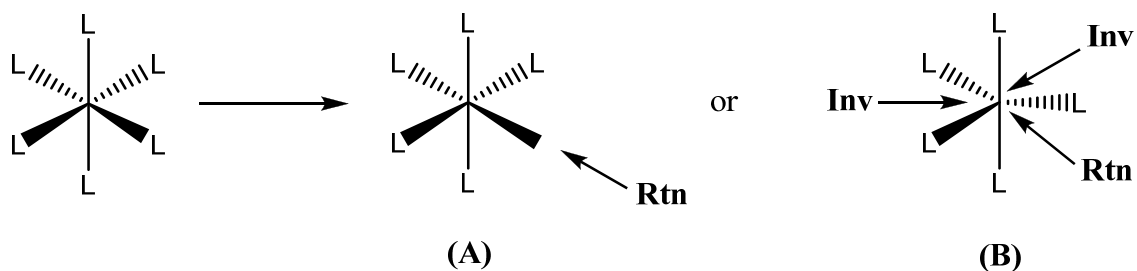


**Figure 2.10:** (A) Retention (**Rtn**) of stereochemistry or (B) retention or inversion (**Inv**) of stereochemistry in octahedral complexes

Substitution rates generally change in the order of third row < second row > first row and are dependent on the metal within a row.<sup>135,136</sup>

### 2.3.3 The Associative (A) Mechanism

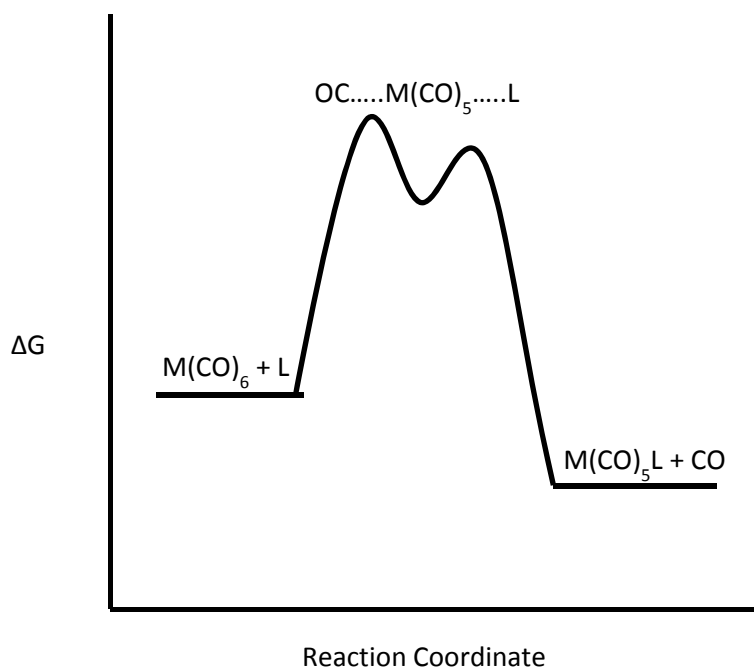
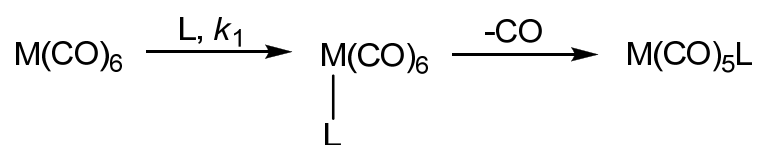


**Figure 2.11:** Free energy diagram for the associative mechanism

The rate determining step in the association mechanism is the attack of the incoming ligand to form an intermediate followed by the rapid loss of CO.<sup>137</sup>



**Scheme 2.4:** The associative mechanism for  $\text{M}(\text{CO})_6$

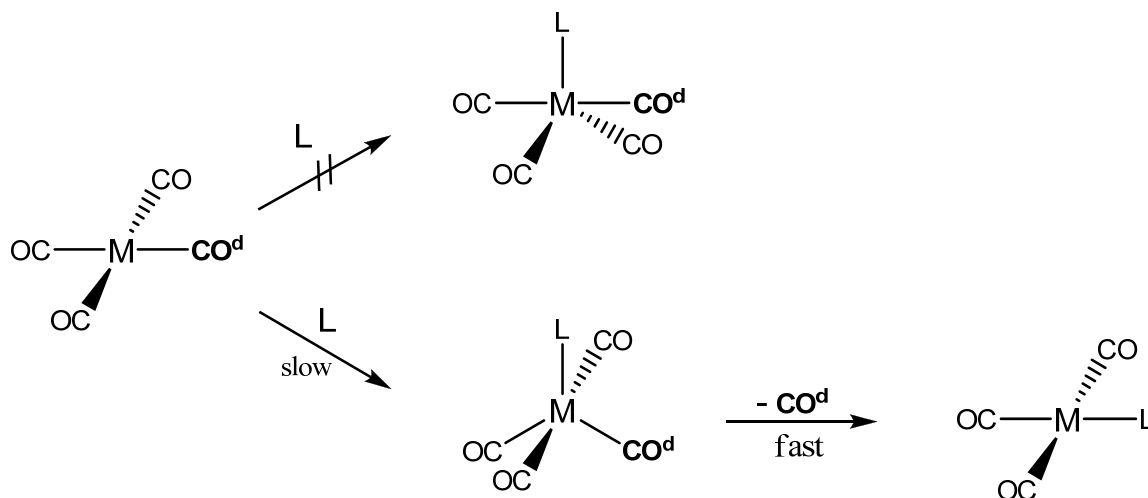
The rate of the overall process is:

(3)

$$\text{Rate} = k_1[\text{M}(\text{CO})_6][\text{L}]$$

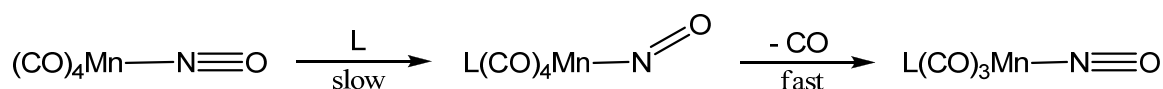
When adopted by a 16-electron complex the 18-electron intermediate offers a lower energy path than a 14-electron intermediate.<sup>138</sup> The reactions are similar to the  $\text{S}_{\text{N}}2$  substitution reactions of alkyl halides and the entropy of activation is negative.<sup>139</sup>

16-electron square planar complexes associative reactions, such as those of Pt(II) or Pd(II), proceed *via* an 18-electron trigonal bipyridmal intermediate where  $\text{CO}^{\text{d}}$  is the departing carbonyl, (**Scheme 2.5**).



**Scheme 2.5:** Retention of symmetry in 16-electron square planar complexes

Should an 18-electron complex undergo an associative reaction, the metal complex must delocalize a pair of electrons onto one of its ligands.<sup>140,141</sup> For example nitrosyls, such as  $\text{Mn}(\text{CO})_4(\text{NO})$ , can undergo a bent to linear rearrangement.



**Scheme 2.6:** Bent to linear rearrangement of  $\text{Mn}(\text{CO})_4(\text{NO})$

Another mechanism by which 18-electron complexes may undergo an associative mechanism would be  $\eta^5$  to  $\eta^3$  ring slippage observed in indenyl and various cyclopentadienyl complexes. This will be discussed further in 2.4.2.

### 2.3.3 The Interchange ( $\text{I}_a$ and $\text{I}_d$ ) Mechanisms

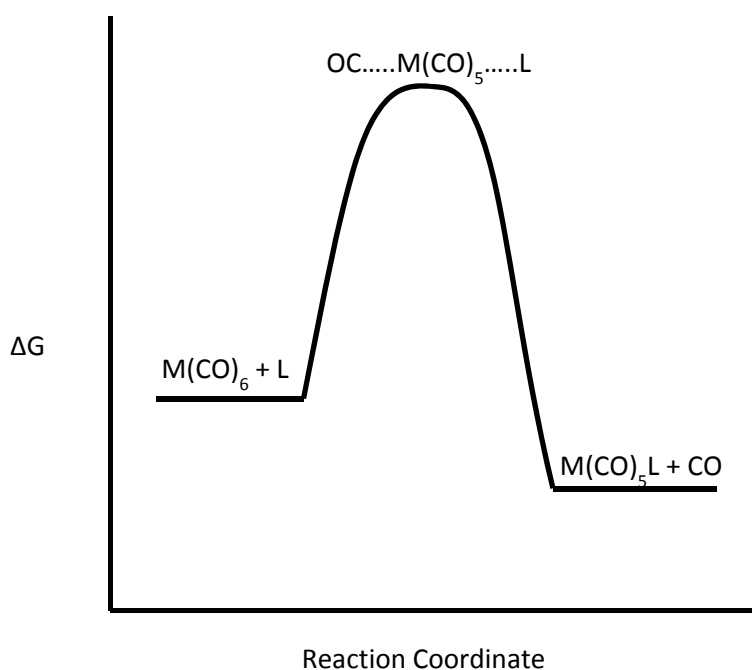
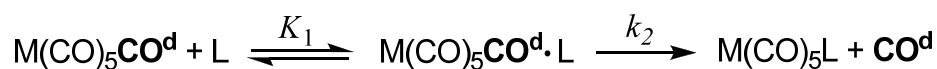


**Figure 2.12:** Free energy diagram for the interchange mechanism

The formation of an outer-sphere complex,  $\text{M}(\text{CO})_5\text{CO}^d\cdot\text{L}$  (**Scheme 2.7**) initiates the dissociative interchange ( $\text{I}_d$ ) mechanism. This is then followed by the replacement of  $\text{CO}^d$  by L in the outer-sphere and then the dissociation from the coordination sphere. The significant difference between the **D**, Equation (1), and  $\text{I}_d$ , Equation (4), mechanism is the dependence of leaving group concentration in the **D** Equation.<sup>142</sup>

The proposed mechanism for the interchange reaction is:



**Scheme 2.7:** The interchange mechanism for  $\text{M}(\text{CO})_6$

The rate for the process is:<sup>140</sup> (4)

$$\text{Rate} = \frac{k_2 K_1 [\text{L}]}{1 + K_1 [\text{L}]}$$

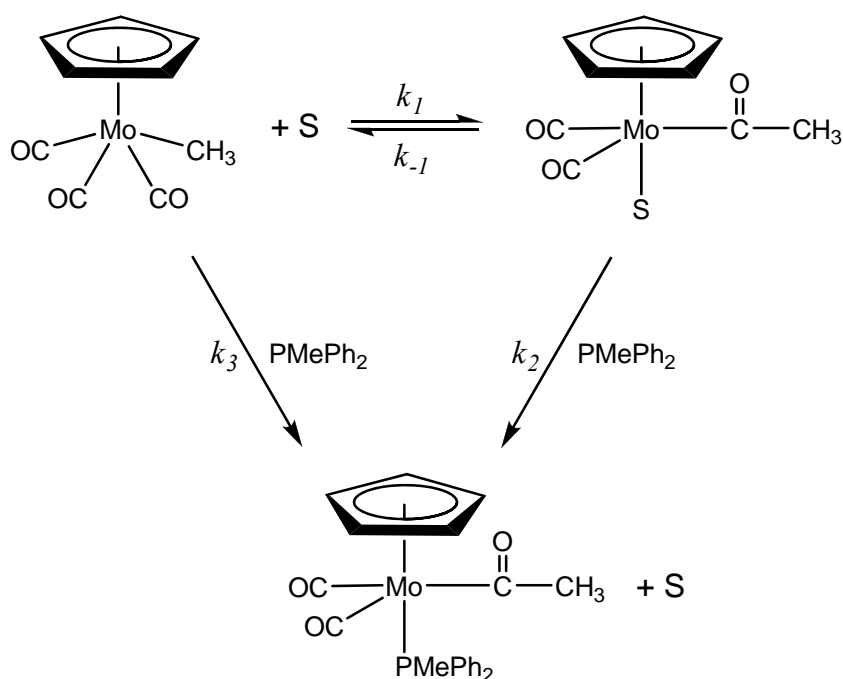
Should  $K_1[\text{L}] \gg 1$  then the rate reduces to: (5)

$$\text{Rate} = k_2$$

And if  $K_1[\text{L}] \ll 1$  then the rate reduces to: (6)

$$\text{Rate} = k_2 K_1 [\text{L}]$$

The  $\text{I}_a$  and  $\text{A}$  classifications are generally ambiguous as it is difficult to distinguish between the two mechanisms. For example the reaction below can also be described by means of an  $\text{I}_a$  pathway.<sup>143</sup>



**Scheme 2.8:** Associative displacement of solvent by phosphine ligand

## 2.4 Carbonyl Substitution Reactions of Cyclopentadienyl Complexes

### 2.4.1 Substitution Reactions of Cyclopentadienyl Iron and Ruthenium Complexes

Brown and co-workers carried out the standard work on  $[\text{MCp}(\text{CO})_2\text{X}]$  ( $\text{M} = \text{Fe}, \text{Ru}$ ,  $\text{X} = \text{Cl}/\text{Br}/\text{I}$ ) complexes in UCD in 1969.<sup>144</sup> They measured the rate of reaction with various phosphine ligands by using IR spectroscopy. They reported an overall first order, dissociative reaction for the iron and ruthenium analogues. The reactions were unaffected by variation in ligand concentration and the nature of the ligand.

Substrate	Solvent	Temp. °C	Ligand	Ligand (molL <sup>-1</sup> )	10 <sup>4</sup> k <sub>obs</sub> (sec <sup>-1</sup> )
[FeCp(CO) <sub>2</sub> I]	<i>n</i> -octane	89.30	P(OPh) <sub>3</sub>	4.0 x 10 <sup>-2</sup>	1.47
[FeCp(CO) <sub>2</sub> I]	<i>n</i> -octane	89.30	P(OPh) <sub>3</sub>	1.6 x 10 <sup>-2</sup>	1.49
[FeCp(CO) <sub>2</sub> I]	<i>n</i> -octane	89.30	P(OC <sub>6</sub> H <sub>13</sub> ) <sub>3</sub>	2.8 x 10 <sup>-2</sup>	1.57
[FeCp(CO) <sub>2</sub> I]	<i>n</i> -octane	98.85	P(OPh) <sub>3</sub>	4.0 x 10 <sup>-2</sup>	3.82
[FeCp(CO) <sub>2</sub> I]	<i>n</i> -butyl ether	98.85	P(OPh) <sub>3</sub>	4.0 x 10 <sup>-2</sup>	3.59
[FeCp(CO) <sub>2</sub> I]	<i>n</i> -octane	98.85	P(OPh) <sub>3</sub>	1.6 x 10 <sup>-2</sup>	3.83
[FeCp(CO) <sub>2</sub> I]	<i>n</i> -butyl ether	98.85	P(OPh) <sub>3</sub>	1.6 x 10 <sup>-2</sup>	3.55
[Fe(η <sup>5</sup> -C <sub>5</sub> H <sub>4</sub> CH <sub>3</sub> )(CO) <sub>2</sub> I]	<i>n</i> -octane	98.60	P(OPh) <sub>3</sub>	5.0 x 10 <sup>-2</sup>	2.45
[Fe(η <sup>5</sup> -C <sub>5</sub> H <sub>4</sub> CH <sub>3</sub> )(CO) <sub>2</sub> I]	<i>n</i> -butyl ether	98.85	P(OPh) <sub>3</sub>	4.0 x 10 <sup>-2</sup>	2.62
[FeCp(CO) <sub>2</sub> Br]	<i>n</i> -octane	74.75	P(OPh) <sub>3</sub>	4.0 x 10 <sup>-2</sup>	5.26
[FeCp(CO) <sub>2</sub> Br]	<i>n</i> -octane	74.75	P(OPh) <sub>3</sub>	1.6 x 10 <sup>-2</sup>	5.27
[FeCp(CO) <sub>2</sub> Br]	<i>n</i> -butyl ether	75.15	P(OPh) <sub>3</sub>	4.0 x 10 <sup>-2</sup>	3.82
[FeCp(CO) <sub>2</sub> Br]	<i>n</i> -butyl ether	75.15	P(OPh) <sub>3</sub>	1.6 x 10 <sup>-2</sup>	3.75
[Fe(η <sup>5</sup> -C <sub>5</sub> H <sub>4</sub> CH <sub>3</sub> )(CO) <sub>2</sub> Br]	<i>n</i> -octane	74.75	P(OPh) <sub>3</sub>	4.0 x 10 <sup>-2</sup>	3.58
[Fe(η <sup>5</sup> -C <sub>5</sub> H <sub>4</sub> CH <sub>3</sub> )(CO) <sub>2</sub> Br]	<i>n</i> -butyl ether	75.15	P(OPh) <sub>3</sub>	4.0 x 10 <sup>-2</sup>	2.56
[Fe(η <sup>5</sup> -C <sub>5</sub> H <sub>4</sub> CH <sub>3</sub> )(CO) <sub>2</sub> Cl]	<i>n</i> -octane	60.5	P(OPh) <sub>3</sub>	4.0 x 10 <sup>-2</sup>	5.03
[Fe(η <sup>5</sup> -C <sub>5</sub> H <sub>4</sub> CH <sub>3</sub> )(CO) <sub>2</sub> Cl]	<i>n</i> -butyl ether	60.5	P(OPh) <sub>3</sub>	4.0 x 10 <sup>-2</sup>	5.39

**Table 2.5:** Rate constants for the reaction of  $[\text{Fe}(\eta^5\text{-C}_5\text{H}_4\text{R})(\text{CO})_2\text{X}]$  ( $\text{R} = \text{H}/\text{Me}$ ) complexes with various phosphine ligands

In both solvents and for both cyclopentadienyl and methylcyclopentadienyl complexes the rate constants decrease in the sequence Cl > Br > I. This is due to an increasing M–CO bond strength which arises from an increased d $\pi$ –p $\pi$  bonding and the increasing polarizability and decreasing electronegativity of the halogens. This is supported by the  $\nu$ MC–O stretching frequencies of these compounds (**Table 2.6**).

Compound	$\nu$ MC–O (cm <sup>-1</sup> )	
[FeCp(CO) <sub>2</sub> I]	2043	2004
[FeCp(CO) <sub>2</sub> Br]	2050	2010
[FeCp(CO) <sub>2</sub> Cl]	2055	2016
[Fe( $\eta^5$ -C <sub>5</sub> H <sub>4</sub> CH <sub>3</sub> )(CO) <sub>2</sub> I]	2038	1998
[Fe( $\eta^5$ -C <sub>5</sub> H <sub>4</sub> CH <sub>3</sub> )(CO) <sub>2</sub> Br]	2047	2005
[Fe( $\eta^5$ -C <sub>5</sub> H <sub>4</sub> CH <sub>3</sub> )(CO) <sub>2</sub> Cl]	2050	2008
[FeCp(CO)P(OPh) <sub>3</sub> I]		1988
[FeCp(CO)P(OPh) <sub>3</sub> Br]		1990
[Fe( $\eta^5$ -C <sub>5</sub> H <sub>4</sub> CH <sub>3</sub> )(CO)P(OPh) <sub>3</sub> I]		1983
[Fe( $\eta^5$ -C <sub>5</sub> H <sub>4</sub> CH <sub>3</sub> )(CO)P(OPh) <sub>3</sub> Br]		1986
[Fe( $\eta^5$ -C <sub>5</sub> H <sub>4</sub> CH <sub>3</sub> )(CO)P(OPh) <sub>3</sub> Cl]		1987

**Table 2.6:**  $\nu$ MC–O (cm<sup>-1</sup>) or [Fe( $\eta^5$ -C<sub>5</sub>H<sub>4</sub>R)(CO)<sub>2</sub>X] (R = H/Me) and its derivatives in *n*-heptane

The activation energies, E<sub>a</sub>, show solvent dependency and in *n*-octane lie in the sequence I < Br > Cl (E<sub>a</sub>) and for *n*-butyl ether I < Br < Cl. However, the generally high E<sub>a</sub> and large positive  $\Delta S^\ddagger$  values are consistent with a purely dissociative mechanism.<sup>145</sup>

Complex	E <sub>a</sub> (kJmol <sup>-1</sup> )	$\Delta S^\ddagger$ (JK <sup>-1</sup> )	Solvent
[FeCp(CO) <sub>2</sub> I]	112.32	-17.66	<i>n</i> -octane
[FeCp(CO) <sub>2</sub> Br]	130.66	+59.13	<i>n</i> -octane
[Fe( $\eta^5$ -C <sub>5</sub> H <sub>4</sub> CH <sub>3</sub> )(CO) <sub>2</sub> I]	118.64	-3.47	<i>n</i> -octane
[Fe( $\eta^5$ -C <sub>5</sub> H <sub>4</sub> CH <sub>3</sub> )(CO) <sub>2</sub> Br]	128.86	+50.60	<i>n</i> -octane
[FeCp(CO) <sub>2</sub> I]	99.81	-52.19	<i>n</i> -butyl ether
[FeCp(CO) <sub>2</sub> Br]	110.32	-2.05	<i>n</i> -butyl ether
[Fe( $\eta^5$ -C <sub>5</sub> H <sub>4</sub> CH <sub>3</sub> )(CO) <sub>2</sub> I]	111.87	-22.77	<i>n</i> -butyl ether
[Fe( $\eta^5$ -C <sub>5</sub> H <sub>4</sub> CH <sub>3</sub> )(CO) <sub>2</sub> Br]	122.62	+29.42	<i>n</i> -butyl ether

**Table 2.7:** Activation energies for reactions of [Fe( $\eta^5$ -C<sub>5</sub>H<sub>4</sub>R)(CO)<sub>2</sub>X] (R = H/Me) complexes with P(OPh)<sub>3</sub>

When compared to the ruthenium analogues, the iron complexes show much greater reactivity with the rate of substitution generally being about 700 times than for the

cyclopentadienyl ruthenium dicarbonyl halides, (**Table 2.8**).<sup>146</sup> The rate sequence is the same as in the iron compounds, Cl > Br > I. This decreased reactivity is in contrast to an enhanced reactivity of some complexes of the second row transition metals. For example, the more rapid substitution of [RhCp(CO)<sub>2</sub>] with phosphines and phosphites when compared to rates reported for the corresponding Co and Ir complexes.<sup>147</sup>

Substrate	Temp. °C	10 <sup>4</sup> k <sub>obs</sub> (sec <sup>-1</sup> )
[FeCp(CO) <sub>2</sub> Br]	72	1.43
[FeCp(CO) <sub>2</sub> Br]	76.7	2.86
[FeCp(CO) <sub>2</sub> Br]	82.4	5.5
[FeCp(CO) <sub>2</sub> I]	91.8	0.81
[FeCp(CO) <sub>2</sub> I]	97.2	1.59
[FeCp(CO) <sub>2</sub> I]	102.2	2.91
[RuCp(CO) <sub>2</sub> Cl]	110.0	1.05
[RuCp(CO) <sub>2</sub> Cl]	115.4	1.75
[RuCp(CO) <sub>2</sub> Cl]	120.4	2.87
[RuCp(CO) <sub>2</sub> Br]	125.4	1.01
[RuCp(CO) <sub>2</sub> Br]	130.4	1.47
[RuCp(CO) <sub>2</sub> Br]	135.4	2.33

**Table 2.8:** Rate constants for the reaction of [MCp(CO)<sub>2</sub>X] with P(OPh)<sub>3</sub> in xylene (M=Fe, Ru, X=Cl, Br, I)

The activation energy of the ruthenium bromide analogue is 14.65 kJmol<sup>-1</sup> less than that of the iron compound in xylene which accounts for the much lower ΔS<sup>‡</sup>. The reverse of this is true in *n*-butyl ether which would suggest that xylene has a greater solvating effect on the ruthenium compounds.

Complex	Solvent	$10^5 k_r$	$E_a$ (kJmol <sup>-1</sup> )	$\Delta S^\ddagger$ (JK <sup>-1</sup> )
[FeCp(CO) <sub>2</sub> Br]	<i>n</i> -octane	27.6	130.57	59.00
	xylene	10.8	144.80	89.98
	<i>n</i> -butyl ether	23.4	110.48	-2.09
	Nitrobenzene	4.4	141.03	73.24
[FeCp(CO) <sub>2</sub> I]	<i>n</i> -octane	1.04	112.16	-17.58
	xylene	0.44	138.94	48.55
	<i>n</i> -butyl ether	0.9	99.60	-52.31
	Nitrobenzene	0.17	140.20	43.94
[RuCp(CO) <sub>2</sub> Cl]	xylene	0.15	125.13	-4.19
[RuCp(CO) <sub>2</sub> Br]	xylene	0.015	130.15	-5.86
	<i>n</i> -butyl ether	0.04	125.97	-8.79

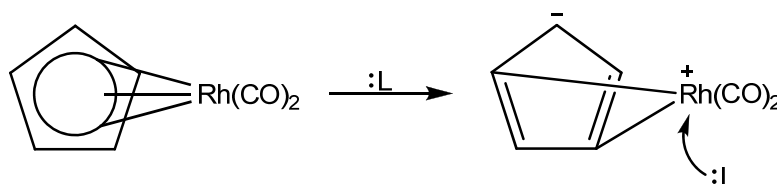
**Table 2.9:** Activation energies for [MCp(CO)<sub>2</sub>X] in xylene at 70°C (M=Fe, Ru, X=Cl, Br, I)

In all cases first-order kinetics were observed. However no kinetic data was reported for the [RuCp(CO)<sub>2</sub>I] complex.

White *et al.* reported on the rate constants for the CO substitution of [Ru( $\eta^5$ -C<sub>5</sub>Me<sub>4</sub>Et)(CO)<sub>2</sub>Br] with tertiary phosphine ligands (P(OPh)<sub>3</sub>, P(OMe)<sub>3</sub> and PPh<sub>3</sub>) in 1981.<sup>148</sup> These reactions were found to be independent of concentration and nature of the incoming ligands. The substitution reactions of pentaphenylcyclopentadienyl analogue were also studied. These too exhibited a dissociative mechanism. When compared to the rates observed for the parent cyclopentadienyl and the ethyltetramethylcyclopentadienyl complexes the [Ru( $\eta^5$ -C<sub>5</sub>Ph<sub>5</sub>)(CO)<sub>2</sub>Br] shows a significant increase in reactivity. At 112.1°C the approximate relative rates for the [RuCp'(CO)<sub>2</sub>Br] complexes were found to be 1:14:20 for Cp' = C<sub>5</sub>H<sub>5</sub>, C<sub>5</sub>Me<sub>4</sub>Et and C<sub>5</sub>Ph<sub>5</sub>, respectively.<sup>149</sup>

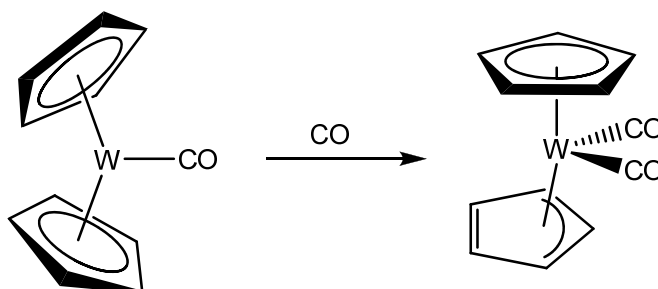
#### 2.4.2 Ring Slippage and the Indenyl Effect

The concept of what was later to be termed “ring slippage”, was first reported by Basolo *et al.* in 1966.<sup>147</sup> Upon reacting [RhCp(CO)<sub>2</sub>] with phosphine ligands a dependence on the concentration of the ligand was noted. He proposed that a pair of electrons were delocalized from the metal or metal–ligand bond, onto the Cp ring forming C<sub>5</sub>H<sub>5</sub><sup>-</sup>.



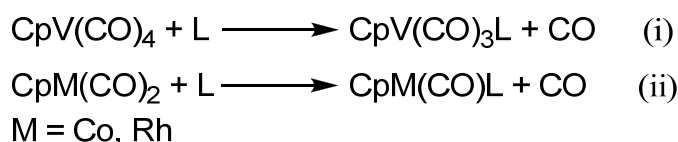
**Scheme 2.9:** Basolo's explanation for the second order kinetics observed in  $[RhCp(CO)_2]$

In 1968 King reported on the synthesis of  $[MoCp_2I(NO)]$ .<sup>150</sup> He proposed that the complex avoided a 20-electron valence shell configuration by donation of only three electrons from the Cp. This was the first report of a proposed  $\eta^3$ -bound Cp ligand. However, the crystal structure later reported for  $[MoCp_2Mo(CO)I]$  disproved his theory.<sup>151</sup> After much debate on the concept of the trihaptocyclopentadienyl–metal bond, Hutner *et al.* reported on the crystal structure of  $[W(\eta^5-C_5H_5)(\eta^3-C_5H_5)(CO)_2]$  (**Scheme 2.10**).<sup>152</sup> The bond distance between the alkene group on the  $\eta^3$ -bound ligand is 2.98Å from the metal centre, which is too great a distance for a bond to occur.

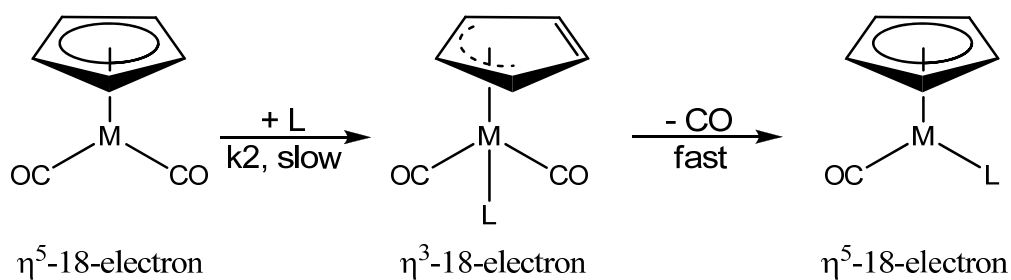


**Scheme 2.10:**  $\eta^3$ -bonding in  $[W(\eta^5-C_5H_5)(\eta^3-C_5H_5)(CO)_2]$

When comparing the carbonyl substitution reactions:

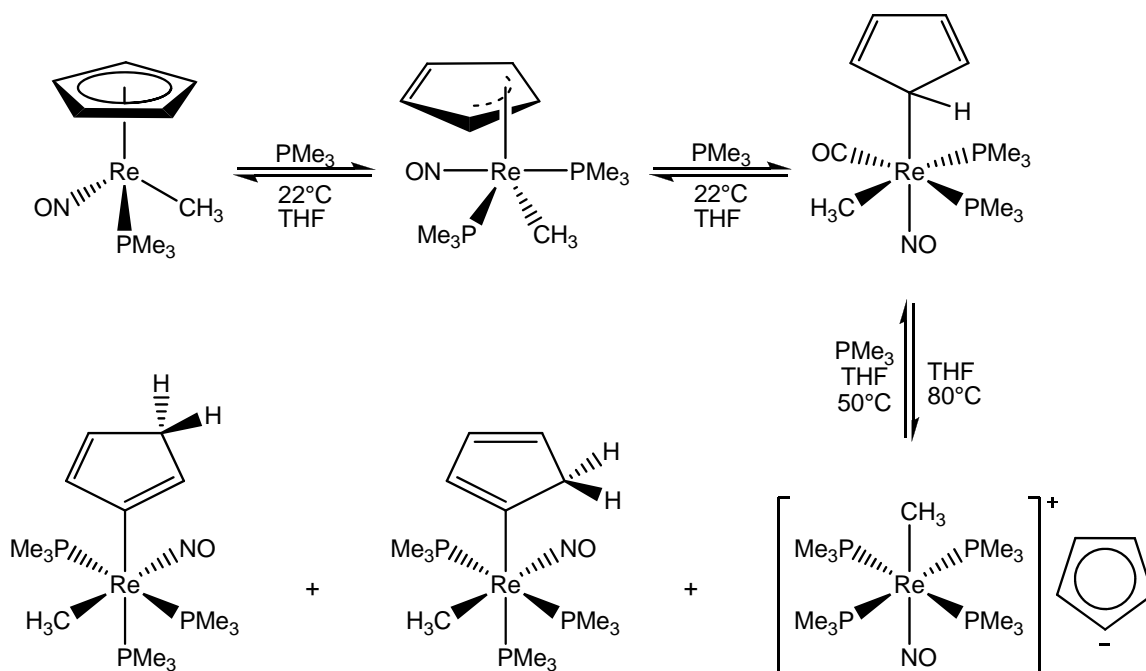


(i) proceeds *via* a dissociative mechanism, whereas, (ii) proceeds *via* an associative mechanism explained by an  $\eta^5 \rightarrow \eta^3 \rightarrow \eta^5$  slippage mechanism.<sup>133</sup>



**Scheme 2.11:** The ring slippage mechanism

An  $\eta^5 \rightarrow \eta^1$  slippage of Cp was observed by Casey and co-workers when investigating the substitution reactions of  $[\text{ReCp}(\text{CO})_3]$  with phosphine ligands.<sup>153,154</sup> The slip mechanism proceeded *via* an  $\eta^3$  intermediate. In 1984 Casey *et al.* reported on the replacement of the Cp ligand by phosphines in a stepwise  $\eta^5 \rightarrow \eta^3 \rightarrow \eta^1 \rightarrow \eta^0$  slippage (**Scheme 2.12**).



**Scheme 2.12:**  $\eta^5 \rightarrow \eta^3 \rightarrow \eta^1 \rightarrow \eta^0$  ring slippage mechanism

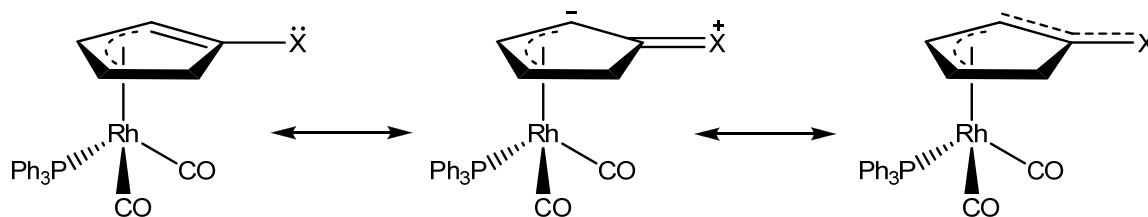
Mawby and Hart-Davies were first to study the rate and mechanisms of reactions of indenyl complexes of the transition metals.<sup>155</sup> The rate constant for the methyl

migration of  $[\text{Mo}(\eta^5\text{-C}_9\text{H}_7)(\text{CO})_3\text{Me}]$  with tertiary phosphine ligands were investigated and compared to those of the parent cyclopentadienyl complex. The mechanisms for both proved to be associative but the rate of substitution for the indenyl complex was greater than the parent by a factor of  $\sim 10$ . Mawby and co-workers group then studied the rate of CO substitution of  $[\text{Mo}(\text{indenyl})(\text{CO})_3\text{X}]$ , ( $\text{X} = \text{Cl}, \text{Br}, \text{I}$ ) and again compared the rates recorded with those reported for the parent cyclopentadienyl complexes.<sup>156</sup> In these reactions the Cp analogues were found to proceed *via* a dissociative mechanism whereas the indenyl complexes *via* an associative mechanism. These changes in rate and mechanism were labelled “the indenyl effect” by Basolo.<sup>157</sup> Just as in the “ring slip” above, the mechanism proceeds via an  $\eta^5 \rightarrow \eta^3 \rightarrow \eta^5$  intermediate, and as before this explains the change from  $\text{S}_{\text{N}}1$  to  $\text{S}_{\text{N}}2$  reactions upon the progression from a cyclopentadienyl to indenyl complex. In the case of the indenyl halides a rate enhancement of  $\sim 6000$  for the  $\text{S}_{\text{N}}1$  path was recorded when compared to the cyclopentadienyl complex.

Basolo *et al.* studied ring slippage and the indenyl effect in depth.<sup>158</sup> He stated that the proposed mechanism (**Scheme 2.13**) predicts that electron withdrawing substituents on the Cp ligand would enhance localization of electron density onto the ring which would assist nucleophilic attack on the metal and thus increase the rate of substitution. By the same measures the presence of electron donating groups on the Cp ligand would decrease the rate of substitution. This theory was investigated using the compounds  $[\text{RhCp}(\text{CO})_2]$ ,  $[\text{Rh}(\eta^5\text{-C}_5\text{H}_4\text{NO}_2)(\text{CO})_2]$  and  $[\text{RhCp}^*(\text{CO})_2]$  for substitution reactions with tertiary phosphines.<sup>159,160</sup> These gave relative reaction rates of 1:104:10<sup>-2</sup> respectively. In the case of the rate reported for the pentamethylcyclopentadienyl analogue it was unclear how much of the decrease in rate was due to the electron donating effects of the methyl groups and how much was due to steric factors.

Reactions of the type  $[\text{Rh}(\eta^5\text{-C}_5\text{H}_4\text{X})(\text{CO})_2]$ , ( $\text{X} = \text{H}, \text{NO}_2, \text{CF}_3, \text{Cl}, \text{CH}_3$  or  $\text{N}(\text{CH}_3)_2$ ) with  $\text{PPh}_3$  were then investigated.<sup>161</sup> These resulted in good linear correlations between the values of  $\nu_{\text{M-CO}}$ , the values of CO stretching frequencies and Hammett  $\sigma$  values of the X ring substituents of the parent and substituted complexes. This reflects the electron density on the metal atom which would then result in greater or lesser  $\pi$ -backbonding from  $\text{M} \rightarrow \text{CO}$ . For the majority of the complexes the rates of

CO substitution were found to decrease with increasing electron density on the metal. However in the cases of  $X = \text{Cl}$  or  $\text{N}(\text{CH}_3)_2$  the rates of substitution were found to increase. Basolo concluded that apart from the electron density on the metal affecting the rate of reaction, the stability of the slipped intermediate also had an effect. He suggested that these particular substituents could resonance stabilize the transition state and increase the rate of reaction (**Scheme 2.13**).



**Scheme 2.13:** Resonance stabilization of the transition state of  $[\text{Rh}(\eta^5\text{-C}_5\text{H}_4\text{X})(\text{CO})_2]$  where  $X = \text{Cl}$  or  $\text{N}(\text{CH}_3)_2$

The substitution reactions of  $[\text{Rh}(\text{indenyl})(\text{CO})_2]$  were shown to proceed  $10^8$  times faster than the relative Cp complexes.<sup>157,159,160</sup>  $[\text{MoCp}(\text{CO})_3]$  was found to be inert to substitution with phosphines and phosphites, however, the indenyl analogue was found to react readily.<sup>162,163</sup>

Basolo compared the kinetics of substitution of the cyclopentadienyl, indenyl and substituted indenyl rhodium dicarbonyl complexes with  $\text{PPh}_3$  (<sup>a</sup>  $\text{L} = \text{P}(\text{n-Bu})_3$ ), (**Table 2.10**).<sup>160</sup>

Compound	$k_{\text{rel}}$	$\nu_{\text{MC-O}} (\text{cm}^{-1})$
$[\text{RhCp}(\text{CO})_2]$	1	2051, 1985
$[\text{Rh}(\text{indenyl})(\text{CO})_2]$	$3.8 \times 10^8$	2048, 1993
$[\text{Rh}(\eta^5\text{-C}_9(\text{CH}_3)_7)(\text{CO})_2]$	$6.1 \times 10^5$	2021, 1965
$[\text{Rh}(\eta^5\text{-C}_5\text{H}_4\text{NO}_2)(\text{CO})_2]$	$1.2 \times 10^4$	2067, 2011
$[\text{Rh}(\eta^5\text{-C}_5\text{H}_4\text{PPh}_3)(\text{CO})_2]^+$	$1.1 \times 10^2$	2062, 2002
$[\text{Rh}(\eta^5\text{-C}_5(\text{CH}_3)_5)(\text{CO})_2]$	$2.2 \times 10^{-2}$ <sup>a</sup>	2020, 1967

**Table 2.10:** Relative rates of substitution for substituted Cp and Indenyl rhodium complexes

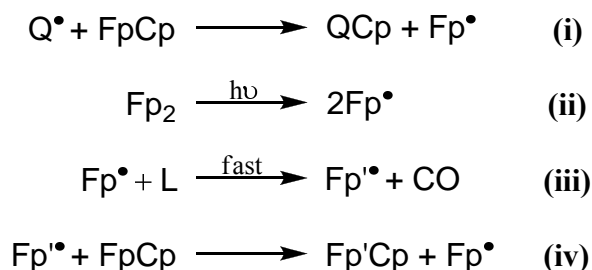
In all cases the mechanism was associative. The slower rate constants recorded for  $[\text{Rh}(\eta^5\text{-C}_9(\text{CH}_3)_7)(\text{CO})_2]$  compared to  $[\text{Rh}(\text{indenyl})(\text{CO})_2]$  can be explained when taking the  $\nu_{\text{MC-O}}$  stretching frequencies into account. These values shift to a lower

frequency which arises from increased back bonding from the metal to the CO and thus making it less susceptible to substitution. Just as in the increase of rate when comparing the Cp complex to the nitro and pentamethyl analogues. In the case of the  $[\text{Rh}(\eta^5\text{-C}_5\text{H}_4\text{NO}_2)(\text{CO})_2]$  there is an increase in the  $\nu_{\text{MC-O}}$  when compared to the parent Cp complex, explaining the increase in rate. The  $[\text{RhCp}^*(\text{CO})_2]$  shows a lower stretching frequency and therefore a slower rate of substitution.

The aromatization of the fused benzene ring in the transition state accounts for the dramatic increase in the reactivities of the indenyl complexes when compared to the cyclopentadienyl analogues.<sup>158</sup> A further increase of rate is noted when progressing from the indenyl to the fluorenyl ligand.<sup>163</sup> The size and basicity of the nucleophile is also a factor in the reactivity of the nucleophile,  $[\text{Mo}(\eta^5\text{-C}_{13}\text{H}_9)(\text{CO})_3]$  was found to react 388 times faster with  $\text{P}(\text{OEt})_3$  than  $[\text{Mo}(\text{indenyl})(\text{CO})_3]$ . Upon increasing the basicity of the incoming ligand ( $\text{P-c-Hx}_3$ ) the rate of substitution for the fluorenyl complex was 45 times faster than the indenyl complex.

### 2.4.3 $[\text{MCp}(\text{CO})_2]_2$ as a Catalyst ( $\text{M} = \text{Fe, Ru}$ )

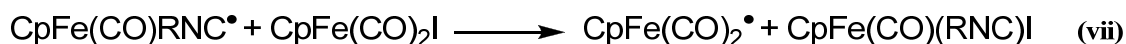
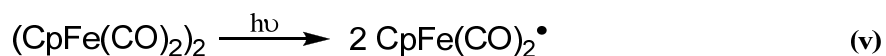
The use of  $[\text{FeCp}(\text{CO})_2]_2$  as a CO substitution catalyst in organometallic chemistry was first reported in 1979.<sup>164</sup> The reaction between  $[\text{Fe}(\eta^5\text{-C}_5\text{H}_5)(\sigma\text{-C}_5\text{H}_5)(\text{CO})_2]$  (denoted FpCp) and tertiary phosphines and phosphites was found to be complex. FpCp reacts with  $\text{P}(\text{OPh})_3$  very slowly in the dark to form  $[\text{Fe}(\eta^5\text{-C}_5\text{H}_5)(\text{CO})\text{P}(\text{OPh})_3](\sigma\text{-C}_5\text{H}_5)]$  (Fp'Cp). No acceleration in the rate of reaction was observed upon irradiation of the reaction solution, but instead the FpCp was converted into ferrocene. Upon addition of the dimer  $[\text{Fe}(\eta^5\text{-C}_5\text{H}_5)\text{Fe}(\text{CO})_2]_2$  (denoted Fp<sub>2</sub>) to the irradiated solution the substitution was markedly enhanced.



**Scheme 2.14:** Radical mechanism in the catalysed reaction of  $[\text{Fe}(\eta^5\text{-C}_5\text{H}_5)(\sigma\text{-C}_5\text{H}_5)(\text{CO})_2]$  with tertiary phosphines

The reaction is initiated either by extrinsic impurities ( $\mathbf{Q}\cdot$ ) (**i**) or by photolysis of ferrocene (**ii**) to yield the 17-electron metal fragment  $\text{Fp}\cdot$ . Propagation then occurs (**iii**) and (**iv**) with (**iv**) being a homolytic displacement of an unsaturated alkyl group.

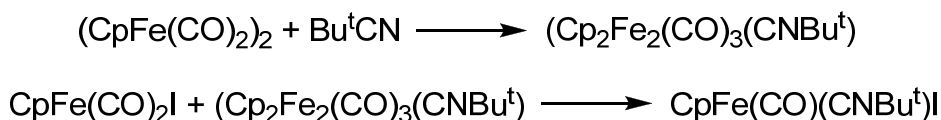
Coville and Albers used the dimer to catalyse the reaction of  $[\text{FeCp}(\text{CO})_2\text{I}]$  with various isonitriles (RNC).<sup>165</sup> Previous attempts using  $[\text{MoCp}(\text{CO})_3]_2$  as a catalyst had been unsuccessful as the molybdenum catalyst underwent a competitive salt formative side reaction. The reaction of  $[\text{FeCp}(\text{CO})_2\text{I}]$  with RNC to yield  $[\text{FeCp}(\text{CO})_{2-n}(\text{CNR})_n\text{I}]$  had been previously reported but the reaction proceeded with difficulty.<sup>166,167</sup> Upon the addition of a small amount of the catalyst ( $\text{Fp}_2$ , 0.05mmol) the reaction went to completion in less than five minutes and in good yield. In the absence of catalyst the reaction proceeded very slowly and resulted in a mixture of the mono- and di-substituted products. Initially the mechanism proposed for such a catalysed reaction was<sup>164,168-170</sup>:



**Scheme 2.15:** Initial proposed radical mechanism in the catalysed reaction of  $\text{CpFe}(\text{CO})_2\text{I}$  with tertiary isonitriles

These reactions were carried out using 1.00 mmol of each reactant and 0.05 mmol of catalyst. In order to better understand the role of the catalyst the concentration of the iron dimer was increased.  $[\text{FeCp}(\text{CO})_2\text{I}]$  (0.5 mmol) was reacted with  $\text{Bu}^t\text{NC}$  (0.55mol) and  $[\text{FeCp}(\text{CO})_2]_2$  (0.25 mmol) in benzene at 42°C. Under these conditions the product  $[\text{FeCp}(\text{CO})(\text{CNBu}^t)\text{I}]$  was formed in 45 mins. In the absence of the catalyst >5% of the product was detected after 2 hours. It was also found if the reaction was left to proceed for ~70mins,  $[\text{FeCp}(\text{CNBu}^t)_2\text{I}]$  and the iron dimer were the only products isolated. From this it can be deduced that the activation barriers to

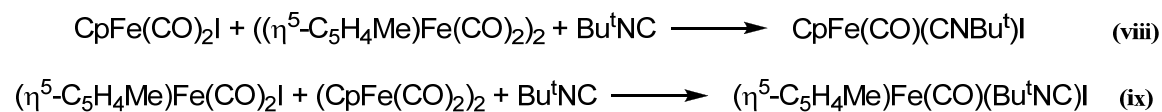
the mono- and di-substituted products are similar. Moreover, the Bu<sup>t</sup>NC substitution of [FeCp(CO)(CNBu<sup>t</sup>)I] occurs in preference to the CO substitution of the dimer.



**Scheme 2.16:** *The interaction between (CpFe(CO)<sub>2</sub>)<sub>2</sub> and Bu<sup>t</sup>CN to form CpFe(CO)(CNBu<sup>t</sup>)I*

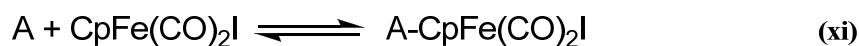
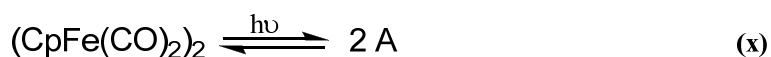
The reactions above (**Scheme 2.16**) proceeded to ~5% completion in 2 hrs under the same reaction conditions (42°C, benzene). Coville stated then that a mechanism such as in reactions (vi) and (vii) (**Scheme 2.15**) were unfeasible.

Labelled cyclopentadienyl rings were then employed to further understand the mechanism.



**Scheme 2.17:** *The catalysed reactions of some labeled cyclopentadienyl iron complexes with Bu<sup>t</sup>CN*

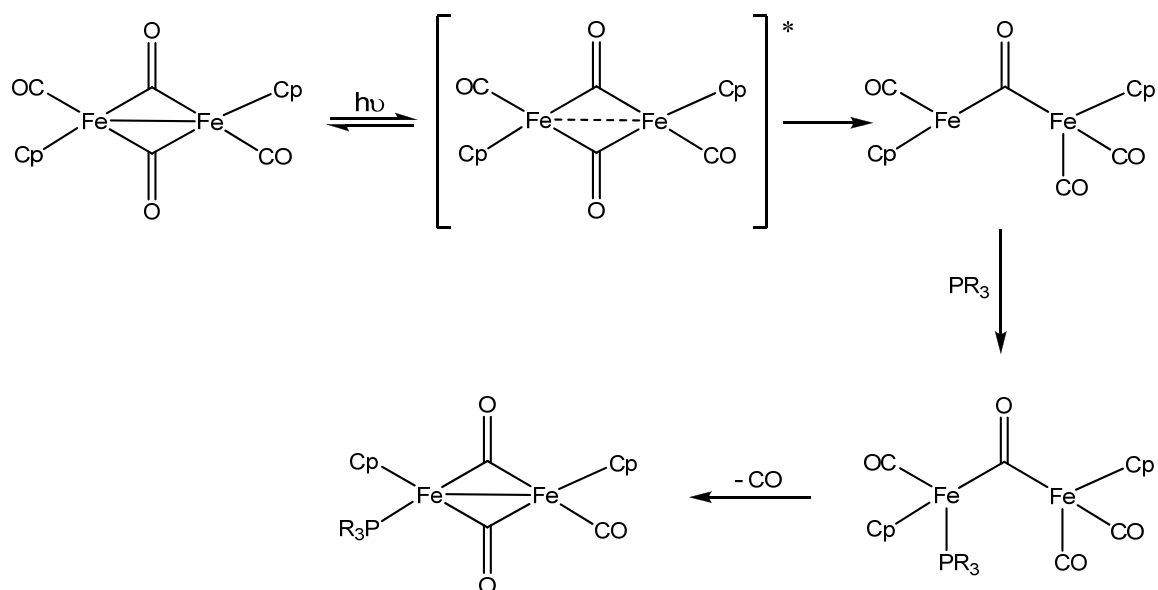
Radical inhibitors were also employed. The addition of hydroquinone or galvinoxyl resulted in a decrease in the rate of reaction. When irradiated the reaction goes to completion in ~1 minute in the presence of the catalyst. However in the absence of the catalyst an irradiated reaction proceeds to completion in ~45min. Metal carbonyls are known to lose CO upon irradiation<sup>171</sup> however the rate of substitution was slower with irradiation compared to when catalysed by [FeCp(CO)<sub>2</sub>]<sub>2</sub>. An alternative mechanism was then proposed.



**Scheme 2.18:** Proposed radical mechanism in the catalysed reaction of  $\text{CpFe}(\text{CO})_2\text{I}$  with tertiary isonitriles

The modified reaction scheme, (**Scheme 2.18**), shows an interaction between the radical, formed from the excitation of the iron dimer (**x**), and the substrate leading to an activation of the ligand, (**xi**) and product formation. This scheme also requires no transfer of ligand between the catalyst and substrate. The mechanism suggests that the mechanism would apply to complexes not containing the  $\text{CpFe}(\text{CO})_2$  moiety. This has been shown to be true for the catalysed reaction between  $\text{Fe}(\text{CO})_5$  and  $\text{PR}_3$  to yield  $\text{Fe}(\text{CO})_4\text{PR}_3$ .<sup>172</sup> The scheme also implies an increase of ligand activation of the substrate.

Coville deduced that species (**A**) could be either monomeric or dimeric. The  $\text{CpFe}(\text{CO})_2\bullet$  radical is generated from the dimer without great difficulty and interaction of the radical with the substrate would lead to  $\text{M-CO}$  bond weakening. This could be achieved *via* a one-electron transfer which would involve either oxidation or reduction of the substrate.<sup>173</sup> It was also suggested that species (**A**) may exist as an activated CO bridged dimer, such as the one proposed by Tyler *et al.* in which the  $\text{M-M}$  bond is cleaved but the dimer is not disrupted.<sup>174</sup>



**Scheme 2.19:** *M–M bond cleavage in  $(\text{CpFe}(\text{CO})_2)_2$*

The M–M cleaved dimer may interact with the substrate to induce M–CO bond weakening via an electron-transfer process between catalyst and substrate.<sup>165</sup> The rate of recombination of the radical monomer  $\text{CpFe}(\text{CO})_2\bullet$  was shown to be  $10^9 \text{ M}^{-1}\text{s}^{-1}$ .<sup>175</sup>

#### 2.4.4 17-Electron Metal-Centred Radicals

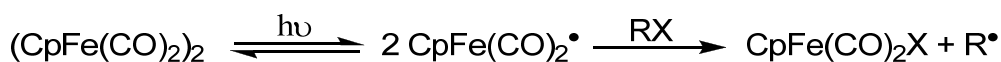
17-electron metal-centered complexes may be formed by electron-transfer reactions of mononuclear carbonyl complexes, (**Figure 2.13**).<sup>176,177</sup>



**Figure 2.13:** *Electron transfer reaction of an 18-electron species*

The 17-electron species may also be formed by photoinduced homolysis of dimeric compounds containing a metal–metal bond.<sup>164,178</sup>

The iron-centred radicals,  $\text{CpFe}(\text{CO})_2\bullet$  and  $\text{Cp}^*\text{Fe}(\text{CO})_2\bullet$  are very reactive species. They recombine to form the relative dimers without difficulty<sup>179</sup> and readily abstract halogen atoms from organic halides.<sup>175</sup>



**Scheme 2.20:** The reactivity of the 17-electron  $\text{CpFe}(\text{CO})_2^\bullet$  radical

The reactions of 17-electron metal centred radicals generally proceed *via* an associative reaction.<sup>180</sup> The rates of reaction when compared to the relative 18-electron complexes show an enhancement of many orders of magnitude.<sup>176</sup> Sweigart reported on the rates of single and double CO substitution in substituted cyclopentadienyl manganese complexes in 1995.<sup>181</sup> The complex  $[\text{Mn}(\eta^5\text{-C}_5\text{H}_4\text{Me})(\text{CO})_3]$  had been previously reported as practically inert to CO substitution<sup>162</sup> but Sweigart found upon oxidation of the metal complex in the presence of  $\text{P}(\text{OEt})_3$  the rates of substitution of one or two CO ligands was rapid.

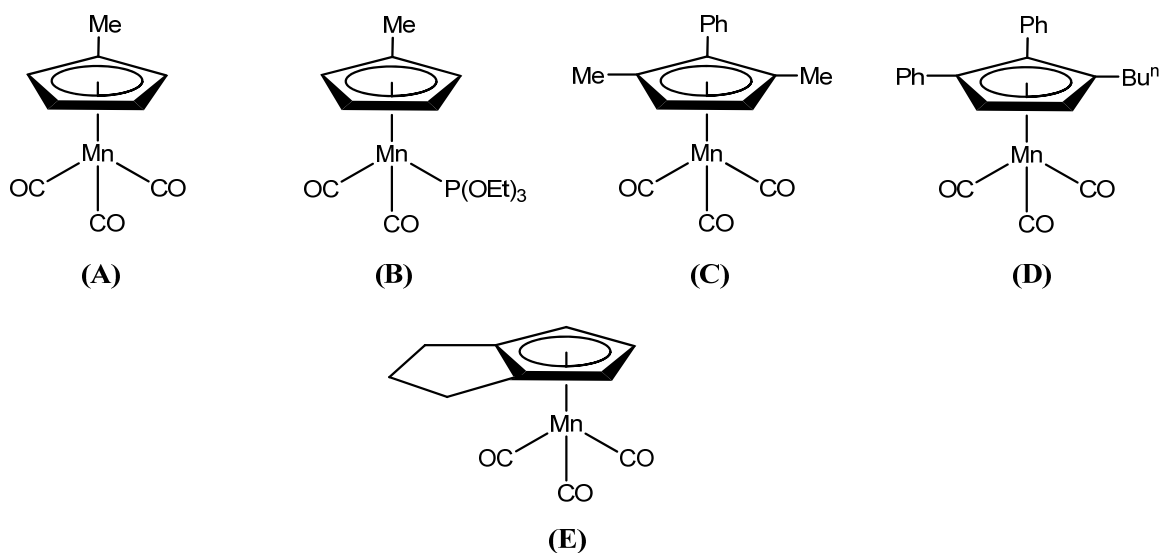
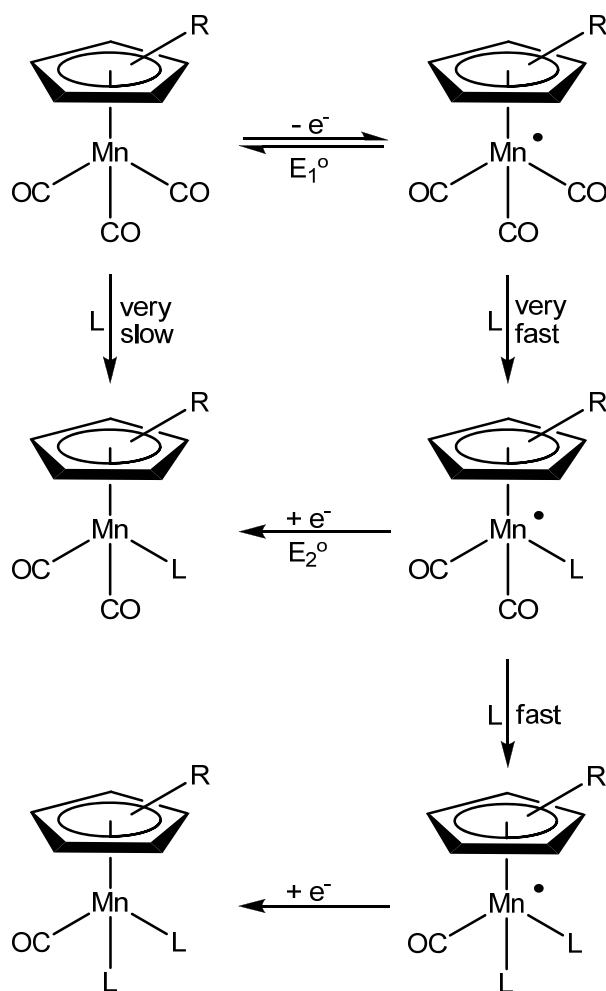


**Figure 2.14:**  $[\text{MnCp}'(\text{CO})_{3-n}\text{L}_n]$  ( $\text{L} = \text{CO}, \text{P}(\text{OEt})_3$ ) complexes investigated

The extent of substitution (single vs. di-substituted) is influenced by steric restrictions in the vicinity of the metal due to the R groups on the cyclopentadienyl ligand. The order of reactivity for the complexes was **(A)** > **(C)** > **(D)** > **(E)**, reflecting the steric hindrance surrounding the metal center.

These reactions are not catalytic, the conversion of  $[\text{MnCp}'(\text{CO})_3]$  to  $[\text{MnCp}'(\text{CO})_2\text{L}]$  requires an initial stoichiometric oxidation followed by CO substitution in the 17-electron radical and then a stoichiometric reduction. In order for the reaction to be catalytic the 18-electron product must be more difficult to oxidize than the reactant, or

$E_2^\circ > E_1^\circ$  (**Scheme 2.21**). In the majority, departing ligands are replaced by ligands that increase the electron density on the metal centre, where  $E_1^\circ > E_2^\circ$ . This then would imply that catalytic oxidative activation of organometallic complexes to substitution is uncommon, with the reverse being true for reductive activation.

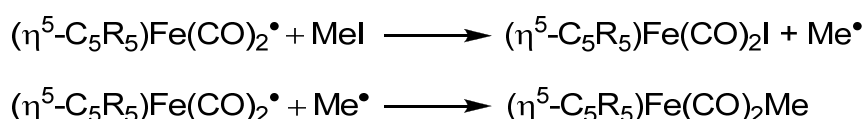


**Scheme 2.21:** Single and double CO substitution of  $RCpMn(CO)_3$

17-electron metal centred catalysts of the type  $(\eta^5-C_5Ph_4Ar)Fe(CO)_2\bullet$  (Ar = Ph, *p*-Tolyl) were reported by Baird in 1994.<sup>182</sup> These were synthesised by treatment of  $[Fe(\eta^5-C_5Ph_5)(CO)_2H]$  with  $Ph_3C\bullet$  to form  $[Fe(\eta^5-C_5Ph_5)(CO)_2]_2$ . This converts to the radical monomer upon radiation. The compound  $[CrCp(CO)_3]_2$  dissociates to its 17-electron radical monomer to the extent of a few percent in solution at room temperature, whereas, the  $[CrCp^*(CO)_3]_2$  dissociates to a much greater extent.<sup>183,184</sup> The 17-electron radicals  $CpCr(CO)_2PPh_3\bullet$  and  $(\eta^5-C_5Ph_5)Cr(CO)_3\bullet$  are completely

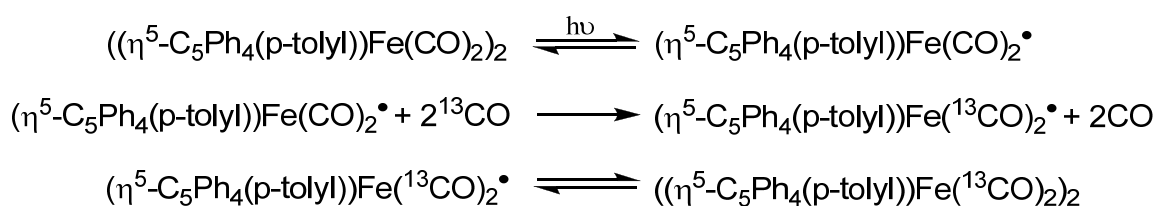
monomeric in solution and in the solid state.<sup>185-187</sup> The iron analogues were not found to convert to the monomeric radical as readily.<sup>188</sup>

Identification of the radical was confirmed by the rapid reaction of the pentaphenylCp dimer with MeI to form the iodo and methyl complexes. The  $[\text{Fe}(\eta^5\text{-C}_5\text{Ph}_4(p\text{-tolyl}))(\text{CO})_2]_2$  analogue was found to behave in a similar fashion. It reacts with methyl,  $\eta^1$ -allyl and (*tert*-butyl)iodides to form  $[\text{Fe}(\eta^5\text{-C}_5\text{Ph}_4(p\text{-tolyl}))(\text{CO})_2\text{I}]$  and the methyl, allyl and *tert*-butyl analogues. The reaction proceeds *via* a two-step mechanism.



**Scheme 2.22:** Reaction of  $(\eta^5\text{-C}_5\text{R}_5)\text{Fe}(\text{CO})_2^\bullet$  with MeI

$[\text{FeCp}(\text{CO})_2]_2$  had been found to be inert to CO substitution under thermal conditions, however, photochemical substitution was found to be facile.<sup>189</sup> This was attributed to the formation of the radical monomer. After photolysis of the dimer,  $(\eta^5\text{-C}_5\text{Ph}_4(p\text{-tolyl}))\text{Fe}(\text{CO})_2^\bullet$  was found to undergo  $^{13}\text{C}$ O substitution easily in relatively small concentrations. The monomers then recombined to form the relative dimer *via* the mechanism below, (**Scheme 2.23**).



**Scheme 2.23:** Substitution reaction of  $[\text{Fe}(\eta^5\text{-C}_5\text{Ph}_4(p\text{-tolyl}))(\text{CO})_2]_2$  with  $^{13}\text{C}$ O

$^{13}\text{C}$ O substitution had been observed for the  $\text{CpCr}(\text{CO})_3^\bullet$  complex, but proceeded at a slower rate.<sup>183</sup> Substitution in the *p*-tolyl iron complex proceeds *via* an associative mechanism as in the chromium complex and it was suggested that in spite of the

bulky ring substituent on the iron, the complex is less sterically hindered than the metal of CpCr(CO)<sub>3</sub>• with the three carbonyl groups attached.<sup>188</sup>

In attempt to stabilize the (η<sup>5</sup>-C<sub>5</sub>Ph<sub>4</sub>(*p*-tolyl))Fe(CO)<sub>2</sub>• radical, suspensions of [Fe(η<sup>5</sup>-C<sub>5</sub>Ph<sub>4</sub>(*p*-tolyl))(CO)<sub>2</sub>]<sub>2</sub> with PMe<sub>3</sub> were reacted in benzene and toluene at room temperature. Instead of the expected substituted monomer or dimer species, the slow formation of [Fe(CO)<sub>3</sub>(PMe<sub>3</sub>)] was observed as well as trace amounts of [Fe(η<sup>5</sup>-C<sub>5</sub>Ph<sub>4</sub>(*p*-tolyl))(CO)<sub>2</sub>H]. Further attempts by reacting [Fe(η<sup>5</sup>-C<sub>5</sub>Ph<sub>4</sub>(*p*-tolyl))(CO)<sub>2</sub>H] with Ph<sub>3</sub>C• and PMe<sub>3</sub> also proved unsuccessful. The reaction between [Fe(η<sup>5</sup>-C<sub>5</sub>Ph<sub>4</sub>(*p*-tolyl))(CO)(PMe<sub>2</sub>Ph)H] with the trityl radical also failed to provide the desired radical. However, upon reaction of (η<sup>5</sup>-C<sub>5</sub>Ph<sub>4</sub>(*p*-tolyl))Fe(CO)<sub>2</sub>• with P(OMe)<sub>3</sub>, three Arbuzov<sup>190</sup> products were formed (**A**), (**B**) and (**C**), (**Figure 2.15**).

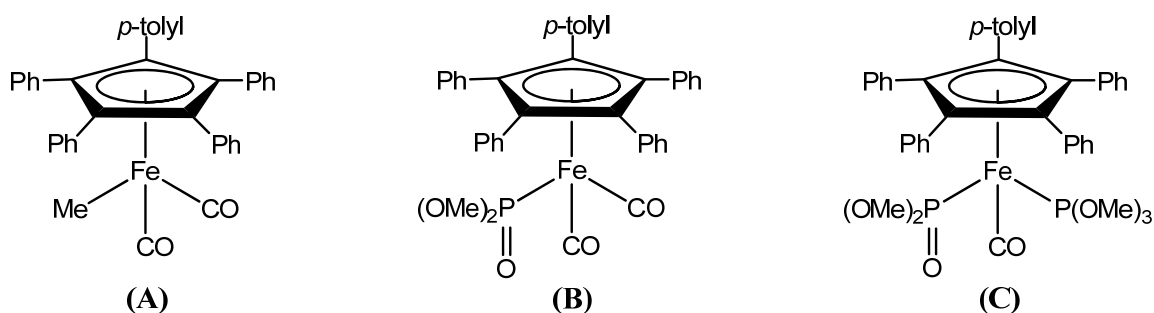
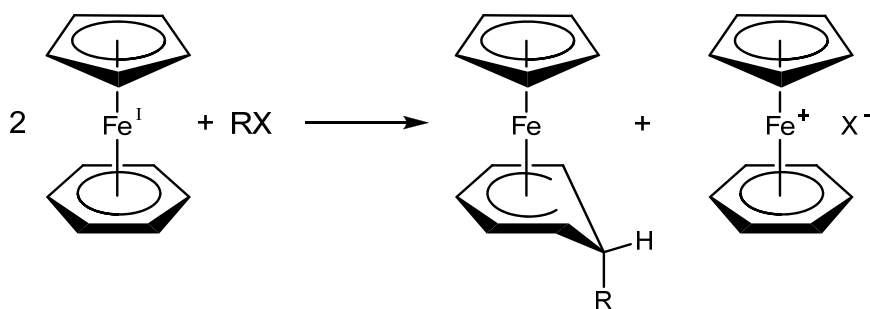


**Figure 2.15:** Arbuzov products formed from the reaction of (η<sup>5</sup>-C<sub>5</sub>Ph<sub>4</sub>(*p*-tolyl))Fe(CO)<sub>2</sub>• with P(OMe)<sub>3</sub>

#### 2.4.5 19-Electron Metal-Centre Radicals

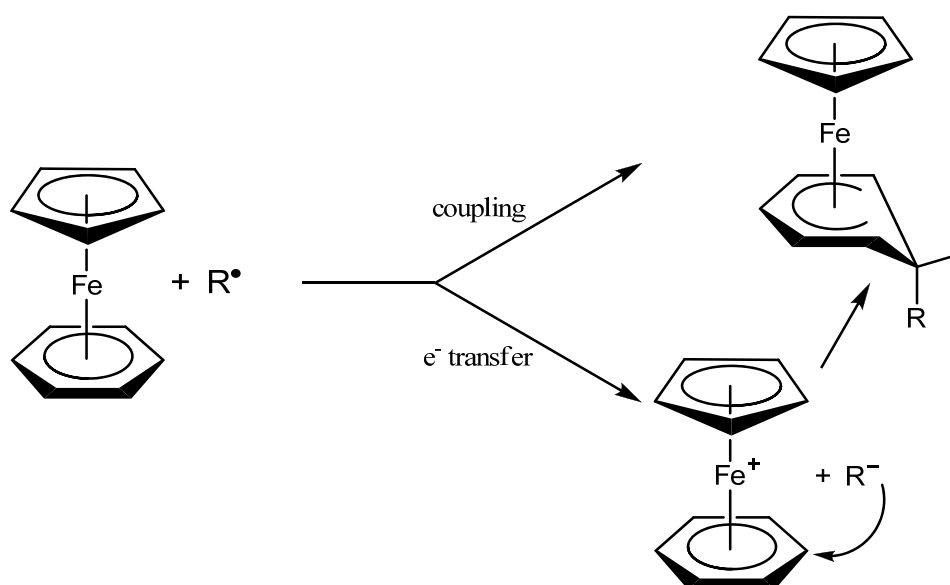
Generation of 19-electron species may be achieved by controlled-potential electrolysis, alkali-metal reduction or by the use of amalgams or alloys.<sup>191</sup> In some cases, such as in nickelocene and Fe(C<sub>6</sub>Me<sub>6</sub>)<sub>2</sub>, the 19-electron complex may be generated from the 20-electron complex by monoelectronic oxidation.<sup>192</sup> Monoelectronic oxidation of 18-electron complexes may provide thermally labile species. Stabilisation may be achieved by the use of ligands that can delocalise the 19<sup>th</sup> electron onto π systems and provide steric crowding, as utilised in the stabilisation of organic radicals.<sup>193</sup> One of the most effective methods of stabilisation is the use of peralkylated or sterically protected Cp or Ph ligands. Several series of 19-electron radicals that are stable at room temperature have been synthesised.<sup>194,195</sup> The

19-electron radical  $(\eta^5\text{-C}_5\text{H}_5)\text{Fe}(\eta^6\text{-C}_6(\text{CH}_3)_6)\cdot$  was shown to be a stable redox catalyst for the electroreduction of  $\text{NO}_2^-$  to  $\text{NH}_3$  in aqueous  $\text{LiOH}$ . The efficiency of this catalyst was further enhanced upon the addition of a carboxylate group on the Cp ring.<sup>196</sup>  $[\text{Fe}(\eta^5\text{-C}_5\text{H}_5)(\eta^6\text{-C}_6\text{H}_6)]$  reacts with various alkyl halides to give equimolecular amounts of Cp(cyclohexadienyl)iron and  $\text{CpFe}^+(\text{arene})$  cation as below, (**Scheme 2.24**).<sup>197</sup>



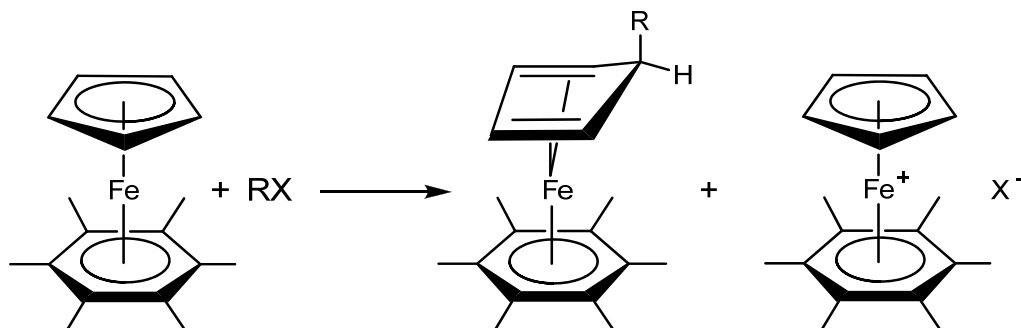
**Scheme 2.24:** The reaction of  $[\text{Fe}(\eta^5\text{-C}_5\text{H}_5)(\eta^6\text{-C}_6\text{H}_6)]$  with  $\text{RX}$  ( $\text{RX} = \text{CH}_3\text{I}, \text{CCl}_4, \text{PhCH}_2\text{Br}$ )

The first step is transfer of an electron from the Fe(I) complex to the alkyl halide, yielding the radical anion of the latter. The alkyl radical may then either couple with another molecule of the Fe(I) complex or oxidize it to give a carbocation which will nucleophilically attack the activated benzene ring, (**Scheme 2.25**).



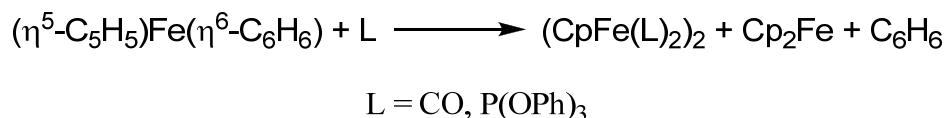
**Scheme 2.25:** Coupling or electron transfer reaction available to the Fe(I) complex

In the case of  $[\text{Fe}(\eta^5\text{-C}_5\text{H}_5)(\eta^6\text{-C}_6(\text{CH}_3)_6)]$ , permethylation of the arene changes the site of reaction to form  $[\text{Fe}^0(\eta^2\text{-C}_5\text{H}_4\text{R})(\eta^6\text{-C}_6(\text{CH}_3)_6)]$ , (**Scheme 2.26**).



**Scheme 2.26:** The reaction of the peralkylated arene complex with  $\text{RX}$

$[\text{Fe}(\eta^5\text{-C}_5\text{H}_5)(\eta^6\text{-C}_6\text{H}_6)]$  was also shown to form ferrocene and benzene upon heating in THF, indicating displacement of the arene.<sup>198</sup> It was also found that the arene ligand may be displaced by CO or triphenylphosphite, (**Scheme 2.27**). This would suggest that the arene moiety is bonded to the complex to a much weaker degree than the Cp.



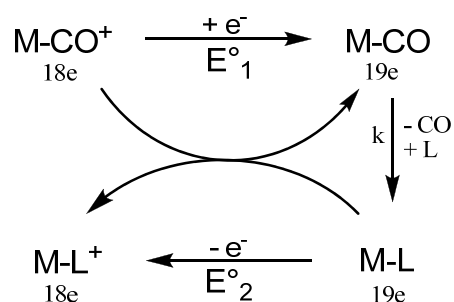
**Scheme 2.27:** The displacement of benzene from  $(\eta^5\text{-C}_5\text{H}_5)\text{Fe}(\eta^6\text{-C}_6\text{H}_6)$  by  $\text{L}$

Astruc *et al.* discovered that the reactions of  $[\text{Fe}(\eta^5\text{-C}_5\text{H}_5)(\eta^6\text{-C}_6\text{H}_6)]$  type complexes also offer a facile route to  $[\text{FeCpL}_2\text{H}]$  complexes ( $\text{L} = \text{PMe}_3, \text{PPh}_3, \text{PPh}_2\text{H}$  or  $\text{L}_2 = \text{dppm}, \text{dppe}$ ).<sup>199</sup> The hydride arises from H atom abstraction by the 17-electron radicals ( $\text{CpFeL}_2\bullet$ ) from the solvent, from a substrate or from impurities. Typically THF was used as the solvent, however, when the reaction was carried out with dppe in DCM,  $[\text{FeCpCl}(\text{dppe})]$  was the only iron complex isolated.

The rate of arene substitution of  $[\text{Fe}(\eta^5\text{-C}_5\text{H}_5)(\eta^6\text{-C}_6\text{H}_5\text{CH}_3)]$  by phosphorus donors was also studied by this group. The rate of substitution of the tolyl ring by  $\text{P}(\text{OMe})_3$  followed an associative mechanism with a rate constant  $k = 5 \times 10^{-3} \text{ m}^{-1}\text{s}^{-1}$  at  $-10^\circ\text{C}$ . The reaction rate for  $\text{PMe}_3$  increased by a factor of three when compared to that of

P(OMe)<sub>3</sub> and 4.5 times larger than that recorded for P(OPh)<sub>3</sub>. The nature of the displaced ligand was also shown to have a significant effect on the rate of substitution. The displacement of toluene proceeded 400 times faster than that recorded for the hexamethylbenzene analogue.

Sweigart *et al.* studied the rate of CO substitution in the 19-electron complexes CpFe(CO)<sub>3</sub><sup>+</sup> and IndFe(CO)<sub>3</sub><sup>+</sup>.<sup>200</sup> When investigating the CO substitution of the manganese analogues the group found the mechanism to proceed *via* a dissociative mechanism.<sup>201</sup> Both CpFe(CO)<sub>3</sub><sup>+</sup> and IndFe(CO)<sub>3</sub><sup>+</sup> were found to rapidly dissociate CO and dimerise upon reduction. The presence of P-donor nucleophiles inhibit the dimerisation reaction and an efficient electron transfer catalysed (ETC) substitution occurs to form CpFe(CO)2L<sup>+</sup> (**Scheme 2.28**).



**Scheme 2.28:** ETC CO substitution reactions of CpFe(CO)<sub>3</sub><sup>+</sup> and IndFe(CO)<sub>3</sub><sup>+</sup>

The rate of CO substitution of the indenyl complex was recorded to investigate whether the indenyl effect is operative in 19-electron systems. Previous reports showed that the rate of CO dissociation of IndMn(CO)<sub>2</sub>NO was very similar to that of the Cp analogue.<sup>202</sup> When the iron complexes were compared it was found that the indenyl complex underwent CO dissociation slower than the Cp complex by a factor of 10<sup>6</sup>. It was suggested that this was due to a relative stabilization of the ground state of the 19-electron radical without ring slippage, therefore increasing the activation energy of CO dissociation.<sup>200</sup>

## Chapter 3 Experimental

### 3.1 Solvents and Starting Materials

All experimental procedures were carried out under an atmosphere of nitrogen unless otherwise stated. All solvents were distilled by standard procedures. Toluene, xylene and diethyl ether were dried using sodium wire/benzophenone and stored over molecular sieves or sodium wire.

Column chromatography was carried out on Merck silica gel 60 (0.04-0.063mm) or Merck aluminium oxide 90 (0.2-0.062).

Triruthenium dodecacarbonyl ( $\text{Ru}_3(\text{CO})_{12}$ ) was supplied by Aldrich Chemicals. Cyclopentadiene and methylcyclopentadiene were prepared immediately before use by thermal cracking of their dimers.<sup>203</sup>

### 3.2 Instrumentation

Carbon, hydrogen and nitrogen analyses were conducted in the NUI, Galway Microanalytical Laboratory, using a Perkin-Elmer Model 2400 elemental analyser. Solution infrared spectra were recorded on a Perkin-Elmer Spectrum 1000 FT-IR spectrophotometer using a 1.0mm KRS-5 solution cell. Diamond-ATR IR spectra were recorded on a Perkin-Elmer Spectrum One FT-IR spectrophotometer fitted with an ATR device. NMR spectra were recorded on a JEOL LMN-LA400.

The molecular weight of 1,4-diphenyl-2-cyclopenta[*d*]pyridazine in solution was determined using a Knauer Vapour Pressure Osmometer K-7000.

Kinetic studies were carried out using a GRANT GP200 temperature controlled oil bath. The reaction mixture was stirred using a magnetic stir bar a magnet rotated by a stirrer motor to promote a homogenous temperature, (*Image 3.1*).

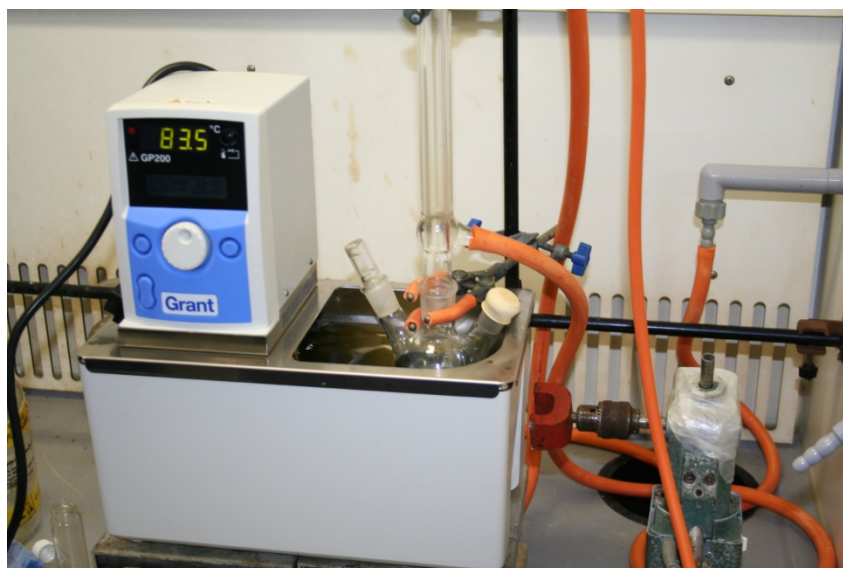


**Image 3.1:** *Kinetic measurement apparatus*

### 3.3 Synthesis of ArCOCl

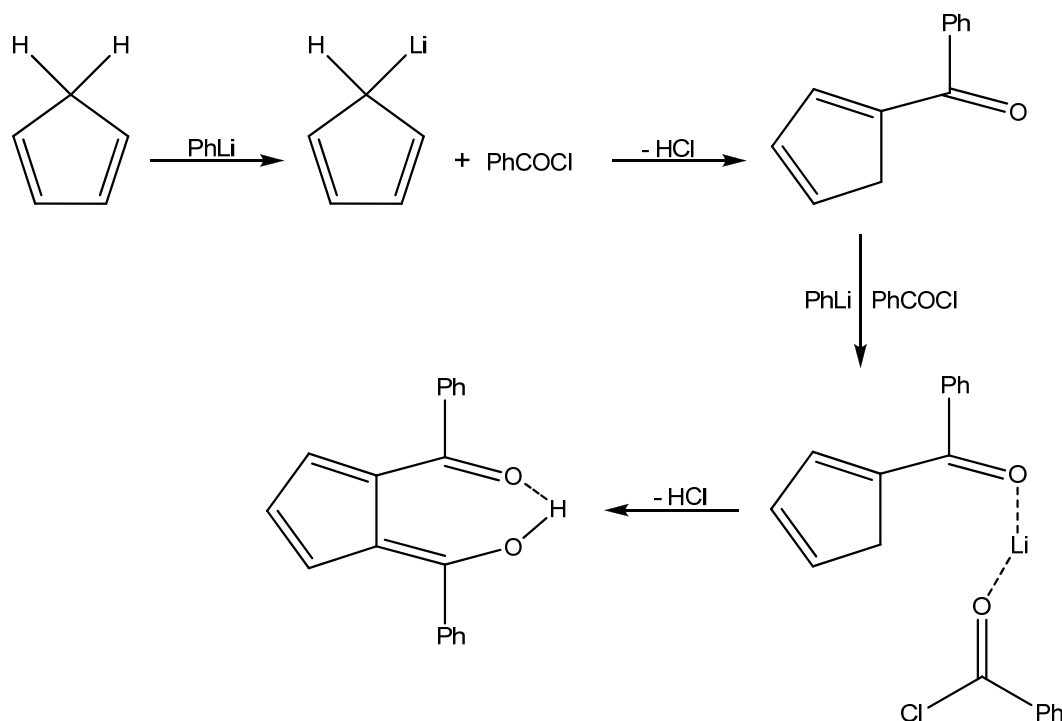
The ArCOCl compounds were synthesised following standard procedures. An excess of thionyl chloride was refluxed overnight with the relative carboxylic acid. The excess thionyl chloride was removed by vacuum distillation affording the desired product in good yield.

Acid	Chloride
Benzoic Acid	Benzoyl Chloride
<i>p</i> -Toluic Acid	<i>p</i> -Toluoyl Chloride
<i>p</i> -Chlorobenzoic Acid	<i>p</i> -Chlorobenzoyl Chloride
<i>o</i> - Chlorobenzoic Acid	<i>o</i> - Chlorobenzoyl Chloride

**Table 3.1:** *Acid chlorides synthesised*

### 3.4 Synthesis of Ligands

#### 3.4.1 Synthesis of dibenzoylcyclopentadiene (dbzCpH)



**Scheme 3.1:** Synthesis of dibenzoylcyclopentadiene

PhLi (25ml, 50 mmol) was added to 100ml of Et<sub>2</sub>O drop wise and the temperature was maintained at 0°C. Cyclopentadiene (3.34ml, 50 mmol) was added and a white precipitate was formed. The solution was then stirred for 15 minutes at room temperature. PhCOCl (7.03g, 50mmol) was added drop wise and the yellow solution was stirred for a further 30 minutes at room temperature. The solution was hydrolysed with dilute Acetic acid, the ether layer separated and the water layer was washed with ether three more times. The solution was then dried over Na<sub>2</sub>SO<sub>4</sub>, filtered and the solvent was removed *in vacuo*. The solid was recrystallised with glacial acetic acid, which yielded an orange-yellow compound. The dbzCpH was purified on a silica column with 50:50 DCM:Pet. Ether. After solvent removal *in vacuo* this produced a bright yellow solid. (3.9g, 28.43%)

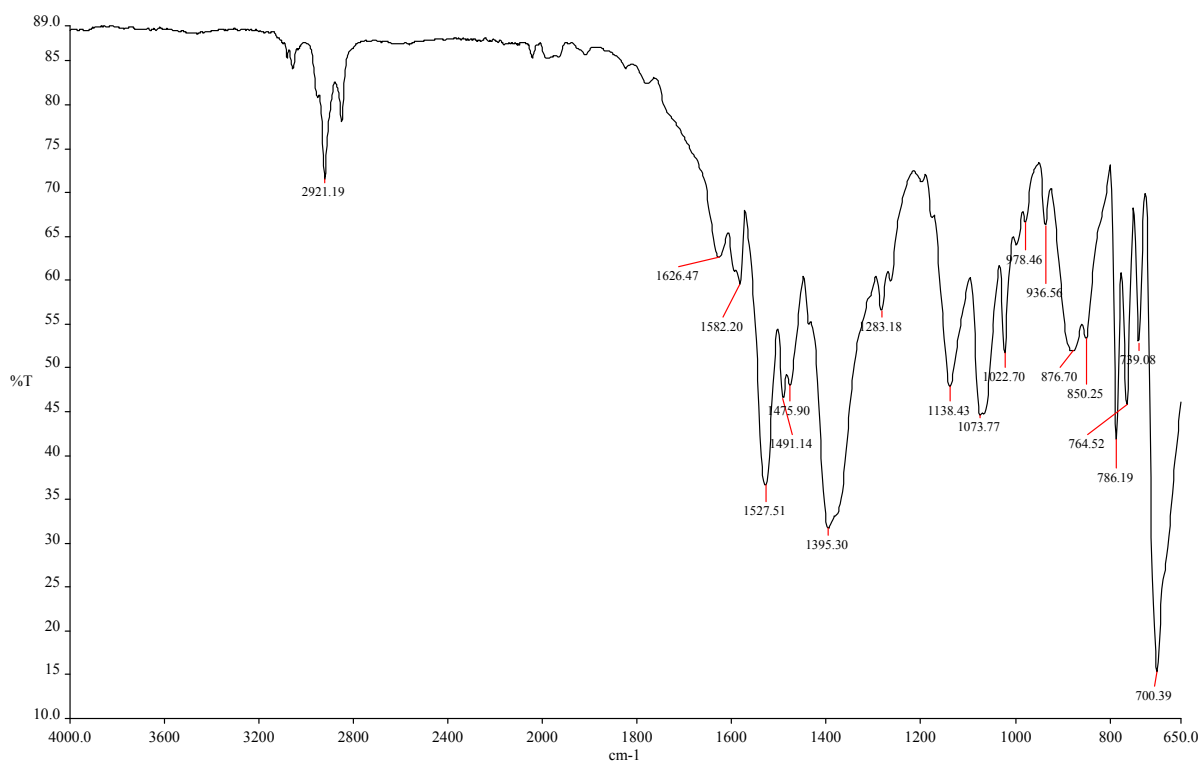


**Figure 3.1:** Infrared spectrum of dbzCpH

$^1\text{H NMR}$  ( $\text{CDCl}_3$ ) (400MHz):  $\delta$ 1.55 (1H),  $\delta$ 6.5 (t, 1H)  $\delta$ 7.79-7.25 (12H)

$\text{M}^+$ : 274

**Elemental Analysis:**

Theory:	%C 83.21	%H 5.11
Found:	%C 83.76	%H 5.90

### 3.4.2 Synthesis of $C_5H_4(CO-p-tol)_2$

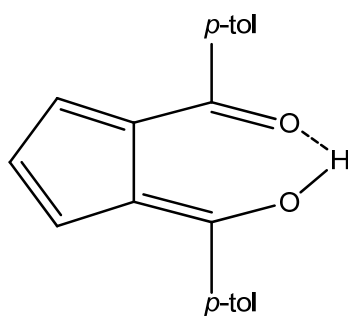
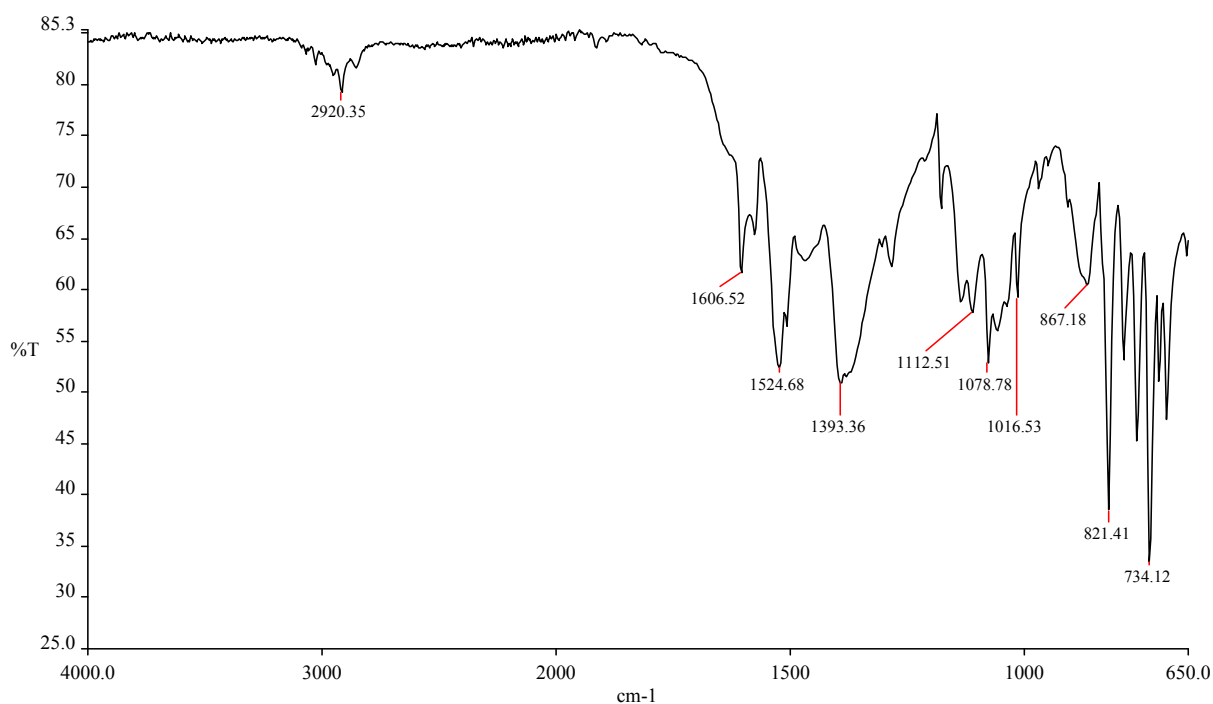


**Figure 3.2:**  $C_5H_4(CO-p-tol)_2$

The synthesis was carried out in a similar fashion to that reported for dbzCpH, where *p*-tolulyl chloride was used in the place of benzoyl chloride to yield a bright yellow crystalline solid. (4.77g, 31.54%)

**$^1H$  NMR ( $CDCl_3$ ) (400MHz):**  $\delta$ 1.55 (s, 1H),  $\delta$ 2.45 (s, 6H),  $\delta$ 6.5 (t, 1H),  $\delta$ 7.77-7.20



(10H)

**Figure 3.3:** Infrared spectrum of  $C_5H_4(CO-p-tol)_2$

#### Elemental analysis

Theory:	%C 83.44	%H 5.96
Found:	%C 81.05	%H 5.76

### 3.4.3 Synthesis of $(\text{CH}_3)\text{C}_5\text{H}_3(\text{CO-}p\text{-tol})_2$

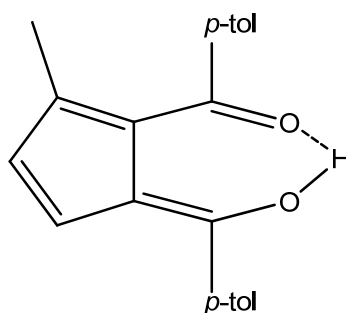


**Figure 3.4:**  $(\text{CH}_3)\text{C}_5\text{H}_3(\text{CO-}p\text{-tol})_2$

This reaction was carried out in a similar fashion to that described in 3.4.1 but with methylcyclopentadiene in the place of CpH. Purification on a silica column with 50:50 DCM:Pet. ether yielded a bright yellow crystalline solid. (5.24g, 33.12%).

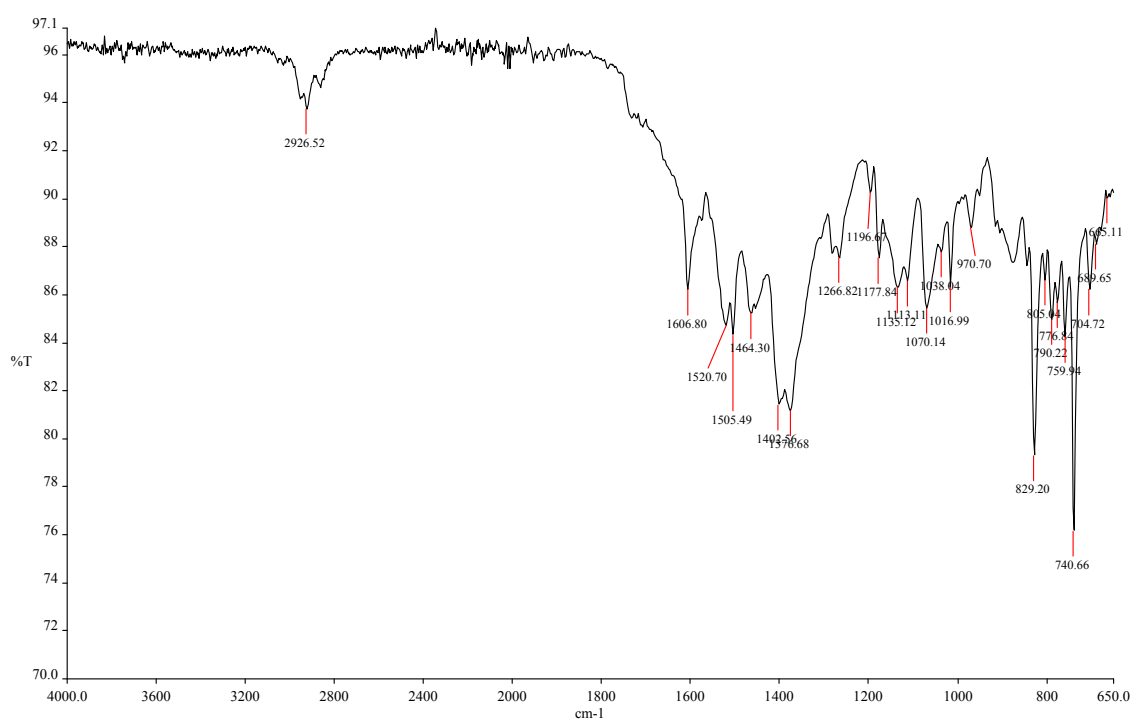


**Figure 3.5:** Infrared spectrum of  $(\text{CH}_3)\text{C}_5\text{H}_3(\text{CO-}p\text{-tol})_2$

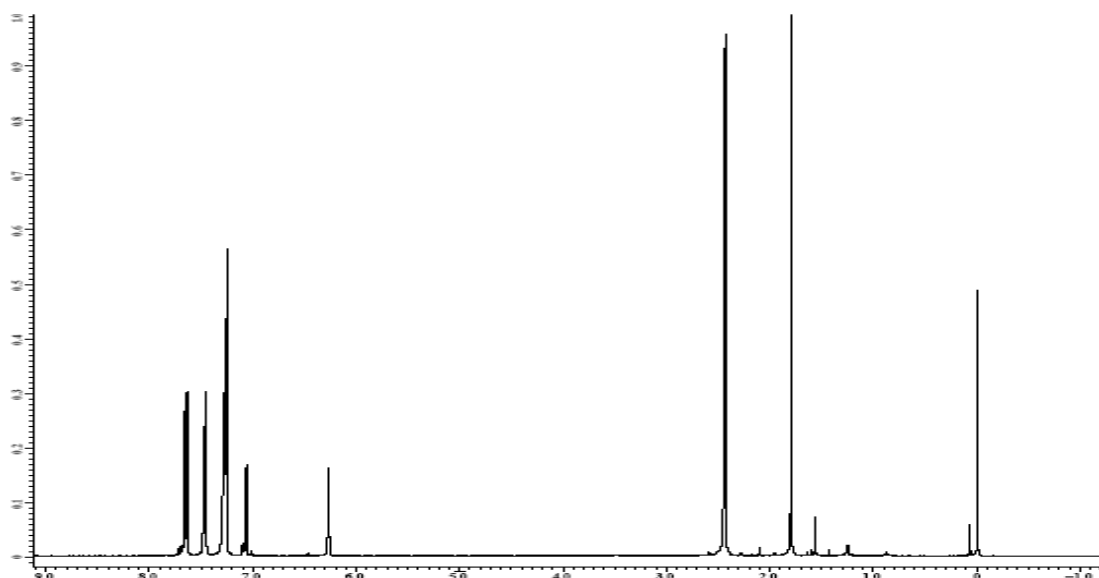


**Figure 3.6:**  $^1\text{H}$  NMR ( $\text{CDCl}_3$ ) of  $(\text{CH}_3)\text{C}_5\text{H}_3(\text{CO-p-tol})_2$

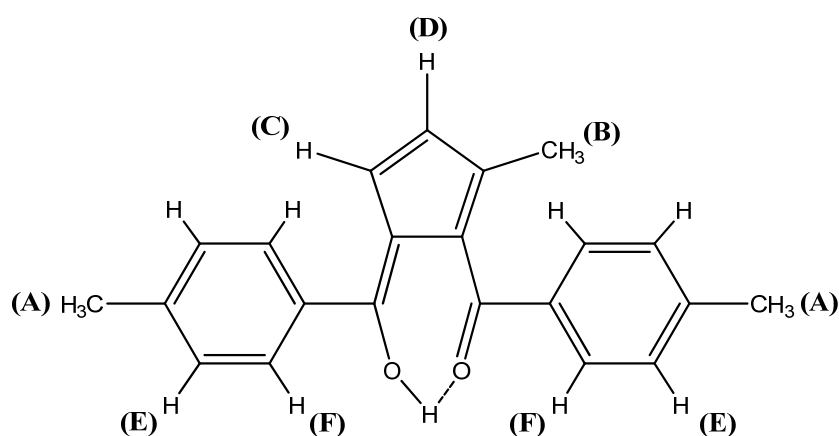


**Figure 3.7:**  $^1\text{H}$  NMR hydrogen assignment

$\delta$ Chemical Shift (ppm)	Hydrogen Assignment
1.79 s	A (6H)
2.49 d	B (3H)
6.27 d	C (1H)
7.06 d	D (1H)
7.24-7.30 m	E (4H)
7.4-7.7 m	F (4H)

**Table 3.2:** Hydrogen assignment for  $(\text{CH}_3)\text{C}_5\text{H}_3(\text{CO-p-tol})_2$

For  $\text{H}_\text{C}$ :  $\text{H}_\text{D}$   $J = 4.12\text{Hz}$ . The  $^1\text{H}$  NMR above confirms the proposed structure of  $(\text{CH}_3)\text{C}_5\text{H}_3(\text{CO-p-tol})_2$

### 3.4.4 Synthesis of $C_5H_4(CO-p-ClC_6H_4)_2$

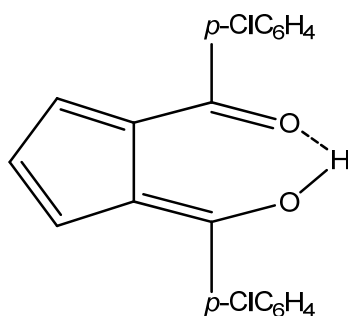


**Figure 3.8:**  $C_5H_4(CO-p-ClC_6H_4)_2$

The reaction was carried out in a similar fashion to the 3.4.1. *p*-Chlorobenzoic acid was used in the place of benzoic acid. Purification on a silica column with 50:50 DCM:Pet ether yielded a bright yellow crystalline compound, (0.832g, 4.86%).

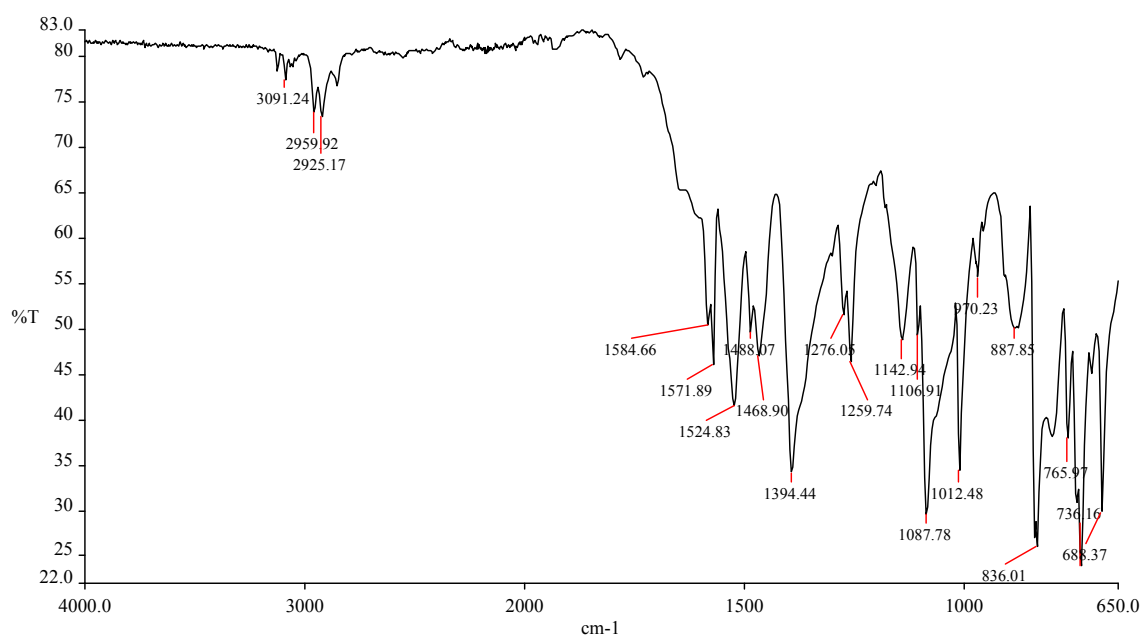


**Figure 3.9:** Infrared spectrum of  $C_5H_4(CO-p-ClC_6H_4)_2$

#### Elemental analysis

Theory:	%C 66.47	%H 3.49
Found:	%C 65.36	%H 3.80

### 3.4.5 Synthesis of $C_5H_4(CO-o-ClC_6H_4)_2$

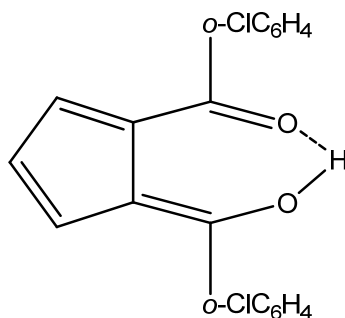


**Figure 3.10:**  $C_5H_4(CO-o-ClC_6H_4)_2$

This reaction was carried out in a similar fashion to **3.4.1**. *o*-Chlorobenzoic acid was used in the place of benzoic acid. Purification on a silica column with 50:50 DCM:Pet ether yielded a bright yellow crystalline compound, (3.15g, 18.42%).

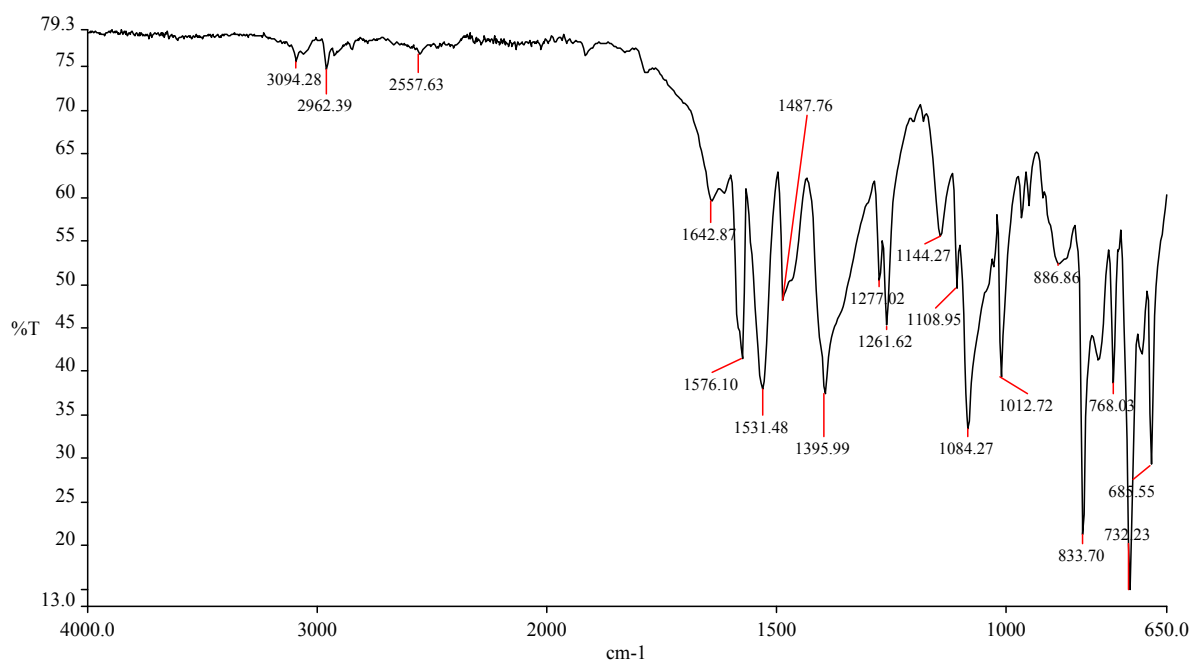


**Figure 3.11:** Infrared spectrum of  $C_5H_4(CO-o-ClC_6H_4)_2$

#### Elemental analysis

Theory:	%C 66.47	%H 3.49
Found:	%C 65.99	%H 4.26

### 3.4.6 Synthesis of 1,4-diphenyl-cyclopenta[d]pyridazine

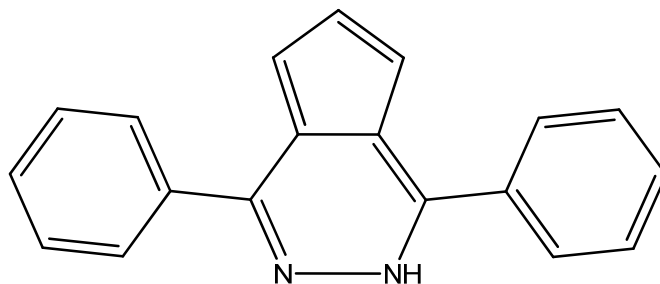


**Figure 3.12:** 1,4-diphenyl-cyclopenta[d]pyridazine

dbzCpH (1.0g, 4.05mmol) and 1g of 85% solution of hydrazine hydrate were heated under reflux in 20ml of absolute ethanol for 2 hours. The product was obtained as fluffy yellow crystals upon cooling, (0.83g, 75.81%). This was then recrystallised from hot ethanol to yield a yellow crystalline solid.

The same quantities of dbzCpH and hydrazine were heated under reflux in 120ml absolute ethanol for two hours. Upon cooling of the reaction solution the product was afforded in a similar yield but in this incidence as orange plates. These plates were then recrystallised with DCM/Hexane to yield bright yellow needle-like crystals. The needle-like crystals could then be reconverted to the plate polymorph by heating in 50ml absolute ethanol with the addition of one drop of hydrazine.

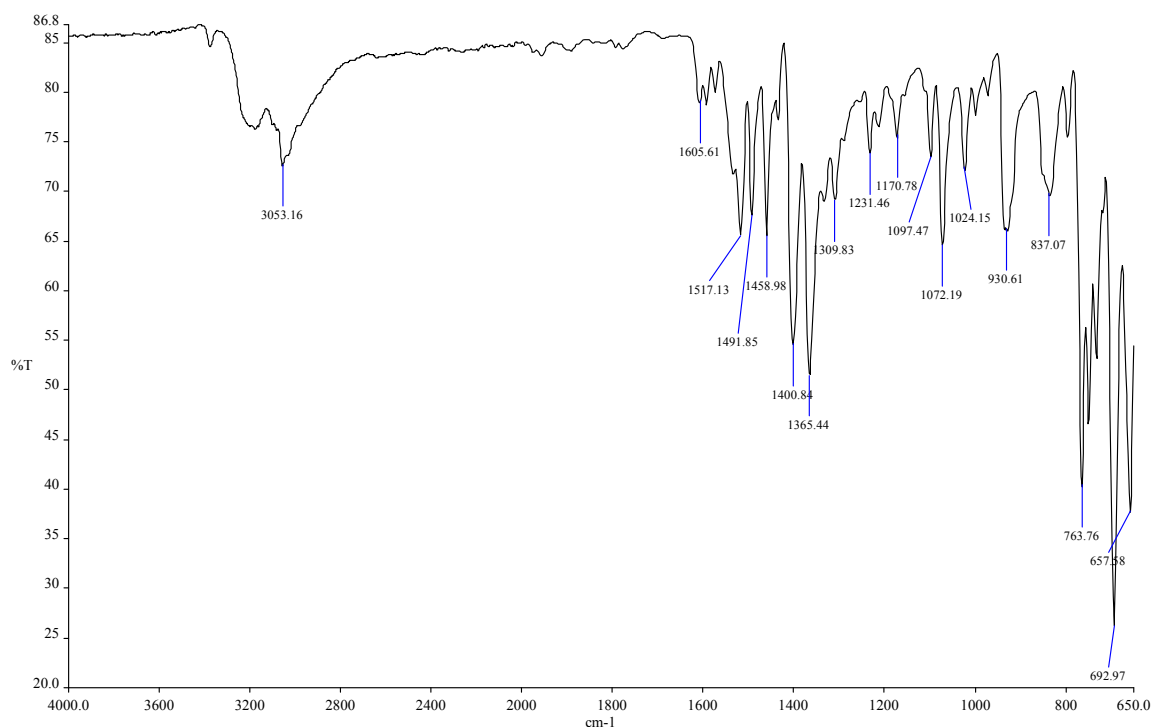


**Figure 3.13:** Infrared spectrum of 1,4-diphenyl-cyclopenta[d]pyridazine

### Elemental analysis

Theory:	%C 84.42	%H 5.22	%N 10.36
Found:	%C 85.29	%H 5.38	%N 10.59

Crystal structures of both polymorphs were obtained.

### 3.4.7 Synthesis of $C_5H_5CPh_3$

Sodium hydride (0.92g, 38.5mmol) was washed twice with 20ml portions of petroleum ether, dried and treated with 100ml THF. The solution was cooled in an ice bath. CpH (3.24ml, 38.5mmol) was added and once the solution had cleared  $Ph_3CCl$  (9.06g, 32.5mmol) was added. The solution was then heated under reflux for 2 hours. The THF was removed *in vacuo* and the resultant liquid was washed four times with 10ml portions of water. The product was purified by recrystallisation from petroleum ether, (7.04g, 59.28%).<sup>204</sup>

### Elemental analysis

Theory:	%C 93.46	%H 6.54
Found:	%C 91.61	%H 6.67

### 3.4.8 Synthesis of $(COPh)_2C_5H_3CPh_3$

PhLi (11.5ml, 23mmol) was added to 100ml of  $Et_2O$  and the temperature was maintained at 0°C.  $C_5H_5CPh_3$  (7.04g, 22.83mmol) was added, upon which a white precipitate formed. The solution was allowed to stir for 15 minutes at room temperature.  $PhCOCl$  (3.21g, 22.83mmol) was then added drop wise and the yellow solution was stirred for a further 30 minutes at room temperature. The solution was hydrolysed with dilute acetic acid, the ether layer separated and the water layer was washed with ether three times. The solution was then dried over  $Na_2SO_4$  and the solvent removed *in vacuo*. The solid was recrystallised with glacial acetic acid, which yielded a bright yellow compound. The product was purified on a silica column and eluted with a 50:50 DCM:Hexane solvent ratio to yield a bright yellow powder, (3.86g, 32.73%).

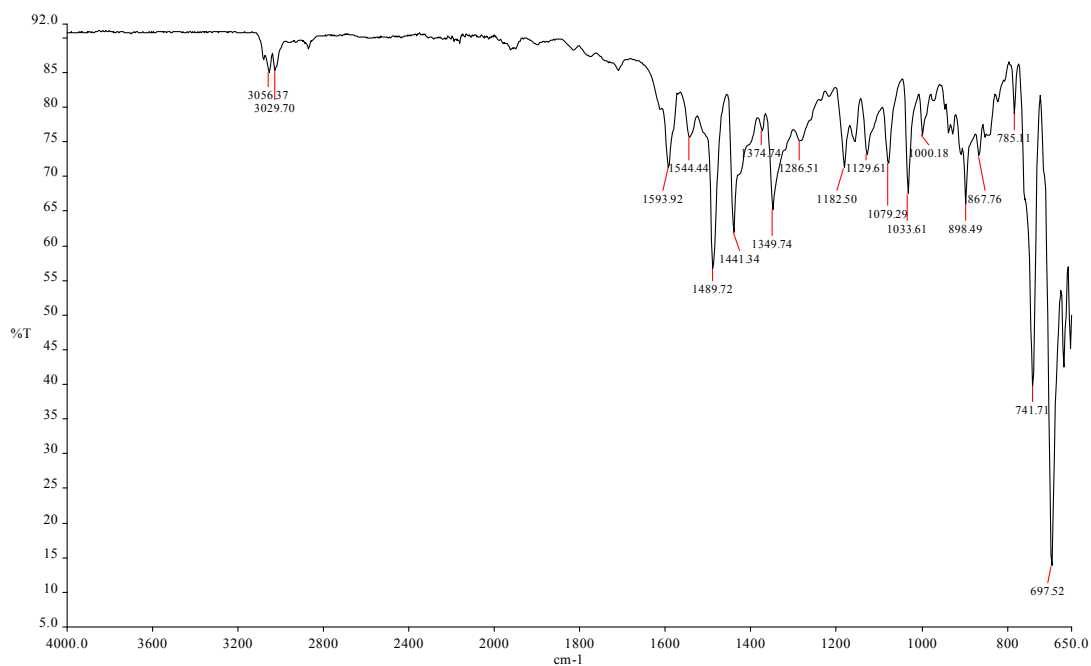


**Figure 3.14:** Infrared spectrum of  $(COPh)_2C_5H_3CPh_3$

### Elemental analysis

Theory:	%C 88.34	%H 5.46
Found:	%C 88.35	%H 5.66

### 3.4.9 Attempted benzoylation of indene

The attempted synthesis of a 1,2-dibenzoyl substituted indene was carried out as for the dibenzoylation of cyclopentadiene, **3.4.1**. However, upon analysis the 1,2-dibenzoylated product was not achieved. X-Ray analysis and the IR spectrum confirmed the production of the ester product formed.

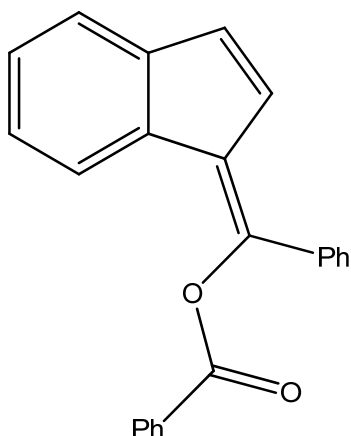


**Figure 3.15:** Product formed from the attempted dibenzoylation of indene

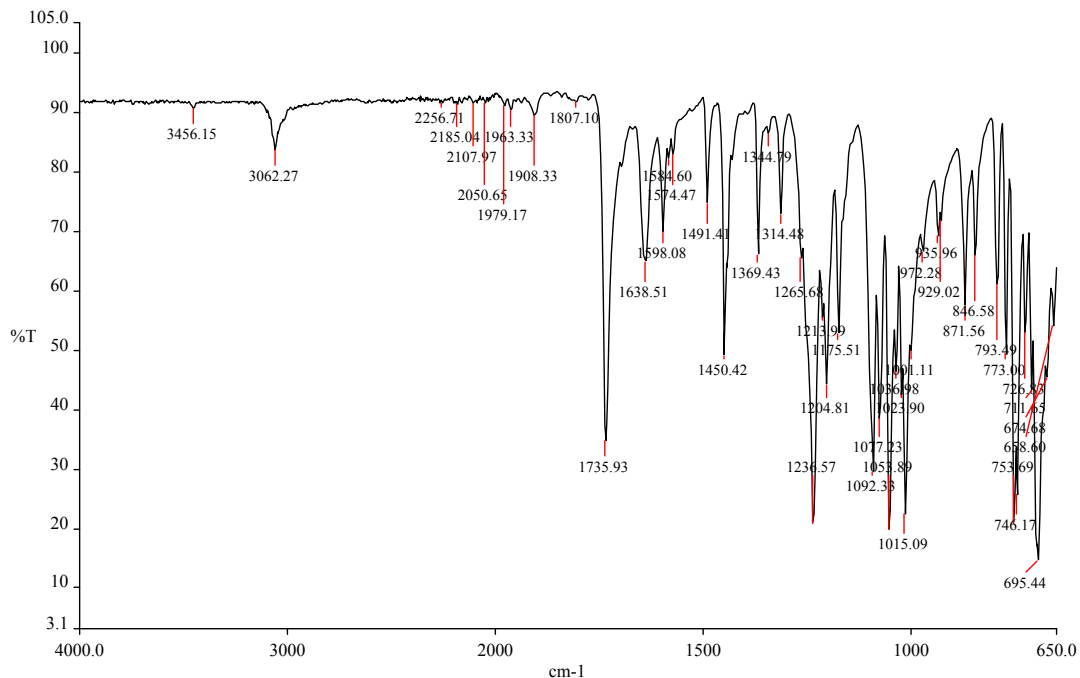
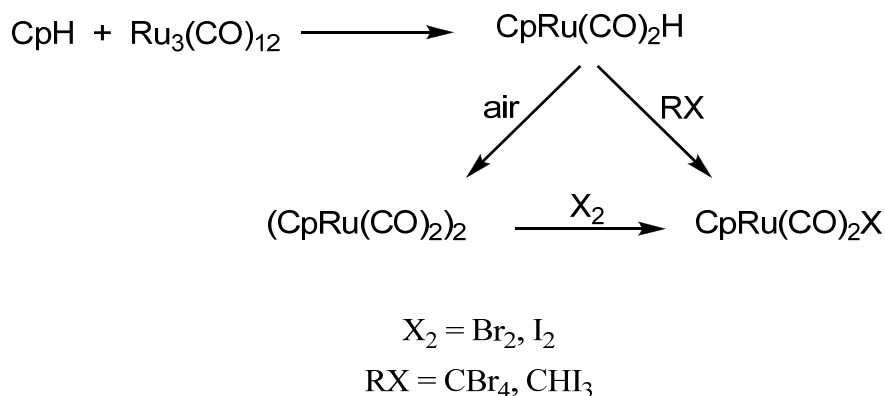


**Figure 3.16:** Infrared spectrum of the ester product

### 3.5 Synthesis of Parent Cyclopentadienyl Complexes

#### 3.5.1 Synthesis of [RuCp(CO)<sub>2</sub>X]



**Scheme 3.2:** Synthesis of parent Cp complexes

$\text{Ru}_3(\text{CO})_{12}$  (0.25g, 0.39mmol) was heated under reflux with freshly cracked cyclopentadiene (0.5ml, 6.13mmol) in 150ml of heptane for 2.5 hours. The solution was then aerated for 5 minutes. This converted the hydride to the dimer. The complex was purified on an alumina column and 3.5:1.5 Hexane:DCM eluted a bright orange band. This was dried to give a bright orange powder, (0.0552g, 20.51%).<sup>27</sup>  $\text{I}_2$  (0.03g, 0.12mmol) was dissolved in the minimum amount of DCM and added drop wise to a stirred solution of  $(\text{CpRu}(\text{CO})_2)_2$  and then stirred for 30 minutes. After drying the compound was separated on an alumina column. The product was eluted with 2:1 Hexane:DCM affording a brown solid, (0.023g, 28.75%).

An alternative to direct reaction of the dimer with halogen also was used.<sup>205</sup> Using the hydride generated above, the relative amount of alkyl halide was added. For the formation of the iodide, iodoform (0.154g, 0.39mmol) was added and heated under reflux for a further 30 minutes. The product was eluted on an alumina column with 2:1 Hexane:DCM affording a brown solid, (0.118g, 86.67%).

The bromide was formed by the addition of  $\text{CBr}_4$  (0.13g, 0.39mmol) to the hydride and left to reflux for a further 30 minutes. Separation on an alumina column with 2:1 Hexane:DCM yielded a brown product, (0.109g, 92.53%).

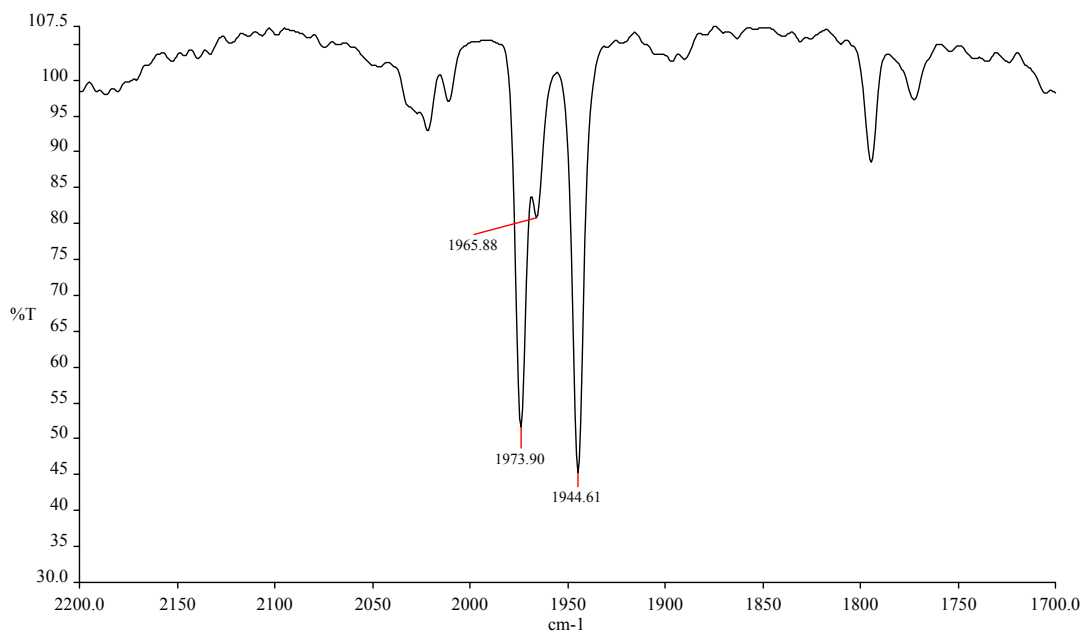


**Figure 3.17:** FT-IR of [RuCp(CO)<sub>2</sub>H]

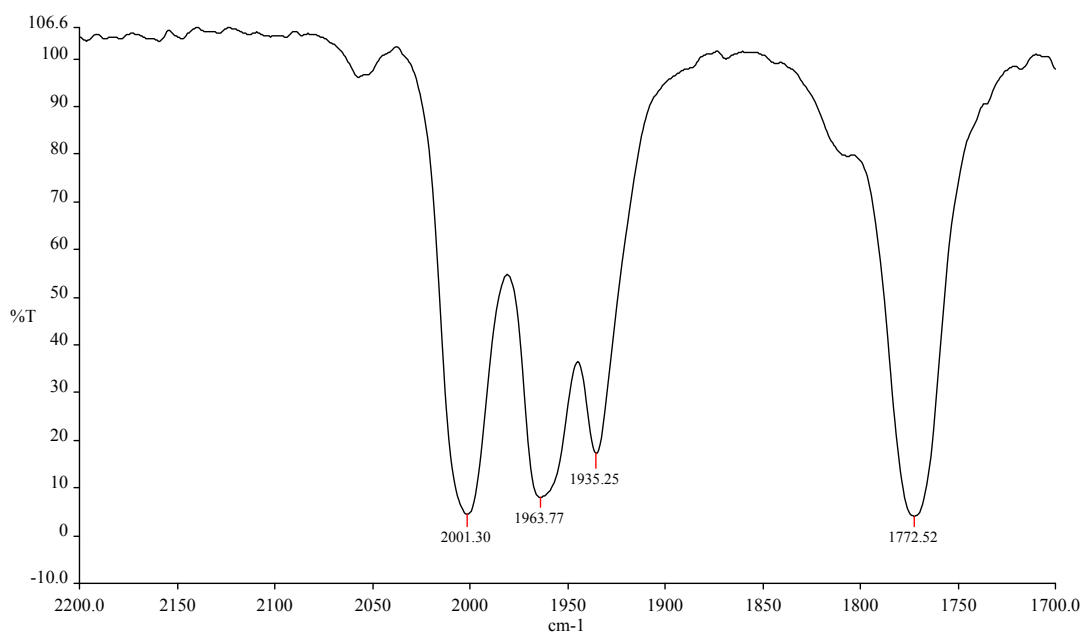


**Figure 3.18:** FT-IR of [RuCp(CO)<sub>2</sub>]<sub>2</sub>

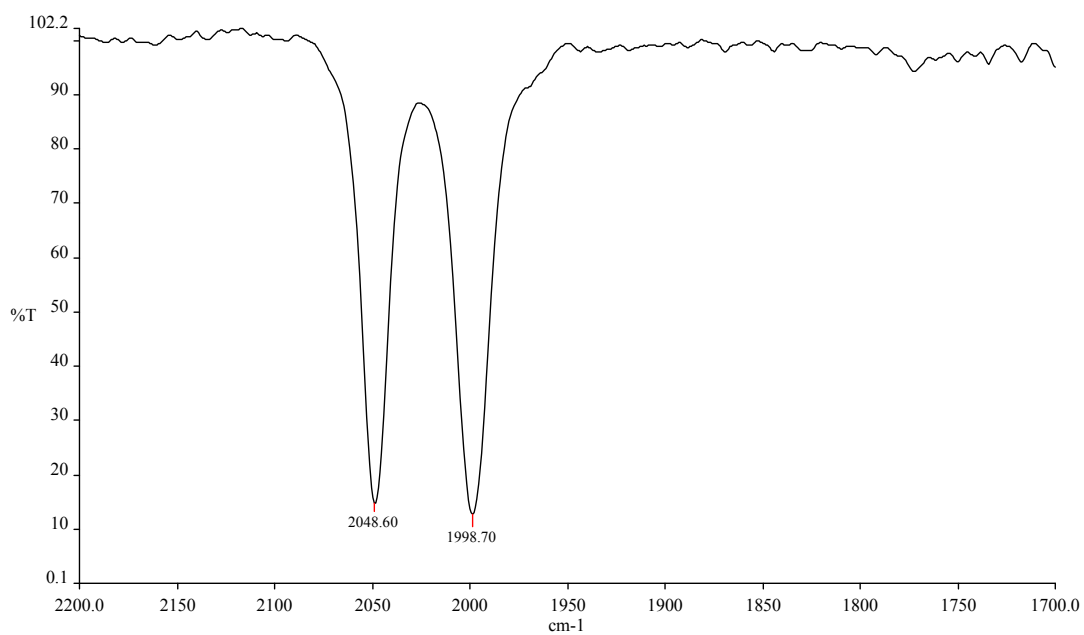


**Figure 3.19:** FT-IR of [RuCp(CO)<sub>2</sub>I]

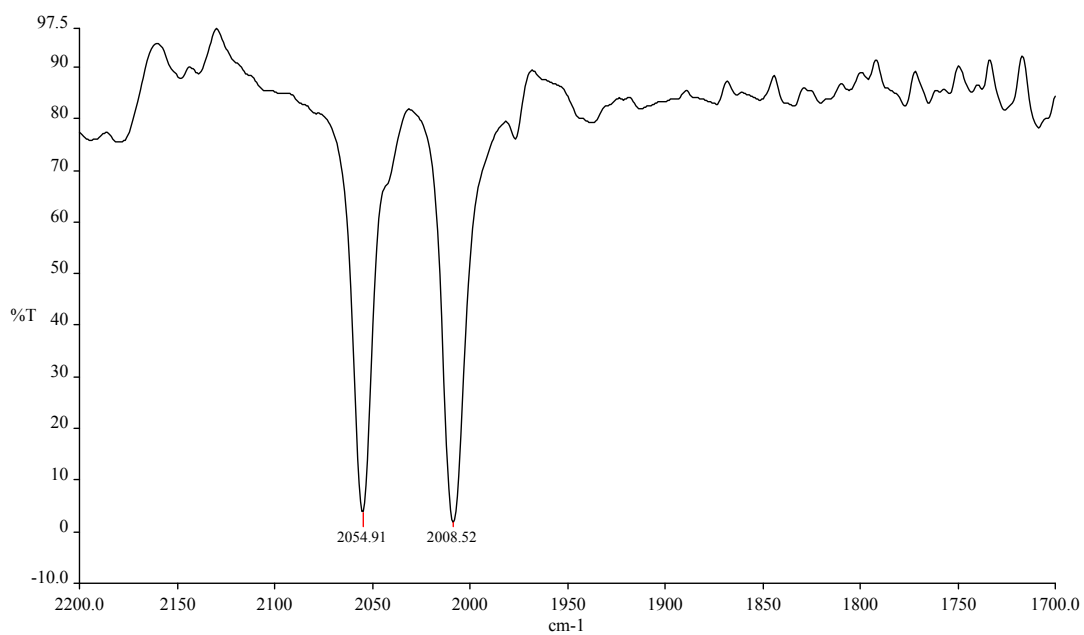


**Figure 3.20:** FT-IR of [RuCp(CO)<sub>2</sub>Br]

### 3.5.2 Synthesis of $[\text{RuCp}(\text{CO})\text{PPh}_3\text{X}]$

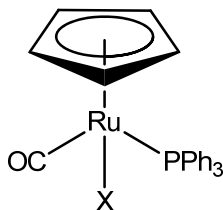


**Figure 3.21:**  $[\text{RuCp}(\text{CO})\text{PPh}_3\text{X}]$ , ( $X = \text{I}, \text{Br}$ )

$[\text{RuCp}(\text{CO})_2\text{I}]$  (0.034g, 0.1mmol) was heated under reflux with a 15 molar excess of triphenylphosphine (0.383g, 1.46mmol) in xylene for 24hrs. The product was separated on an alumina column with 2:1 Hexane:DCM, (0.049g, 85.89%).

$[\text{RuCp}(\text{CO})_2\text{Br}]$  (0.05g, 0.165mmol) was heated under reflux with a 50% excess of triphenylphosphine (0.065g, 0.25mmol) in xylene for 24hrs. The product was separated on an alumina column with 2:1 Hexane:DCM, (0.074g, 84.1%).

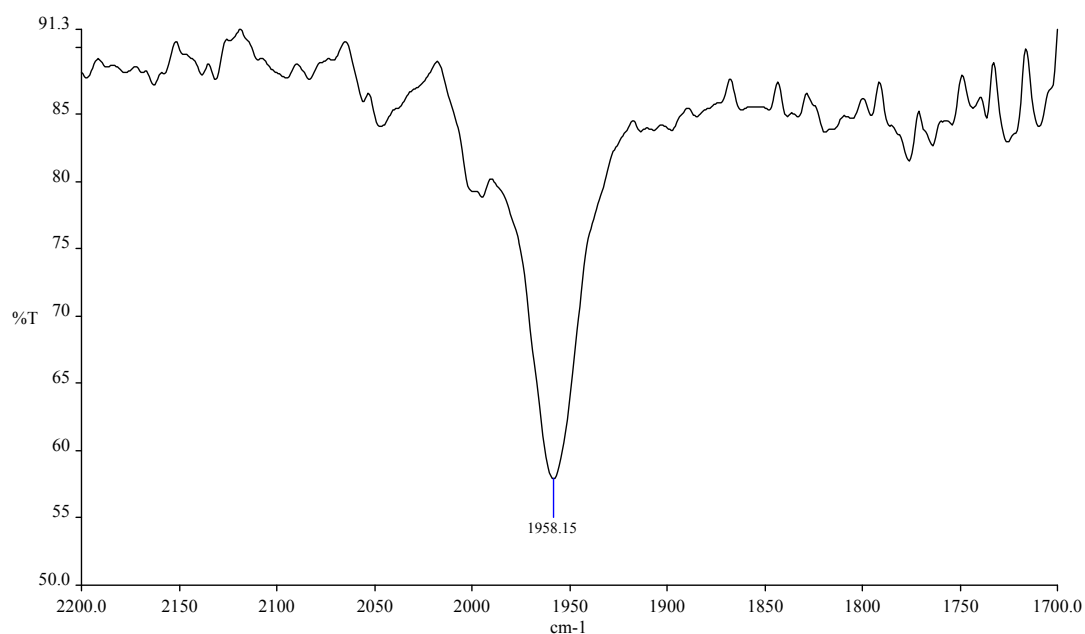


**Figure 3.22:** FT-IR of  $[\text{RuCp}(\text{CO})\text{IPPh}_3]$

### 3.6 Synthesis of dbzCp Ruthenium Dimeric Complexes

#### 3.6.1 Synthesis of $[\text{Ru}(\eta^5\text{-1,2-C}_5\text{H}_3(\text{COPh})_2)(\text{CO})_2]_2$

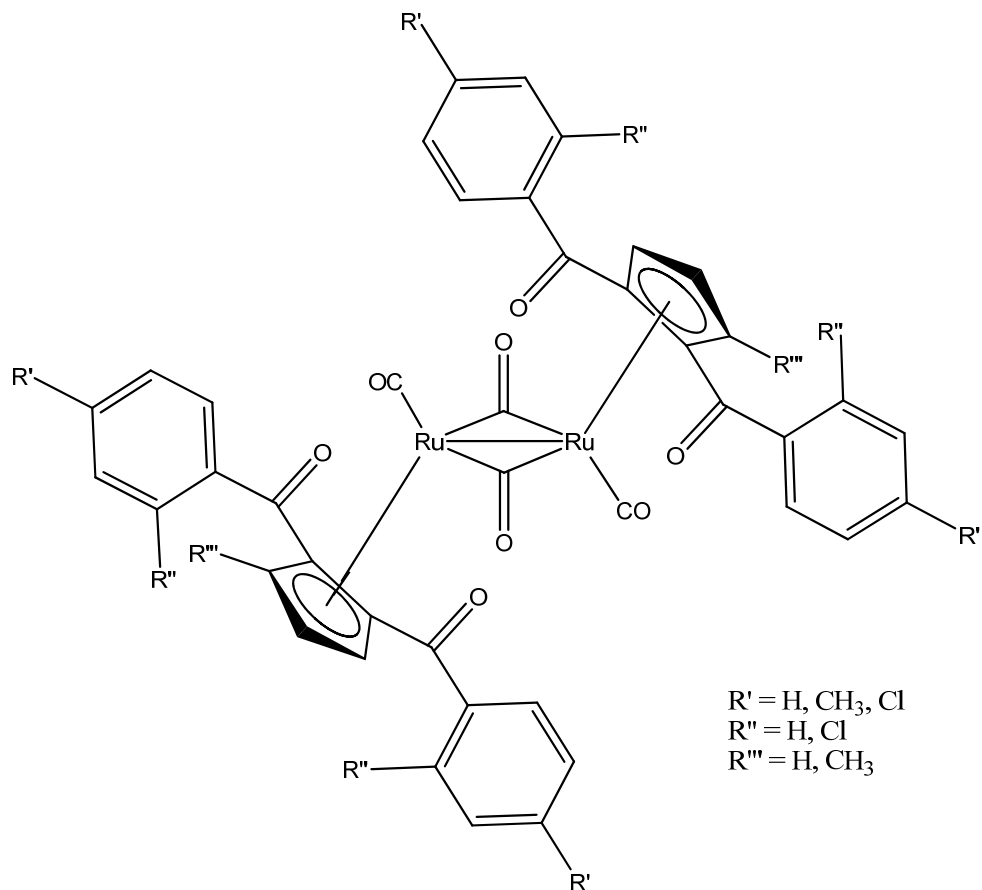


**Figure 3.23:** Dimeric complexes

$\text{Ru}_3(\text{CO})_{12}$  (0.17g, 0.26mmol) and dbzCpH (0.22g, 0.79mmol) were heated under reflux in toluene for 8hrs. The dimer was purified on an alumina column and eluted with 80:20 DCM:Et<sub>2</sub>O, (0.22g, 63.53%).

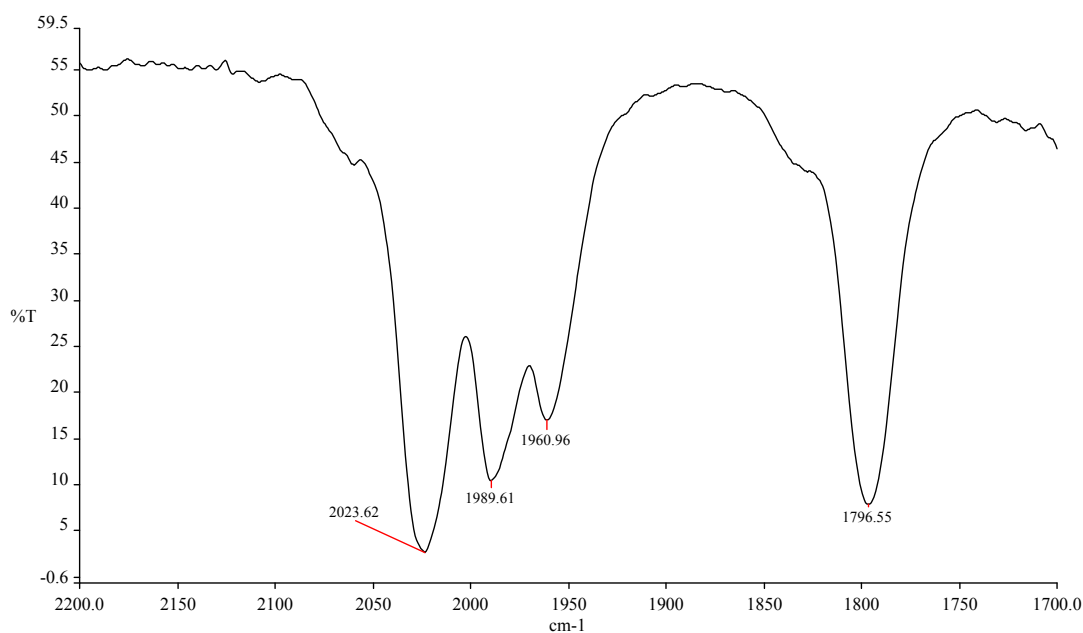


**Figure 3.24:** FT-IR of  $[Ru(\eta^5-1,2-C_5H_3(COPh)_2(CO)_2)_2]$

#### Elemental Analysis:

Theory:	%C 58.60	%H 3.02
Found:	%C 59.49	%H 2.91

#### 3.6.2 Synthesis of $[Ru(\eta^5-1,2-C_5H_3(CO-p-tol)_2(CO)_2)_2]$

$C_5H_4(CO-p-tol)_2$  (0.22g, 0.79mmol) was heated under reflux with  $Ru_3(CO)_{12}$  (0.17g, 0.26mmol) in **3.6.1**. The product was purified on an alumina column and eluted with 80:20 DCM:Et<sub>2</sub>O, (0.296g, 82.68%).

#### Elemental analysis

Theory:	%C 60.26	%H 3.71
Found:	%C 59.30	%H 3.68

#### 3.6.3 Synthesis of $[Ru(\eta^5-1,2-(CH_3)C_5H_2(CO-p-tol)_2(CO)_2)_2]$

$(CH_3)C_5H_3(CO-p-tol)_2$  (0.475g, 1.5mmol) was reacted with  $Ru_3(CO)_{12}$  (0.32g, 0.5mmol) as in **3.6.1**. Elution on an alumina column with 80:20 DCM:Et<sub>2</sub>O resulted in a brown crystalline solid, (0.265g, 86.36%).

### Elemental analysis

Theory:        %C 60.95        %H 4.02  
Found:        %C 59.56        %H 3.36

### 3.6.4 Synthesis of $[\text{Ru}(\eta^5\text{-1,2-C}_5\text{H}_3(\text{CO-}p\text{-ClC}_6\text{H}_4)_2(\text{CO})_2)_2]$

$\text{C}_5\text{H}_4(\text{CO-}p\text{-ClC}_6\text{H}_4)_2$  (0.271g, 0.79mmol) and  $\text{Ru}_3(\text{CO})_{12}$  (0.17g, 0.26mmol) were heated under reflux overnight as in 3.6.1. Elution on an alumina column with 80:20 DCM:Et<sub>2</sub>O resulted in a brown crystalline solid, (0.3g, 76.92%).

### Elemental analysis

Theory:        %C 50.54        %H 2.22  
Found:        %C 52.69        %H 2.29

### 3.6.5 Synthesis of $[\text{Ru}(\eta^5\text{-1,2-C}_5\text{H}_3(\text{CO-}o\text{-ClC}_6\text{H}_4)_2(\text{CO})_2)_2]$

$\text{C}_5\text{H}_4(\text{CO-}o\text{-ClC}_6\text{H}_4)_2$  (0.27g, 0.79mmol) and  $\text{Ru}_3(\text{CO})_{12}$  (0.17g, 0.26mmol) were heated under reflux overnight as in 3.6.1. The product was eluted with 80:20 DCM:Et<sub>2</sub>O, yielding a brown crystalline solid, (0.282g, 71.8%).

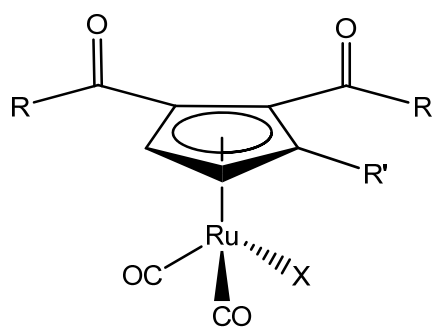
### Elemental analysis

Theory:        %C 50.54        %H 2.22  
Found:        %C 51.86        %H 3.12

Metal Complex	$\nu_{\text{MC-O}}$ (cm <sup>-1</sup> ) in DCM	$\Delta$
$[\text{RuCp}(\text{CO})_2]_2$	2001, 1964, 1935, 1772	
$[\text{Ru}(\eta^5\text{-1,2-C}_5\text{H}_3(\text{COPh})_2)(\text{CO})_2]_2$	2024, 1990, 1961, 1797	23, 34, 26, 25
$[\text{Ru}(\eta^5\text{-1,2-C}_5\text{H}_3(\text{CO-}p\text{-tol})_2)(\text{CO})_2]_2$	2020, 1988, 1950, 1794	19, 24, 25, 22
$[\text{Ru}(\eta^5\text{-1,2-}(\text{CH}_3)\text{C}_5\text{H}_3(\text{CO-}p\text{-tol})_2)(\text{CO})_2]_2$	2020, 1979, 1789	19, 15, -, 17
$[\text{Ru}(\eta^5\text{-1,2-C}_5\text{H}_3(\text{CO-}p\text{-ClC}_6\text{H}_4)_2)(\text{CO})_2]_2$	2024, 1989, 1957, 1796	23, 25, 22, 24
$[\text{Ru}(\eta^5\text{-1,2-C}_5\text{H}_3(\text{CO-}o\text{-ClC}_6\text{H}_4)_2)(\text{CO})_2]_2$	2026, 1989, 1803	25, 22, -, 31

**Table 3.3:**  $\nu_{\text{MC-O}}$  for dimeric complexes

### 3.7 Synthesis of dbzCp Ruthenium Halide Complexes



R = Ph, p-tol, p-Cl-C<sub>6</sub>H<sub>4</sub>, o-Cl-C<sub>6</sub>H<sub>4</sub>

R' = H, CH<sub>3</sub>

**Figure 3.25:** *dbzCp Ruthenium Dicarboxyl Halide Complexes*

#### 3.7.1 Synthesis of [Ru( $\eta^5$ -1,2-C<sub>5</sub>H<sub>3</sub>(COPh)<sub>2</sub>)(CO)<sub>2</sub>I]

I<sub>2</sub> (0.065g, 0.0256mmol) was dissolved in the minimal amount of DCM and added drop wise to a stirred solution of [Ru( $\eta^5$ -1,2-C<sub>5</sub>H<sub>3</sub>)(CO)<sub>2</sub>]<sub>2</sub> (0.22g, 0.256mmol) in 100ml DCM. This was left to stir for a further 30 minutes. The product was eluted with 80:20 DCM:Et<sub>2</sub>O on an alumina column. This yielded a brown crystalline compound, (0.175g, 61.33 %). The absence of a bridging carbonyl peak in the FT-IR indicates a successful cleavage of the M–M bond.<sup>206</sup>

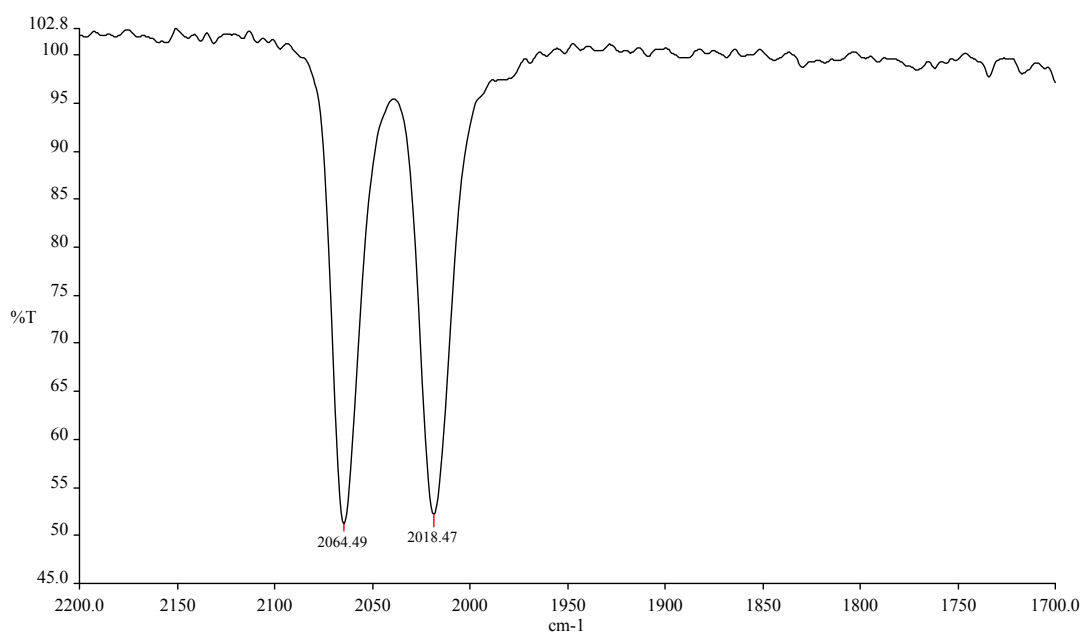


**Figure 3.26:** *FT-IR of [Ru( $\eta^5$ -1,2-C<sub>5</sub>H<sub>3</sub>(COPh)<sub>2</sub>)(CO)<sub>2</sub>I]*

### Elemental Analysis:

Theory:	%C 45.24	%H 2.33
Found:	%C 43.52	%H 2.91

#### 3.7.2 Synthesis of $[\text{Ru}(\eta^5\text{-1,2-C}_5\text{H}_3(\text{COPh})_2)(\text{CO})_2\text{Br}]$

25.6ml of a 0.01M  $\text{Br}_2$  solution in DCM was added to a stirred solution of  $[\text{Ru}(\eta^5\text{-1,2-C}_5\text{H}_3(\text{CO})_2)_2]$  (0.22g, 0.256mmol) in 100ml DCM. This was then left to stir for a further 30 minutes. The product was eluted with 80:20 DCM:Et<sub>2</sub>O on an alumina column. This yielded a brown crystalline compound, (0.162g, 62.0%).

### Elemental analysis

Theory:	%C 45.24	%H 2.33
Found:	%C 43.52	%H 2.91

#### 3.7.3 Synthesis of $[\text{Ru}(\eta^5\text{-1,2-C}_5\text{H}_3(\text{CO-}i>p\text{-tol})_2)(\text{CO})_2\text{I}]$

The *p*-tol analogue was synthesized and purified in a similar fashion to 3.7.1 to yield a brown crystalline complex, (0.512g, 50.7%).

### Elemental analysis

Theory:	%C 47.17	%H 2.91
Found:	%C 46.78	%H 2.98

#### 3.7.4 Synthesis of $[\text{Ru}(\eta^5\text{-1,2-(CH}_3\text{)C}_5\text{H}_2(\text{CO-}i>p\text{-tol})_2)(\text{CO})_2\text{I}]$

The synthesis and purification was carried out in a similar fashion to 3.7.1 to yield a brown crystalline solid, (0.143g, 44.64%).

### Elemental analysis

Theory:	%C 48.32	%H 3.19
Found:	%C 48.43	%H 3.45

### 3.7.5 Synthesis of $[\text{Ru}(\eta^5\text{-1,2-C}_5\text{H}_3(\text{CO-}p\text{-ClC}_6\text{H}_4)_2(\text{CO})_2\text{I}]$

The synthesis and purification was carried out in a similar fashion to 3.7.1 to yield a brown crystalline solid, (0.134g, 41.02%).

#### Elemental analysis

Theory:        %C 50.49        %H 2.20  
 Found:        %C 48.56        %H 3.51

### 3.7.6 Synthesis of $[\text{Ru}(\eta^5\text{-1,2-C}_5\text{H}_3(\text{CO-}o\text{-ClC}_6\text{H}_4)_2(\text{CO})_2\text{I}]$

The synthesis and purification was carried out in a similar fashion 3.7.1 to yield a brown crystalline solid, (0.110g, 33.67%).

#### Elemental analysis

Theory:        %C 50.49        %H 2.20  
 Found:        %C 49.62        %H 3.10

Metal Complex	$\nu_{\text{MC-O}}$ ( $\text{cm}^{-1}$ ) in DCM	$\Delta(\text{Parent})$
$[\text{RuCp}(\text{CO})_2\text{I}]$	2047, 1997	
$[\text{Ru}(\eta^5\text{-1,2-C}_5\text{H}_3(\text{COPh})_2)(\text{CO})_2\text{I}]$	2064, 2019	17, 22
$[\text{Ru}(\eta^5\text{-1,2-C}_5\text{H}_4(\text{CO-}p\text{-tol})_2)(\text{CO})_2\text{I}]$	2063, 2014	16, 19
$[\text{Ru}(\eta^5\text{-1,2-}(\text{CH}_3)\text{C}_5\text{H}_3(\text{CO-}p\text{-tol})_2)(\text{CO})_2\text{I}]$	2061, 2013	14, 18
$[\text{Ru}(\eta^5\text{-1,2-C}_5\text{H}_4(\text{CO-}p\text{-ClC}_6\text{H}_4)_2)(\text{CO})_2\text{I}]$	2060, 2014	13, 17
$[\text{Ru}(\eta^5\text{-1,2-C}_5\text{H}_4(\text{CO-}o\text{-ClC}_6\text{H}_4)_2)(\text{CO})_2\text{I}]$	2060, 2015	13, 18

**Table 3.4:**  $\nu_{\text{MC-O}}$  for iodo complexes

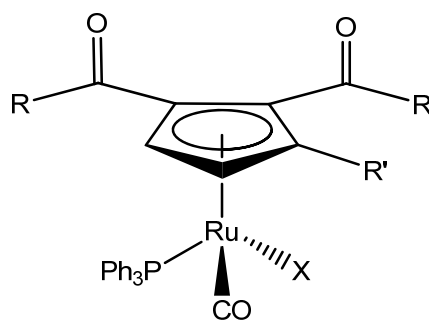
Metal Complex	$\nu_{\text{MC-O}}$ ( $\text{cm}^{-1}$ ) in DCM	$\Delta(\text{Parent})$
$[\text{RuCp}(\text{CO})_2\text{Br}]$	2055, 2008	
$[\text{Ru}(\eta^5\text{-1,2-C}_5\text{H}_3(\text{COPh})_2)(\text{CO})_2\text{Br}]$	2071, 2024	16, 16
$[\text{Ru}(\eta^5\text{-1,2-C}_5\text{H}_4(\text{CO-}p\text{-tol})_2)(\text{CO})_2\text{Br}]$	2065, 2019	10, 9
$[\text{Ru}(\eta^5\text{-1,2-}(\text{CH}_3)\text{C}_5\text{H}_3(\text{CO-}p\text{-tol})_2)(\text{CO})_2\text{Br}]$	2066, 2018	11, 10

**Table 3.5:**  $\nu_{\text{MC-O}}$  for bromo complexes

Metal Complex	$\nu_{\text{MC-O}}$ ( $\text{cm}^{-1}$ ) in DCM	$\Delta(\text{Parent})$
$[\text{RuCp}(\text{CO})_2\text{Cl}]$	2058, 2008	
$[\text{Ru}(\eta^5\text{-1,2-C}_5\text{H}_3(\text{COPh})_2)(\text{CO})_2\text{Cl}]$	2073, 1926	15, 18

**Table 3.6:**  $\nu_{\text{MC-O}}$  for chloro complexes

### 3.8 Synthesis of Triphenylphosphine Derivatives



R = Ph, p-tol, p-Cl-C<sub>6</sub>H<sub>4</sub>, o-Cl-C<sub>6</sub>H<sub>4</sub>

R' = H, CH<sub>3</sub>

**Figure 3.27:** *dbzCp Ruthenium Triphenylphosphine Complexes*

#### 3.8.1 Synthesis of [Ru( $\eta^5$ -1,2-C<sub>5</sub>H<sub>3</sub>(COPh)<sub>2</sub>)(CO)IPPh<sub>3</sub>]

[Ru( $\eta^5$ -1,2-C<sub>5</sub>H<sub>3</sub>)(CO)<sub>2</sub>I] (0.2g, 0.35mmol) and PPh<sub>3</sub> (0.14g, 0.53mmol) were heated under reflux in 150ml xylene for 30 minutes. The product was eluted with an 80:20 DCM:Et<sub>2</sub>O solvent ratio on an alumina column, (0.26g, 93.86%).

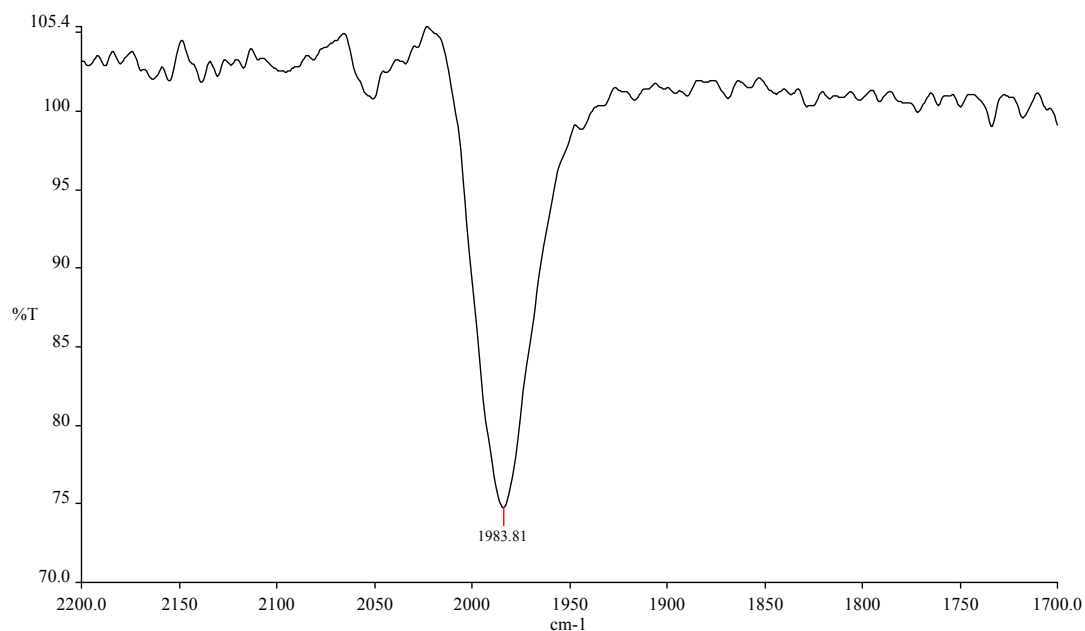


**Figure 3.28:** *FT-IR of [Ru( $\eta^5$ -1,2-C<sub>5</sub>H<sub>3</sub>(COPh)<sub>2</sub>)(CO)IPPh<sub>3</sub>]*

#### Elemental analysis

Theory:	%C 57.66	%H 3.57
Found:	%C 56.50	%H 3.09

### 3.8.2 Synthesis of $[\text{Ru}(\eta^5\text{-1,2-C}_5\text{H}_3(\text{CO-}i>p\text{-tol})_2)_2(\text{CO})\text{IPPh}_3]$

The synthesis and purification were carried out as in 3.8.1 and the product was recorded in a similar yield.

### 3.8.3 Synthesis of $[\text{Ru}(\eta^5\text{-1,2-(CH}_3\text{)C}_5\text{H}_2(\text{CO-}i>p\text{-tol})_2)_2(\text{CO})\text{IPPh}_3]$

The procedure was as in 3.8.1.

### 3.8.4 Synthesis of $[\text{Ru}(\eta^5\text{-1,2-C}_5\text{H}_3(\text{CO-}i>p\text{-ClC}_6\text{H}_4)_2)_2(\text{CO})\text{IPPh}_3]$

The procedure was as in 3.8.1.

Metal Complex	$\nu_{\text{MC-O}}$ ( $\text{cm}^{-1}$ ) in DCM	$\Delta(\text{Parent})$
$[\text{RuCp}(\text{CO})\text{IPPh}_3]$	1958	
$[\text{Ru}(\eta^5\text{-1,2-C}_5\text{H}_3(\text{COPh})_2)(\text{CO})\text{IPPh}_3]$	1984	26
$[\text{Ru}(\eta^5\text{-1,2-C}_5\text{H}_4(\text{CO-}i>p\text{-tol})_2)(\text{CO})\text{IPPh}_3]$	1986	28
$[\text{Ru}(\eta^5\text{-1,2-(CH}_3\text{)C}_5\text{H}_3(\text{CO-}i>p\text{-tol})_2)(\text{CO})\text{IPPh}_3]$	1978	20
$[\text{Ru}(\eta^5\text{-1,2-C}_5\text{H}_4(\text{CO-}i>p\text{-ClC}_6\text{H}_4)_2)(\text{CO})\text{IPPh}_3]$	1974	16
$[\text{Ru}(\eta^5\text{-1,2-C}_5\text{H}_4(\text{CO-}i>o\text{-ClC}_6\text{H}_4)_2)(\text{CO})\text{IPPh}_3]$	1975	17

**Table 3.7:**  $\nu_{\text{MC-O}}$  for  $\text{PPh}_3$  substituted complexes

## 3.9 Synthesis of Indenyl Complexes

### 3.9.1 Synthesis of $[\text{RuInd}(\text{CO})_2]_2$

Indene (0.694g, 6.0mmol) was heated under reflux with  $\text{Ru}_3(\text{CO})_{12}$  (0.2g, 0.31mmol) in xylene for 14 hours. The dimer was purified on an Alumina column and eluted with 50:50 DCM:Hexane to yield an orange product, (0.24g, 93.71%).<sup>207</sup>

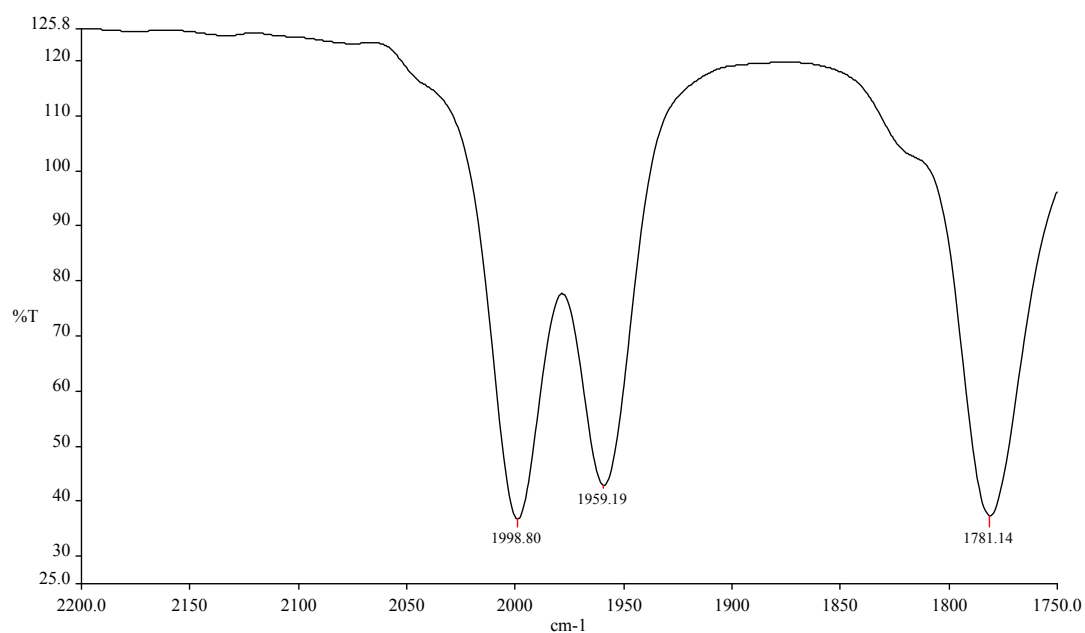


**Figure 3.29:** FT-IR of  $[\text{RuInd}(\text{CO})_2]_2$

#### Elemental analysis

Theory:	%C 48.53	%H 2.59
Found:	%C 48.76	%H 2.48

### 3.9.2 Synthesis of [RuInd(CO)<sub>2</sub>I]

I<sub>2</sub> (0.1g, 0.4mmol) was dissolved in the minimal amount of DCM and added dropwise to a stirred solution of [RuInd(CO)<sub>2</sub>]<sub>2</sub> (0.22g, 0.4mmol) in DCM and stirred for a further 30 minutes. The product was eluted off an alumina column with 50:50 DCM:Hexane to yield an orange product, (0.287g, 89.72%).

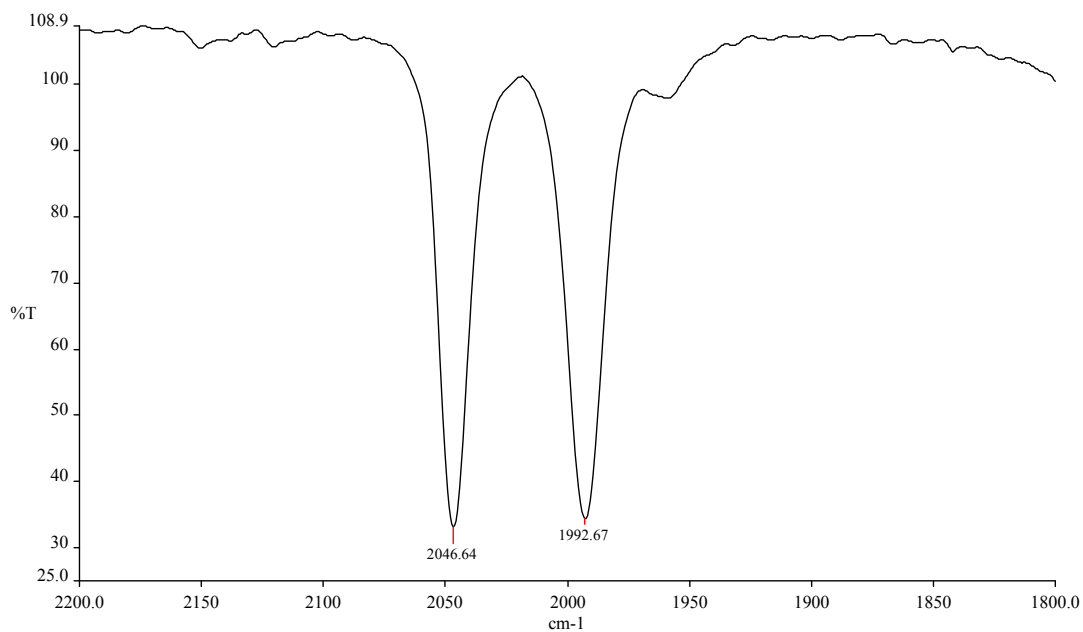


**Figure 3.30:** FT-IR of [RuInd(CO)<sub>2</sub>I]

#### Elemental analysis

Theory:	%C 33.04	%H 1.76
Found:	%C 32.58	%H 1.58

### 3.10 Kinetic Studies

0.2g of the complex was reacted with 10 and 20M excesses of PPh<sub>3</sub> or P(OPh)<sub>3</sub> in 25ml of xylene at 135.4°C. This allowed a direct comparison with the rates reported by Brown *et al.*<sup>144</sup> Xylene was distilled and dried over sodium wire/benzophenone and stored in an argon environment over molecular sieves. Glassware was dried overnight and cooled in a desiccator prior to use. Experimental conditions were kept as constant as possible. The reactions were carried out in the absence of light.

Prior to reaction, each complex was repurified using preparative TLC to ensure no dimer was present. Nitrogen was passed through the xylene for 10 minutes to ensure complete deaeration before reactions were started.

The reaction progress was monitored by solution IR in xylene and allowed to proceed for the duration of at least 3 half-lives. Rate calculations were carried out by plotting absorbance vs time using OLIS program by Online Instrumental Systems Inc.

### 3.11 Molecular Mass Determination of 1,4-diphenyl-2-cyclopenta[*d*]pyridazine

The instrument was calibrated with five solutions of benzil of known concentration (0.01 – 0.05 M). These were prepared in DCM and the weight of the solution measured. Starting with the lowest concentration after zeroing the instrument, a droplet of each solution was attached to each thermistor and left for three minutes and repeated ten times to get an average measurement value.

Three solutions of known concentration (0.01, 0.03 and 0.04 M) of 1,4-diphenyl-2-cyclopenta[*d*]pyridazine were then prepared in DCM and the weight of the solutions measured. Measurement values (MV) were obtained in the same fashion as for the benzil.

The molecular weight of the 1,4-diphenyl-2-cyclopenta[*d*]pyridazine was determined by:

$$\text{Molecular weight} = \frac{k_{\text{calib}}}{k_{\text{measured}}}$$

Where  $k$  is the slope of the graph generated from the plot of concentration ( $\text{gmol}^{-1}$ ) vs. MV.

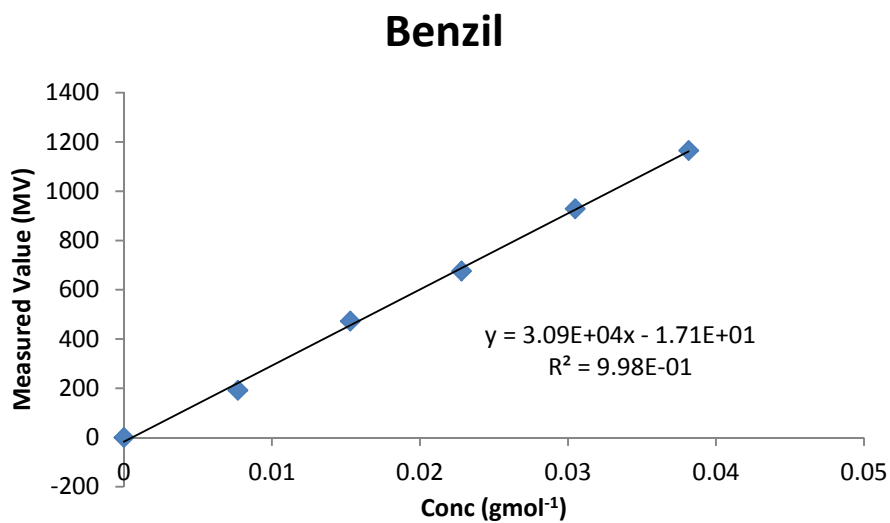


*Figure 3.31: Plot of conc. ( $\text{gmol}^{-1}$ ) vs. measured value for benzil*

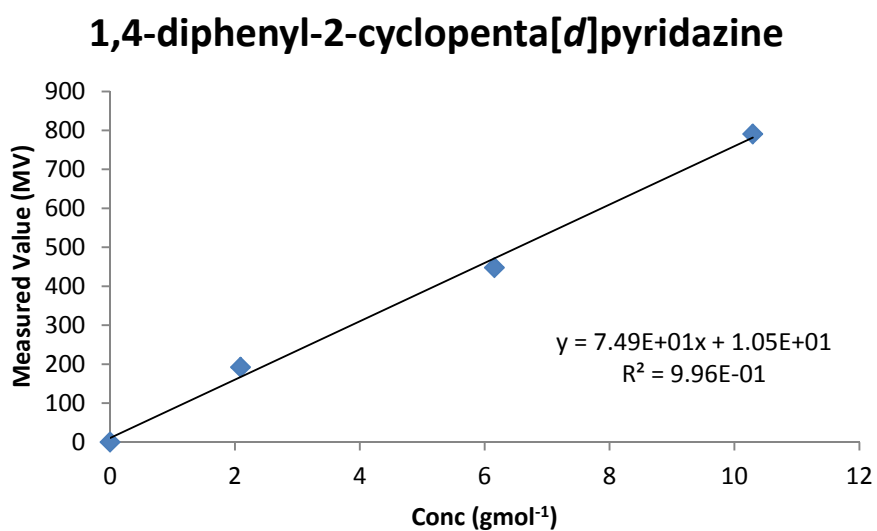


*Figure 3.32: Plot of conc. ( $\text{gmol}^{-1}$ ) vs. measured value for 1,4-diphenyl-2-cyclopenta[d]pyridazine*

## Chapter 4      Theoretical Studies

### 4.1 Introduction

The first theoretical calculations in chemistry were carried out by Heitler and London in 1927,<sup>208</sup> since then the use of theoretical methods have become an important tool in both computational and synthetic chemistry. Molecular Mechanics and Quantum Chemical calculations are the two most important techniques used in theoretical chemistry. Molecular Mechanics is used to perform calculations on systems containing significant numbers of atoms. It is a method employed to model the behavior of matter. It disregards the electronic motions and calculates the energy of a system as a function of the nuclear positions. The collection of atoms studied is treated as a mechanical system moving with its potential energy. Details about the system, such as the equilibrium structure, the vibrational spectrum, thermodynamic properties, equations of state and reaction rates can then be computed. Quantum mechanics focuses on the electrons in a system. These calculations may prove to be extremely time consuming as even if some electrons in a system are ignored, a large number of particles must still be considered.<sup>209</sup>

The term Molecular Mechanics (MM) was first used in the 1970s to describe the application of classical mechanics to the determination of molecular structure and conformation. Some well known packages available for the calculations of conformational space for C, H, N and O, are AMBER,<sup>210</sup> MM3<sup>211</sup> and TINKER.<sup>212</sup> One deficiency of MM, however, is that parameterizations of systems beyond one bond angle coordination is more difficult. Although more accurate, an important limitation to Quantum Chemical (QC) calculations is that all, e.g., methods like Density Functional Theory (DFT) or Hartree Fock techniques scale very badly and can only be applied to relatively small numbers of atoms.

### 4.2 Quantum Mechanical Methods

The basic Hückel theory is somewhat limited but does not apply to conjugated  $\pi$ -systems and was originally devised to explain the non-additive nature of certain properties of aromatic compounds.<sup>213</sup> The Extended Hückel theory (EHT), however,

which takes all the valence electrons in the molecule into account, has been widely applied. EHT was one of the first QC techniques to have a major impact in organometallic and coordination chemistry. Hoffmann developed EHT methods for both organic and inorganic chemistry.<sup>214-216</sup> For earlier work on orbital symmetry rules for organic reactions he won the Nobel Prize. His Nobel address rated an application in transition metal chemistry. His work made extensive use of symmetry and perturbation theory. The technique proved to be more successful than other semi-empirical techniques as it described d and f-orbitals more accurately than other methods.

*Ab initio* Hartree-Fock (HF) calculations account for molecular equilibrium and transition state geometries for organic systems but yield poor results when applied to organometallic or coordination compounds. *Ab initio* techniques like Møller-Plesset Type 2 (MP2) have shown some success in providing better calculations for organometallic molecules. This technique, however, is only feasible for small molecules as it scales poorly when compared to DFT. The major obstacle for HF calculations is their inability to deal with electron correlation which is only partly dealt with by MP2 methods. DFT approaches this problem in a different manner. It can explicitly account for electron correlation and therefore provide more accurate results. DFT methods are now the method of choice for inorganic calculation. The development of new gradient corrected functionals and new sets of one-electron equations, which allow all problems associated with local density approximation to be diminished, aided the progress of DFT.

### 4.3 Density Functional Theory

DFT is concerned with the electronic structure of atoms and molecules. There has been an increased interest with DFT since the 1980s.<sup>217,218</sup> The approach is based on a theory presented by Hohenberg and Kohn 1964 which states that all the ground-state properties of a system are functions of the charge density.<sup>219</sup> The Hohenberg-Kohn theorem allows the total electronic energy to be written as a function of the electronic density  $\rho$ .

$$E(\rho) = E_{KE}(\rho) + E_C(\rho) + E_H(\rho) + E_{XC}(\rho)$$

$E_{KE}(\rho)$  = Kinetic energy

$E_C(\rho)$  = Electron-nuclear interaction

$E_H(\rho)$  = Electron-electron Coulombic energy

$E_{XC}(\rho)$  = Contains the exchange and correlation contributions

The Hohenberg-Kohn theorem concludes that the ground-state properties of a system are determined by the density. An incorrect density results in an energy value above the true energy.

DFT may give a clear description of ground state properties, however, practical applications of DFT are based on approximations for the exchange correlation potential. This potential describes the effects of the Coulomb potential and the Pauli principle beyond a pure electrostatic interaction of the electrons. One common approximation is the local density approximation (LDA), which locally substitutes the exchange correlation energy density of an inhomogeneous system with that of an electron gas evaluated at the local density.

The Thomas-Fermi model shows one of the first attempts to employ electron density in the place of the wave function.<sup>220</sup> The Hartree-Fock-Slater or  $X\alpha$  method was one of the first DFT-based schemes to be used in systems with more than one atom.<sup>221</sup> This method was then replaced by the more accurate Kohn-Sham equations.<sup>222</sup>

### 4.3.1 Brief Summary of Calculation Methods

#### 1. Molecular Mechanics Methods:

The advantage of these methods is the ability to search conformational space in an efficient way, incorporating speed and low computational cost. However, they are only effective in describing molecular equilibrium geometry and conformation.

#### 2. Semi-empirical Methods:

These methods are suitable for equilibrium and determination of the structure of the transition state for large molecules where HF or DFT models may be too slow to perform calculations. A disadvantage of this method is their inability to calculate reaction energies and differences in conformational energies reliably.

### **3. Hartree-Fock Methods:**

These methods are useful for structural determination of organic and some main group inorganic molecules. They also may be used for calculations on reaction energies. They are, however, unsuitable for calculations of reaction energies that involve net bond making or breaking and structural determinations of transition metal inorganic and organometallic compounds which had occupied d-orbitals.

### **4. Density Functional Models:**

These calculations are similar to HF models for molecules of moderate sizes but are more computationally cost effective for larger molecules. DFT methods are also effective for calculations on moderately-sized transition metal coordination and organometallic compounds where HF models are inaccurate. DFT calculations, however, are considered unsuitable for calculations on very small systems.

#### **4.3.2 Strengths and Weakness of DFT**

DFT involves electron correlation in its theoretical basis. This method can calculate geometries and relative energies with an accuracy comparable to MP2 calculations in much the same time as that needed for HF calculations. DFT tends to be the favoured method for geometry and energy calculations on transition metal compounds.<sup>223,224</sup>

### **4.4 Molecular Modelling Packages**

Gaussian, GAMESS and Firefly (previously PC-GAMESS) are currently the two of the most popular high level modelling packages. Firefly is free for academic use whereas Gaussian is somewhat less accessible being a commercial program. Firefly provides speed and an ability to allow for efficient calculation on multiprocessor systems.

Some of the applications of Firefly are:

- Calculation of the electron correlation energy correction for SCF wave functions using DFT, CI, MP2 or coupled-cluster methodologies
- Calculation of semi-empirical MNDO, AM1 and PM3 models
- Calculation of energy gradients
- Optimisation of molecular geometries using energy gradients

- Transition states searches on the potential energy surface
- Calculation of molecular properties such as multiple moments, electrostatic potential, electronic field gradients, electron and spin density, infrared and Raman intensities, relativistic effects and solvation effects
- Surface IMOMM-type (integrated molecular orbital and molecular mechanics) simulations can also be performed when Firefly is combined with the add-on TINKER Molecular Mechanics program

Spartan (Wavefunction, Inc.) contains code for MM, semi-empirical methods, ab initio models, DFT, HF methods and thermochemical recipes such as T1.<sup>225</sup> One of its features, PM3-TM, is a semi-empirical method that has been parameterised for transition metals. This provides quick results of moderate quality.

There are two general categories of basis sets, minimal and extended. Minimal basis sets describe the most basic aspects of the orbitals and extended basis sets give a much more detailed description. Split-valence basis sets are an example of an extended basis set.

In the 3-21G basis set, three Gaussian functions are used to describe the core orbitals. Valence electrons are also represented by three Gaussians, the contracted part by two Gaussians and the diffuse part by one. 6-31G basis sets are constructed in a similar way with the core orbitals represented in terms of six Gaussian and valence orbitals split into three and one Gaussian components. The \* notation (6-31G\*) is used to indicate polarization basis sets. They are constructed from 6-31G by adding a set of d-type polarization functions written in terms of a single Gaussian for each heavy atom.<sup>226</sup>

## 4.5 Calculation of Atom Charges

### 4.5.1 Mulliken Population Analysis Method

Mulliken suggested a method for performing population analysis. This is now the most widely used method. Mulliken population analysis is easy to perform once a self-consistent field has been established and the elements of the density matrix have been determined.<sup>227</sup>

$$q_A = Z_A - \sum_{\mu=1; \mu \text{ on } A}^K P_{\mu\mu} - \sum_{\mu=1; \mu \text{ on } A}^K \sum_{v=1; v \neq \mu}^K P_{\mu v} S_{\mu v}$$

**Equation 4.2**

The above equation (**Equation 4.2**) relates the total number of electrons to the density matrix and to the overlap integrals. In the Mulliken method the total electron density ( $P_{\mu\mu}$ ) in an orbital is allocated to the atom on which  $\Phi_{\mu}$  is allocated. The remaining electron density is associated with the overlap population,  $\Phi_{\mu}\Phi_{\nu}$ . For each element  $\Phi_{\mu}\Phi_{\nu}$  of the density matrix, half of the density is assigned to the atom on which  $\Phi_{\nu}$  is located. The net charge on atom A is then calculated by subtracting the number of electrons from the nuclear charge,  $Z_A$ .

A Mulliken analysis depends on the use of a balanced basis set, in which an equivalent number of basis functions is present on each atom in the molecule. If taking water as an example, calculation of a wavefunction for the molecule with all the basis functions residing on the oxygen atom is possible. Providing a large enough basis set is used, a reasonable wavefunction for this whole molecule may be obtained. However, the Mulliken method would place the total charge on the oxygen. This exemplifies the general problem of the designated positions of p, d and f orbitals being spread quite far from the corresponding nucleus. The issue associated with this situation is that while they are very close to other atoms, the charge associated with electron occupation of such orbitals is assigned to the atom on which the orbital is centred. The equal distribution of electrons between pairs of atoms, even if their electronegativities are very different can very well lead to unrealistic values for the net atomic charge.

CHELPG (CHarges from Electrostatic Potentials using a Grid based method) is an atomic charge calculation scheme in which atomic charges are fitted to reproduce the molecular electrostatic potential (MESP) at a number of points around the molecule.<sup>228</sup> This method is popular with those modeling solid state properties.<sup>229</sup>

## 4.6 The Eyring Equation

The Eyring equation, developed in 1935, describes the temperature dependence on reaction rate.<sup>230</sup>

The general form of the Eyring equation is:

$$k = \frac{k_B T}{h} e^{\frac{-\Delta G^\ddagger}{RT}}$$

$k$  = rate of reaction

$T$  = absolute temperature

$\Delta G^\ddagger$  = Gibbs energy of activation

$k_B$  = Boltzmann's constant

$h$  = Planck's constant

This can be rewritten as:

$$k = \frac{k_B T}{h} e^{\frac{\Delta S^\ddagger}{R}} e^{\frac{-\Delta H^\ddagger}{RT}}$$

To calculate the linear form of the Eyring Equation:

$$\ln \frac{k}{T} = \frac{-\Delta H^\ddagger}{RT} + \ln \frac{k_B}{h} + \frac{\Delta S^\ddagger}{R}$$

$\Delta H^\ddagger$  = Enthalpy of activation

$\Delta S^\ddagger$  = Entropy of activation

Complex	vMC–O (cm <sup>-1</sup> )	Intensity	vMC–O (cm <sup>-1</sup> )	Intensity
[RuCp(CO) <sub>2</sub> H]	2036.66	12.41	1988.05	17.81
[RuCp(CO) <sub>2</sub> Cl]	2056.51	11	2012.65	15.58
[RuCp(CO) <sub>2</sub> Br]	2051.5	11.22	2008.44	15.1
[RuCp(CO) <sub>2</sub> I]	2048.82	11.22	2009.92	14.59
[RuCp*(CO) <sub>2</sub> H]	2016.46	14.35	1970.41	17.75
[RuCp*(CO) <sub>2</sub> Cl]	2036.04	12.57	1994.9	15.67
[Ru(dbzCp)(CO) <sub>2</sub> H]	2053.69	12.12	2004.89	15.54
[Ru(dbzCp)(CO) <sub>2</sub> Cl]	2075.87	9.96	2032.59	12.56
[Ru(dbzCp)(CO) <sub>2</sub> Br]	2071.53	10.04	2026.12	12.41
[Ru(dbzCp)(CO) <sub>2</sub> I]	2065.8	9.23	2023.35	12.18

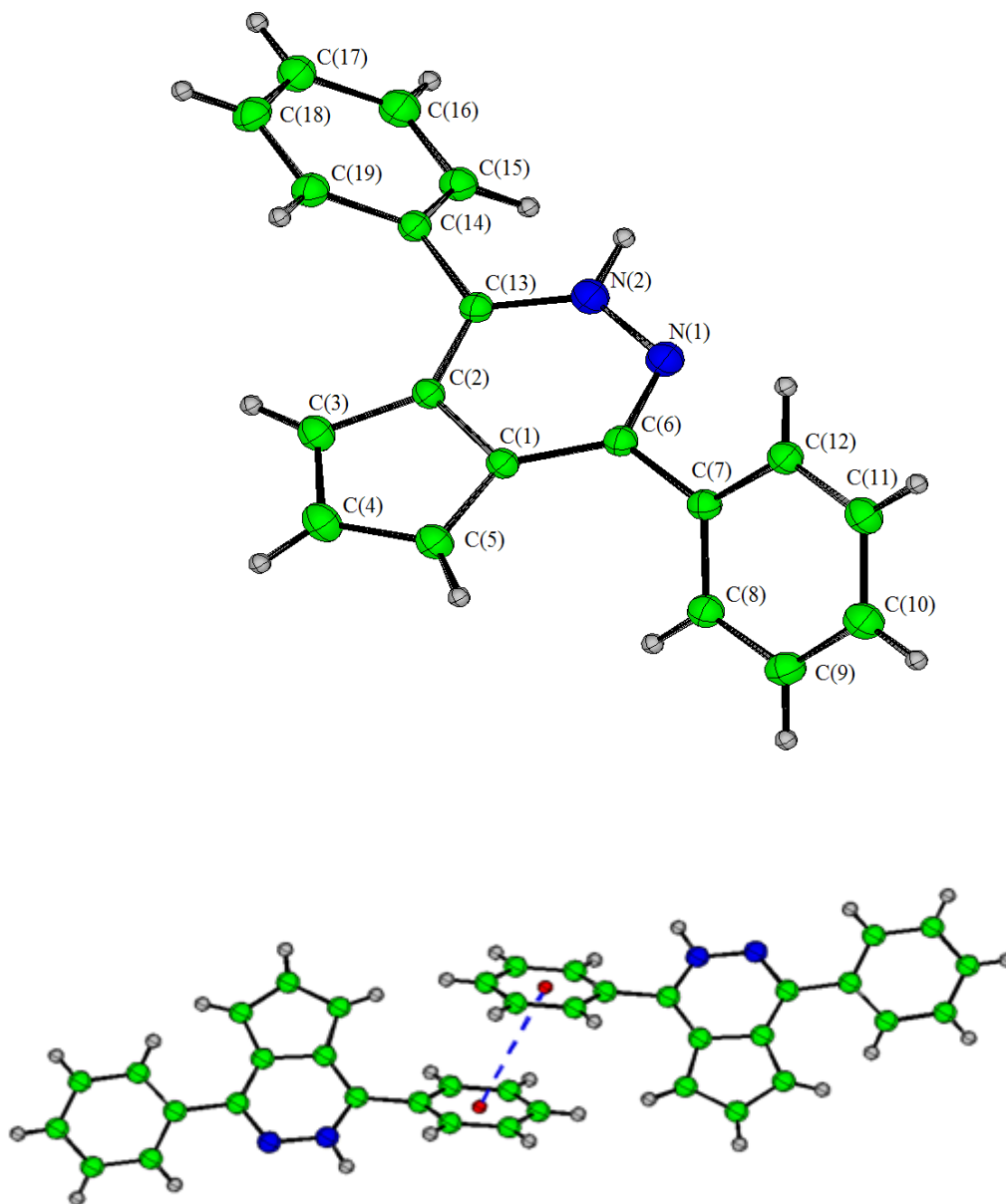
**Table 4.1:** Calculated IR Hessian vMC–O values

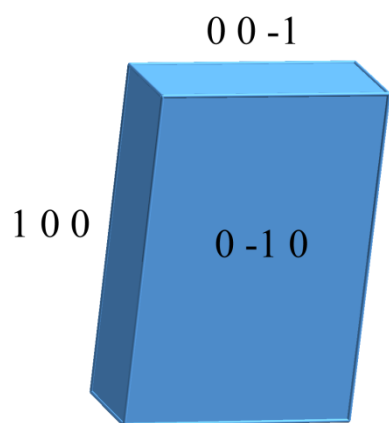
## Chapter 5 Crystallographic Data

The structures were solved by direct methods, SHELXS-97, and refined by full matrix least squares using SHELXL-97.<sup>231</sup> SHELX operations were performed using the Oscail package which was also used to obtain the drawings. Data were corrected for Lorentz and polarization effects and for absorption. Hydrogen atoms were included in calculated positions with thermal parameters 30% larger than the atom to which they were attached. The non-hydrogen atoms were refined anisotropically.

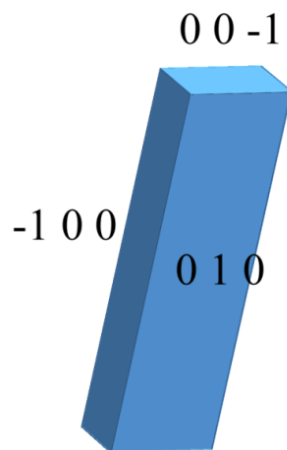
The crystal structures in this chapter are of those of 1,4-diphenyl-2-cyclopenta[d]pyridizine, Forms I and II,  $\text{Ph}_3\text{C}-\text{C}_5\text{H}_3(\text{COPh})_2$ , (1H-inden-1-yl)(phenyl)methyl benzoate,  $[\text{Ru}(\text{dbzCp})(\text{CO})\text{IPPh}_3]$ ,  $[\text{Ru}((\text{CO}-p\text{-tolyl})_2\text{C}_5\text{H}_3)(\text{CO})\text{IPPh}_3]$ ,  $[\text{Ru}(\text{indenyl})(\text{CO})_2\text{I}]$  and  $[\text{Ru}(\text{indenyl})(\text{CO})\text{IPPh}_3]$ .

## 5.1 Crystal Structure of C<sub>19</sub>H<sub>14</sub>N<sub>2</sub> Form I

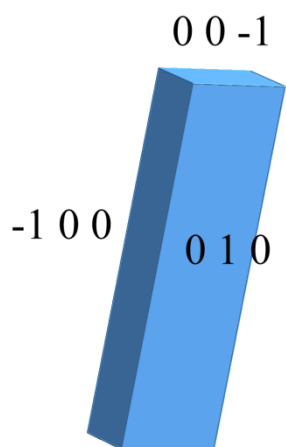




Calculated BFDH



Calculated ASE (Habit)



Observed shape.

**Table 5.1:** *Crystal data and structure refinement for 1,4-diphenyl-2-cyclopenta[d]pyridizine Form I*

Identification code	mc5
Empirical formula	C <sub>19</sub> H <sub>14</sub> N <sub>2</sub>
Formula weight	270.32
Temperature	293(2) K
Wavelength	0.7107 Å
Crystal system	Monoclinic
Space group	P21/c
Unit cell dimensions	a = 8.8290(7)Å b = 25.4203(19)Å β = 92.144(8)° c = 6.1530(5)Å
Volume	1379.99(19) Å <sup>3</sup>
Z	4
Density (calculated)	1.301 Mg/m <sup>3</sup>
Absorption coefficient	0.077 mm <sup>-1</sup>
F(000)	568
Crystal size	0.58 x 0.17 x 0.10 mm
Theta range for data collection	3.2084 to 28.6929 °.
Index ranges	-7<=h<=7; -24<=k<=33; -11<=l<=11
Reflections collected	8041
Independent reflections	2456 [R <sub>int</sub> = 0.0309]
Reflections observed (>2σ)	1662
Data Completeness	0.970
Absorption correction	Semi-empirical from equivalents
Max. and min. transmission	1.00000 and 0.85850
Refinement method	Full-matrix least-squares on F <sup>2</sup>
Data / restraints / parameters	2456 / 0 / 194
Goodness-of-fit on F <sup>2</sup>	1.045
Final R indices [I>2σ(I)]	R <sub>1</sub> = 0.0422 wR <sub>2</sub> = 0.1062
R indices (all data)	R <sub>1</sub> = 0.0703 wR <sub>2</sub> = 0.1135
Largest diff. peak and hole	0.130 and -0.178 e.Å <sup>-3</sup>

$${}^aR_1 = \Sigma||F_o| - |F_c||/\Sigma|F_o|. \quad {}^b wR_2 = |\Sigma w(|F_o|^2 - |F_c|^2)|/\Sigma|w(F_o)^2|^{1/2}, \quad w = 1/[\sigma^2(F_o^2) + (.0603P)^2 + .07P]. \quad P = (F_o^2 + 2F_c^2)/3.$$

**Table 5.2:** Atomic coordinates ( $\times 10^4$ ) and equivalent isotropic displacement parameters ( $\text{\AA}^2 \times 10^3$ ) for 1,4-diphenyl-2-cyclopenta[d]pyridazine Form I.  $U(eq)$  is defined as one third of the trace of the orthogonalized  $U_{ij}$  tensor.

Atom	x	y	z	U(eq)
N(1)	562(2)	4193(1)	5171(2)	52(1)
N(2)	-295(2)	4427(1)	6692(3)	51(1)
C(1)	-1258(2)	3492(1)	5161(3)	39(1)
C(2)	-2124(2)	3771(1)	6762(3)	39(1)
C(3)	-3414(2)	3463(1)	7178(3)	51(1)
C(4)	-3324(2)	3015(1)	5916(3)	58(1)
C(5)	-2020(2)	3023(1)	4678(3)	50(1)
C(6)	84(2)	3728(1)	4442(3)	42(1)
C(7)	1081(2)	3477(1)	2856(3)	41(1)
C(8)	506(2)	3247(1)	949(3)	48(1)
C(9)	1462(2)	3020(1)	-511(3)	54(1)
C(10)	3006(2)	3012(1)	-72(3)	55(1)
C(11)	3601(2)	3237(1)	1809(3)	53(1)
C(12)	2653(2)	3469(1)	3267(3)	48(1)
C(13)	-1577(2)	4247(1)	7541(2)	41(1)
C(14)	-2264(2)	4578(1)	9219(3)	42(1)
C(15)	-2342(2)	5122(1)	9009(3)	50(1)
C(16)	-2989(2)	5423(1)	10592(3)	59(1)
C(17)	-3565(2)	5189(1)	12398(3)	58(1)
C(18)	-3496(2)	4652(1)	12631(3)	59(1)
C(19)	-2849(2)	4345(1)	11060(3)	52(1)

**Table 5.3:** Bond lengths [ $\text{\AA}$ ] and angles [ $^\circ$ ] for 1,4-diphenyl-2-cyclopenta[d]pyridizine Form I

N(1)-C(6)	1.328(2)	N(1)-N(2)	1.362(2)
N(2)-C(13)	1.345(2)	C(1)-C(5)	1.395(2)
C(1)-C(6)	1.414(2)	C(1)-C(2)	1.454(2)
C(2)-C(13)	1.380(2)	C(2)-C(3)	1.413(2)
C(3)-C(4)	1.381(3)	C(4)-C(5)	1.404(3)
C(6)-C(7)	1.483(2)	C(7)-C(8)	1.389(2)
C(7)-C(12)	1.401(2)	C(8)-C(9)	1.383(3)
C(9)-C(10)	1.380(3)	C(10)-C(11)	1.377(3)
C(11)-C(12)	1.383(2)	C(13)-C(14)	1.480(2)
C(14)-C(15)	1.391(3)	C(14)-C(19)	1.394(2)
C(15)-C(16)	1.379(3)	C(16)-C(17)	1.375(3)
C(17)-C(18)	1.374(3)	C(18)-C(19)	1.382(3)
C(6)-N(1)-N(2)	116.32(14)	C(13)-N(2)-N(1)	127.95(16)
C(5)-C(1)-C(6)	134.30(17)	C(5)-C(1)-C(2)	107.44(15)
C(6)-C(1)-C(2)	118.26(16)	C(13)-C(2)-C(3)	134.14(16)
C(13)-C(2)-C(1)	118.42(15)	C(3)-C(2)-C(1)	107.44(16)
C(4)-C(3)-C(2)	106.92(16)	C(3)-C(4)-C(5)	111.03(17)
C(1)-C(5)-C(4)	107.16(17)	N(1)-C(6)-C(1)	122.08(15)
N(1)-C(6)-C(7)	114.64(15)	C(1)-C(6)-C(7)	123.27(16)
C(8)-C(7)-C(12)	118.36(16)	C(8)-C(7)-C(6)	121.95(16)
C(12)-C(7)-C(6)	119.70(16)	C(9)-C(8)-C(7)	120.78(18)
C(8)-C(9)-C(10)	120.12(18)	C(11)-C(10)-C(9)	120.07(17)
C(10)-C(11)-C(12)	120.11(18)	C(11)-C(12)-C(7)	120.56(17)
N(2)-C(13)-C(2)	116.92(15)	N(2)-C(13)-C(14)	116.72(16)
C(2)-C(13)-C(14)	126.36(15)	C(15)-C(14)-C(19)	118.56(16)
C(15)-C(14)-C(13)	121.42(15)	C(19)-C(14)-C(13)	120.01(17)
C(16)-C(15)-C(14)	120.48(17)	C(17)-C(16)-C(15)	120.4(2)
C(16)-C(17)-C(18)	119.88(18)	C(17)-C(18)-C(19)	120.39(17)
C(18)-C(19)-C(14)	120.30(19)		

**Table 5.4:** *Anisotropic displacement parameters ( $\text{\AA}^2 \times 10^3$ ) for 1,4-diphenyl-2-cyclopenta[d]pyridazine Form I. The anisotropic displacement factor exponent takes the form:*

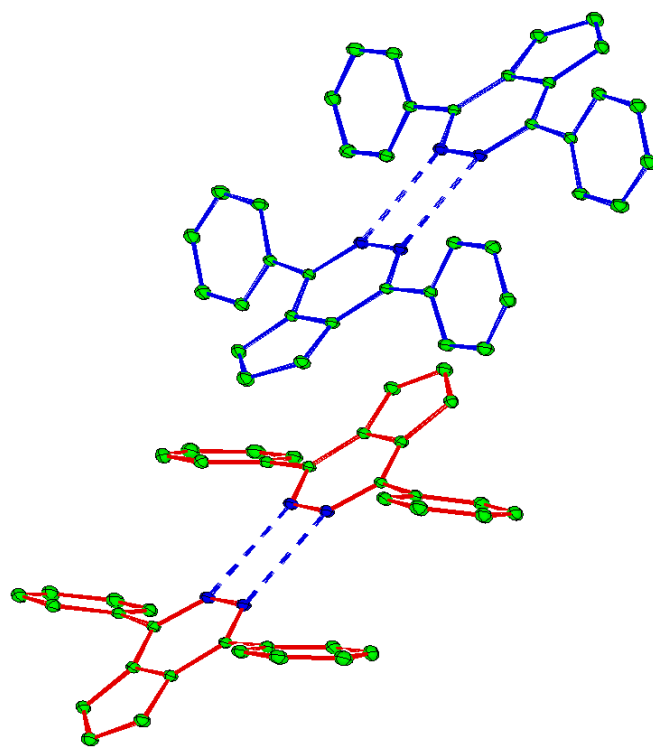
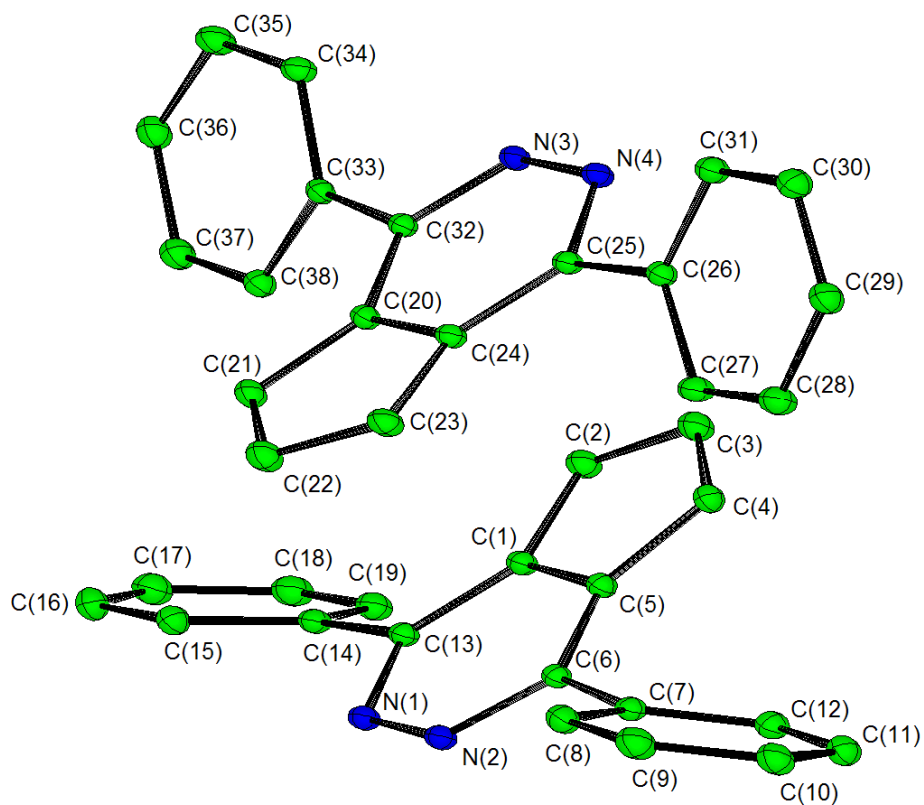
$$-2 \pi^2 [ h^2 a^{*2} U11 + \dots + 2 h k a^* b^* U12 ]$$

Atom	U11	U22	U33	U23	U13	U12
N(1)	47(1)	61(1)	50(1)	-15(1)	19(1)	-15(1)
N(2)	48(1)	54(1)	53(1)	-13(1)	18(1)	-15(1)
C(1)	35(1)	44(1)	40(1)	6(1)	0(1)	0(1)
C(2)	33(1)	44(1)	40(1)	7(1)	2(1)	0(1)
C(3)	39(1)	56(1)	59(1)	8(1)	9(1)	-5(1)
C(4)	46(1)	52(1)	76(1)	10(1)	3(1)	-14(1)
C(5)	48(1)	43(1)	58(1)	2(1)	1(1)	-5(1)
C(6)	39(1)	48(1)	38(1)	0(1)	3(1)	-3(1)
C(7)	43(1)	41(1)	40(1)	2(1)	7(1)	-1(1)
C(8)	46(1)	51(1)	47(1)	0(1)	0(1)	1(1)
C(9)	65(1)	50(1)	47(1)	-7(1)	6(1)	0(1)
C(10)	59(1)	43(1)	63(1)	-2(1)	20(1)	7(1)
C(11)	42(1)	54(1)	64(1)	5(1)	10(1)	3(1)
C(12)	42(1)	54(1)	47(1)	-1(1)	3(1)	-5(1)
C(13)	38(1)	48(1)	37(1)	5(1)	6(1)	0(1)
C(14)	35(1)	54(1)	39(1)	1(1)	4(1)	2(1)
C(15)	52(1)	52(1)	48(1)	1(1)	8(1)	-4(1)
C(16)	60(1)	56(1)	62(1)	-9(1)	7(1)	3(1)
C(17)	47(1)	76(2)	53(1)	-13(1)	5(1)	9(1)
C(18)	51(1)	86(2)	41(1)	9(1)	12(1)	12(1)
C(19)	48(1)	62(1)	46(1)	12(1)	8(1)	10(1)

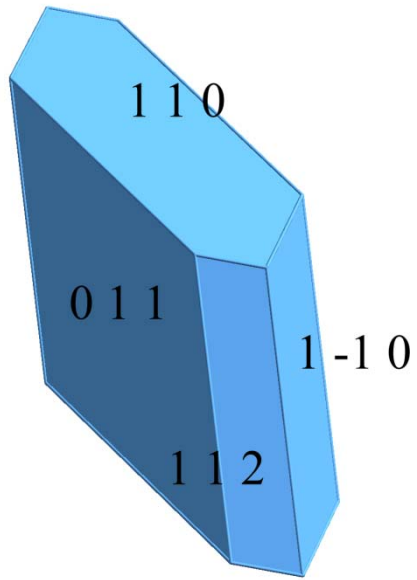
**Table 5.5:** Hydrogen coordinates ( $\times 10^4$ ) and isotropic displacement parameters ( $\text{\AA}^2 \times 10^3$ ) for 1,4-diphenyl-2-cyclopenta[d]pyridizine Form I

Atom	x	y	z	U(eq)
H(3)	-4177	3546	8122	66
H(4)	-4033	2745	5890	75
H(5)	-1720	2764	3717	65
H(8)	-535	3247	652	62
H(9)	1063	2872	-1792	70
H(10)	3645	2854	-1047	71
H(11)	4642	3232	2098	69
H(12)	3061	3621	4532	62
H(15)	-1956	5284	7793	66
H(16)	-3036	5787	10437	77
H(17)	-4000	5394	13461	76
H(18)	-3887	4494	13852	77
H(19)	-2804	3982	11232	67
H(2N)	140(30)	4727(10)	7240(30)	86(8)

## 5.2 Crystal Structure of C<sub>19</sub>H<sub>14</sub>N<sub>2</sub> Form II

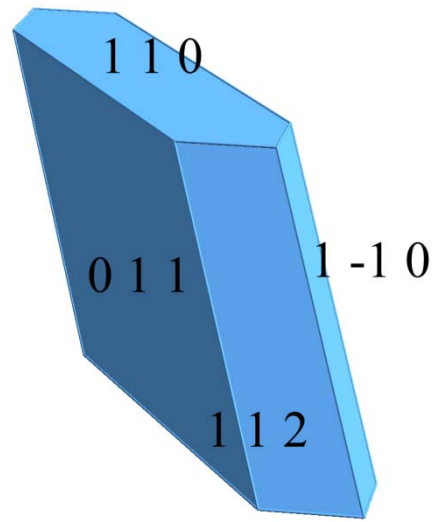


MC5\_1

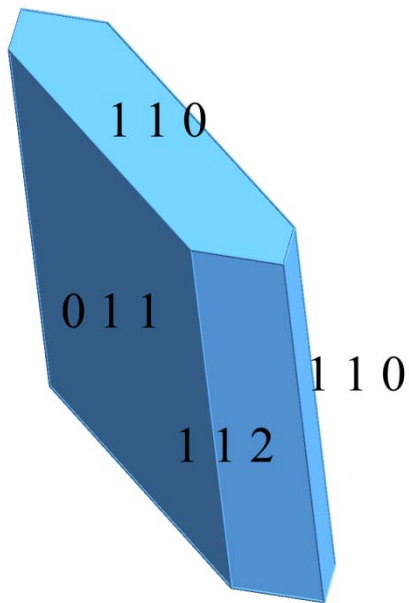


Calculated shape

BFDH



ASE (Habit)



Observed shape

**Table 5.6:** Crystal data and structure refinement for 1,4-diphenyl-2-cyclopenta[d]pyridizine Form I.

Identification code	mc5_1
Empirical formula	C <sub>19</sub> H <sub>14</sub> N <sub>2</sub>
Formula weight	270.32
Temperature	293(2) K
Wavelength	0.7107 Å
Crystal system	Triclinic
Space group	P-1
Unit cell dimensions	a = 7.9764(4) Å α = 74.892(4)° b = 13.3709(6) Å β = 84.132(4)° c = 14.0867(7) Å γ = 76.765(4)°
Volume	1410.47(12) Å <sup>3</sup>
Z	4
Density (calculated)	1.273 Mg/m <sup>3</sup>
Absorption coefficient	0.076 mm <sup>-1</sup>
F(000)	568
Crystal size	0.34 x 0.28 x 0.10 mm
Theta range for data collection	2.7685 to 29.0845 °.
Index ranges	-10 ≤ h ≤ 6; -17 ≤ k ≤ 18; -18 ≤ l ≤ 19
Reflections collected	12551
Independent reflections	4835 [R <sub>int</sub> = 0.0288]
Reflections observed (>2σ)	3173
Data Completeness	0.936
Absorption correction	Semi-empirical from equivalents
Max. and min. transmission	1.00000 and 0.89561
Refinement method	Full-matrix least-squares on F <sup>2</sup>
Data / restraints / parameters	4835 / 0 / 379
Goodness-of-fit on F <sup>2</sup>	0.991
Final R indices [I > 2 σ (I)]	R <sub>1</sub> = 0.0451 wR <sub>2</sub> = 0.1179
R indices (all data)	R <sub>1</sub> = 0.0788 wR <sub>2</sub> = 0.1295
Largest diff. peak and hole	0.198 and -0.249 e.Å <sup>-3</sup>

$${}^aR_1 = \Sigma |F_o| - |F_c| / \Sigma |F_o|. \quad {}^b wR_2 = | \Sigma w(|F_o|^2 - |F_c|^2) / \Sigma |w(F_o)^2|^{1/2}, \quad w = 1/[\sigma^2(F_o^2) + (.0798P)^2]. \quad P = (F_o^2 + 2F_c^2)/3.$$

**Table 5.7:** Atomic coordinates ( $\times 10^4$ ) and equivalent isotropic displacement parameters ( $\text{\AA}^2 \times 10^3$ ) for 1,4-diphenyl-2-cyclopenta[d]pyridizine Form II.  $U(eq)$  is defined as one third of the trace of the orthogonalized  $U_{ij}$  tensor.

Atom	x	y	z	U(eq)
N(1)	5507(2)	4701(1)	1132(1)	40(1)
N(2)	6746(2)	4298(1)	516(1)	41(1)
N(3)	8300(2)	649(1)	4419(1)	41(1)
N(4)	9607(2)	250(1)	3836(1)	41(1)
C(1)	7428(2)	4009(1)	2440(1)	38(1)
C(2)	8117(2)	3669(2)	3369(1)	50(1)
C(3)	9760(3)	3060(2)	3277(1)	54(1)
C(4)	10158(2)	2997(1)	2313(1)	48(1)
C(5)	8726(2)	3585(1)	1768(1)	39(1)
C(6)	8321(2)	3767(1)	794(1)	37(1)
C(7)	9551(2)	3390(1)	36(1)	39(1)
C(8)	9083(2)	2866(1)	-586(1)	50(1)
C(9)	10281(3)	2479(2)	-1250(1)	65(1)
C(10)	11938(3)	2623(2)	-1306(1)	66(1)
C(11)	12413(3)	3155(2)	-701(1)	57(1)
C(12)	11232(2)	3533(1)	-31(1)	48(1)
C(13)	5829(2)	4577(1)	2070(1)	37(1)
C(14)	4407(2)	5056(1)	2678(1)	42(1)
C(15)	2720(2)	4986(2)	2619(1)	53(1)
C(16)	1420(3)	5414(2)	3221(2)	65(1)
C(17)	1798(3)	5918(2)	3881(2)	68(1)
C(18)	3460(3)	6002(2)	3938(1)	64(1)
C(19)	4761(3)	5574(1)	3349(1)	51(1)

C(20)	6458(2)	1396(1)	3104(1)	39(1)
C(21)	4994(2)	1845(2)	2547(1)	53(1)
C(22)	5439(3)	1690(2)	1613(1)	61(1)
C(23)	7147(3)	1162(2)	1547(1)	51(1)
C(24)	7824(2)	964(1)	2469(1)	38(1)
C(25)	9395(2)	407(1)	2879(1)	36(1)
C(26)	10864(2)	-69(1)	2295(1)	39(1)
C(27)	11271(2)	479(1)	1350(1)	49(1)
C(28)	12582(3)	26(2)	783(1)	57(1)
C(29)	13514(3)	-979(2)	1145(2)	59(1)
C(30)	13141(3)	-1527(2)	2077(2)	58(1)
C(31)	11827(2)	-1084(1)	2659(1)	48(1)
C(32)	6770(2)	1211(1)	4094(1)	36(1)
C(33)	5456(2)	1553(1)	4835(1)	38(1)
C(34)	5259(2)	896(1)	5752(1)	46(1)
C(35)	3967(3)	1211(2)	6411(1)	56(1)
C(36)	2869(3)	2181(2)	6155(2)	61(1)
C(37)	3078(3)	2850(2)	5251(1)	60(1)
C(38)	4355(2)	2542(1)	4595(1)	49(1)

**Table 5.8:** Bond lengths [ $\text{\AA}$ ] and angles [ $^\circ$ ] for 1,4-diphenyl-2-cyclopenta[d]pyridazine Form II

N(1)-C(13)	1.3321(19)	N(1)-N(2)	1.3584(17)
N(2)-C(6)	1.335(2)	N(3)-C(32)	1.334(2)
N(3)-N(4)	1.3581(17)	N(4)-C(25)	1.3305(18)
C(1)-C(2)	1.395(2)	C(1)-C(13)	1.401(2)
C(1)-C(5)	1.448(2)	C(2)-C(3)	1.389(3)
C(3)-C(4)	1.383(2)	C(4)-C(5)	1.402(2)
C(5)-C(6)	1.389(2)	C(6)-C(7)	1.482(2)
C(7)-C(8)	1.380(2)	C(7)-C(12)	1.387(2)
C(8)-C(9)	1.378(2)	C(9)-C(10)	1.370(3)
C(10)-C(11)	1.371(3)	C(11)-C(12)	1.372(2)
C(13)-C(14)	1.478(2)	C(14)-C(15)	1.382(2)
C(14)-C(19)	1.393(2)	C(15)-C(16)	1.387(3)
C(16)-C(17)	1.373(3)	C(17)-C(18)	1.368(3)
C(18)-C(19)	1.376(2)	C(20)-C(32)	1.389(2)
C(20)-C(21)	1.400(2)	C(20)-C(24)	1.450(2)
C(21)-C(22)	1.383(2)	C(22)-C(23)	1.390(3)
C(23)-C(24)	1.395(2)	C(24)-C(25)	1.399(2)
C(25)-C(26)	1.480(2)	C(26)-C(27)	1.387(2)
C(26)-C(31)	1.391(2)	C(27)-C(28)	1.375(2)
C(28)-C(29)	1.372(3)	C(29)-C(30)	1.366(3)
C(30)-C(31)	1.384(2)	C(32)-C(33)	1.484(2)
C(33)-C(34)	1.377(2)	C(33)-C(38)	1.389(2)
C(34)-C(35)	1.383(2)	C(35)-C(36)	1.371(3)
C(36)-C(37)	1.371(3)	C(37)-C(38)	1.370(2)
C(13)-N(1)-N(2)	120.18(14)	C(6)-N(2)-N(1)	123.54(13)
C(32)-N(3)-N(4)	123.97(13)	C(25)-N(4)-N(3)	119.95(14)
C(2)-C(1)-C(13)	134.94(16)	C(2)-C(1)-C(5)	106.90(15)
C(13)-C(1)-C(5)	118.04(14)	C(3)-C(2)-C(1)	107.63(16)

C(4)-C(3)-C(2)	110.77(16)	C(3)-C(4)-C(5)	106.95(16)
C(6)-C(5)-C(4)	133.79(16)	C(6)-C(5)-C(1)	118.34(15)
C(4)-C(5)-C(1)	107.75(14)	N(2)-C(6)-C(5)	119.18(15)
N(2)-C(6)-C(7)	117.56(14)	C(5)-C(6)-C(7)	123.26(15)
C(8)-C(7)-C(12)	118.94(16)	C(8)-C(7)-C(6)	121.55(17)
C(12)-C(7)-C(6)	119.47(15)	C(9)-C(8)-C(7)	120.16(19)
C(10)-C(9)-C(8)	120.25(18)	C(9)-C(10)-C(11)	120.13(18)
C(10)-C(11)-C(12)	120.0(2)	C(11)-C(12)-C(7)	120.55(18)
N(1)-C(13)-C(1)	120.68(15)	N(1)-C(13)-C(14)	116.15(15)
C(1)-C(13)-C(14)	123.17(14)	C(15)-C(14)-C(19)	118.29(17)
C(15)-C(14)-C(13)	121.91(16)	C(19)-C(14)-C(13)	119.78(17)
C(14)-C(15)-C(16)	120.65(19)	C(17)-C(16)-C(15)	120.1(2)
C(18)-C(17)-C(16)	119.75(19)	C(17)-C(18)-C(19)	120.57(19)
C(18)-C(19)-C(14)	120.60(19)	C(32)-C(20)-C(21)	133.97(16)
C(32)-C(20)-C(24)	118.08(15)	C(21)-C(20)-C(24)	107.63(14)
C(22)-C(21)-C(20)	106.93(16)	C(21)-C(22)-C(23)	111.00(16)
C(22)-C(23)-C(24)	107.27(15)	C(23)-C(24)-C(25)	134.31(16)
C(23)-C(24)-C(20)	107.17(15)	C(25)-C(24)-C(20)	118.33(13)
N(4)-C(25)-C(24)	120.61(15)	N(4)-C(25)-C(26)	116.88(14)
C(24)-C(25)-C(26)	122.46(13)	C(27)-C(26)-C(31)	118.39(15)
C(27)-C(26)-C(25)	120.31(15)	C(31)-C(26)-C(25)	121.27(15)
C(28)-C(27)-C(26)	120.89(17)	C(29)-C(28)-C(27)	120.27(18)
C(30)-C(29)-C(28)	119.67(17)	C(29)-C(30)-C(31)	120.86(18)
C(30)-C(31)-C(26)	119.91(17)	N(3)-C(32)-C(20)	119.02(15)
N(3)-C(32)-C(33)	117.19(14)	C(20)-C(32)-C(33)	123.69(15)
C(34)-C(33)-C(38)	118.72(16)	C(34)-C(33)-C(32)	121.43(16)
C(38)-C(33)-C(32)	119.81(15)	C(33)-C(34)-C(35)	120.33(18)
C(36)-C(35)-C(34)	120.17(18)	C(37)-C(36)-C(35)	119.93(18)
C(38)-C(37)-C(36)	120.14(19)	C(37)-C(38)-C(33)	120.69(17)

Symmetry transformations used to generate equivalent atoms:

**Table 5.9:** Anisotropic displacement parameters ( $\text{\AA}^2 \times 10^3$ ) for 1,4-diphenyl-2-cyclopenta[d]pyridazine Form II. The anisotropic displacement factor exponent takes the form:

$$-2 \pi^2 [ h^2 a^{*2} U11 + \dots + 2 h k a^* b^* U12 ]$$

Atom	U11	U22	U33	U23	U13	U12
N(1)	40(1)	45(1)	34(1)	-10(1)	-7(1)	-3(1)
N(2)	41(1)	45(1)	35(1)	-8(1)	-11(1)	-1(1)
N(3)	38(1)	48(1)	32(1)	-5(1)	-10(1)	0(1)
N(4)	40(1)	48(1)	32(1)	-9(1)	-6(1)	-2(1)
C(1)	37(1)	41(1)	37(1)	-7(1)	-9(1)	-8(1)
C(2)	50(1)	63(1)	36(1)	-10(1)	-13(1)	-11(1)
C(3)	51(1)	65(1)	45(1)	-4(1)	-25(1)	-10(1)
C(4)	37(1)	53(1)	52(1)	-12(1)	-16(1)	-1(1)
C(5)	37(1)	39(1)	41(1)	-8(1)	-11(1)	-7(1)
C(6)	34(1)	35(1)	40(1)	-6(1)	-10(1)	-3(1)
C(7)	40(1)	36(1)	36(1)	-4(1)	-9(1)	0(1)
C(8)	43(1)	63(1)	44(1)	-17(1)	-11(1)	-3(1)
C(9)	62(2)	88(2)	49(1)	-32(1)	-10(1)	-1(1)
C(10)	54(1)	85(2)	48(1)	-20(1)	1(1)	7(1)
C(11)	45(1)	63(1)	55(1)	-6(1)	2(1)	-7(1)
C(12)	46(1)	45(1)	52(1)	-11(1)	-5(1)	-8(1)
C(13)	37(1)	36(1)	35(1)	-5(1)	-7(1)	-7(1)
C(14)	44(1)	40(1)	35(1)	-1(1)	-7(1)	-3(1)
C(15)	45(1)	55(1)	56(1)	-8(1)	-9(1)	-6(1)
C(16)	39(1)	69(1)	73(1)	-3(1)	2(1)	-1(1)
C(17)	65(2)	70(2)	58(1)	-14(1)	10(1)	3(1)
C(18)	70(2)	68(1)	50(1)	-20(1)	2(1)	-5(1)
C(19)	52(1)	58(1)	43(1)	-15(1)	-3(1)	-7(1)
C(20)	34(1)	45(1)	35(1)	-4(1)	-9(1)	-6(1)
C(21)	37(1)	69(1)	45(1)	-8(1)	-14(1)	0(1)
C(22)	52(1)	87(2)	41(1)	-6(1)	-23(1)	-10(1)

C(23)	51(1)	68(1)	32(1)	-8(1)	-10(1)	-13(1)
C(24)	39(1)	42(1)	32(1)	-4(1)	-7(1)	-9(1)
C(25)	39(1)	36(1)	33(1)	-6(1)	-6(1)	-8(1)
C(26)	37(1)	43(1)	39(1)	-13(1)	-9(1)	-6(1)
C(27)	53(1)	46(1)	43(1)	-8(1)	1(1)	-5(1)
C(28)	59(1)	63(1)	48(1)	-14(1)	9(1)	-14(1)
C(29)	46(1)	71(1)	59(1)	-26(1)	3(1)	-2(1)
C(30)	51(1)	53(1)	65(1)	-17(1)	-8(1)	8(1)
C(31)	46(1)	50(1)	44(1)	-8(1)	-8(1)	-3(1)
C(32)	34(1)	39(1)	33(1)	-4(1)	-7(1)	-6(1)
C(33)	33(1)	46(1)	36(1)	-10(1)	-7(1)	-9(1)
C(34)	51(1)	51(1)	36(1)	-8(1)	-6(1)	-12(1)
C(35)	62(1)	74(1)	37(1)	-12(1)	2(1)	-28(1)
C(36)	45(1)	87(2)	55(1)	-30(1)	5(1)	-10(1)
C(37)	47(1)	70(1)	57(1)	-21(1)	-4(1)	3(1)
C(38)	40(1)	53(1)	45(1)	-7(1)	-4(1)	-1(1)

**Table 5.10:** Hydrogen coordinates ( $\times 10^4$ ) and isotropic displacement parameters ( $\text{\AA}^2 \times 10^3$ ) for 1,4-diphenyl-2-cyclopenta[d]pyridazine Form II

Atom	x	y	z	U(eq)
H(2N)	6504	4391	-86	54
H(3N)	8469	533	5035	53
H(2)	7574	3823	3946	64
H(3)	10492	2737	3794	71
H(4)	11181	2634	2072	62
H(8)	7956	2775	-557	65
H(9)	9964	2117	-1661	85
H(10)	12742	2360	-1755	85
H(11)	13534	3259	-745	74
H(12)	11561	3888	382	63
H(15)	2454	4649	2171	69
H(16)	290	5360	3178	85
H(17)	927	6201	4288	89
H(18)	3713	6351	4380	83
H(19)	5887	5631	3399	66
H(21)	3927	2183	2764	68
H(22)	4693	1910	1097	79
H(23)	7731	976	992	66
H(27)	10648	1161	1098	64
H(28)	12837	402	150	75
H(29)	14396	-1286	759	77
H(30)	13777	-2207	2323	76
H(31)	11589	-1464	3293	62
H(34)	5999	237	5929	60
H(35)	3843	765	7030	73
H(36)	1983	2385	6593	79
H(37)	2350	3515	5083	77
H(38)	4486	2999	3983	63

### 5.3 Crystal Structure of $\text{Ph}_3\text{C-C}_5\text{H}_3(\text{COPh})_2$

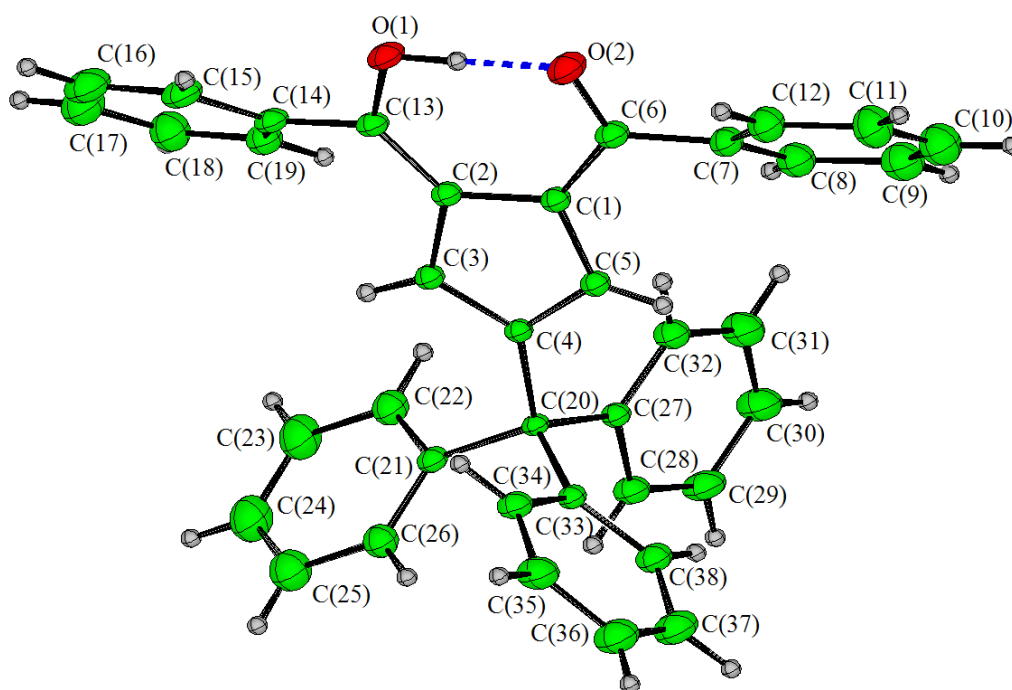


**Table 5.11:** Crystal data and structure refinement for  $Ph_3C-C_5H_2(COPh)_2$ 

Identification code	mc13
Empirical formula	C30.40 H22.40 O1.60
Formula weight	413.28
Temperature	293(2) K
Wavelength	0.7107 Å
Crystal system	Orthorhombic
Space group	Pna21
Unit cell dimensions	a = 18.055(4) Å $\alpha = 90^\circ$ b = 14.1131(17) Å $\beta = 90^\circ$ c = 11.1883(12) Å $\gamma = 90^\circ$
Volume	2850.9(7) Å <sup>3</sup>
Z	5
Density (calculated)	1.204 Mg/m <sup>3</sup>
Absorption coefficient	0.073 mm <sup>-1</sup>
F(000)	1088
Crystal size	0.42 x 0.34 x 0.20 mm
Theta range for data collection	3.2298 to 28.8326 °.
Index ranges	-14 ≤ h ≤ 23; -8 ≤ k ≤ 19; -14 ≤ l ≤ 9
Reflections collected	8939
Independent reflections	3914 [ $R_{int} = 0.0207$ ]
Reflections observed (>2 $\sigma$ )	2834
Data Completeness	0.997
Absorption correction	Semi-empirical from equivalents
Max. and min. transmission	1.00000 and 0.98591
Refinement method	Full-matrix least-squares on F <sup>2</sup>
Data / restraints / parameters	3914 / 1 / 365
Goodness-of-fit on F <sup>2</sup>	0.891
Final R indices [ $I > 2 \sigma(I)$ ]	$R_1 = 0.0338$ $wR_2 = 0.0690$
R indices (all data)	$R_1 = 0.0522$ $wR_2 = 0.0724$
Absolute structure parameter	2.2(13)
Largest diff. peak and hole	0.128 and -0.144 e.Å <sup>-3</sup>

$${}^aR_1 = \Sigma||F_o| - |F_c||/\Sigma|F_o|. \quad {}^b wR_2 = |\Sigma w(|F_o|^2 - |F_c|^2)|/\Sigma|w(F_o)^2|^{1/2}, \quad w = 1/[\sigma^2(F_o^2) + (.0428P)^2]. \quad P = (F_o^2 + 2F_c^2)/3.$$

**Table 5.12:** Atomic coordinates ( $\times 10^4$ ) and equivalent isotropic displacement parameters ( $\text{\AA}^2 \times 10^3$ ) for  $Ph_3C-C_5H_2(COPh)_2$ .  $U(eq)$  is defined as one third of the trace of the orthogonalized  $U_{ij}$  tensor.

Atom	x	y	z	U(eq)
O(1)	2445(1)	6616(1)	5069(1)	54(1)
O(2)	3692(1)	6352(1)	5896(2)	65(1)
C(1)	2960(1)	6387(1)	7641(2)	36(1)
C(2)	2216(1)	6569(1)	7151(2)	36(1)
C(3)	1748(1)	6703(1)	8157(2)	35(1)
C(4)	2144(1)	6604(1)	9198(2)	31(1)
C(5)	2888(1)	6420(1)	8875(2)	36(1)
C(6)	3638(1)	6218(2)	7009(2)	45(1)
C(7)	4321(1)	5891(2)	7618(2)	48(1)
C(8)	4318(1)	5180(2)	8476(2)	61(1)
C(9)	4976(2)	4869(2)	8979(3)	77(1)
C(10)	5640(2)	5264(2)	8623(3)	83(1)
C(11)	5647(1)	5954(2)	7784(3)	79(1)
C(12)	4999(1)	6274(2)	7272(3)	63(1)
C(13)	1984(1)	6612(1)	5968(2)	39(1)
C(14)	1195(1)	6649(2)	5613(2)	43(1)
C(15)	982(2)	7214(2)	4658(2)	62(1)
C(16)	242(2)	7214(2)	4291(3)	82(1)
C(17)	-270(2)	6660(3)	4868(3)	87(1)
C(18)	-64(1)	6103(2)	5798(3)	75(1)
C(19)	664(1)	6093(2)	6170(2)	54(1)
C(20)	1860(1)	6683(1)	10484(2)	30(1)
C(21)	1032(1)	6967(2)	10500(2)	40(1)
C(22)	516(1)	6335(2)	10043(2)	61(1)
C(23)	-233(2)	6545(3)	10073(3)	91(1)

C(24)	-481(2)	7376(3)	10560(3)	96(1)
C(25)	12(2)	8004(2)	11008(3)	82(1)
C(26)	766(1)	7804(2)	10979(2)	55(1)
C(27)	1916(1)	5719(1)	11134(2)	34(1)
C(28)	1604(1)	5627(2)	12259(2)	50(1)
C(29)	1651(2)	4787(2)	12886(2)	67(1)
C(30)	1986(2)	4013(2)	12393(2)	72(1)
C(31)	2275(1)	4081(2)	11282(3)	70(1)
C(32)	2245(1)	4929(2)	10655(2)	51(1)
C(33)	2325(1)	7453(1)	11116(2)	33(1)
C(34)	2410(1)	8330(2)	10559(2)	46(1)
C(35)	2761(1)	9068(2)	11117(3)	65(1)
C(36)	3030(2)	8978(2)	12251(3)	76(1)
C(37)	2971(2)	8115(2)	12802(2)	76(1)
C(38)	2626(1)	7356(2)	12234(2)	52(1)

**Table 5.13:** Bond lengths [ $\text{\AA}$ ] and angles [ $^\circ$ ] for  $\text{Ph}_3\text{C}-\text{C}_5\text{H}_2(\text{COPh})_2$ 

O(1)-C(13)	1.305(2)	O(2)-C(6)	1.263(3)
C(1)-C(5)	1.387(3)	C(1)-C(6)	1.434(3)
C(1)-C(2)	1.474(3)	C(2)-C(13)	1.390(3)
C(2)-C(3)	1.420(3)	C(3)-C(4)	1.374(3)
C(4)-C(5)	1.414(3)	C(4)-C(20)	1.531(3)
C(6)-C(7)	1.482(3)	C(7)-C(8)	1.389(3)
C(7)-C(12)	1.392(3)	C(8)-C(9)	1.387(3)
C(9)-C(10)	1.381(4)	C(10)-C(11)	1.352(4)
C(11)-C(12)	1.380(4)	C(13)-C(14)	1.479(3)
C(14)-C(19)	1.387(3)	C(14)-C(15)	1.388(3)
C(15)-C(16)	1.398(4)	C(16)-C(17)	1.373(4)
C(17)-C(18)	1.355(4)	C(18)-C(19)	1.380(3)
C(20)-C(33)	1.544(3)	C(20)-C(27)	1.546(3)
C(20)-C(21)	1.548(3)	C(21)-C(26)	1.383(3)
C(21)-C(22)	1.388(3)	C(22)-C(23)	1.384(4)
C(23)-C(24)	1.369(5)	C(24)-C(25)	1.353(5)
C(25)-C(26)	1.390(3)	C(27)-C(32)	1.372(3)
C(27)-C(28)	1.385(3)	C(28)-C(29)	1.381(3)
C(29)-C(30)	1.365(4)	C(30)-C(31)	1.351(4)
C(31)-C(32)	1.388(3)	C(33)-C(38)	1.371(3)
C(33)-C(34)	1.394(3)	C(34)-C(35)	1.369(3)
C(35)-C(36)	1.365(4)	C(36)-C(37)	1.369(4)
C(37)-C(38)	1.392(3)		
C(5)-C(1)-C(6)	125.3(2)	C(5)-C(1)-C(2)	106.12(19)
C(6)-C(1)-C(2)	128.6(2)	C(13)-C(2)-C(3)	124.70(18)
C(13)-C(2)-C(1)	129.54(19)	C(3)-C(2)-C(1)	105.75(17)
C(4)-C(3)-C(2)	110.34(16)	C(3)-C(4)-C(5)	107.27(18)
C(3)-C(4)-C(20)	127.89(17)	C(5)-C(4)-C(20)	124.84(17)
C(1)-C(5)-C(4)	110.51(19)	O(2)-C(6)-C(1)	121.8(2)
O(2)-C(6)-C(7)	115.87(18)	C(1)-C(6)-C(7)	122.4(2)

C(8)-C(7)-C(12)	118.5(2)	C(8)-C(7)-C(6)	122.6(2)
C(12)-C(7)-C(6)	118.8(2)	C(9)-C(8)-C(7)	120.4(2)
C(10)-C(9)-C(8)	119.9(3)	C(11)-C(10)-C(9)	119.9(3)
C(10)-C(11)-C(12)	121.1(3)	C(11)-C(12)-C(7)	120.1(3)
O(1)-C(13)-C(2)	122.81(19)	O(1)-C(13)-C(14)	114.01(19)
C(2)-C(13)-C(14)	123.17(19)	C(19)-C(14)-C(15)	118.6(2)
C(19)-C(14)-C(13)	121.7(2)	C(15)-C(14)-C(13)	119.5(2)
C(14)-C(15)-C(16)	119.4(3)	C(17)-C(16)-C(15)	120.4(3)
C(18)-C(17)-C(16)	120.5(3)	C(17)-C(18)-C(19)	119.9(3)
C(18)-C(19)-C(14)	121.2(2)	C(4)-C(20)-C(33)	107.43(15)
C(4)-C(20)-C(27)	110.84(15)	C(33)-C(20)-C(27)	111.62(15)
C(4)-C(20)-C(21)	110.71(15)	C(33)-C(20)-C(21)	109.74(16)
C(27)-C(20)-C(21)	106.53(14)	C(26)-C(21)-C(22)	117.20(19)
C(26)-C(21)-C(20)	124.16(18)	C(22)-C(21)-C(20)	118.6(2)
C(23)-C(22)-C(21)	120.6(3)	C(24)-C(23)-C(22)	120.9(3)
C(25)-C(24)-C(23)	119.5(3)	C(24)-C(25)-C(26)	120.2(3)
C(21)-C(26)-C(25)	121.6(2)	C(32)-C(27)-C(28)	117.1(2)
C(32)-C(27)-C(20)	124.01(18)	C(28)-C(27)-C(20)	118.91(18)
C(29)-C(28)-C(27)	121.2(2)	C(30)-C(29)-C(28)	120.6(2)
C(31)-C(30)-C(29)	119.1(2)	C(30)-C(31)-C(32)	120.7(3)
C(27)-C(32)-C(31)	121.3(2)	C(38)-C(33)-C(34)	116.89(19)
C(38)-C(33)-C(20)	124.27(19)	C(34)-C(33)-C(20)	118.70(17)
C(35)-C(34)-C(33)	121.5(2)	C(36)-C(35)-C(34)	121.2(2)
C(35)-C(36)-C(37)	118.3(2)	C(36)-C(37)-C(38)	120.9(2)
C(33)-C(38)-C(37)	121.1(2)		

**Table 5.14:** Anisotropic displacement parameters ( $\text{\AA}^2 \times 10^3$ ) for  $\text{Ph}_3\text{C-C}_5\text{H}_2(\text{COPh})_2$ . The anisotropic displacement factor exponent takes the form:

$$-2 \pi^2 [ h^2 a^{*2} U11 + \dots + 2 h k a^* b^* U12 ]$$

Atom	U11	U22	U33	U23	U13	U12
O(1)	62(1)	73(1)	26(1)	2(1)	5(1)	1(1)
O(2)	59(1)	97(1)	38(1)	4(1)	13(1)	3(1)
C(1)	42(1)	34(1)	32(1)	-3(1)	4(1)	-4(1)
C(2)	46(1)	31(1)	30(1)	0(1)	1(1)	-4(1)
C(3)	41(1)	34(1)	31(1)	-3(1)	-1(1)	-3(1)
C(4)	38(1)	29(1)	27(1)	1(1)	0(1)	-4(1)
C(5)	41(1)	36(1)	32(1)	0(1)	-4(1)	-4(1)
C(6)	56(1)	45(1)	35(1)	-1(1)	9(1)	-5(1)
C(7)	48(1)	53(2)	42(1)	-7(1)	8(1)	1(1)
C(8)	67(2)	55(2)	61(2)	2(1)	9(1)	7(1)
C(9)	86(2)	68(2)	78(2)	12(2)	-2(2)	24(2)
C(10)	69(2)	89(2)	91(3)	-5(2)	-16(2)	18(2)
C(11)	52(2)	91(2)	95(3)	-5(2)	0(2)	-3(2)
C(12)	54(1)	74(2)	63(2)	2(2)	7(1)	-1(1)
C(13)	55(1)	34(1)	29(1)	2(1)	2(1)	-1(1)
C(14)	60(1)	42(1)	26(1)	-5(1)	-5(1)	7(1)
C(15)	84(2)	68(2)	34(1)	-3(1)	-5(1)	17(1)
C(16)	102(2)	99(2)	44(2)	-5(2)	-28(2)	45(2)
C(17)	68(2)	121(3)	73(2)	-14(2)	-23(2)	13(2)
C(18)	60(2)	84(2)	83(2)	-10(2)	-14(2)	-6(1)
C(19)	60(1)	55(2)	48(2)	-1(1)	-12(1)	-2(1)
C(20)	36(1)	32(1)	21(1)	0(1)	1(1)	-2(1)
C(21)	40(1)	51(1)	28(1)	10(1)	3(1)	-2(1)
C(22)	47(1)	80(2)	56(2)	1(2)	-5(1)	-15(1)
C(23)	45(2)	133(3)	96(3)	15(2)	-12(2)	-24(2)
C(24)	47(2)	140(3)	101(3)	49(3)	1(2)	21(2)

C(25)	62(2)	99(2)	83(2)	29(2)	22(2)	28(2)
C(26)	48(1)	63(2)	55(2)	6(1)	6(1)	11(1)
C(27)	41(1)	35(1)	28(1)	2(1)	-4(1)	-7(1)
C(28)	71(1)	40(1)	38(1)	5(1)	9(1)	-11(1)
C(29)	101(2)	64(2)	36(2)	14(1)	2(1)	-29(2)
C(30)	116(2)	44(2)	58(2)	18(2)	-18(2)	-11(2)
C(31)	98(2)	41(2)	69(2)	8(1)	-9(2)	8(1)
C(32)	68(1)	41(1)	44(1)	5(1)	4(1)	4(1)
C(33)	34(1)	39(1)	27(1)	-2(1)	6(1)	-3(1)
C(34)	66(1)	38(1)	36(1)	-2(1)	4(1)	-8(1)
C(35)	96(2)	42(2)	57(2)	-6(1)	17(2)	-27(1)
C(36)	98(2)	77(2)	53(2)	-16(2)	9(2)	-51(2)
C(37)	91(2)	94(2)	43(2)	1(2)	-13(1)	-49(2)
C(38)	61(1)	58(2)	37(1)	11(1)	-12(1)	-26(1)

**Table 5.15:** Hydrogen coordinates ( $\times 10^4$ ) and isotropic displacement parameters ( $\text{\AA}^2 \times 10^3$ ) for  $\text{Ph}_3\text{C-C}_3\text{H}_2(\text{COPh})_2$

Atom	x	y	z	U(eq)
H(1)	2958(14)	6551(16)	5380(20)	66(8)
H(3)	1244	6838	8117	46
H(5)	3274	6333	9414	47
H(8)	3871	4911	8714	79
H(9)	4970	4394	9556	100
H(10)	6082	5056	8959	108
H(11)	6096	6217	7549	103
H(12)	5014	6747	6693	82
H(15)	1329	7588	4265	81
H(16)	96	7592	3652	106
H(17)	-761	6667	4620	113
H(18)	-414	5729	6184	98
H(19)	801	5707	6806	71
H(22)	674	5765	9713	80
H(23)	-572	6116	9759	119
H(24)	-986	7509	10582	124
H(25)	-153	8571	11337	106
H(26)	1099	8243	11288	72
H(28)	1359	6141	12597	65
H(29)	1453	4748	13652	87
H(30)	2014	3446	12815	94
H(31)	2497	3554	10934	90
H(32)	2451	4962	9894	66
H(34)	2225	8416	9792	60
H(35)	2816	9641	10715	84
H(36)	3247	9490	12640	99
H(37)	3164	8035	13566	99
H(38)	2600	6774	12620	68

## 5.4 Crystal Structure for C<sub>23</sub>H<sub>16</sub>O<sub>2</sub>

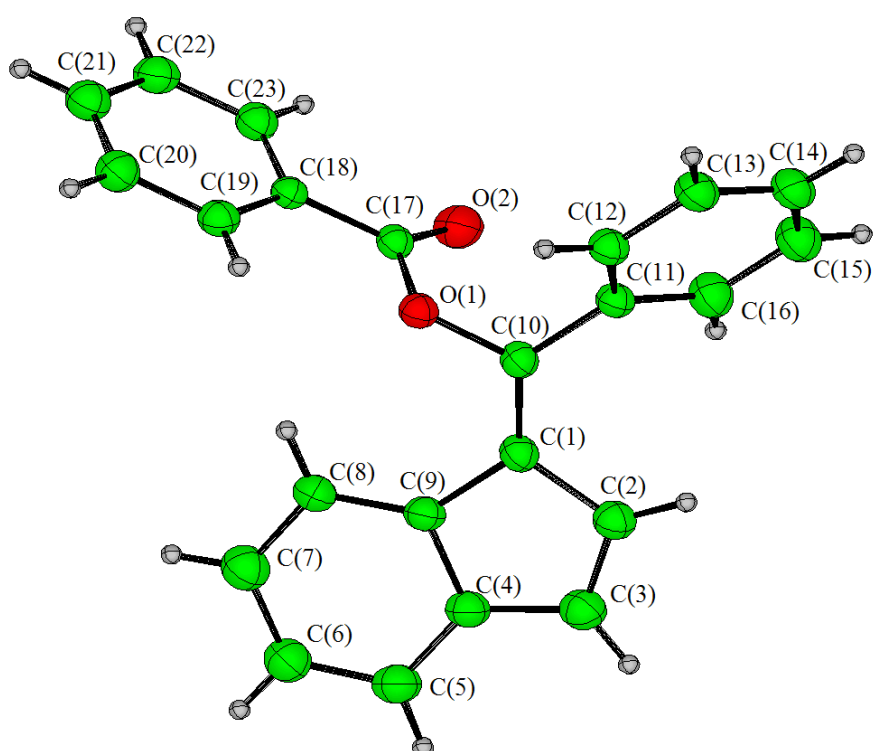


**Table 5.16:** Crystal data and structure refinement for  $C_{23}H_{16}O_2$ 

Identification code	mc8
Empirical formula	$C_{23}H_{16}O_2$
Formula weight	324.36
Temperature	293(2) K
Wavelength	0.7107 Å
Crystal system	Triclinic
Space group	P-1
Unit cell dimensions	$a = 9.0224(7)\text{Å}$ $\alpha = 90.002(7)^\circ$ $b = 9.0509(7)\text{Å}$ $\beta = 88.001(8)^\circ$ $c = 21.338(2)\text{Å}$ $\gamma = 83.266(7)^\circ$
Volume	1729.3(3) Å <sup>3</sup>
Z	4
Density (calculated)	1.246 Mg/m <sup>3</sup>
Absorption coefficient	0.079 mm <sup>-1</sup>
F(000)	680
Crystal size	0.50 x 0.40 x 0.20 mm
Theta range for data collection	2.9521 to 28.8248 °.
Index ranges	-11 ≤ h ≤ 12; -12 ≤ k ≤ 12; -27 ≤ l ≤ 26
Reflections collected	9731
Independent reflections	5515 [ $R_{\text{int}} = 0.0503$ ]
Reflections observed (>2 $\sigma$ )	4047
Data Completeness	0.872
Absorption correction	Semi-empirical from equivalents
Max. and min. transmission	1.00000 and 0.64187
Refinement method	Full-matrix least-squares on $F^2$
Data / restraints / parameters	5515 / 0 / 453
Goodness-of-fit on $F^2$	1.988
Final R indices [ $I > 2 \sigma(I)$ ]	$R_1 = 0.1710$ $wR_2 = 0.4959$
R indices (all data)	$R_1 = 0.1908$ $wR_2 = 0.5117$
Largest diff. peak and hole	0.536 and -0.415 e.Å <sup>-3</sup>

$${}^aR_1 = \Sigma|F_o| - |F_c|/\Sigma|F_o|. \quad {}^b wR_2 = |\Sigma w(|F_o|^2 - |F_c|^2)|/\Sigma|w(F_o)^2|^{1/2}, \quad w = 1/[\sigma^2(F_o^2) + (0.2P)^2]. \quad P = (F_o^2 + 2F_c^2)/3.$$

**Table 5.17:** Atomic coordinates ( $\times 10^4$ ) and equivalent isotropic displacement parameters ( $\text{\AA}^2 \times 10^3$ ) for  $C_{23}H_{16}O_2$ .  $U(eq)$  is defined as one third of the trace of the orthogonalized  $U_{ij}$  tensor.

Atom	x	y	z	U(eq)
O(3)	5078(5)	8842(5)	815(2)	56(1)
O(4)	4762(7)	7049(7)	1505(2)	84(2)
O(1)	3835(5)	5120(5)	4182(2)	59(1)
O(2)	2048(6)	4809(7)	3504(2)	85(2)
C(1)	5778(8)	5162(8)	3432(3)	62(2)
C(2)	6780(9)	5802(9)	2979(4)	72(2)
C(3)	7920(10)	4800(11)	2819(4)	81(2)
C(4)	7750(8)	3425(9)	3124(4)	71(2)
C(5)	8630(9)	2033(11)	3097(4)	87(3)
C(6)	8172(11)	910(12)	3460(4)	87(3)
C(7)	6893(11)	1065(12)	3830(5)	94(3)
C(8)	6023(9)	2454(9)	3873(4)	70(2)
C(9)	6449(8)	3617(8)	3522(3)	63(2)
C(10)	4566(8)	5868(8)	3715(3)	57(2)
C(11)	3913(7)	7431(8)	3622(3)	58(2)
C(12)	3526(8)	8344(8)	4144(3)	65(2)
C(13)	2925(9)	9802(9)	4073(4)	79(2)
C(14)	2705(10)	10369(10)	3476(4)	81(2)
C(15)	3037(11)	9443(10)	2950(5)	90(3)
C(16)	3657(11)	8004(10)	3029(4)	86(3)
C(17)	2518(7)	4624(7)	4027(3)	55(2)
C(18)	1811(7)	3883(7)	4543(3)	52(2)
C(19)	2460(8)	3636(8)	5111(3)	66(2)

C(20)	1757(10)	2872(10)	5575(4)	76(2)
C(21)	435(9)	2367(10)	5470(4)	78(2)
C(22)	-219(9)	2588(10)	4905(4)	77(2)
C(23)	479(8)	3341(8)	4448(4)	69(2)
C(24)	5010(7)	10809(8)	1535(3)	56(2)
C(25)	5592(9)	11850(9)	1983(3)	69(2)
C(26)	4511(9)	12879(9)	2157(4)	72(2)
C(27)	3114(8)	12648(8)	1852(3)	63(2)
C(28)	1713(9)	13409(9)	1887(4)	75(2)
C(29)	602(9)	12928(11)	1528(4)	81(2)
C(30)	898(9)	11712(10)	1155(4)	74(2)
C(31)	2302(8)	10927(8)	1097(3)	63(2)
C(32)	3442(7)	11393(7)	1454(3)	54(2)
C(33)	5794(7)	9594(7)	1280(3)	53(2)
C(34)	7358(7)	8980(8)	1374(3)	62(2)
C(35)	7928(8)	8888(9)	1956(4)	72(2)
C(36)	9409(9)	8278(11)	2041(5)	86(3)
C(37)	10266(9)	7752(10)	1524(5)	85(2)
C(38)	9723(9)	7858(11)	937(5)	90(3)
C(39)	8283(8)	8461(9)	850(4)	70(2)
C(40)	4614(7)	7533(8)	982(3)	57(2)
C(41)	3868(6)	6825(7)	477(3)	50(2)
C(42)	3658(7)	7473(8)	-104(3)	58(2)
C(43)	2887(9)	6756(10)	-546(4)	73(2)
C(44)	2399(9)	5435(10)	-432(4)	75(2)
C(45)	2582(9)	4792(9)	148(4)	74(2)
C(46)	3359(8)	5473(8)	602(3)	62(2)

**Table 5.18:** Bond lengths [ $\text{\AA}$ ] and angles [ $^\circ$ ] for  $C_{23}H_{16}O_2$ 

O(3)-C(40)	1.346(8)	O(3)-C(33)	1.420(7)
O(4)-C(40)	1.205(8)	O(1)-C(17)	1.369(8)
O(1)-C(10)	1.394(8)	O(2)-C(17)	1.211(8)
C(1)-C(10)	1.327(10)	C(1)-C(2)	1.466(11)
C(1)-C(9)	1.472(10)	C(2)-C(3)	1.324(11)
C(3)-C(4)	1.427(12)	C(4)-C(5)	1.408(11)
C(4)-C(9)	1.418(11)	C(5)-C(6)	1.371(13)
C(6)-C(7)	1.368(14)	C(7)-C(8)	1.403(12)
C(8)-C(9)	1.375(11)	C(10)-C(11)	1.484(10)
C(11)-C(16)	1.383(10)	C(11)-C(12)	1.397(9)
C(12)-C(13)	1.377(11)	C(13)-C(14)	1.386(13)
C(14)-C(15)	1.403(13)	C(15)-C(16)	1.369(12)
C(17)-C(18)	1.456(9)	C(18)-C(19)	1.370(9)
C(18)-C(23)	1.372(10)	C(19)-C(20)	1.385(11)
C(20)-C(21)	1.352(12)	C(21)-C(22)	1.365(12)
C(22)-C(23)	1.369(10)	C(24)-C(33)	1.339(9)
C(24)-C(32)	1.467(9)	C(24)-C(25)	1.493(10)
C(25)-C(26)	1.311(11)	C(26)-C(27)	1.475(10)
C(27)-C(28)	1.366(10)	C(27)-C(32)	1.415(9)
C(28)-C(29)	1.392(12)	C(29)-C(30)	1.353(12)
C(30)-C(31)	1.380(10)	C(31)-C(32)	1.405(9)
C(33)-C(34)	1.475(9)	C(34)-C(35)	1.359(10)
C(34)-C(39)	1.417(10)	C(35)-C(36)	1.402(11)
C(36)-C(37)	1.377(13)	C(37)-C(38)	1.359(13)
C(38)-C(39)	1.368(11)	C(40)-C(41)	1.475(9)
C(41)-C(46)	1.380(9)	C(41)-C(42)	1.381(9)
C(42)-C(43)	1.395(10)	C(43)-C(44)	1.341(11)
C(44)-C(45)	1.376(12)	C(45)-C(46)	1.400(10)
C(40)-O(3)-C(33)	116.5(5)	C(17)-O(1)-C(10)	116.6(5)

C(10)-C(1)-C(2)	126.4(7)	C(10)-C(1)-C(9)	128.2(7)
C(2)-C(1)-C(9)	105.3(6)	C(3)-C(2)-C(1)	110.0(8)
C(2)-C(3)-C(4)	109.8(7)	C(5)-C(4)-C(9)	119.6(9)
C(5)-C(4)-C(3)	131.6(8)	C(9)-C(4)-C(3)	108.8(7)
C(6)-C(5)-C(4)	117.6(8)	C(7)-C(6)-C(5)	123.5(9)
C(6)-C(7)-C(8)	119.5(10)	C(9)-C(8)-C(7)	119.0(8)
C(8)-C(9)-C(4)	120.8(7)	C(8)-C(9)-C(1)	133.1(7)
C(4)-C(9)-C(1)	106.0(7)	C(1)-C(10)-O(1)	118.3(6)
C(1)-C(10)-C(11)	127.5(7)	O(1)-C(10)-C(11)	114.1(6)
C(16)-C(11)-C(12)	119.1(7)	C(16)-C(11)-C(10)	121.6(6)
C(12)-C(11)-C(10)	119.4(6)	C(13)-C(12)-C(11)	120.8(7)
C(12)-C(13)-C(14)	119.5(7)	C(13)-C(14)-C(15)	120.0(8)
C(16)-C(15)-C(14)	119.6(8)	C(15)-C(16)-C(11)	121.0(8)
O(2)-C(17)-O(1)	120.7(6)	O(2)-C(17)-C(18)	126.2(7)
O(1)-C(17)-C(18)	113.1(5)	C(19)-C(18)-C(23)	118.5(7)
C(19)-C(18)-C(17)	122.7(6)	C(23)-C(18)-C(17)	118.7(6)
C(18)-C(19)-C(20)	119.9(7)	C(21)-C(20)-C(19)	120.3(7)
C(20)-C(21)-C(22)	120.7(8)	C(21)-C(22)-C(23)	118.9(8)
C(22)-C(23)-C(18)	121.8(7)	C(33)-C(24)-C(32)	129.1(6)
C(33)-C(24)-C(25)	125.4(6)	C(32)-C(24)-C(25)	105.5(6)
C(26)-C(25)-C(24)	109.2(7)	C(25)-C(26)-C(27)	110.7(6)
C(28)-C(27)-C(32)	120.8(7)	C(28)-C(27)-C(26)	132.2(7)
C(32)-C(27)-C(26)	106.9(6)	C(27)-C(28)-C(29)	119.1(7)
C(30)-C(29)-C(28)	120.5(7)	C(29)-C(30)-C(31)	122.3(8)
C(30)-C(31)-C(32)	118.1(7)	C(31)-C(32)-C(27)	119.1(6)
C(31)-C(32)-C(24)	133.3(6)	C(27)-C(32)-C(24)	107.6(6)
C(24)-C(33)-O(3)	116.4(5)	C(24)-C(33)-C(34)	129.3(6)
O(3)-C(33)-C(34)	114.1(5)	C(35)-C(34)-C(39)	119.1(7)
C(35)-C(34)-C(33)	121.2(6)	C(39)-C(34)-C(33)	119.7(6)
C(34)-C(35)-C(36)	120.7(7)	C(37)-C(36)-C(35)	118.6(9)
C(38)-C(37)-C(36)	121.5(8)	C(37)-C(38)-C(39)	120.2(7)
C(38)-C(39)-C(34)	119.8(8)	O(4)-C(40)-O(3)	121.6(6)
O(4)-C(40)-C(41)	124.9(7)	O(3)-C(40)-C(41)	113.4(6)

C(46)-C(41)-C(42)	119.8(6)	C(46)-C(41)-C(40)	117.7(6)
C(42)-C(41)-C(40)	122.4(6)	C(41)-C(42)-C(43)	118.7(7)
C(44)-C(43)-C(42)	122.0(7)	C(43)-C(44)-C(45)	119.7(7)
C(44)-C(45)-C(46)	119.8(7)	C(41)-C(46)-C(45)	119.8(7)

**Table 5.19:** Anisotropic displacement parameters ( $\text{\AA}^2 \times 10^3$ ) for  $C_{23}H_{16}O_2$ . The anisotropic displacement factor exponent takes the form:

$$-2 \pi^2 [ h^2 a^{*2} U11 + \dots + 2 h k a^* b^* U12 ]$$

Atom	U11	U22	U33	U23	U13	U12
O(3)	61(3)	52(3)	57(3)	-1(2)	-7(2)	-9(2)
O(4)	111(4)	89(4)	58(3)	9(3)	-11(3)	-31(3)
O(1)	61(3)	60(3)	57(3)	3(2)	-2(2)	-12(2)
O(2)	90(4)	113(5)	58(3)	12(3)	-14(3)	-35(3)
C(1)	70(4)	53(4)	62(4)	-11(3)	-1(3)	-6(3)
C(2)	75(5)	72(5)	67(4)	-5(4)	11(4)	-6(4)
C(3)	80(5)	89(6)	72(5)	-13(4)	11(4)	-10(5)
C(4)	64(4)	81(5)	66(4)	-20(4)	-12(3)	4(4)
C(5)	70(5)	103(7)	78(5)	-19(5)	-19(4)	33(5)
C(6)	94(6)	88(6)	73(5)	-3(5)	-22(5)	23(5)
C(7)	101(7)	86(6)	89(6)	-3(5)	-20(5)	16(5)
C(8)	67(4)	66(5)	76(5)	0(4)	-7(4)	0(4)
C(9)	57(4)	65(5)	65(4)	-11(3)	-16(3)	2(3)
C(10)	69(4)	59(4)	45(3)	3(3)	-5(3)	-12(3)
C(11)	59(4)	58(4)	57(4)	-4(3)	-2(3)	-5(3)
C(12)	68(4)	64(5)	61(4)	-3(3)	10(3)	-2(3)
C(13)	79(5)	62(5)	94(6)	-15(4)	21(4)	-7(4)
C(14)	86(6)	56(5)	97(6)	7(4)	10(5)	2(4)
C(15)	106(7)	72(6)	87(6)	23(5)	9(5)	4(5)
C(16)	106(7)	80(6)	65(5)	3(4)	4(4)	10(5)
C(17)	61(4)	50(4)	53(4)	-7(3)	-7(3)	0(3)
C(18)	52(3)	48(4)	55(3)	-6(3)	-4(3)	1(3)
C(19)	66(4)	70(5)	62(4)	4(3)	-5(3)	-12(4)
C(20)	88(5)	81(5)	61(4)	7(4)	-13(4)	-15(4)
C(21)	80(5)	76(5)	79(5)	14(4)	6(4)	-12(4)
C(22)	68(5)	82(6)	81(5)	8(4)	5(4)	-18(4)
C(23)	73(5)	65(5)	69(4)	2(3)	-11(4)	-11(4)

C(24)	57(4)	58(4)	54(4)	0(3)	-6(3)	-7(3)
C(25)	70(4)	70(5)	69(4)	-4(4)	-11(3)	-12(4)
C(26)	88(5)	63(5)	65(4)	-10(3)	-9(4)	-6(4)
C(27)	72(4)	62(4)	54(4)	-5(3)	-3(3)	0(3)
C(28)	83(5)	67(5)	68(4)	-5(4)	8(4)	13(4)
C(29)	59(4)	93(6)	89(5)	1(5)	-2(4)	6(4)
C(30)	60(4)	84(6)	76(5)	4(4)	-9(3)	-1(4)
C(31)	64(4)	54(4)	72(4)	-1(3)	-13(3)	-3(3)
C(32)	56(4)	49(4)	57(3)	6(3)	-3(3)	-4(3)
C(33)	53(4)	54(4)	54(3)	1(3)	0(3)	-14(3)
C(34)	55(4)	55(4)	77(5)	-2(3)	-1(3)	-8(3)
C(35)	67(4)	75(5)	73(5)	-5(4)	-4(4)	2(4)
C(36)	65(5)	89(6)	101(6)	7(5)	-1(4)	5(4)
C(37)	54(4)	85(6)	112(7)	-14(5)	-2(4)	2(4)
C(38)	69(5)	88(6)	109(7)	-32(5)	16(5)	3(4)
C(39)	58(4)	72(5)	79(5)	-21(4)	-1(3)	-5(3)
C(40)	61(4)	50(4)	59(4)	1(3)	0(3)	-7(3)
C(41)	46(3)	48(4)	56(4)	-2(3)	2(3)	-7(3)
C(42)	60(4)	62(4)	55(4)	4(3)	-4(3)	-16(3)
C(43)	77(5)	82(6)	63(4)	3(4)	-17(3)	-22(4)
C(44)	77(5)	72(5)	76(5)	-10(4)	-9(4)	-11(4)
C(45)	73(5)	59(5)	93(6)	-9(4)	-4(4)	-18(4)
C(46)	66(4)	56(4)	65(4)	-1(3)	0(3)	-7(3)

**Table 5.20:** Hydrogen coordinates ( $\times 10^4$ ) and isotropic displacement parameters ( $\text{\AA}^2 \times 10^3$ ) for  $C_{23}H_{16}O_2$

Atom	x	y	z	U(eq)
H(2)	6637	6770	2827	93
H(3)	8712	4968	2548	105
H(5)	9491	1880	2841	113
H(6)	8762	-4	3455	113
H(7)	6603	256	4051	122
H(8)	5172	2587	4135	91
H(12)	3676	7962	4545	85
H(13)	2668	10401	4423	103
H(14)	2338	11364	3424	105
H(15)	2838	9805	2550	117
H(16)	3909	7402	2680	111
H(19)	3371	3979	5184	85
H(20)	2196	2707	5960	99
H(21)	-33	1865	5786	102
H(22)	-1124	2232	4833	100
H(23)	39	3490	4062	89
H(25)	6568	11780	2117	90
H(26)	4611	13649	2435	93
H(28)	1504	14237	2148	97
H(29)	-352	13446	1545	106
H(30)	128	11395	931	96
H(31)	2489	10111	828	82
H(35)	7330	9233	2301	94
H(36)	9804	8231	2438	112
H(37)	11238	7314	1577	110
H(38)	10332	7519	594	117
H(39)	7913	8530	449	91
H(42)	4023	8369	-199	76

H(43)	2705	7209	-932	95
H(44)	1938	4957	-744	97
H(45)	2190	3907	239	96
H(46)	3532	5015	987	81

## 5.5 Crystal structure of [Ru(dbzCp)(CO)IPPh<sub>3</sub>]

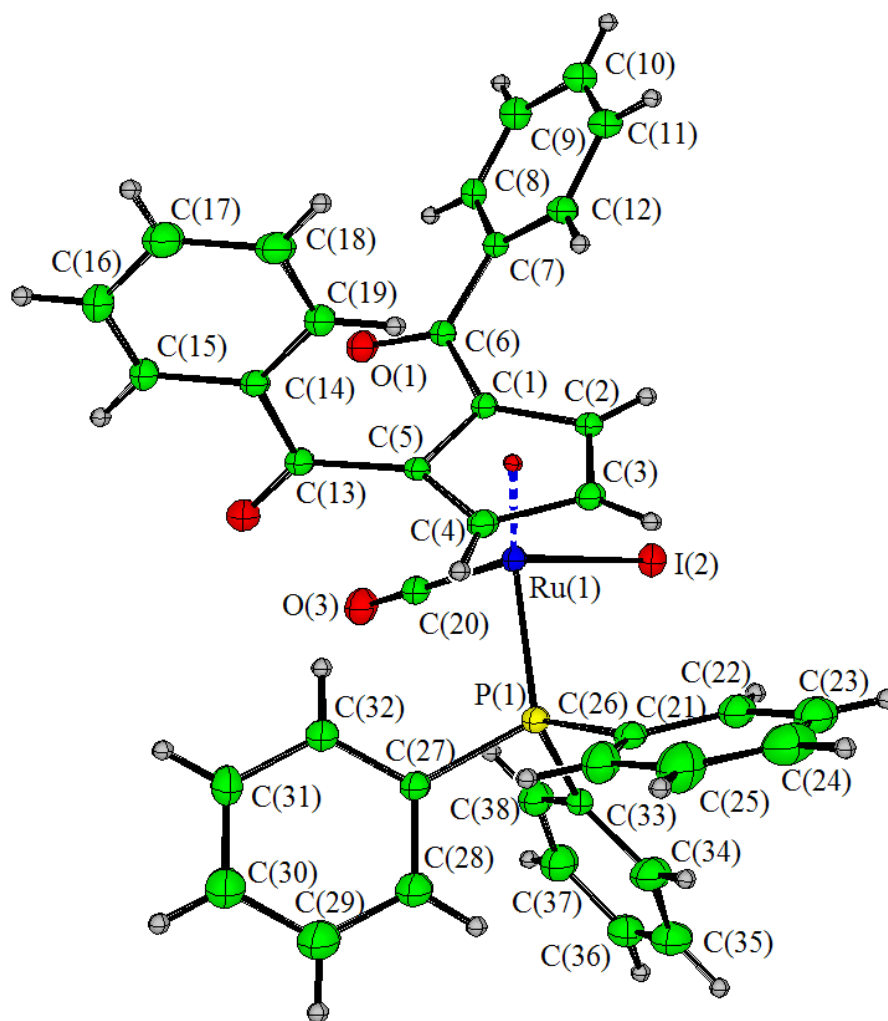


**Table 5.21:** Crystal data and structure refinement of  $[Ru(dbzCp)(CO)IPPh_3]$

Identification code	mc4c
Empirical formula	C <sub>38</sub> H <sub>28</sub> I O <sub>3</sub> P Ru
Formula weight	791.54
Temperature	293(2) K
Wavelength	0.7107 Å
Crystal system	Monoclinic
Space group	P2 <sub>1</sub> /n
Unit cell dimensions	a = 10.0096(3) Å $\alpha$ = 90° b = 32.9682(8) Å $\beta$ = 106.043(3)° c = 10.2968(3) Å $\gamma$ = 90°
Volume	3265.59(16) Å <sup>3</sup>
Z	4
Density (calculated)	1.610 Mg/m <sup>3</sup>
Absorption coefficient	1.511 mm <sup>-1</sup>
F(000)	1568
Crystal size	0.45 x 0.32 x 0.28 mm
Theta range for data collection	2.4594 to 25.1510 °.
Index ranges	-11 ≤ h ≤ 10; -35 ≤ k ≤ 39; -12 ≤ l ≤ 9
Reflections collected	13267
Independent reflections	5179 [R <sub>int</sub> = 0.0361]
Reflections observed (>2σ)	3316
Data Completeness	0.875
Absorption correction	Semi-empirical from equivalents
Max. and min. transmission	1.00000 and 0.89692
Refinement method	Full-matrix least-squares on F <sup>2</sup>
Data / restraints / parameters	5179 / 0 / 397
Goodness-of-fit on F <sup>2</sup>	0.974
Final R indices [I > 2σ(I)]	R <sub>1</sub> = 0.0337 wR <sub>2</sub> = 0.0876
R indices (all data)	R <sub>1</sub> = 0.0715 wR <sub>2</sub> = 0.1042
Largest diff. peak and hole	0.588 and -0.539 e.Å <sup>-3</sup>

$${}^aR_1 = \Sigma|F_o| - |F_c|/\Sigma|F_o|. \quad {}^b wR_2 = |\Sigma w(|F_o|^2 - |F_c|^2)|/\Sigma w(F_o)^2|^{1/2}, \quad w = 1/[\sigma^2(F_o^2) + (0.0530P)^2]. \quad P = (F_o^2 + 2F_c^2)/3.$$

**Table 5.22:** Atomic coordinates ( $\times 10^4$ ) and equivalent isotropic displacement parameters ( $\text{\AA}^2 \times 10^3$ ) for  $[\text{Ru}(\text{dbzCp})(\text{CO})\text{IPPh}_3]$ .  $U(\text{eq})$  is defined as one third of the trace of the orthogonalized  $U_{ij}$  tensor.

Atom	x	y	z	U(eq)
Ru(1)	633(1)	1490(1)	6921(1)	32(1)
I(2)	3090(1)	1390(1)	6385(1)	52(1)
P(1)	707(2)	857(1)	7876(2)	36(1)
O(1)	-1062(5)	2348(1)	4557(5)	52(1)
O(3)	-768(5)	1151(2)	4209(5)	62(2)
O(2)	-3027(5)	1686(1)	5490(5)	66(2)
C(1)	113(6)	2164(2)	6770(6)	35(2)
C(2)	1342(7)	2111(2)	7869(6)	39(2)
C(3)	1007(7)	1862(2)	8844(6)	41(2)
C(4)	-419(7)	1750(2)	8367(6)	39(2)
C(5)	-977(6)	1927(2)	7069(6)	33(2)
C(6)	-150(7)	2435(2)	5560(7)	38(2)
C(7)	592(6)	2827(2)	5657(7)	39(2)
C(8)	633(6)	3024(2)	4470(7)	46(2)
C(9)	1243(8)	3392(2)	4521(9)	65(2)
C(10)	1817(8)	3582(2)	5717(11)	75(3)
C(11)	1779(8)	3396(2)	6909(9)	69(3)
C(12)	1164(7)	3015(2)	6894(7)	49(2)
C(13)	-2479(7)	1947(2)	6293(7)	41(2)
C(14)	-3260(7)	2305(2)	6558(6)	36(2)
C(15)	-4660(7)	2335(2)	5907(7)	42(2)
C(16)	-5408(8)	2651(2)	6158(8)	54(2)

C(17)	-4790(9)	2937(2)	7081(8)	63(2)
C(18)	-3407(8)	2913(2)	7745(8)	58(2)
C(19)	-2647(7)	2597(2)	7482(7)	47(2)
C(20)	-251(7)	1270(2)	5185(8)	45(2)
C(21)	1434(7)	899(2)	9688(7)	45(2)
C(22)	2844(8)	988(2)	10190(8)	60(2)
C(23)	3408(10)	1052(2)	11573(10)	83(3)
C(24)	2574(14)	1027(3)	12438(10)	92(3)
C(25)	1210(12)	946(3)	11956(9)	89(3)
C(26)	624(9)	882(2)	10576(8)	64(2)
C(27)	-999(7)	623(2)	7684(6)	40(2)
C(28)	-1121(8)	238(2)	8185(8)	60(2)
C(29)	-2421(10)	78(3)	8058(9)	74(3)
C(30)	-3589(10)	285(3)	7438(10)	81(3)
C(31)	-3487(8)	657(3)	6916(9)	77(3)
C(32)	-2190(7)	829(2)	7039(8)	55(2)
C(33)	1653(6)	433(2)	7395(7)	41(2)
C(34)	2440(9)	167(2)	8327(8)	66(2)
C(35)	3010(9)	-173(2)	7911(11)	80(3)
C(36)	2826(9)	-248(2)	6614(11)	75(3)
C(37)	2069(9)	8(3)	5681(9)	72(2)
C(38)	1492(8)	349(2)	6058(8)	61(2)

**Table 5.23:** Bond lengths [ $\text{\AA}$ ] and angles [ $^\circ$ ] for  $[\text{Ru}(\text{dbzCp})(\text{CO})\text{IPPh}_3]$ 

Ru(1)-C(20)	1.906(8)	Ru(1)-C(5)	2.197(6)
Ru(1)-C(4)	2.219(6)	Ru(1)-C(3)	2.270(6)
Ru(1)-C(1)	2.277(6)	Ru(1)-C(2)	2.295(6)
Ru(1)-P(1)	2.3003(17)	Ru(1)-I(2)	2.6860(7)
P(1)-C(21)	1.811(7)	P(1)-C(33)	1.830(6)
P(1)-C(27)	1.833(6)	O(1)-C(6)	1.209(7)
O(3)-C(20)	1.069(8)	O(2)-C(13)	1.214(7)
C(1)-C(2)	1.433(8)	C(1)-C(5)	1.443(8)
C(1)-C(6)	1.497(8)	C(2)-C(3)	1.408(8)
C(3)-C(4)	1.423(8)	C(4)-C(5)	1.422(8)
C(5)-C(13)	1.496(8)	C(6)-C(7)	1.480(9)
C(7)-C(12)	1.390(9)	C(7)-C(8)	1.395(9)
C(8)-C(9)	1.354(9)	C(9)-C(10)	1.359(11)
C(10)-C(11)	1.381(11)	C(11)-C(12)	1.396(10)
C(13)-C(14)	1.483(9)	C(14)-C(19)	1.373(9)
C(14)-C(15)	1.380(8)	C(15)-C(16)	1.349(9)
C(16)-C(17)	1.360(10)	C(17)-C(18)	1.366(10)
C(18)-C(19)	1.361(9)	C(21)-C(26)	1.380(10)
C(21)-C(22)	1.393(9)	C(22)-C(23)	1.396(10)
C(23)-C(24)	1.382(13)	C(24)-C(25)	1.344(13)
C(25)-C(26)	1.395(11)	C(27)-C(32)	1.372(9)
C(27)-C(28)	1.388(9)	C(28)-C(29)	1.377(10)
C(29)-C(30)	1.352(11)	C(30)-C(31)	1.353(11)
C(31)-C(32)	1.390(10)	C(33)-C(38)	1.370(9)
C(33)-C(34)	1.377(9)	C(34)-C(35)	1.379(10)
C(35)-C(36)	1.320(11)	C(36)-C(37)	1.343(11)
C(37)-C(38)	1.367(10)		
C(20)-Ru(1)-C(5)	98.9(2)	C(20)-Ru(1)-C(4)	126.4(3)
C(5)-Ru(1)-C(4)	37.6(2)	C(20)-Ru(1)-C(3)	161.1(3)

C(5)-Ru(1)-C(3)	62.2(2)	C(4)-Ru(1)-C(3)	36.9(2)
C(20)-Ru(1)-C(1)	105.6(2)	C(5)-Ru(1)-C(1)	37.6(2)
C(4)-Ru(1)-C(1)	61.7(2)	C(3)-Ru(1)-C(1)	60.8(2)
C(20)-Ru(1)-C(2)	138.4(3)	C(5)-Ru(1)-C(2)	62.1(2)
C(4)-Ru(1)-C(2)	61.2(2)	C(3)-Ru(1)-C(2)	35.9(2)
C(1)-Ru(1)-C(2)	36.5(2)	C(20)-Ru(1)-P(1)	90.4(2)
C(5)-Ru(1)-P(1)	120.18(17)	C(4)-Ru(1)-P(1)	91.69(16)
C(3)-Ru(1)-P(1)	98.00(17)	C(1)-Ru(1)-P(1)	153.42(17)
C(2)-Ru(1)-P(1)	131.18(16)	C(20)-Ru(1)-I(2)	88.6(2)
C(5)-Ru(1)-I(2)	145.61(16)	C(4)-Ru(1)-I(2)	144.68(17)
C(3)-Ru(1)-I(2)	107.78(17)	C(1)-Ru(1)-I(2)	108.08(16)
C(2)-Ru(1)-I(2)	90.17(17)	P(1)-Ru(1)-I(2)	93.07(5)
C(21)-P(1)-C(33)	104.3(3)	C(21)-P(1)-C(27)	103.9(3)
C(33)-P(1)-C(27)	100.7(3)	C(21)-P(1)-Ru(1)	109.1(2)
C(33)-P(1)-Ru(1)	122.3(2)	C(27)-P(1)-Ru(1)	114.6(2)
C(2)-C(1)-C(5)	107.5(5)	C(2)-C(1)-C(6)	130.1(6)
C(5)-C(1)-C(6)	122.2(5)	C(2)-C(1)-Ru(1)	72.4(3)
C(5)-C(1)-Ru(1)	68.2(3)	C(6)-C(1)-Ru(1)	128.6(4)
C(3)-C(2)-C(1)	108.2(6)	C(3)-C(2)-Ru(1)	71.1(3)
C(1)-C(2)-Ru(1)	71.1(3)	C(2)-C(3)-C(4)	108.6(6)
C(2)-C(3)-Ru(1)	73.0(4)	C(4)-C(3)-Ru(1)	69.6(3)
C(5)-C(4)-C(3)	108.4(6)	C(5)-C(4)-Ru(1)	70.4(3)
C(3)-C(4)-Ru(1)	73.5(4)	C(4)-C(5)-C(1)	107.3(5)
C(4)-C(5)-C(13)	126.6(6)	C(1)-C(5)-C(13)	124.7(5)
C(4)-C(5)-Ru(1)	72.1(3)	C(1)-C(5)-Ru(1)	74.2(3)
C(13)-C(5)-Ru(1)	129.8(4)	O(1)-C(6)-C(7)	120.7(6)
O(1)-C(6)-C(1)	119.2(6)	C(7)-C(6)-C(1)	119.7(6)
C(12)-C(7)-C(8)	119.4(6)	C(12)-C(7)-C(6)	121.6(6)
C(8)-C(7)-C(6)	118.9(6)	C(9)-C(8)-C(7)	120.4(7)
C(8)-C(9)-C(10)	121.4(8)	C(9)-C(10)-C(11)	119.5(8)
C(10)-C(11)-C(12)	120.6(8)	C(7)-C(12)-C(11)	118.8(7)
O(2)-C(13)-C(14)	121.8(6)	O(2)-C(13)-C(5)	122.1(6)
C(14)-C(13)-C(5)	116.1(6)	C(19)-C(14)-C(15)	119.1(6)

C(19)-C(14)-C(13)	121.9(6)	C(15)-C(14)-C(13)	118.9(6)
C(16)-C(15)-C(14)	120.3(7)	C(15)-C(16)-C(17)	120.0(7)
C(16)-C(17)-C(18)	120.9(7)	C(19)-C(18)-C(17)	119.3(7)
C(18)-C(19)-C(14)	120.5(7)	O(3)-C(20)-Ru(1)	178.5(7)
C(26)-C(21)-C(22)	118.9(7)	C(26)-C(21)-P(1)	122.4(6)
C(22)-C(21)-P(1)	118.4(6)	C(21)-C(22)-C(23)	119.5(8)
C(24)-C(23)-C(22)	120.2(9)	C(25)-C(24)-C(23)	120.4(9)
C(24)-C(25)-C(26)	120.3(9)	C(21)-C(26)-C(25)	120.6(9)
C(32)-C(27)-C(28)	118.5(6)	C(32)-C(27)-P(1)	120.2(5)
C(28)-C(27)-P(1)	121.2(5)	C(29)-C(28)-C(27)	119.5(7)
C(30)-C(29)-C(28)	121.5(8)	C(29)-C(30)-C(31)	119.7(8)
C(30)-C(31)-C(32)	120.3(8)	C(27)-C(32)-C(31)	120.5(7)
C(38)-C(33)-C(34)	117.1(7)	C(38)-C(33)-P(1)	120.1(5)
C(34)-C(33)-P(1)	122.5(6)	C(33)-C(34)-C(35)	120.6(8)
C(36)-C(35)-C(34)	120.8(8)	C(35)-C(36)-C(37)	120.0(8)
C(36)-C(37)-C(38)	120.8(8)	C(37)-C(38)-C(33)	120.7(7)

**Table 5.24:** *Anisotropic displacement parameters ( $\text{\AA}^2 \times 10^3$ ) for  $[\text{Ru}(\text{dbzCp})(\text{CO})\text{IPPh}_3]$ . The anisotropic displacement factor exponent takes the form:*

$$-2 \pi^2 [h^2 a^{*2} U11 + \dots + 2 h k a^* b^* U12]$$

Atom	U11	U22	U33	U23	U13	U12
Ru(1)	32(1)	32(1)	30(1)	0(1)	8(1)	2(1)
I(2)	41(1)	61(1)	59(1)	-4(1)	21(1)	0(1)
P(1)	39(1)	32(1)	38(1)	0(1)	12(1)	4(1)
O(1)	52(3)	54(3)	39(3)	5(2)	-8(2)	-4(2)
O(3)	58(4)	73(4)	42(3)	-15(3)	-5(3)	12(3)
O(2)	48(3)	51(3)	84(4)	-18(3)	-3(3)	6(2)
C(1)	34(4)	33(4)	34(4)	-2(3)	1(3)	4(3)
C(2)	40(4)	29(4)	43(4)	-5(3)	3(3)	0(3)
C(3)	49(4)	37(4)	31(4)	-7(3)	0(3)	5(3)
C(4)	50(5)	38(4)	33(4)	4(3)	17(3)	10(3)
C(5)	35(4)	26(3)	37(4)	-4(3)	9(3)	4(3)
C(6)	37(4)	36(4)	39(4)	1(3)	9(3)	9(3)
C(7)	34(4)	35(4)	46(5)	-1(3)	8(3)	6(3)
C(8)	35(4)	52(5)	52(5)	12(4)	11(3)	4(3)
C(9)	55(5)	62(5)	80(7)	25(5)	23(5)	-2(4)
C(10)	58(6)	50(5)	113(9)	16(6)	17(5)	-8(4)
C(11)	59(5)	43(5)	89(7)	-16(4)	-7(5)	-1(4)
C(12)	52(5)	38(4)	52(5)	5(3)	5(4)	4(3)
C(13)	39(4)	37(4)	45(4)	1(3)	9(3)	-1(3)
C(14)	42(4)	32(4)	38(4)	8(3)	16(3)	5(3)
C(15)	36(4)	47(4)	44(4)	9(3)	12(3)	3(3)
C(16)	43(5)	68(5)	55(5)	19(4)	20(4)	14(4)
C(17)	75(6)	57(5)	67(6)	13(4)	37(5)	30(4)
C(18)	72(6)	45(5)	62(6)	-4(4)	24(4)	9(4)
C(19)	45(4)	46(4)	50(5)	3(4)	14(4)	13(3)
C(20)	42(4)	40(4)	54(5)	8(4)	16(4)	13(3)

C(21)	56(5)	31(4)	46(5)	1(3)	13(4)	7(3)
C(22)	72(6)	48(5)	49(5)	11(4)	0(4)	-3(4)
C(23)	100(8)	57(6)	66(7)	2(5)	-19(6)	-13(5)
C(24)	156(11)	73(6)	37(6)	-13(5)	9(7)	15(7)
C(25)	118(9)	108(8)	47(6)	-5(5)	34(6)	32(7)
C(26)	71(6)	76(6)	46(5)	-2(4)	20(4)	16(4)
C(27)	45(4)	36(4)	45(4)	-1(3)	21(3)	-4(3)
C(28)	62(6)	48(5)	71(6)	13(4)	18(4)	-6(4)
C(29)	80(7)	60(6)	93(7)	10(5)	40(5)	-17(5)
C(30)	65(7)	63(6)	127(9)	-9(6)	47(6)	-33(5)
C(31)	38(5)	67(6)	126(8)	-11(6)	24(5)	5(4)
C(32)	48(5)	42(4)	79(6)	1(4)	23(4)	2(4)
C(33)	36(4)	30(4)	58(5)	0(3)	17(3)	-1(3)
C(34)	90(6)	49(5)	62(6)	6(4)	28(5)	23(4)
C(35)	92(7)	48(5)	103(8)	10(5)	31(6)	24(5)
C(36)	67(6)	45(5)	115(9)	-28(6)	27(6)	1(4)
C(37)	78(6)	69(6)	68(6)	-31(5)	18(5)	9(5)
C(38)	67(5)	59(5)	50(5)	-15(4)	9(4)	18(4)

**Table 5.25:** Hydrogen coordinates ( $\times 10^4$ ) and isotropic displacement parameters ( $\text{\AA}^2 \times 10^3$ ) for  $[\text{Ru}(\text{dbzCp})(\text{CO})\text{IPPh}_3]$

Atom	x	y	z	U(eq)
H(2)	2210	2222	7927	51
H(3)	1615	1783	9663	53
H(4)	-902	1589	8825	51
H(8)	239	2901	3638	60
H(9)	1271	3518	3720	84
H(10)	2232	3835	5733	97
H(11)	2166	3526	7728	90
H(12)	1138	2890	7696	64
H(15)	-5091	2136	5292	55
H(16)	-6346	2674	5700	70
H(17)	-5315	3151	7263	82
H(18)	-2989	3111	8370	76
H(19)	-1705	2578	7931	61
H(22)	3405	1006	9607	77
H(23)	4348	1112	11914	107
H(24)	2958	1066	13361	120
H(25)	654	933	12544	116
H(26)	-321	827	10251	83
H(28)	-329	89	8604	78
H(29)	-2498	-179	8406	96
H(30)	-4458	173	7371	105
H(31)	-4288	798	6472	100
H(32)	-2128	1085	6682	72
H(34)	2590	217	9245	86
H(35)	3530	-352	8552	104
H(36)	3220	-477	6346	98
H(37)	1935	-48	4769	94
H(38)	986	525	5399	79

## 5.6 Crystal Structure of $[\text{Ru}((\text{CO}-p\text{-tolyl})_2\text{C}_5\text{H}_3)(\text{CO})\text{IPPh}_3]$

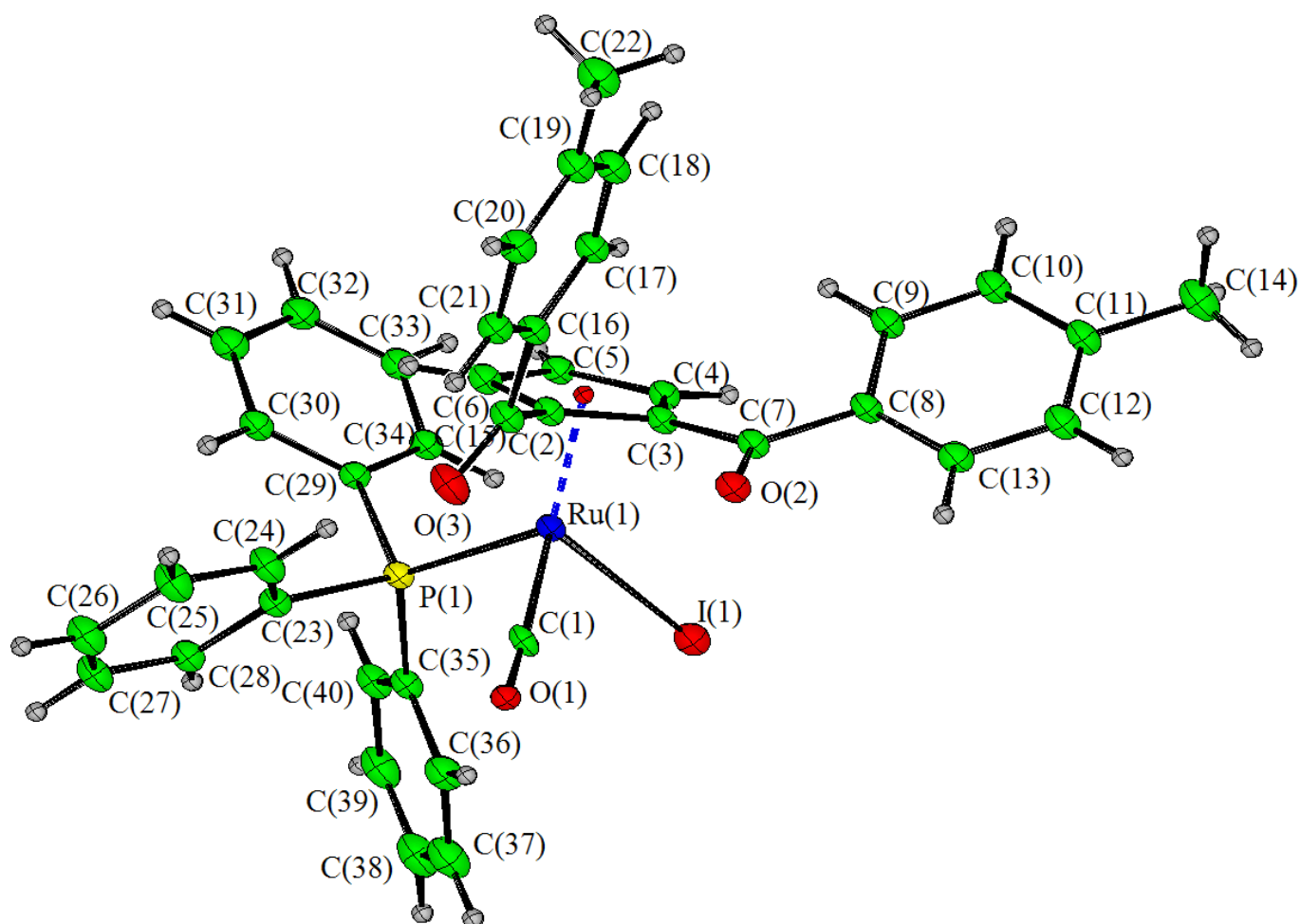


**Table 5.26:** *Crystal data and structure refinement for [Ru((CO-p-tolyl)<sub>2</sub>C<sub>5</sub>H<sub>3</sub>)(CO)IPPh<sub>3</sub>]*

Identification code	h06pma l
Empirical formula	C <sub>39.80</sub> H <sub>32</sub> I <sub>1.20</sub> O <sub>2.80</sub> P Ru
Formula weight	839.37
Temperature	150(2) K
Wavelength	0.71073 Å
Crystal system	Monoclinic
Space group	P2 <sub>1</sub> /n
Unit cell dimensions	a = 10.1950(1)Å b = 32.3310(4)Å $\beta$ = 108.496(1) <sup>o</sup> c = 11.0430(1)Å
Volume	3451.91(6) Å <sup>3</sup>
Z	4
Density (calculated)	1.615 Mg/m <sup>3</sup>
Absorption coefficient	1.610 mm <sup>-1</sup>
F(000)	1663
Crystal size	0.25 x 0.15 x 0.05 mm
Theta range for data collection	3.78 to 27.48 <sup>o</sup>
Index ranges	-13<=h<=12; -41<=k<=41; -14<=l<=14
Reflections collected	44034
Independent reflections	7873 [R(int) = 0.0486]
Reflections observed (>2σ)	6203
Data Completeness	0.994
Absorption correction	Semi-empirical from equivalents
Max. and min. transmission	0.83 and 0.76
Refinement method	Full-matrix least-squares on F <sup>2</sup>
Data / restraints / parameters	7873 / 0 / 428
Goodness-of-fit on F <sup>2</sup>	1.144
Final R indices [I>2σ(I)]	R1 = 0.0518 wR2 = 0.1342
R indices (all data)	R1 = 0.0708 wR2 = 0.1425
Largest diff. peak and hole	1.087 and -1.549 eÅ <sup>-3</sup>

**Table 5.27:** Atomic coordinates ( $\times 10^4$ ) and equivalent isotropic displacement parameters ( $\text{\AA}^2 \times 10^3$ ) for  $[\text{Ru}((\text{CO-p-tolyl})_2\text{C}_5\text{H}_3)(\text{CO})\text{IPPh}_3]$ .  $U(\text{eq})$  is defined as one third of the trace of the orthogonalized  $U_{ij}$  tensor.

Atom	x	y	z	U(eq)
I(1)	3773(1)	1577(1)	-951(1)	44(1)
I(2A)	5465(9)	1170(2)	2339(7)	60(2)
Ru(1)	3069(1)	1514(1)	1182(1)	25(1)
P(1)	2081(1)	867(1)	678(1)	25(1)
O(1)	5800(20)	1076(6)	2560(19)	67(6)
O(2)	5472(4)	2354(1)	3118(4)	39(1)
O(3)	4449(6)	1533(1)	4599(4)	54(1)
C(1)	4726(10)	1252(3)	2006(9)	33(2)
C(2)	2946(5)	1885(2)	2806(5)	30(1)
C(3)	3204(5)	2175(2)	1910(5)	29(1)
C(4)	2041(5)	2150(2)	768(5)	32(1)
C(5)	1087(5)	1868(2)	952(6)	32(1)
C(6)	1640(6)	1703(2)	2223(5)	32(1)
C(7)	4429(5)	2451(2)	2240(5)	30(1)
C(8)	4347(6)	2853(2)	1563(5)	32(1)
C(9)	3112(6)	3070(2)	1055(5)	33(1)
C(10)	3104(6)	3462(2)	545(6)	39(1)
C(11)	4338(7)	3647(2)	503(6)	40(1)
C(12)	5546(7)	3429(2)	1006(6)	41(1)
C(13)	5573(6)	3041(2)	1541(6)	39(1)
C(14)	4331(8)	4068(2)	-78(7)	56(2)
C(15)	3781(6)	1840(2)	4196(6)	34(1)
C(16)	3632(5)	2184(2)	5047(5)	30(1)
C(17)	2753(6)	2521(2)	4583(6)	34(1)
C(18)	2593(6)	2825(2)	5396(6)	39(1)
C(19)	3320(6)	2806(2)	6697(6)	38(1)

C(20)	4184(6)	2472(2)	7152(6)	38(1)
C(21)	4345(6)	2160(2)	6352(5)	34(1)
C(22)	3163(8)	3141(2)	7596(7)	52(2)
C(23)	2504(5)	501(2)	2018(5)	29(1)
C(24)	2985(7)	650(2)	3266(6)	40(1)
C(25)	3262(8)	379(2)	4293(6)	50(2)
C(26)	3074(8)	-41(2)	4076(6)	48(2)
C(27)	2620(7)	-191(2)	2851(6)	43(1)
C(28)	2323(6)	78(2)	1820(6)	33(1)
C(29)	197(5)	903(2)	179(5)	28(1)
C(30)	-557(6)	745(2)	941(6)	33(1)
C(31)	-1984(6)	805(2)	578(6)	41(1)
C(32)	-2655(6)	1026(2)	-524(7)	44(2)
C(33)	-1908(6)	1183(2)	-1273(6)	39(1)
C(34)	-500(6)	1123(2)	-936(5)	32(1)
C(35)	2424(6)	560(2)	-589(5)	30(1)
C(36)	3802(6)	496(2)	-505(7)	42(1)
C(37)	4117(8)	254(2)	-1426(8)	52(2)
C(38)	3076(9)	84(2)	-2414(7)	52(2)
C(39)	1704(9)	145(2)	-2504(6)	52(2)
C(40)	1374(7)	382(2)	-1579(5)	39(1)

**Table 5.28:** Bond lengths [ $\text{\AA}$ ] and angles [ $^\circ$ ] for  $[\text{Ru}((\text{CO}-p\text{-tolyl})_2\text{C}_5\text{H}_3)(\text{CO})\text{IPPh}_3]$ .

I(1)-Ru(1)	2.6790(6)	I(2A)-Ru(1)	2.619(9)
Ru(1)-C(1)	1.850(10)	Ru(1)-C(2)	2.196(5)
Ru(1)-C(6)	2.209(5)	Ru(1)-C(5)	2.266(5)
Ru(1)-C(3)	2.273(5)	Ru(1)-C(4)	2.287(5)
Ru(1)-P(1)	2.3098(13)	P(1)-C(29)	1.826(5)
P(1)-C(23)	1.836(6)	P(1)-C(35)	1.838(5)
O(1)-C(1)	1.215(18)	O(2)-C(7)	1.231(6)
O(3)-C(15)	1.205(7)	C(2)-C(6)	1.412(7)
C(2)-C(3)	1.446(8)	C(2)-C(15)	1.508(8)
C(3)-C(4)	1.433(7)	C(3)-C(7)	1.482(7)
C(4)-C(5)	1.394(8)	C(5)-C(6)	1.439(8)
C(7)-C(8)	1.489(8)	C(8)-C(9)	1.395(7)
C(8)-C(13)	1.397(8)	C(9)-C(10)	1.384(8)
C(10)-C(11)	1.407(9)	C(11)-C(12)	1.375(9)
C(11)-C(14)	1.503(9)	C(12)-C(13)	1.383(8)
C(15)-C(16)	1.495(7)	C(16)-C(21)	1.396(8)
C(16)-C(17)	1.400(8)	C(17)-C(18)	1.374(8)
C(18)-C(19)	1.393(9)	C(19)-C(20)	1.382(9)
C(19)-C(22)	1.513(8)	C(20)-C(21)	1.385(8)
C(23)-C(28)	1.390(7)	C(23)-C(24)	1.393(8)
C(24)-C(25)	1.390(9)	C(25)-C(26)	1.382(9)
C(26)-C(27)	1.372(9)	C(27)-C(28)	1.386(8)
C(29)-C(30)	1.403(7)	C(29)-C(34)	1.405(8)
C(30)-C(31)	1.395(8)	C(31)-C(32)	1.391(9)
C(32)-C(33)	1.385(9)	C(33)-C(34)	1.378(8)
C(35)-C(40)	1.389(8)	C(35)-C(36)	1.393(8)
C(36)-C(37)	1.399(9)	C(37)-C(38)	1.372(11)
C(38)-C(39)	1.384(11)	C(39)-C(40)	1.402(8)

C(1)-Ru(1)-C(2)	97.3(3)	C(1)-Ru(1)-C(6)	121.4(3)
C(2)-Ru(1)-C(6)	37.38(19)	C(1)-Ru(1)-C(5)	158.3(3)
C(2)-Ru(1)-C(5)	62.3(2)	C(6)-Ru(1)-C(5)	37.5(2)
C(1)-Ru(1)-C(3)	108.2(3)	C(2)-Ru(1)-C(3)	37.7(2)
C(6)-Ru(1)-C(3)	62.1(2)	C(5)-Ru(1)-C(3)	61.06(19)
C(1)-Ru(1)-C(4)	142.9(3)	C(2)-Ru(1)-C(4)	62.0(2)
C(6)-Ru(1)-C(4)	61.3(2)	C(5)-Ru(1)-C(4)	35.6(2)
C(3)-Ru(1)-C(4)	36.63(19)	C(1)-Ru(1)-P(1)	88.0(3)
C(2)-Ru(1)-P(1)	123.94(15)	C(6)-Ru(1)-P(1)	93.82(15)
C(5)-Ru(1)-P(1)	97.20(14)	C(3)-Ru(1)-P(1)	155.39(14)
C(4)-Ru(1)-P(1)	128.93(14)	C(1)-Ru(1)-I(2A)	2.2(3)
C(2)-Ru(1)-I(2A)	96.86(19)	C(6)-Ru(1)-I(2A)	122.0(2)
C(5)-Ru(1)-I(2A)	158.4(2)	C(3)-Ru(1)-I(2A)	106.50(19)
C(4)-Ru(1)-I(2A)	140.9(2)	P(1)-Ru(1)-I(2A)	90.07(17)
C(1)-Ru(1)-I(1)	90.5(3)	C(2)-Ru(1)-I(1)	141.03(15)
C(6)-Ru(1)-I(1)	147.30(16)	C(5)-Ru(1)-I(1)	109.97(16)
C(3)-Ru(1)-I(1)	103.69(14)	C(4)-Ru(1)-I(1)	89.42(15)
P(1)-Ru(1)-I(1)	94.31(4)	I(2A)-Ru(1)-I(1)	89.58(18)
C(29)-P(1)-C(23)	103.8(2)	C(29)-P(1)-C(35)	103.9(2)
C(23)-P(1)-C(35)	102.2(2)	C(29)-P(1)-Ru(1)	110.66(17)
C(23)-P(1)-Ru(1)	114.60(18)	C(35)-P(1)-Ru(1)	119.92(17)
O(1)-C(1)-Ru(1)	178.8(15)	C(6)-C(2)-C(3)	108.0(5)
C(6)-C(2)-C(15)	124.7(5)	C(3)-C(2)-C(15)	126.4(5)
C(6)-C(2)-Ru(1)	71.8(3)	C(3)-C(2)-Ru(1)	74.1(3)
C(15)-C(2)-Ru(1)	128.2(4)	C(4)-C(3)-C(2)	106.6(5)
C(4)-C(3)-C(7)	130.4(5)	C(2)-C(3)-C(7)	122.9(5)
C(4)-C(3)-Ru(1)	72.2(3)	C(2)-C(3)-Ru(1)	68.2(3)
C(7)-C(3)-Ru(1)	127.2(4)	C(5)-C(4)-C(3)	109.3(5)
C(5)-C(4)-Ru(1)	71.4(3)	C(3)-C(4)-Ru(1)	71.2(3)
C(4)-C(5)-C(6)	108.0(5)	C(4)-C(5)-Ru(1)	73.0(3)
C(6)-C(5)-Ru(1)	69.1(3)	C(2)-C(6)-C(5)	108.1(5)
C(2)-C(6)-Ru(1)	70.8(3)	C(5)-C(6)-Ru(1)	73.4(3)
O(2)-C(7)-C(3)	119.3(5)	O(2)-C(7)-C(8)	121.1(5)

C(3)-C(7)-C(8)	119.5(5)	C(9)-C(8)-C(13)	118.2(5)
C(9)-C(8)-C(7)	122.8(5)	C(13)-C(8)-C(7)	118.7(5)
C(10)-C(9)-C(8)	120.8(5)	C(9)-C(10)-C(11)	120.9(5)
C(12)-C(11)-C(10)	117.6(5)	C(12)-C(11)-C(14)	121.3(6)
C(10)-C(11)-C(14)	121.1(6)	C(11)-C(12)-C(13)	122.1(6)
C(12)-C(13)-C(8)	120.4(6)	O(3)-C(15)-C(16)	122.6(5)
O(3)-C(15)-C(2)	121.7(5)	C(16)-C(15)-C(2)	115.5(5)
C(21)-C(16)-C(17)	119.0(5)	C(21)-C(16)-C(15)	118.9(5)
C(17)-C(16)-C(15)	122.0(5)	C(18)-C(17)-C(16)	120.8(6)
C(17)-C(18)-C(19)	120.5(6)	C(20)-C(19)-C(18)	118.6(5)
C(20)-C(19)-C(22)	120.6(6)	C(18)-C(19)-C(22)	120.9(6)
C(19)-C(20)-C(21)	121.9(6)	C(20)-C(21)-C(16)	119.3(6)
C(28)-C(23)-C(24)	118.9(5)	C(28)-C(23)-P(1)	121.5(4)
C(24)-C(23)-P(1)	119.6(4)	C(25)-C(24)-C(23)	120.4(5)
C(26)-C(25)-C(24)	119.8(6)	C(27)-C(26)-C(25)	120.2(6)
C(26)-C(27)-C(28)	120.4(6)	C(27)-C(28)-C(23)	120.3(5)
C(30)-C(29)-C(34)	119.3(5)	C(30)-C(29)-P(1)	121.3(4)
C(34)-C(29)-P(1)	119.1(4)	C(31)-C(30)-C(29)	119.8(5)
C(32)-C(31)-C(30)	120.1(6)	C(33)-C(32)-C(31)	119.9(5)
C(34)-C(33)-C(32)	120.7(6)	C(33)-C(34)-C(29)	120.1(5)
C(40)-C(35)-C(36)	120.0(5)	C(40)-C(35)-P(1)	122.5(4)
C(36)-C(35)-P(1)	117.4(4)	C(35)-C(36)-C(37)	119.6(6)
C(38)-C(37)-C(36)	120.3(6)	C(37)-C(38)-C(39)	120.7(6)
C(38)-C(39)-C(40)	119.7(7)	C(35)-C(40)-C(39)	119.8(6)

**Table 5.29:** Anisotropic displacement parameters ( $\text{\AA}^2 \times 10^3$ ) for  $[\text{Ru}((\text{CO-p-tolyl})_2\text{C}_5\text{H}_3)(\text{CO})\text{IPPh}_3)]$ . The anisotropic displacement factor exponent takes the form:

$$-2 \pi^2 [h^2 a^{*2} U_{11} + \dots + 2 h k a^* b^* U_{12}]$$

Atom	U11	U22	U33	U23	U13	U12
I(1)	39(1)	47(1)	49(1)	8(1)	19(1)	5(1)
I(2A)	52(4)	68(3)	61(3)	-19(3)	17(3)	-5(3)
Ru(1)	20(1)	26(1)	29(1)	-3(1)	9(1)	1(1)
P(1)	23(1)	27(1)	27(1)	-4(1)	12(1)	-1(1)
O(1)	50(10)	72(9)	76(8)	9(6)	16(6)	2(6)
O(2)	30(2)	37(2)	40(2)	-4(2)	-1(2)	-1(2)
O(3)	77(3)	39(2)	36(2)	-2(2)	5(2)	15(2)
C(1)	28(4)	30(4)	43(5)	-7(3)	14(4)	-8(4)
C(2)	29(3)	27(3)	32(3)	-8(2)	9(2)	3(2)
C(3)	27(3)	25(2)	32(3)	-5(2)	6(2)	2(2)
C(4)	29(3)	29(3)	33(3)	-3(2)	6(2)	8(2)
C(5)	19(2)	31(3)	45(3)	-10(2)	8(2)	6(2)
C(6)	32(3)	34(3)	34(3)	-12(2)	15(2)	2(2)
C(7)	27(3)	30(3)	33(3)	-7(2)	8(2)	3(2)
C(8)	31(3)	27(3)	36(3)	-5(2)	9(2)	0(2)
C(9)	33(3)	29(3)	37(3)	-5(2)	10(2)	2(2)
C(10)	39(3)	32(3)	43(3)	-7(2)	7(3)	7(2)
C(11)	48(3)	29(3)	40(3)	-7(2)	11(3)	-4(2)
C(12)	41(3)	37(3)	42(3)	-4(3)	8(3)	-9(3)
C(13)	29(3)	38(3)	46(4)	-4(3)	7(3)	1(2)
C(14)	68(5)	38(3)	57(4)	4(3)	10(4)	-9(3)
C(15)	38(3)	31(3)	35(3)	-3(2)	12(3)	1(2)
C(16)	29(3)	31(3)	34(3)	-6(2)	13(2)	-5(2)
C(17)	27(3)	34(3)	44(3)	-5(2)	15(2)	-3(2)
C(18)	36(3)	35(3)	52(4)	-9(3)	24(3)	-6(2)
C(19)	38(3)	39(3)	50(4)	-14(3)	30(3)	-14(2)

C(20)	39(3)	48(3)	30(3)	-11(3)	17(3)	-18(3)
C(21)	31(3)	40(3)	34(3)	-1(2)	14(2)	-8(2)
C(22)	59(4)	48(4)	64(5)	-24(3)	40(4)	-15(3)
C(23)	26(2)	32(3)	31(3)	-1(2)	14(2)	-1(2)
C(24)	54(4)	33(3)	34(3)	-3(2)	17(3)	-5(3)
C(25)	71(5)	45(4)	28(3)	-2(3)	9(3)	-8(3)
C(26)	66(4)	43(3)	33(3)	9(3)	13(3)	-5(3)
C(27)	55(4)	32(3)	43(4)	1(3)	17(3)	-2(3)
C(28)	33(3)	35(3)	33(3)	-5(2)	12(2)	-2(2)
C(29)	23(2)	30(2)	31(3)	-7(2)	11(2)	-3(2)
C(30)	30(3)	31(3)	42(3)	-4(2)	19(2)	0(2)
C(31)	35(3)	41(3)	55(4)	-5(3)	27(3)	-5(2)
C(32)	25(3)	43(3)	62(4)	-11(3)	13(3)	0(2)
C(33)	31(3)	36(3)	43(3)	-6(3)	2(3)	1(2)
C(34)	30(3)	33(3)	34(3)	-6(2)	10(2)	-6(2)
C(35)	34(3)	28(3)	33(3)	-3(2)	19(2)	-1(2)
C(36)	39(3)	40(3)	54(4)	-9(3)	26(3)	-1(2)
C(37)	63(4)	41(3)	73(5)	-3(3)	51(4)	4(3)
C(38)	88(6)	43(4)	41(4)	-1(3)	43(4)	11(4)
C(39)	84(5)	39(3)	34(3)	-8(3)	21(3)	0(3)
C(40)	50(3)	33(3)	32(3)	-4(2)	13(3)	2(3)

**Table 5.30:** Hydrogen coordinates ( $\times 10^4$ ) and isotropic displacement parameters ( $\text{\AA}^2 \times 10^3$ ) for  $[\text{Ru}((\text{CO-p-tolyl})_2\text{C}_5\text{H}_3)(\text{CO})\text{IPPh}_3]$ .

Atom	x	y	z	U(eq)
H(4)	1937	2301	6	38
H(5)	223	1798	345	39
H(6)	1203	1505	2603	38
H(9)	2266	2948	1059	40
H(10)	2255	3607	218	47
H(12)	6390	3548	985	49
H(13)	6430	2902	1897	46
H(14A)	4301	4281	544	85
H(14B)	3516	4094	-839	85
H(14C)	5171	4102	-318	85
H(17)	2261	2540	3696	41
H(18)	1982	3049	5069	47
H(20)	4680	2456	8038	45
H(21)	4935	1932	6689	41
H(22A)	2292	3101	7780	78
H(22B)	3156	3412	7198	78
H(22C)	3938	3127	8394	78
H(24)	3124	939	3415	48
H(25)	3581	482	5142	60
H(26)	3260	-227	4777	58
H(27)	2508	-480	2708	52
H(28)	1995	-28	975	40
H(30)	-96	597	1702	39
H(31)	-2498	694	1085	49
H(32)	-3625	1071	-763	52
H(33)	-2372	1333	-2027	47
H(34)	1	1231	-1459	39
H(36)	4522	616	173	50

H(37)	5055	208	-1368	63
H(38)	3299	-76	-3041	63
H(39)	989	25	-3190	62
H(40)	435	422	-1630	46

## 5.7 Crystal Structure of [Ru(indenyl)(CO)<sub>2</sub>I]

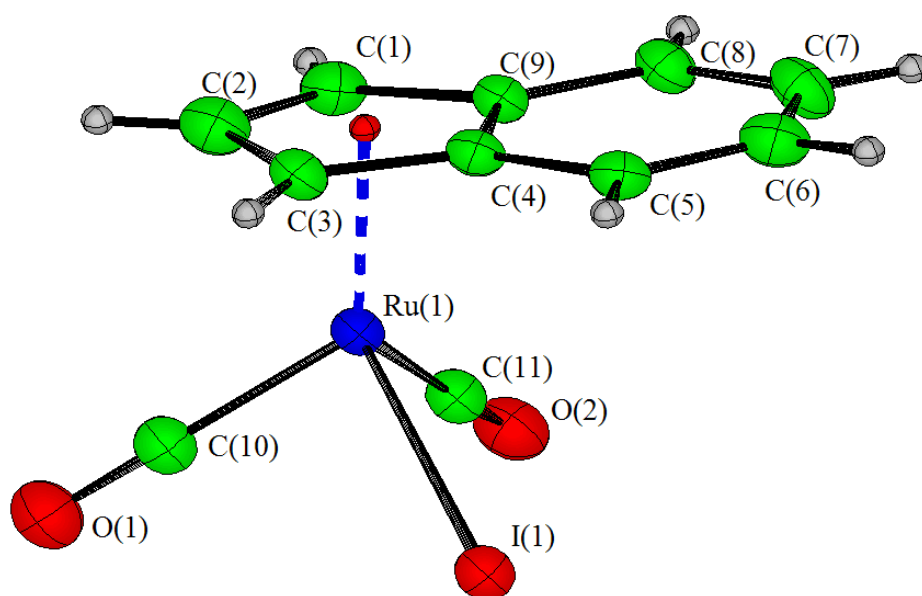


**Table 5.31:** *Crystal data and structure refinement for Crystal Structure of [Ru(indenyl)(CO)<sub>2</sub>I]*

Identification code	mc15
Empirical formula	C <sub>11</sub> H <sub>7</sub> I O <sub>2</sub> Ru
Formula weight	399.14
Temperature	293(2) K
Wavelength	0.7107 Å
Crystal system	Triclinic
Space group	P-1
Unit cell dimensions	a = 6.9018(5)Å α = 81.124(5)° b = 6.9858(4)Å β = 87.985(5)° c = 12.3276(7)Å γ = 79.161(5)°
Volume	576.77(6) Å <sup>3</sup>
Z	2
Density (calculated)	2.298 Mg/m <sup>3</sup>
Absorption coefficient	4.011 mm <sup>-1</sup>
F(000)	372
Crystal size	0.34 x 0.31 x 0.18 mm
Theta range for data collection	2.9967 to 29.2075 °.
Index ranges	-9<=h<=9; -9<=k<=9; -15<=l<=15
Reflections collected	4308
Independent reflections	2632 [R <sub>int</sub> = 0.0236]
Reflections observed (>2σ)	1770
Data Completeness	0.835
Absorption correction	Semi-empirical from equivalents
Max. and min. transmission	1.00000 and 0.46262
Refinement method	Full-matrix least-squares on F <sup>2</sup>
Data / restraints / parameters	2632 / 0 / 136
Goodness-of-fit on F <sup>2</sup>	0.928
Final R indices [I>2σ(I)]	R <sub>1</sub> = 0.0404 wR <sub>2</sub> = 0.0921
R indices (all data)	R <sub>1</sub> = 0.0685 wR <sub>2</sub> = 0.1001
Largest diff. peak and hole	1.569 and -1.097 e.Å <sup>-3</sup>

$${}^aR_1 = \Sigma||F_o| - |F_c||/\Sigma|F_o|. \quad {}^b wR_2 = |\Sigma w(|F_o|^2 - |F_c|^2)|/\Sigma|w(F_o)^2|^{1/2}, \quad w = 1/[\sigma^2(F_o^2) + (.0596P)^2]. \quad P = (F_o^2 + 2F_c^2)/3.$$

**Table 5.32:** *Atomic coordinates ( $\times 10^4$ ) and equivalent isotropic displacement parameters ( $\text{\AA}^2 \times 10^3$ ) for [Ru(indenyl)(CO)<sub>2</sub>I]. U(eq) is defined as one third of the trace of the orthogonalized Uij tensor*

Atom	x	y	z	U(eq)
I(1)	3212(1)	3615(1)	3359(1)	48(1)
Ru(1)	4379(1)	7141(1)	2899(1)	37(1)
O(2)	1006(8)	8947(10)	1371(5)	76(2)
O(1)	1942(8)	8495(9)	4787(5)	75(2)
C(1)	6408(10)	9081(10)	2226(7)	52(2)
C(2)	6926(10)	8323(12)	3314(7)	58(2)
C(3)	7512(9)	6267(10)	3427(6)	45(2)
C(4)	7547(9)	5730(10)	2359(6)	42(2)
C(5)	8109(9)	3874(10)	1969(6)	46(2)
C(6)	8029(10)	3844(12)	880(7)	57(2)
C(7)	7358(11)	5518(13)	118(6)	62(2)
C(8)	6795(10)	7325(11)	472(6)	52(2)
C(9)	6874(9)	7455(9)	1596(5)	40(1)
C(10)	2861(11)	7984(10)	4067(6)	53(2)
C(11)	2235(11)	8228(10)	1946(6)	49(2)

**Table 5.33:** Bond lengths [ $\text{\AA}$ ] and angles [ $^\circ$ ] for  $[\text{Ru}(\text{indenyl})(\text{CO})_2\text{I}]$ .

I(1)-Ru(1)	2.7055(7)	Ru(1)-C(10)	1.854(7)
Ru(1)-C(11)	1.890(8)	Ru(1)-C(1)	2.184(7)
Ru(1)-C(2)	2.185(7)	Ru(1)-C(3)	2.226(7)
Ru(1)-C(9)	2.331(6)	Ru(1)-C(4)	2.342(6)
O(2)-C(11)	1.116(8)	O(1)-C(10)	1.137(8)
C(1)-C(2)	1.398(11)	C(1)-C(9)	1.454(9)
C(2)-C(3)	1.404(10)	C(3)-C(4)	1.422(9)
C(4)-C(9)	1.422(9)	C(4)-C(5)	1.433(9)
C(5)-C(6)	1.348(10)	C(6)-C(7)	1.398(11)
C(7)-C(8)	1.381(10)	C(8)-C(9)	1.406(9)
C(10)-Ru(1)-C(11)	89.6(3)	C(10)-Ru(1)-C(1)	114.0(3)
C(11)-Ru(1)-C(1)	98.4(3)	C(10)-Ru(1)-C(2)	94.1(3)
C(11)-Ru(1)-C(2)	131.6(3)	C(1)-Ru(1)-C(2)	37.3(3)
C(10)-Ru(1)-C(3)	108.7(3)	C(11)-Ru(1)-C(3)	157.5(3)
C(1)-Ru(1)-C(3)	62.6(3)	C(2)-Ru(1)-C(3)	37.1(3)
C(10)-Ru(1)-C(9)	151.3(3)	C(11)-Ru(1)-C(9)	96.8(3)
C(1)-Ru(1)-C(9)	37.4(2)	C(2)-Ru(1)-C(9)	61.0(3)
C(3)-Ru(1)-C(9)	60.8(2)	C(10)-Ru(1)-C(4)	144.5(3)
C(11)-Ru(1)-C(4)	125.5(3)	C(1)-Ru(1)-C(4)	61.2(2)
C(2)-Ru(1)-C(4)	60.3(2)	C(3)-Ru(1)-C(4)	36.2(2)
C(9)-Ru(1)-C(4)	35.4(2)	C(10)-Ru(1)-I(1)	89.5(2)
C(11)-Ru(1)-I(1)	92.9(2)	C(1)-Ru(1)-I(1)	153.84(18)
C(2)-Ru(1)-I(1)	135.3(2)	C(3)-Ru(1)-I(1)	100.08(18)
C(9)-Ru(1)-I(1)	117.98(15)	C(4)-Ru(1)-I(1)	93.12(16)
C(2)-C(1)-C(9)	107.2(7)	C(2)-C(1)-Ru(1)	71.4(4)
C(9)-C(1)-Ru(1)	76.8(4)	C(1)-C(2)-C(3)	109.9(7)
C(1)-C(2)-Ru(1)	71.3(4)	C(3)-C(2)-Ru(1)	73.0(4)
C(2)-C(3)-C(4)	107.4(6)	C(2)-C(3)-Ru(1)	69.9(4)
C(4)-C(3)-Ru(1)	76.4(4)	C(9)-C(4)-C(3)	108.6(6)

C(9)-C(4)-C(5)	119.3(6)	C(3)-C(4)-C(5)	132.2(6)
C(9)-C(4)-Ru(1)	71.9(3)	C(3)-C(4)-Ru(1)	67.4(3)
C(5)-C(4)-Ru(1)	126.6(5)	C(6)-C(5)-C(4)	118.3(7)
C(5)-C(6)-C(7)	123.3(7)	C(8)-C(7)-C(6)	119.6(7)
C(7)-C(8)-C(9)	119.7(7)	C(8)-C(9)-C(4)	119.8(6)
C(8)-C(9)-C(1)	133.5(7)	C(4)-C(9)-C(1)	106.7(6)
C(8)-C(9)-Ru(1)	127.1(5)	C(4)-C(9)-Ru(1)	72.7(3)
C(1)-C(9)-Ru(1)	65.8(4)	O(1)-C(10)-Ru(1)	179.5(8)
O(2)-C(11)-Ru(1)	176.8(7)		

**Table 5.34:** *Anisotropic displacement parameters ( $\text{\AA}^2 \times 10^3$ ) for  $[\text{Ru}(\text{indenyl})(\text{CO})_2\text{I}]$ . The anisotropic displacement factor exponent takes the form:  
 $-2 \pi^2 [ h^2 a^{*2} U11 + \dots + 2 h k a^* b^* U12 ]$*

Atom	U11	U22	U33	U23	U13	U12
I(1)	55(1)	40(1)	52(1)	-12(1)	3(1)	-14(1)
Ru(1)	41(1)	33(1)	40(1)	-13(1)	3(1)	-7(1)
O(2)	61(3)	89(4)	72(4)	-1(3)	-15(3)	-4(3)
O(1)	85(4)	76(4)	67(4)	-36(3)	26(3)	-8(3)
C(1)	53(4)	40(4)	68(5)	-15(3)	3(4)	-17(3)
C(2)	54(4)	65(5)	69(5)	-36(4)	4(4)	-25(4)
C(3)	44(3)	52(4)	42(4)	-15(3)	-3(3)	-11(3)
C(4)	34(3)	45(4)	49(4)	-11(3)	2(3)	-11(3)
C(5)	40(3)	42(4)	57(4)	-15(3)	5(3)	-2(3)
C(6)	47(4)	61(5)	71(5)	-34(4)	13(4)	-14(4)
C(7)	59(5)	94(6)	40(4)	-25(4)	10(4)	-24(4)
C(8)	49(4)	63(5)	44(4)	-1(3)	6(3)	-16(4)
C(9)	39(3)	40(3)	43(4)	-10(3)	6(3)	-15(3)
C(10)	62(4)	45(4)	56(5)	-20(3)	2(4)	-9(3)
C(11)	53(4)	46(4)	51(4)	-11(3)	8(3)	-15(3)

**Table 5.35:** Hydrogen coordinates ( $\times 10^4$ ) and isotropic displacement parameters ( $\text{\AA}^2 \times 10^3$ ) for  $[\text{Ru}(\text{indenyl})(\text{CO})_2\text{I}]$ .

Atom	x	y	z	U(eq)
H(1)	5866	10382	1955	68
H(2)	6889	9070	3880	75
H(3)	7821	5413	4080	58
H(5)	8518	2720	2454	60
H(6)	8442	2648	624	74
H(7)	7292	5417	-622	80
H(8)	6366	8451	-31	68

## 5.8 Crystal structure of [Ru(indenyl)COIPPh<sub>3</sub>]

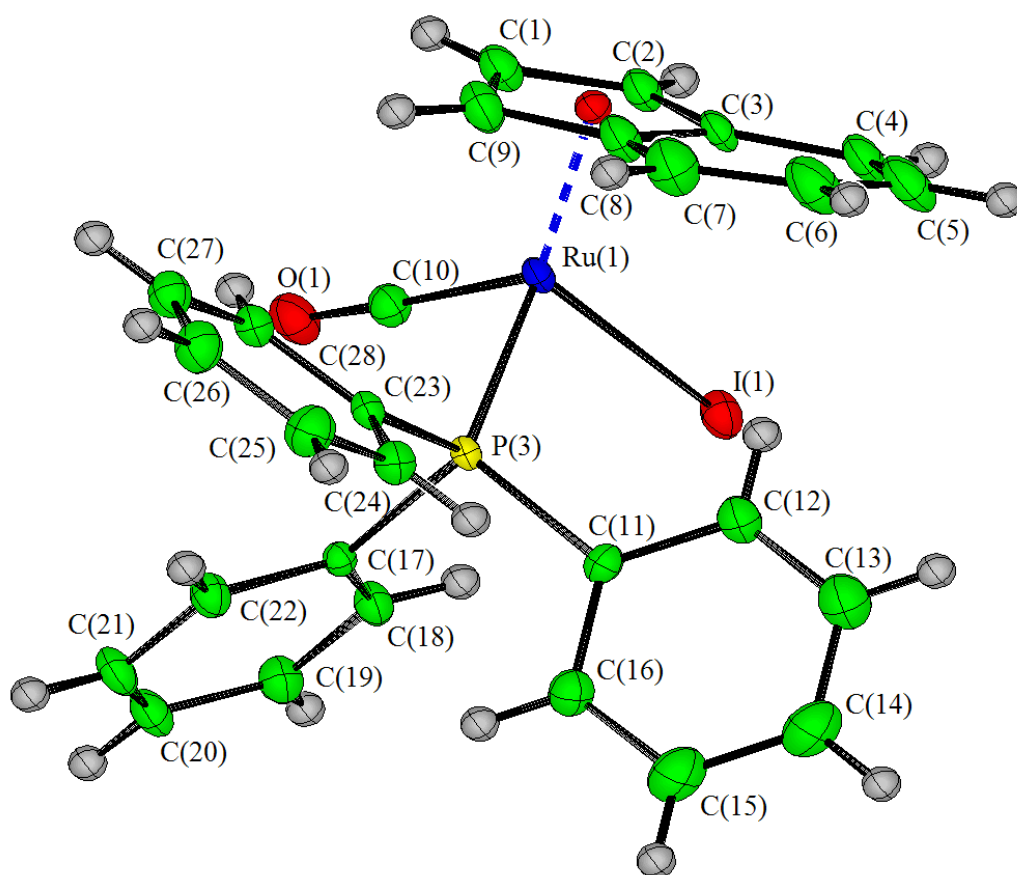


**Table 5.36:** Crystal data and structure refinement for [Ru(indenyl)COIPPh<sub>3</sub>].

Identification code	mc11
Empirical formula	C <sub>28</sub> H <sub>22</sub> I O P Ru
Formula weight	633.40
Temperature	293(2) K
Wavelength	0.7107 Å
Crystal system	Triclinic
Space group	P-1
Unit cell dimensions	a = 9.2229(4) Å α = 85.196(4)° b = 10.2986(5) Å β = 83.290(4)° c = 12.7686(7) Å γ = 85.861(4)°
Volume	1197.87(10) Å <sup>3</sup>
Z	2
Density (calculated)	1.756 Mg/m <sup>3</sup>
Absorption coefficient	2.028 mm <sup>-1</sup>
F(000)	620
Crystal size	0.35 x 0.32 x 0.20 mm
Theta range for data collection	2.8859 to 29.1176 °.
Index ranges	-10 ≤ h ≤ 12; -13 ≤ k ≤ 13; -12 ≤ l ≤ 16
Reflections collected	8850
Independent reflections	4367 [R <sub>int</sub> = 0.0182]
Reflections observed (>2σ)	3647
Data Completeness	0.995
Absorption correction	Semi-empirical from equivalents
Max. and min. transmission	1.00000 and 0.71996
Refinement method	Full-matrix least-squares on F <sup>2</sup>
Data / restraints / parameters	4367 / 0 / 289
Goodness-of-fit on F <sup>2</sup>	0.948
Final R indices [I > 2σ(I)]	R <sub>1</sub> = 0.0208 wR <sub>2</sub> = 0.0475
R indices (all data)	R <sub>1</sub> = 0.0281 wR <sub>2</sub> = 0.0488
Largest diff. peak and hole	0.391 and -0.555 e.Å <sup>-3</sup>

$${}^aR_1 = \Sigma|F_o| - |F_c|/\Sigma|F_o|. \quad {}^b wR_2 = |\Sigma w(|F_o|^2 - |F_c|^2)|/\Sigma|w(F_o)^2|^{1/2}, \quad w = 1/[\sigma^2(F_o^2) + (.0271P)^2]. \quad P = (F_o^2 + 2F_c^2)/3.$$

**Table 5.37:** Atomic coordinates ( $\times 10^4$ ) and equivalent isotropic displacement parameters ( $\text{\AA}^2 \times 10^3$ ) for  $[\text{Ru}(\text{indenyl})\text{COIPPh}_3]$ .  $U(\text{eq})$  is defined as one third of the trace of the orthogonalized  $U_{ij}$  tensor.

Atom	x	y	z	U(eq)
Ru(1)	2068(1)	924(1)	6996(1)	16(1)
I(1)	4970(1)	1317(1)	6732(1)	27(1)
P(3)	1514(1)	2627(1)	8098(1)	14(1)
O(1)	2300(2)	-899(2)	8900(2)	34(1)
C(1)	974(3)	-541(3)	6284(2)	27(1)
C(2)	2202(3)	-209(3)	5582(2)	23(1)
C(3)	1916(3)	1112(2)	5158(2)	21(1)
C(4)	2727(3)	1910(3)	4383(2)	30(1)
C(5)	2101(4)	3100(3)	4068(2)	43(1)
C(6)	718(4)	3543(3)	4512(3)	45(1)
C(7)	-52(4)	2839(3)	5302(3)	39(1)
C(8)	534(3)	1590(3)	5647(2)	26(1)
C(9)	-10(3)	577(3)	6403(2)	29(1)
C(10)	2232(3)	-174(3)	8178(2)	22(1)
C(11)	2366(3)	4168(2)	7704(2)	18(1)
C(12)	2772(3)	4513(3)	6653(2)	27(1)
C(13)	3383(3)	5694(3)	6336(3)	38(1)
C(14)	3597(3)	6530(3)	7091(3)	38(1)
C(15)	3214(3)	6194(3)	8144(3)	36(1)
C(16)	2592(3)	5017(3)	8464(2)	25(1)
C(17)	1952(3)	2252(2)	9458(2)	14(1)
C(18)	3349(3)	1752(3)	9622(2)	22(1)

C(19)	3729(3)	1408(3)	10624(2)	26(1)
C(20)	2710(3)	1558(3)	11486(2)	28(1)
C(21)	1324(3)	2074(3)	11342(2)	28(1)
C(22)	945(3)	2425(3)	10336(2)	23(1)
C(23)	-435(3)	3092(2)	8302(2)	17(1)
C(24)	-1013(3)	4377(3)	8221(2)	23(1)
C(25)	-2500(3)	4658(3)	8450(2)	31(1)
C(26)	-3418(3)	3669(3)	8752(2)	31(1)
C(27)	-2860(3)	2390(3)	8842(2)	25(1)
C(28)	-1380(3)	2108(3)	8615(2)	21(1)

**Table 5.38:** Bond lengths [ $\text{\AA}$ ] and angles [ $^\circ$ ] for  $[\text{Ru}(\text{indenyl})\text{COIPPh}_3]$ .

Ru(1)-C(10)	1.823(3)	Ru(1)-C(1)	2.188(2)
Ru(1)-C(9)	2.204(3)	Ru(1)-C(2)	2.218(2)
Ru(1)-P(3)	2.3306(6)	Ru(1)-C(3)	2.358(2)
Ru(1)-C(8)	2.381(3)	Ru(1)-I(1)	2.7138(3)
P(3)-C(23)	1.821(2)	P(3)-C(11)	1.828(2)
P(3)-C(17)	1.832(3)	O(1)-C(10)	1.141(3)
C(1)-C(2)	1.404(4)	C(1)-C(9)	1.421(4)
C(2)-C(3)	1.438(4)	C(3)-C(4)	1.413(4)
C(3)-C(8)	1.425(4)	C(4)-C(5)	1.366(4)
C(5)-C(6)	1.395(5)	C(6)-C(7)	1.354(5)
C(7)-C(8)	1.414(4)	C(8)-C(9)	1.437(4)
C(11)-C(12)	1.375(4)	C(11)-C(16)	1.402(4)
C(12)-C(13)	1.387(4)	C(13)-C(14)	1.385(4)
C(14)-C(15)	1.371(4)	C(15)-C(16)	1.389(4)
C(17)-C(22)	1.385(3)	C(17)-C(18)	1.385(3)
C(18)-C(19)	1.377(4)	C(19)-C(20)	1.373(4)
C(20)-C(21)	1.375(4)	C(21)-C(22)	1.383(4)
C(23)-C(28)	1.388(3)	C(23)-C(24)	1.391(4)
C(24)-C(25)	1.383(4)	C(25)-C(26)	1.373(4)
C(26)-C(27)	1.380(4)	C(27)-C(28)	1.377(3)
C(10)-Ru(1)-C(1)	90.73(11)	C(10)-Ru(1)-C(9)	107.38(11)
C(1)-Ru(1)-C(9)	37.75(10)	C(10)-Ru(1)-C(2)	110.23(11)
C(1)-Ru(1)-C(2)	37.16(9)	C(9)-Ru(1)-C(2)	62.87(10)
C(10)-Ru(1)-P(3)	87.98(8)	C(1)-Ru(1)-P(3)	139.97(8)
C(9)-Ru(1)-P(3)	105.42(8)	C(2)-Ru(1)-P(3)	160.31(7)
C(10)-Ru(1)-C(3)	146.58(10)	C(1)-Ru(1)-C(3)	60.28(10)
C(9)-Ru(1)-C(3)	60.63(10)	C(2)-Ru(1)-C(3)	36.48(9)
P(3)-Ru(1)-C(3)	124.63(6)	C(10)-Ru(1)-C(8)	143.65(11)
C(1)-Ru(1)-C(8)	60.29(10)	C(9)-Ru(1)-C(8)	36.27(10)

C(2)-Ru(1)-C(8)	60.50(10)	P(3)-Ru(1)-C(8)	100.45(7)
C(3)-Ru(1)-C(8)	35.00(9)	C(10)-Ru(1)-I(1)	92.65(8)
C(1)-Ru(1)-I(1)	126.82(7)	C(9)-Ru(1)-I(1)	152.82(8)
C(2)-Ru(1)-I(1)	93.36(7)	P(3)-Ru(1)-I(1)	93.194(17)
C(3)-Ru(1)-I(1)	92.55(6)	C(8)-Ru(1)-I(1)	121.72(7)
C(23)-P(3)-C(11)	104.20(11)	C(23)-P(3)-C(17)	101.90(11)
C(11)-P(3)-C(17)	103.15(11)	C(23)-P(3)-Ru(1)	113.07(8)
C(11)-P(3)-Ru(1)	117.77(9)	C(17)-P(3)-Ru(1)	114.92(8)
C(2)-C(1)-C(9)	109.4(3)	C(2)-C(1)-Ru(1)	72.58(14)
C(9)-C(1)-Ru(1)	71.73(14)	C(1)-C(2)-C(3)	107.2(2)
C(1)-C(2)-Ru(1)	70.26(14)	C(3)-C(2)-Ru(1)	77.08(14)
C(4)-C(3)-C(8)	120.2(3)	C(4)-C(3)-C(2)	131.5(3)
C(8)-C(3)-C(2)	108.3(2)	C(4)-C(3)-Ru(1)	127.19(18)
C(8)-C(3)-Ru(1)	73.38(15)	C(2)-C(3)-Ru(1)	66.44(14)
C(5)-C(4)-C(3)	118.0(3)	C(4)-C(5)-C(6)	121.7(3)
C(7)-C(6)-C(5)	121.9(3)	C(6)-C(7)-C(8)	118.8(3)
C(7)-C(8)-C(3)	119.3(3)	C(7)-C(8)-C(9)	133.3(3)
C(3)-C(8)-C(9)	107.4(3)	C(7)-C(8)-Ru(1)	131.17(18)
C(3)-C(8)-Ru(1)	71.62(15)	C(9)-C(8)-Ru(1)	65.12(15)
C(1)-C(9)-C(8)	107.2(2)	C(1)-C(9)-Ru(1)	70.51(15)
C(8)-C(9)-Ru(1)	78.61(15)	O(1)-C(10)-Ru(1)	177.0(2)
C(12)-C(11)-C(16)	119.3(2)	C(12)-C(11)-P(3)	120.0(2)
C(16)-C(11)-P(3)	120.6(2)	C(11)-C(12)-C(13)	120.9(3)
C(14)-C(13)-C(12)	119.4(3)	C(15)-C(14)-C(13)	120.4(3)
C(14)-C(15)-C(16)	120.4(3)	C(15)-C(16)-C(11)	119.6(3)
C(22)-C(17)-C(18)	118.1(2)	C(22)-C(17)-P(3)	123.18(19)
C(18)-C(17)-P(3)	118.75(19)	C(19)-C(18)-C(17)	121.5(2)
C(20)-C(19)-C(18)	119.8(3)	C(19)-C(20)-C(21)	119.6(3)
C(20)-C(21)-C(22)	120.5(3)	C(21)-C(22)-C(17)	120.5(2)
C(28)-C(23)-C(24)	118.6(2)	C(28)-C(23)-P(3)	117.57(19)
C(24)-C(23)-P(3)	123.7(2)	C(25)-C(24)-C(23)	120.3(3)
C(26)-C(25)-C(24)	120.2(3)	C(25)-C(26)-C(27)	120.2(3)
C(28)-C(27)-C(26)	119.7(3)	C(27)-C(28)-C(23)	121.0(3)

**Table 5.39:** Anisotropic displacement parameters ( $\text{\AA}^2 \times 10^3$ ). The anisotropic displacement factor exponent takes the form:

$$-2 \pi^2 [h^2 a^{*2} U11 + \dots + 2 h k a^* b^* U12]$$

Atom	U11	U22	U33	U23	U13	U12
Ru(1)	20(1)	17(1)	10(1)	-3(1)	-3(1)	-1(1)
I(1)	20(1)	43(1)	20(1)	-9(1)	1(1)	2(1)
P(3)	16(1)	16(1)	11(1)	-2(1)	-2(1)	-1(1)
O(1)	58(1)	23(1)	23(1)	4(1)	-10(1)	0(1)
C(1)	41(2)	27(2)	16(2)	-7(1)	-6(1)	-14(1)
C(2)	33(2)	22(1)	15(1)	-8(1)	-4(1)	-1(1)
C(3)	34(2)	23(1)	10(1)	-7(1)	-9(1)	2(1)
C(4)	47(2)	30(2)	14(2)	-2(1)	-4(1)	-2(1)
C(5)	85(3)	29(2)	16(2)	0(1)	-12(2)	-9(2)
C(6)	87(3)	25(2)	25(2)	-4(1)	-25(2)	14(2)
C(7)	48(2)	43(2)	32(2)	-20(2)	-24(2)	18(2)
C(8)	35(2)	31(2)	16(2)	-9(1)	-15(1)	0(1)
C(9)	28(2)	46(2)	19(2)	-14(1)	-6(1)	-10(1)
C(10)	30(2)	18(1)	21(2)	-7(1)	-6(1)	-2(1)
C(11)	15(1)	16(1)	23(2)	1(1)	-1(1)	1(1)
C(12)	30(2)	27(2)	22(2)	1(1)	-2(1)	-3(1)
C(13)	43(2)	37(2)	31(2)	15(2)	1(2)	-7(2)
C(14)	36(2)	20(2)	55(2)	9(2)	-4(2)	-7(1)
C(15)	39(2)	19(2)	51(2)	-7(2)	-9(2)	-4(1)
C(16)	26(2)	22(1)	28(2)	-3(1)	-3(1)	-2(1)
C(17)	18(1)	12(1)	14(1)	-2(1)	-3(1)	-3(1)
C(18)	20(1)	30(2)	17(2)	-7(1)	-2(1)	1(1)
C(19)	26(2)	30(2)	24(2)	-7(1)	-13(1)	3(1)
C(20)	42(2)	28(2)	15(2)	1(1)	-10(1)	-5(1)
C(21)	30(2)	41(2)	13(2)	-2(1)	4(1)	-5(1)
C(22)	18(1)	32(2)	20(2)	-4(1)	-1(1)	2(1)
C(23)	17(1)	22(1)	12(1)	-2(1)	-5(1)	1(1)

C(24)	22(1)	24(1)	22(2)	4(1)	-3(1)	0(1)
C(25)	26(2)	30(2)	36(2)	1(1)	-5(1)	6(1)
C(26)	17(1)	44(2)	31(2)	0(1)	-4(1)	4(1)
C(27)	19(1)	33(2)	24(2)	-1(1)	-4(1)	-7(1)
C(28)	23(1)	23(1)	18(2)	-3(1)	-6(1)	1(1)

**Table 5.40:** Hydrogen coordinates ( $\times 10^4$ ) and isotropic displacement parameters ( $\text{\AA}^2 \times 10^3$ ) for  $[\text{Ru}(\text{indenyl})\text{COIPPh}_3]$ .

Atom	x	y	z	U(eq)
H(1)	827	-1366	6620	35
H(2)	3042	-742	5420	30
H(4)	3660	1633	4094	39
H(5)	2609	3628	3545	55
H(6)	314	4344	4258	58
H(7)	-950	3170	5613	51
H(9)	-849	642	6881	38
H(12)	2635	3946	6148	35
H(13)	3647	5922	5623	50
H(14)	4003	7324	6883	49
H(15)	3372	6757	8646	46
H(16)	2327	4793	9178	33
H(18)	4046	1646	9042	29
H(19)	4674	1074	10716	33
H(20)	2957	1313	12164	36
H(21)	636	2187	11926	37
H(22)	7	2781	10249	30
H(24)	-397	5050	8013	30
H(25)	-2880	5519	8398	40
H(26)	-4418	3862	8898	40
H(27)	-3481	1722	9054	33
H(28)	-1008	1244	8673	27

## Chapter 6      Results and Discussion

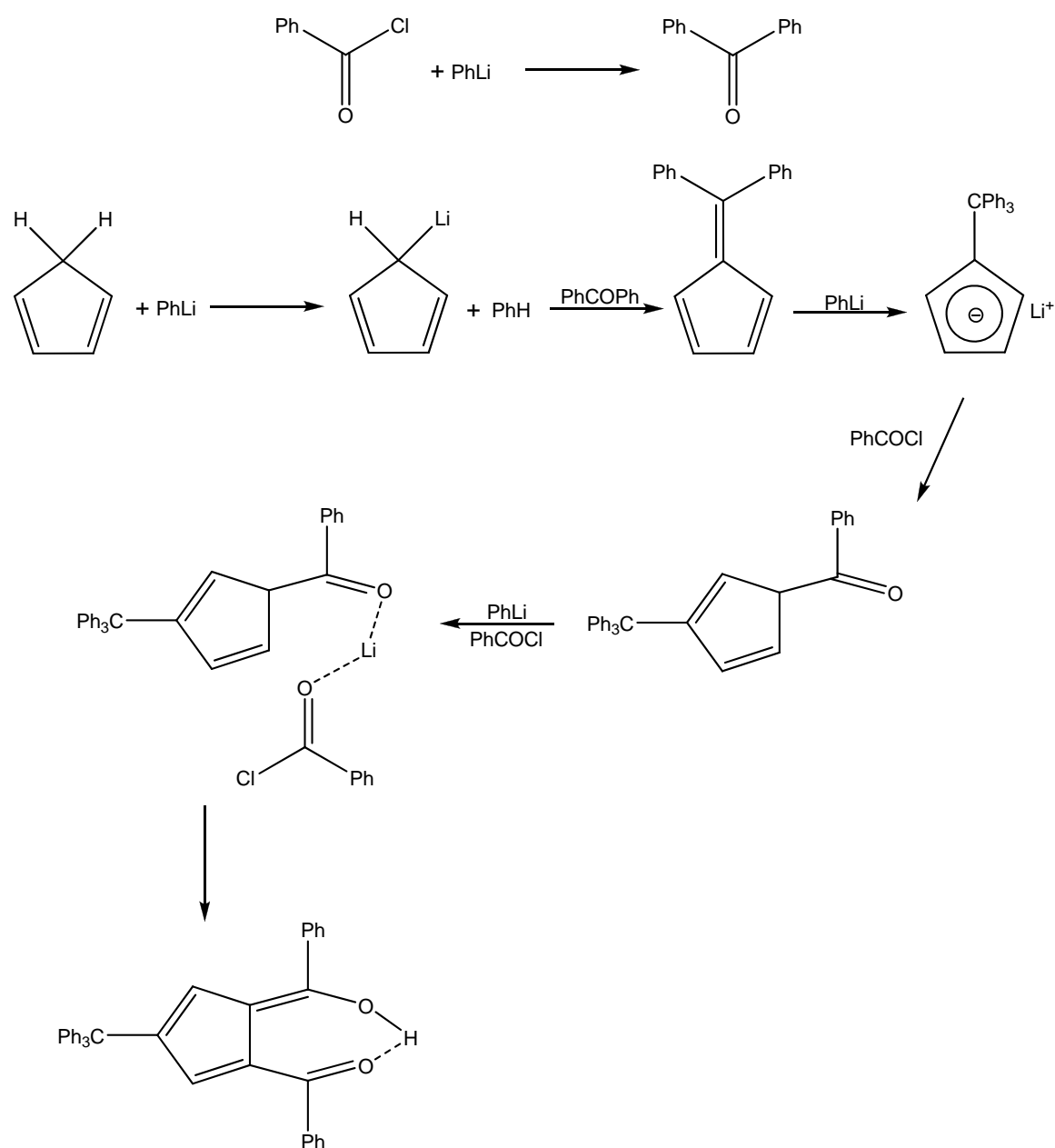
Despite the large number of substituted cyclopentadienyl ligands in the literature there are just a few examples which have electron-withdrawing substituents.<sup>232</sup> The dbzCpH synthesis discovered by Linn and Sharkey seemed to provide an interesting source of cyclopentadienyl ligands with electron-withdrawing substituents. Although some sandwich and half-sandwich transition metal complexes containing the dbzCp ligand have been reported, the effects of these ligands on the chemistry of their transition metal complexes have not been investigated.

### 6.1    Dibenzoylcyclopentadienyl Ligands

#### 6.1.1    Dibenzoylcyclopentadiene

The 1,2-disubstituted products arise from  $\text{Li}^+$  coordination of the incoming second benzoyl group adjacent to the position of first attack. Upon the addition of TMEDA, a known  $\text{Li}^+$  complexing agent to the reaction the yield of dbzCpH was suppressed by a factor of five.<sup>229</sup> The infrared spectrum shows strong intramolecular hydrogen bonding, as no carbonyl peak appears above  $1642\text{ cm}^{-1}$ .

During her investigations of the Linn and Sharkey reaction, Fitzgerald isolated some bright green crystals during work up.<sup>229</sup> The crystal structure was determined and the crystals were found to contain an unexpected side product, triphenylmethyldibenzoyl cyclopentadiene. This would suggest the reaction is more complicated than previously suggested. It was proposed that this side reaction proceeds via the formation of benzophenone and then diphenyl fulvene in sequence. The diphenylfulvene is alkylated and benzoylated. The sequence which incorporates five phenyl rings onto a cyclopentadienyl ring in a one pot synthesis is remarkable.



**Scheme 6.1:** Proposed mechanism for the formation of the triphenylmethyl derivative

However, the green crystals were of poor quality. The crystal structure confirmed the presence of  $(\text{COPh})_2\text{C}_5\text{H}_3\text{CPh}_3$  co-crystallisation with benzoic acid.

The compound was directly synthesised by benzylation of  $\text{C}_5\text{H}_5\text{CPh}_3$ . All attempts to grow co-crystals with benzoic acid were unsuccessful.

### 6.1.2 $(\text{CH}_3)_2\text{C}_5\text{H}_3(\text{CO}-p\text{-tol})_2$

The structure of the  $(\text{CH}_3)_2\text{C}_5\text{H}_3(\text{CO}-p\text{-tol})_2$  compound has been confirmed by  $^1\text{H}$  NMR spectroscopy.

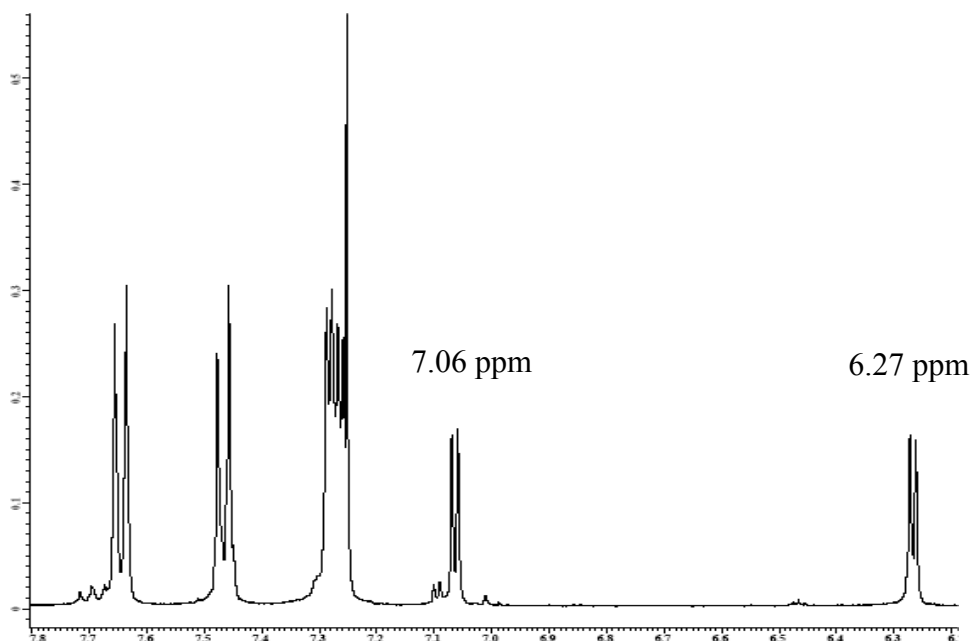


**Figure 6.1:** Expanded  $^1\text{H}$  NMR spectrum for  $(\text{CH}_3)_2\text{C}_5\text{H}_3(\text{CO}-p\text{-tol})_2$

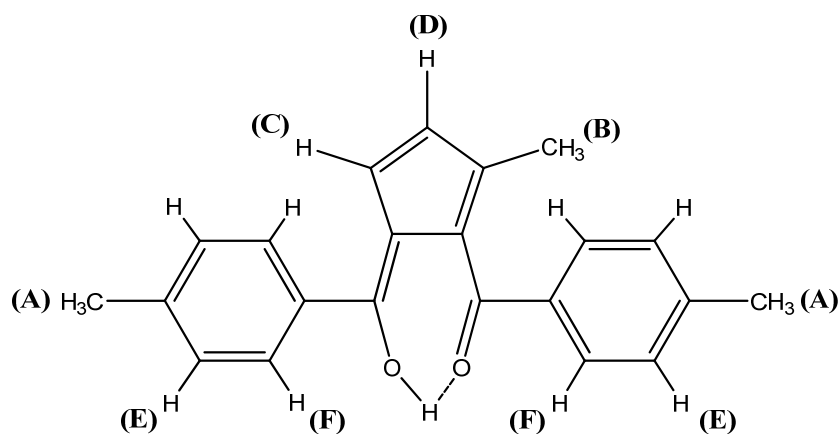


**Figure 6.2:**  $^1\text{H}$  NMR hydrogen assignment

$\delta$ Chemical Shift (ppm)	Hydrogen Assignment
1.79 s	A (6H)
2.49 d	B (3H)
6.27 d	C (1H)
7.06 d	D (1H)
7.24-7.30 m	E (4H)
7.4-7.7 m	F (4H)

**Table 6.1:** Hydrogen assignment for  $(CH_3)C_5H_3(CO-p-tol)_2$

The resonances at 6.27 ppm and 7.06 ppm indicate un-equivalent protons on the Cp ring and not a symmetrical product as was expected. This arises due to the orientation of the oxygen after the first benzylation which occurs at the carbon furthest away from the electron releasing methyl group on the Cp.

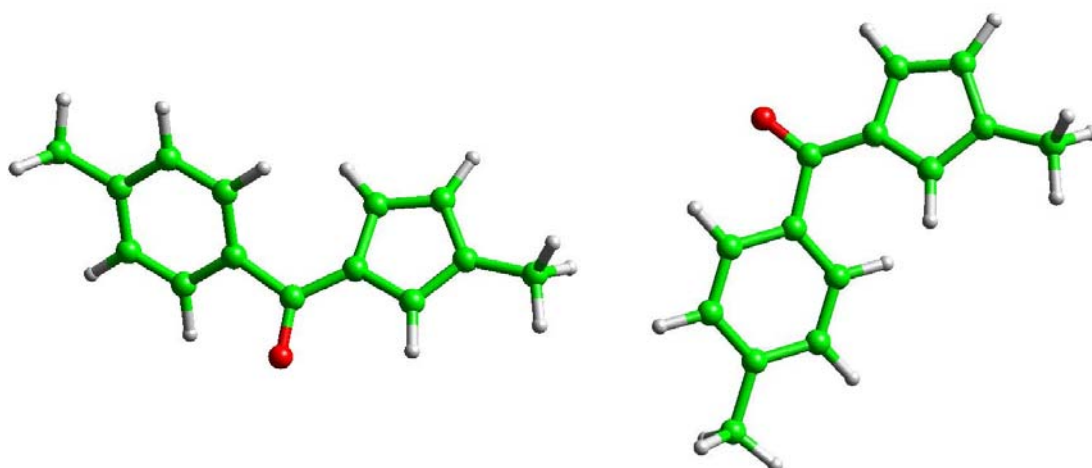


**Figure 6.3:** Two possible orientations for the oxygen atom after the initial benzylation

The figure on the left (**Figure 6.3**) indicates the more stable configuration after the initial benzylation of cyclopentadiene, calculated using B3LYP (6-31G\*). The 1,2-disubstituted product is then formed by lithium direction of the second benzoyl group adjacent to the site of first attack.

These dbzCp ligands react with transition metals *via* their cyclopentadienyl tautomer.

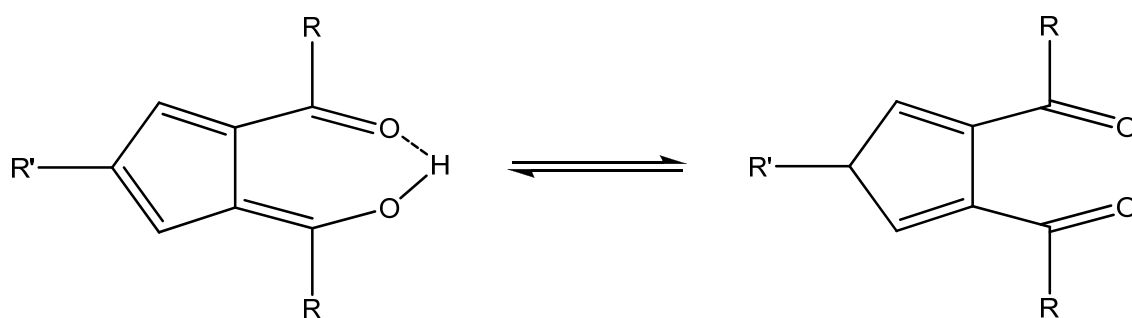


**Figure 6.4:** Tautomerism in dbzCpH compounds

## 6.2 Crystallographic Data

Two polymorphs of the pyridazine ligand were obtained (**5.1** and **5.2**). The needle polymorph (Form I) is the stable form and was obtained after recrystallization from DCM/hexane. The diamond habit form (Form II) is a metastable form and was isolated upon cooling of the reaction solution when the reaction was carried out in EtOH. X-ray powder diffraction showed the “fluffy” crystals reported by Linn and Sharkey to be a mixture of the two polymorphs. The polymorphs can be interconverted by recrystallization from the solvents described above. Crystallization of Form II was more efficient if a few drops of hydrazine were added to the solution. Single crystal X-ray diffraction studies show that the Form I has one molecule per asymmetric unit in space group  $P2_1/a$ , whereas the Form II crystallised in the triclinic space group  $P-1$  with two independent molecules per asymmetric unit. In the lattice of Form II there are hydrogen bonded dimers and it is interesting that in the stable form there is no hydrogen bonding. This is not common as unused hydrogen bonding capacity is rare. Indeed it breaks Etter’s first rule.<sup>233</sup> However Form I has a face to face 1D  $\pi$ -stacking motif which is in the  $c$  direction. This motif is probably the reason for needle growth in the  $c$  direction and the stability of Form I.

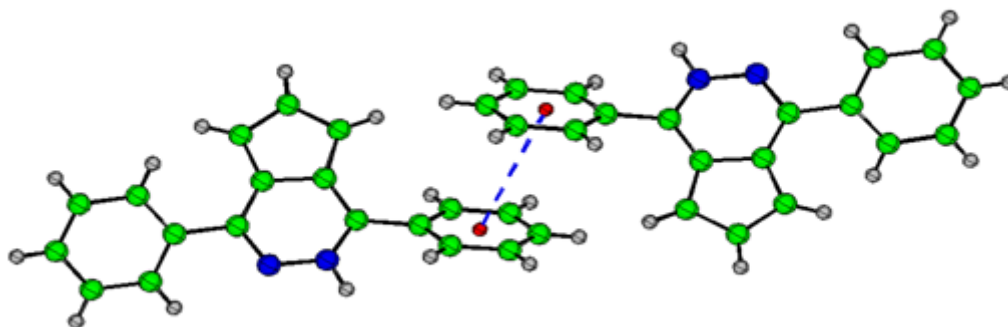


*Figure 6.5:* Unit cell pack for Form I

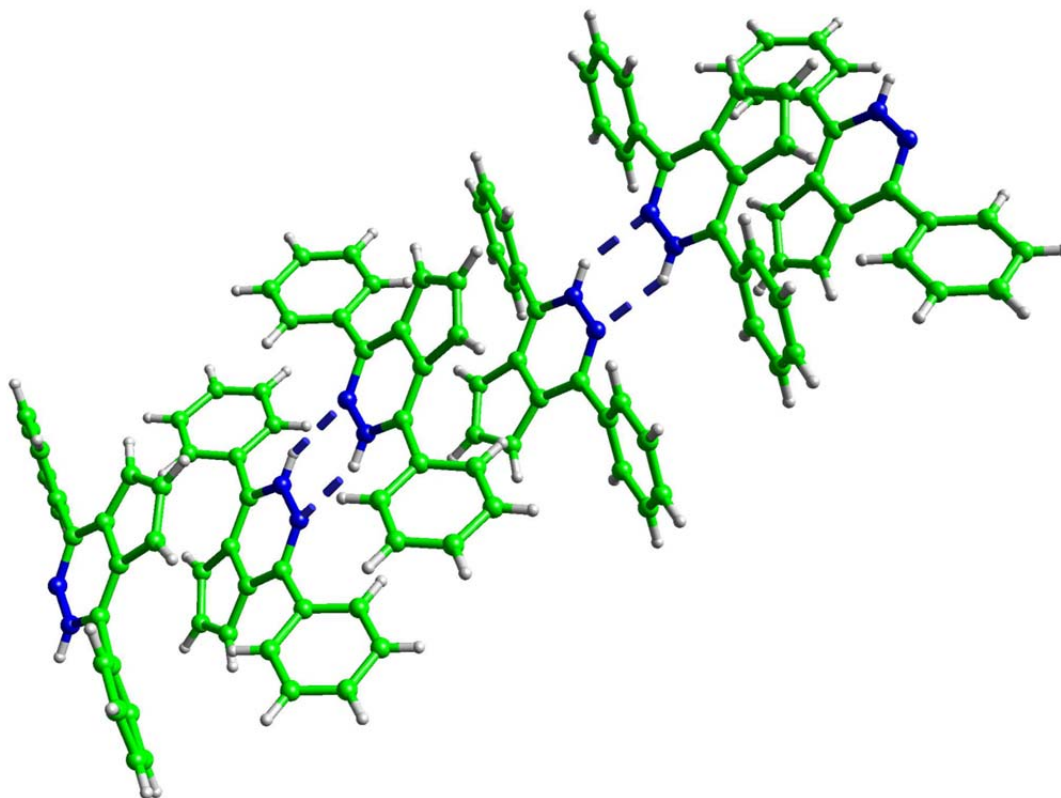


**Figure 6.6:** *Hydrogen bonded dimers of Form II*

The hydrogen bonding in Form II has N...N distances of 2.920 and 2.943 Å in the dimers formed by the molecules of the asymmetric unit.

Habit lattice energy calculations show Form I to be the more stable polymorph with a density equals to 1.312 Mg/m<sup>3</sup> and  $E = -24.023\text{kJ}$ . Form II has a density of 1.29 Mg/m<sup>3</sup> and a lattice energy of  $E = -22.263$ .

The molecular weight of 1,4-diphenyl-2-cyclopenta[*d*]pyridazine in DCM solution was determined as 412.55 gmol<sup>-1</sup>. This suggests that in solution there is an equilibrium between monomeric and dimeric forms.

The observed and calculated crystal habit for Forms I and II are shown in 5.1 and 5.2. While the simple BFDH model is reasonably accurate for Form II which has no extensive hydrogen bonding or  $\pi$ -stacking motif it is interesting that Form I which has a habit controlling 1D  $\pi$ -stacking motif, in the needle direction, is only reproduced by the more accurate added slice energy model (ASE).

**5.3**, the crystal structure of  $\text{Ph}_3\text{C}-\text{C}_5\text{H}_3(\text{COPh})_2$  has a strong intra molecular hydrogen bond. The O-H...O distance was 1.47(2) and the O...O was 2.462(2) Å. The O-H hydrogen was located and refined. The C-C bond lengths within the five membered ring indicate that there is just one resonance form as the C1-C2, C2-C3 and C4-C5 bonds are long, 1.390(3), 1.420(3) and 1.414(3) and the C1-C5 and C3-C4 bonds are short 1.387(3) and 1.374(3) respectively.

There are no inter molecular O-H...O or C-H...O contacts or  $\pi$ -stacking interactions as all Ph ring centroids are more than 4 Å apart. This combined with the awkward shape of the molecule leads to a density of 1.20 Mg/m<sup>3</sup> which is on the low side of normal.

**5.4**, the crystal structure of  $\text{C}_{23}\text{H}_{16}\text{O}_2$ , has a pseudo symmetry problem. The inversion centre in the P-1 space group in which the structure was refined is imperfect and this affects the R factors. Attempts to solve the structure and refine it in P1 which has no symmetry gave unsatisfactory results. In P1 the aromatic rings were not planar and the bond lengths were poor. The present refinement in P-1 gives reasonable bond lengths and angles and there are no significant peaks in the difference map.

**5.5**, the crystal structure of  $[\text{Ru}(\text{dbzCp})(\text{CO})\text{IPPh}_3]$ , shows one benzoyl group attempts to enter the plane of the Cp ligand to the best of its ability whereas the other's attempt is hampered due to the phenyl groups of the triphenylphosphine substituent. In contrast to the para-tolyl analogue no disorder is exhibited between the CO and I moieties. The Ru – CO bond distance is 1.906(8), the RuC – O 1.069(8) and the Ru – P 2.003(1) Å.

**5.6**, the crystal structure of  $[\text{Ru}((\text{CO}-p\text{-tolyl})_2\text{C}_5\text{H}_3)(\text{CO})\text{IPPh}_3]$  the carbonyl ligand exhibits 80:20 disorder with the iodide. However, all aromatic bond lengths are within normal range.

**5.7**,  $[\text{Ru}(\text{indenyl})(\text{CO})_2\text{I}]$ , the Ru – C bond distances are 1.854(7) and 1.890(8) Å for C10 and C11 respectively. The RuC – O bond distances are 1.137(8) and 1.116(8) Å for C10 and C11 respectively. The Ru – I bond distance is 2.7055(7) Å. No disorder was exhibited in this structure.

**5.8**, [Ru(indenyl)(CO)IPPh<sub>3</sub>], the Ru – C bond distance is 1.823(3) and the RuC – O is 1.141(3) Å. When compared to the unsubstituted analogue, (**5.7**), it is clear that the phosphine group shortens the M – C bond length. This is due to an increase in back-bonding to the CO group upon substitution. The M – C bond length in the phosphine substituted dibenzoyl complex, (**5.5**), is 1.906(8) Å. This slightly longer M – C bond length may be due to a decrease in back-bonding arising from the electron withdrawing abilities of the dibenzoyl substituents. This is also visible in the IR spectra where the  $\nu_{MC-O}$  stretching frequencies for the dibenzoyl metal complexes differing to those of the indenyl complexes by  $\sim 27$  wavenumbers.

### 6.3 Carbonyl Stretching Frequencies

The extent electron-withdrawing capability of the dbzCp ligand is evident in  $\nu_{MC-O}$  stretching frequencies.

Compound	$\nu_{MC-O}$ (cm <sup>-1</sup> ) in DCM	$\Delta$
[CpRu(CO) <sub>2</sub> ] <sub>2</sub>	2001, 1964, 1935, 1772	
[Ru(dbzCp)(CO) <sub>2</sub> ] <sub>2</sub>	2024, 1990, 1961, 1797	23, 34, 26, 25

**Table 6.2:** Carbonyl stretching frequencies in parent and substituted dimeric complexes

These frequency differences of more than 22 cm<sup>-1</sup> are shown (**Table 6.2**).  $\nu_{MC-O}$  shifts to a lower frequency upon the addition of electron-releasing methyl groups to the Cp ring. However, the shifts are  $< 2$  cm<sup>-1</sup> per CH<sub>3</sub> group added.

Costa *et al.* developed a series of metal complexes containing slightly electron-withdrawing substituents and their effects evident in the  $\nu(CO)$  values recorded.<sup>32</sup>

Compound	$\nu_{MC-O}$ (cm <sup>-1</sup> )	Solvent	$\Delta$
[RuCp(CO) <sub>2</sub> ] <sub>2</sub>	2001, 1964, 1772	CH <sub>2</sub> Cl <sub>2</sub>	
[Ru(MDMCp)(CO) <sub>2</sub> ] <sub>2</sub> <sup>*</sup>	2014, 1973, 1787	CH <sub>2</sub> Cl <sub>2</sub>	13, 9, 15

<sup>\*</sup>MDMCp = 1-methoxycarbonyl-3,4-di(dimethoxycarbonylmethylene)cyclopentadienyl

**Table 6.3:** The effects of electron-withdrawing and electron-releasing substituents on  $\nu_{MC-O}$  of Cp ruthenium complexes

As illustrated in **Tables 6.2** and **6.3**, both ligands are withdrawing electron density from the metal centre, reducing back-bonding and increasing the  $\nu_{MC-O}$  frequencies. However, the dbzCp ligand exhibits a greater extent of electron-withdrawal from the metal centre. This is due to the methyl group hindering the electron-withdrawing capabilities of the COOMe group on the MDMCp ligand.

Compound	$\nu_{MC-O}$ (cm <sup>-1</sup> ) in DCM
[Ru(dbzCp)(CO) <sub>2</sub> Cl]	2073, 2026
[Ru(dbzCp)(CO) <sub>2</sub> Br]	2071, 2024
[Ru(dbzCp)(CO) <sub>2</sub> I]	2064, 2019

**Table 6.4:** Comparison of the  $\nu_{MC-O}$  frequencies of the dbzCp halide complexes

The lower value obtained for the  $\nu_{MC-O}$  of the iodide complex when compared to the bromide complex indicate competition between the ligand and the iodide for the metal electron density. The calculated charges on the metal in dbzCp and parent Cp complexes have been calculated using DFT 3-21G\* methods.

Complex	Cl	Br	I
[RuCp(CO) <sub>2</sub> X]	0.687	0.582	0.560
[RudbzCp(CO) <sub>2</sub> X]	0.899	0.728	0.788

**Table 6.5:** Calculated metal centre charges

This also holds true for the observed parent Cp  $\nu_{MC-O}$  stretching frequencies.

Compound	$\nu_{MC-O}$ (cm <sup>-1</sup> ) in DCM
[RuCp(CO) <sub>2</sub> H]	1966, 1774
[RuCp(CO) <sub>2</sub> Cl]	2058, 2008
[RuCp(CO) <sub>2</sub> Br]	2055, 2008
[RuCp(CO) <sub>2</sub> I]	2047, 1997

**Table 6.6:** Comparison of the  $\nu_{MC-O}$  frequencies of the Cp halide and hydride complexes

IR Hessian calculations show good correlation between calculated and experimental results, (**Table 6.7**).

Metal Complex	Experimental (DCM)	Calculated
[RuCp(CO) <sub>2</sub> H]	1973.90, 1944.61	2036.66, 1988.05
[RuCp(CO) <sub>2</sub> Cl]	2057.95, 2008.95	2056.51, 2012.65
[RuCp(CO) <sub>2</sub> Br]	2054.91, 2008.52	2051.50, 2008.44
[RuCp(CO) <sub>2</sub> I]	2048.60, 1998.70	2048.82, 2009.92
[Ru(dbzCp)(CO) <sub>2</sub> Cl]	2072.98, 2026.87	2075.87, 2032.59
[Ru(dbzCp)(CO) <sub>2</sub> Br]	2071.57, 2024.91	2071.53, 2026.12
[Ru(dbzCp)(CO) <sub>2</sub> I]	2064.73, 2019.25	2065.80, 2023.35

**Table 6.7:** Comparison of calculated and experimental  $\nu_{MC-O}$  for metal complexes

#### 6.4 Kinetics and Mechanism of Carbonyl Substitution on [RuCp(CO)<sub>2</sub>X] with PPh<sub>3</sub>

In order to understand the effects of the electron-withdrawing substituents on [Ru(dbzCp)(CO)<sub>2</sub>I], the rates of CO substitution by tertiary phosphines were measured and compared to those reported by Brown *et al.* in 1970.<sup>146</sup> The Brown group examined the rates of CO substitution by tertiary phosphines on [FeCp(CO)<sub>2</sub>X] and [RuCp(CO)<sub>2</sub>X], (X = Cl, Br, I). All the reactions proceed *via* a dissociative mechanism with no dependence on the concentration of the incoming ligand. However, although mentioning that the rate of CO substitution on the [RuCp(CO)<sub>2</sub>I] complex is ~100 times slower than the corresponding iron complex, no kinetic or thermodynamic data were provided for these reactions.<sup>144</sup> To compare the rates of reaction of the dibenzoyl complexes with the parent Cp complexes, the rate constants of these reactions were measured.

Complex	[PPh <sub>3</sub> ] (molL <sup>-1</sup> )	10 <sup>5</sup> k <sub>obs</sub> (sec <sup>-1</sup> )
[RuCp(CO) <sub>2</sub> I]	2.29 x 10 <sup>-2</sup>	0.72 ± .02
	3.44 x 10 <sup>-2</sup>	1.24 ± 0.2
	4.60 x 10 <sup>-2</sup>	1.5 ± 0.2
[RuCp(CO) <sub>2</sub> Br]	2.65 x 10 <sup>-2</sup>	12.1 ± 1
	5.30 x 10 <sup>-2</sup>	14.0 ± 4

**Table 6.8:** Rates of CO substitution on CpRu(CO)<sub>2</sub>X (X = I, Br)

The rate constants of CO substitution recorded for  $[\text{RuCp}(\text{CO})_2\text{Br}]$  are consistent with a dissociative mechanism having shown no dependence on the concentration of the incoming ligand. The rates recorded also were in accordance with those reported by Brown *et al.* for the reactions at a similar temperature.

The rate constants recorded for  $\text{CpRu}(\text{CO})_2\text{I}$  appeared associative, with the rate dependent on the concentration of the  $\text{PPh}_3$  (**Figure 6.7**). The rate of substitution on the iodide complex, at a 20 M excess of ligand, is  $\sim 10$  times slower than the corresponding bromide complex at the same molar excess of ligand. This is as expected from the  $\nu_{\text{MC-O}}$  recorded for both the bromide and iodide complexes, (**Table 6.6**).

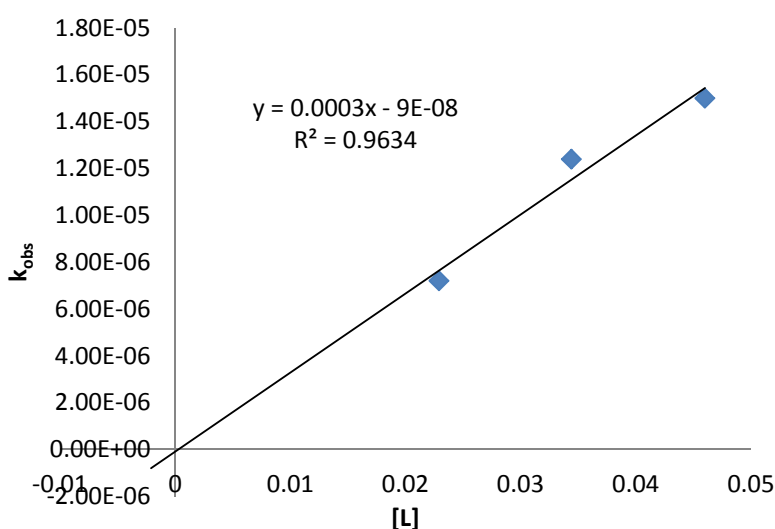


**Figure 6.7:** Linear dependence of  $k_{\text{obs}}$  on  $[\text{L}]$

To further understand the mechanism of reaction of the parent iodide complex, the kinetics of reaction were measured at three different temperatures to calculate the activation parameters for the reaction. General practice would be to carry out the reactions at temperatures spanning at least 60 °C, however, experimental constraints reduced this to 10° in the present case. This is the reason for the significant error values obtained.

[RuCp(CO) <sub>2</sub> I]	134.5°C	129.5°C	124.5°C
10 <sup>5</sup> k <sub>obs</sub> (s <sup>-1</sup> )	1.240	0.405	0.275

**Table 6.9:** *k<sub>obs</sub>* for CO substitution reaction of [RuCp(CO)<sub>2</sub>I] at varying temperatures

The activation values of the system was calculated using the Eyring equation, (**Table 6.10**)

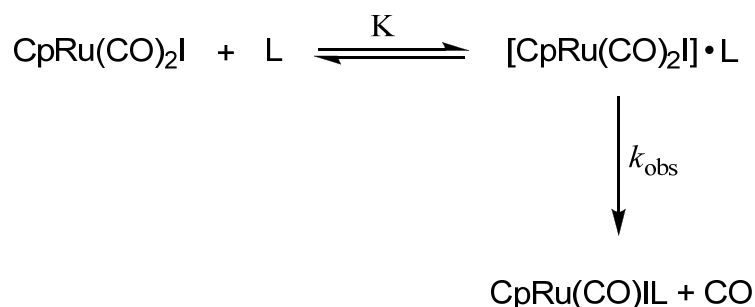
Complex	$\Delta H^\ddagger$ (kJmol <sup>-1</sup> )	$\Delta S^\ddagger$ (JK <sup>-1</sup> mol <sup>-1</sup> )
[RuCp(CO) <sub>2</sub> I]	199.1 ± 58.3	145.7 ± 61.5
[RuCp(CO) <sub>2</sub> Br]*	109.7 ± 7.4	-49.0 ± 6.0

\* Values calculated using the Eyring equation and the kinetic data reported by Brown<sup>146</sup>

**Table 6.10:** Activation parameters for the reaction of CpRu(CO)<sub>2</sub>X with PPh<sub>3</sub>

While the negative  $\Delta S^\ddagger$  recorded suggests a dissociative mechanism, the rate constants were shown to be dependent on the concentration of the incoming ligand. These factors suggest that the reaction proceeds *via* an interchange dissociative (I<sub>d</sub>) mechanism.

Such a mechanism would involve a pre-equilibrium step between the reactants and the incoming ligand, (L), involving only weak bonding to both the incoming ligand and the departing CO, (**Scheme 6.2**).<sup>140</sup>



**Scheme 6.2:** The proposed I<sub>d</sub> mechanism employed by CpRu(CO)<sub>2</sub>I

The rate law for such a mechanism is:

$$\text{Rate} = \frac{k_{\text{obs}}K[\text{L}]}{1 + K[\text{L}]}$$

If  $K \gg 1$  the rate equation becomes:

$$\text{Rate} = k_{\text{obs}}$$

If  $K \ll 1$  the rate equation becomes:

$$\text{Rate} = k_{\text{obs}}K[\text{L}]$$

The  $I_d$  mechanism may be operative in the case of the  $[\text{RuCp}(\text{CO})_2\text{I}]$  due to the slow rate of reaction. The reaction requires 4 days to go to completion at a temperature of  $134.5^\circ\text{C}$ .

Complexes of the type  $\text{M}(\text{CO})_5\text{-amine}$  ( $\text{M} = \text{Cr}, \text{Mo}, \text{W}$ ) undergo amine substitution with CO to form  $\text{M}(\text{CO})_6$  in the absence of added amines.<sup>140</sup> In reactions with other incoming ligands such as phosphines or phosphites, both ligand-independent and ligand-dependent terms are observed in the rate constant expression. The ligand-independent rate parameters, when  $\text{L} = \text{CO}$ , phosphines, are identical. This signifies a rate-determining dissociation of the amine. However, the ligand-dependent term exhibits a significant dependence on both the leaving and entering groups.<sup>234</sup> These ligand-dependent pathways exhibit activation parameters that parallel those for a dissociative mechanism thus inferring an  $I_d$  mechanism.

Reaction	$\Delta H^\ddagger$ (kJmol <sup>-1</sup> )	
	Ligand-independent	Ligand-dependent
$\text{Cr}(\text{CO})_6 + \text{P}(n\text{-Bu})_3$	168.23	106.72
$\text{Mo}(\text{CO})_6 + \text{P}(n\text{-Bu})_3$	132.66	90.81
$\text{W}(\text{CO})_6 + \text{P}(n\text{-Bu})_3$	166.98	122.20

**Table 6.11:** Enthalpies of activation for the reactions of  $\text{M}(\text{CO})_6$  with  $\text{P}(n\text{-Bu})_3$

## 6.5 Kinetics and Mechanism of CO Substitution on $\text{dbzCpRu}(\text{CO})_2\text{X}$ with Tertiary Phosphines

Complex	L	[L] ( $\text{molL}^{-1}$ )	$10^4 k_{\text{obs}}$ ( $\text{sec}^{-1}$ )
[Ru(dbzCp)(CO) <sub>2</sub> I]	PPh <sub>3</sub>	$1.44 \times 10^{-2}$	$4.7 \pm 0.7$
		$2.87 \times 10^{-2}$	$4.6 \pm 0.3$
	P(OPh) <sub>3</sub>	$1.44 \times 10^{-2}$	$4.5 \pm 0.2$
		$2.87 \times 10^{-2}$	$4.6 \pm 0.4$
[Ru(dbzCp)(CO) <sub>2</sub> Br]	PPh <sub>3</sub>	$1.57 \times 10^{-2}$	$24 \pm 6$
		$3.14 \times 10^{-2}$	$24 \pm 4$
	P(OPh) <sub>3</sub>	$1.57 \times 10^{-2}$	$23 \pm 3$
		$3.14 \times 10^{-2}$	$24 \pm 3$

**Table 6.12:** Rates of CO substitution on [Ru(dbzCp)(CO)<sub>2</sub>X] (X = Br, I) with PPh

The rates of CO substitution on both the [Ru(dbzCp)(CO)<sub>2</sub>Br] and [Ru(dbzCp)(CO)<sub>2</sub>I] complexes show no dependence on the concentration or the nature of the incoming ligand. The bromide complex underwent substitution at a rate 5 times greater than the iodide. This is in accordance with the decreased back bonding from the metal centre to the carbonyl ligands, as evident in the  $\nu_{\text{MC-O}}$  stretching frequencies, (**Table 6.4**).

The activation parameters were calculated using the Eyring equation.

[Ru(dbzCp)(CO) <sub>2</sub> I]	134.5 °C	114.5 °C	94.5 °C
$10^4 k_{\text{obs}}$ ( $\text{s}^{-1}$ )	$4.7 \pm 0.7$	$1.49 \pm 0.4$	$0.14 \pm 0.03$

**Table 6.13:**  $k_{\text{obs}}$  for CO substitution reaction of [Ru(dbzCp)(CO)<sub>2</sub>I] at interval temperatures

Complex	$\Delta H^\ddagger$ ( $\text{kJmol}^{-1}$ )	$\Delta S^\ddagger$ ( $\text{JK}^{-1}\text{mol}^{-1}$ )
[Ru(dbzCp)(CO) <sub>2</sub> I]	$98.7 \pm 12$	$-68.4 \pm 16$

**Table 6.14:** Activation parameters for the reaction of [Ru(dbzCp)(CO)<sub>2</sub>I] with PPh<sub>3</sub>

The negative entropy of activation recorded is in accordance with the negative entropies reported by Brown *et al.* for the reactions of the ruthenium complexes in xylene.

Complex	Solvent	$\Delta S^\ddagger$ (JK <sup>-1</sup> mol <sup>-1</sup> )	Reference
[RuCp(CO) <sub>2</sub> Cl]	Xylene	-15.9 ± 0.56	<sup>146</sup> (calc)
[RuCp(CO) <sub>2</sub> Br]	Xylene	-49.0 ± 6.0	<sup>146</sup> (calc)
	Di-n-butyl ether	-8.8	<sup>146</sup>
	Diglyme	67 ± 8.0	<sup>148</sup>

**Table 6.15:** Entropies of activation for the reactions of [RuCp(CO)<sub>2</sub>X] (X = Cl, Br) with PPh<sub>3</sub>

Generally, large positive  $\Delta H^\ddagger$  and  $\Delta S^\ddagger$  are suggestive of a dissociative process while smaller positive  $\Delta H^\ddagger$  and negative  $\Delta S^\ddagger$  are indicative of an associative process.<sup>133</sup>

Angelici and Leach reported on solvent effects on the kinetics of substitution of nickel carbonyl in 1968.<sup>235</sup> The rate of reaction of Ni(CO)<sub>4</sub> with PPh<sub>3</sub> were measured over various temperatures and in cyclohexane and toluene and the activation parameters were measured.

Solvent	Temperature	10 <sup>3</sup> k <sub>obs</sub> (s <sup>-1</sup> )
Cyclohexane	19.0	2.77
	23.5	5.35
Toluene	19.0	9.40
	23.5	15.8

**Table 6.16:** k<sub>obs</sub> for the reaction of Ni(CO)<sub>4</sub> with PPh<sub>3</sub>

Solvent	$\Delta H^\ddagger$ (kJmol <sup>-1</sup> )	$\Delta S^\ddagger$ (JK <sup>-1</sup> mol <sup>-1</sup> )
Cyclohexane	108.81 ± 2.93	87.47 ± 9.63
Toluene	85.37 ± 2.51	8.37 ± 7.95

**Table 6.17:** Activation parameters for the reaction of Ni(CO)<sub>4</sub> with PPh<sub>3</sub>

The results show a more negative entropy for the reaction in toluene. This is a similar trend to that measured for the dibenzoyl and parent ruthenium complexes and most likely indicates that the aromatic solvent is involved in the reaction. Negative entropies of activation have also been observed for dissociative reactions involving

bulky ligands, for example, phosphine substitutions of complexes of the type  $[M(CO)_4L_2]$  ( $M = Co, Ir, W$   $L =$  phosphines, phosphites).<sup>149,236</sup>

The increase in reactivity of the dibenzoyl complex when compared to the parent may be attributed to the decrease in back-bonding from the metal to the carbonyl ligands as a consequence of the electron-withdrawing abilities of the dibenzoyl ligand. This is evident in the  $\nu_{MC-O}$  stretching frequencies, (**Table 6.7**). The calculated charges on the metal in  $[Ru(dbzCp)(CO)_2X]$  complexes also show a higher positive charge on the metal. The electron-withdrawing abilities of the dibenzoylcyclopentadienyl ligand is clearly labilizing the CO ligand. The relative rate constants for the substitution reactions of  $CpRu(CO)_2I$  and  $dbzCpRu(CO)_2I$  are 1:37 respectively.

Basolo *et al.* demonstrated the effects of electron-withdrawing substituents on the cyclopentadienyl ligand on the rate of CO substitution of  $[Rh(\eta^5-C_5H_5X)(CO)_2]$  with tertiary phosphines.<sup>161</sup> The rate of reaction was found to decrease with an increase of electron density on the metal and increase with a decrease of electron density.<sup>158</sup>

White *et al.* compared the rates of reaction of  $[RuCp'(CO)_2Br]$ , ( $Cp' = C_5H_5, C_5Me_4Et, C_5Ph_5$ ).<sup>149</sup> Both the substituted cyclopentadienyl ligands contain electron-releasing substituents, as evident in the  $\nu_{MC-O}$  stretching frequencies, (**Table 6.18**).

Complex	Solvent	$\nu_{MC-O}$ ( $cm^{-1}$ )
$[RuCp(CO)_2Br]$	Diglyme	2052, 1987
$[Ru(\eta^5-C_5Me_4Et)(CO)_2Br]$	Diglyme	2026, 1967
$[RuCp(CO)_2Br]$	DCM	2055, 2005
$[Ru(\eta^5-C_5Ph_5)(CO)_2Br]$	DCM	2047, 2000

**Table 6.18:**  $\nu_{MC-O}$  stretching frequencies for  $[RuCp'(CO)_2Br]$

However, instead of a decrease in the rate of CO substitution by tertiary phosphines, an increase in the rate of substitution was observed in the order 1:14:20 along the series  $Cp: C_5Me_4Et: C_5Ph_5$  for the reactions carried out in diglyme.

Complex	Temperature, °C	$10^5 k_{\text{obs}}$ (s <sup>-1</sup> )
[RuCp(CO) <sub>2</sub> Br]	115.3	2.7
[Ru( $\eta^5$ -C <sub>5</sub> Me <sub>4</sub> Et)(CO) <sub>2</sub> Br]	112.5	25.0
[Ru( $\eta^5$ -C <sub>5</sub> Ph <sub>5</sub> )(CO) <sub>2</sub> Br]	112.1	37.6

**Table 6.19:** Rates of CO substitution for [RuCp'(CO)<sub>2</sub>Br]

The activation energies were also recorded and reported for the reactions in diglyme.

Complex	$\Delta H^\ddagger$ (kJmol <sup>-1</sup> )	$\Delta S^\ddagger$ (JK <sup>-1</sup> mol <sup>-1</sup> )
[RuCp(CO) <sub>2</sub> Br]	108.9 ± 4.2	67 ± 8.0
[Ru( $\eta^5$ -C <sub>5</sub> Me <sub>4</sub> Et)(CO) <sub>2</sub> Br]	132.0 ± 2.6	27 ± 6.0
[Ru( $\eta^5$ -C <sub>5</sub> Ph <sub>5</sub> )(CO) <sub>2</sub> Br]	155 ± 3.9	-28 ± 8.0

**Table 6.20:** Activation parameters for the CO substitution reaction of [RuCp'(CO)<sub>2</sub>Br]

The rate increase is in contrast to that expected for a complex containing electron releasing substituents, as one would expect the increase in M–CO back-bonding to strengthen the M–CO bond, thus decreasing the rate of reaction. In the case of the [Ru( $\eta^5$ -C<sub>5</sub>Ph<sub>5</sub>)(CO)<sub>2</sub>Br] complex, it might have been expected that the steric bulk of the pentaphenylcyclopentadienyl ligand would encumber nucleophilic attack. In fact, the rate of reaction was found to be independent of the nature of the ligand. No decrease in the rate of reaction was observed for the reaction with the bulkier P(OPh)<sub>3</sub> ligand. The authors attributed the increase in rate along the series Cp: C<sub>5</sub>Me<sub>4</sub>Et: C<sub>5</sub>Ph<sub>5</sub> to the increasing activation enthalpy. This would imply that the more substituted the Cp, the greater its ability to stabilize its transition state.<sup>149</sup>

## 6.6 Ring Slippage and the Indenyl Effect

The occurrence of an associative mechanism in 18-electron complexes is well documented.<sup>237</sup> During their initial investigations into the reaction mechanisms of metal carbonyls, Basolo *et al.* found the square-planar [Ni(CO)<sub>4</sub>] complex to undergo a dissociative mechanism yet the isoelectric compounds [Co(CO)<sub>3</sub>NO], [Fe(CO)<sub>2</sub>(NO)<sub>2</sub>] and [Mn(NO)<sub>3</sub>CO] readily undergo associative carbonyl substitution reactions.<sup>139,238-240</sup> These reactions were found to proceed *via* the localisation of a pair



The  $\eta^5$  to  $\eta^3$  slippage accommodates the associative reaction by vacating a coordination site on the metal centre after the shift in hapticity of the Ind/fluorenyl ligand.

Mawby and Jones reported on the substitution reactions of indenyl and tetrahydroindenyl iron carbonyl complexes in 1972.<sup>243</sup> The tetrahydroindenyl complex was investigated as the aromatic character of the fused six-membered is eliminated. The relative rates of reaction for the Cp:C<sub>9</sub>H<sub>7</sub>:C<sub>9</sub>H<sub>11</sub> complexes in *n*-octane at 95.2°C are 1:575:0.5.

Complex	Solvent	$\Delta H^\ddagger$ (kJmol <sup>-1</sup> )	$\Delta S^\ddagger$ (JK <sup>-1</sup> mol <sup>-1</sup> )
[FeCp(CO) <sub>2</sub> I]	<i>n</i> -octane	127.22	33.06
[Fe( $\eta^5$ -C <sub>9</sub> H <sub>7</sub> )(CO) <sub>2</sub> I]	<i>n</i> -octane	121.37	65.70
[Fe( $\eta^5$ -C <sub>9</sub> H <sub>11</sub> )(CO) <sub>2</sub> I]	<i>n</i> -octane	123.04	15.90
[FeCp(CO) <sub>2</sub> I]	di- <i>n</i> -butyl ether	118.44	54.41
[Fe( $\eta^5$ -C <sub>9</sub> H <sub>7</sub> )(CO) <sub>2</sub> I]	di- <i>n</i> -butyl ether	116.76	46.45

**Table 6.21:** Activation parameters for the substitution reactions of [FeCp'(CO)<sub>2</sub>I] with P(OEt)<sub>3</sub> (Cp' = C<sub>5</sub>H<sub>5</sub>, C<sub>9</sub>H<sub>7</sub>, C<sub>9</sub>H<sub>11</sub>)

Complex	$\nu_{MC-O}$ (cm <sup>-1</sup> )
[FeCp(CO) <sub>2</sub> I]	2043, 2004
[Fe( $\eta^5$ -C <sub>9</sub> H <sub>7</sub> )(CO) <sub>2</sub> I]	2038, 1997
[Fe( $\eta^5$ -C <sub>9</sub> H <sub>11</sub> )(CO) <sub>2</sub> I]	2037, 1995

**Table 6.22:**  $\nu_{MC-O}$  for [FeCp'(CO)<sub>2</sub>I]

There is no indication from the  $\nu_{MC-O}$  stretching frequencies that the M–CO bonding in the indenyl complexes ground state differs from that in the Cp or tetrahydroindenyl complexes. The author concluded that the increase in rate of reaction is due to a lowering in the energy of the activated state relative to that of the ground state. This would imply involvement of the aromatic six-membered ring in the bonding in the activated state to compensate for the weakening M–CO bond of the leaving carbonyl.

The increase in rate when progressing from Cp to Ind is reflected in the entropy of activation. The positive entropy and independence of rate on ligand concentration infers a dissociative mechanism.

A comparison of the rates of ligand substitution on  $[\text{RuCp}(\text{PPh}_3)_2\text{Cl}]$  and  $[\text{Ru}(\text{indenyl})(\text{PPh}_3)_2\text{Cl}]$  was reported by Gamasa *et al.*<sup>244</sup>

Complex	Temperature, °C	$10^5 k_{\text{obs}} (\text{s}^{-1})$
$[\text{RuCp}(\text{PPh}_3)_2\text{Cl}]$	30.0	2.8
$[\text{Ru}(\text{indenyl})(\text{PPh}_3)_2\text{Cl}]$	30.0	20.4

**Table 6.23:** Rates of  $\text{PPh}_3$  substitution for  $[\text{RuCp}(\text{PPh}_3)_2\text{Cl}]$  and  $[\text{Ru}(\text{indenyl})(\text{PPh}_3)_2\text{Cl}]$

Complex	$\Delta H^\ddagger$	$\Delta S^\ddagger$
$[\text{RuCp}(\text{PPh}_3)_2\text{Cl}]$	$29 \pm 1$	$17 \pm 2$
$[\text{Ru}(\text{indenyl})(\text{PPh}_3)_2\text{Cl}]$	$26 \pm 1$	$11 \pm 2$

**Table 6.24:** Activation parameters for the substitution reactions of  $[\text{RuCp}(\text{PPh}_3)_2\text{Cl}]$  and  $[\text{Ru}(\text{indenyl})(\text{PPh}_3)_2\text{Cl}]$

Both complexes were found to undergo substitution *via* a dissociative mechanism. No dependence on the concentration of the incoming ligand was observed and positive enthalpies were recorded. The indenyl analogue was found to react at a rate  $\sim 7$  times greater than the cyclopentadienyl complex. The reactions were carried out in toluene and THF and no strong solvent effects were found. This behaviour is attributed to the ability of the indenyl ligand to act as an electron sink towards the metal fragments  $[\text{Fe}(\text{CO})_3]$  and  $[\text{RuCl}(\text{PPh}_3)_2]$ , favouring the cleavage of the M–CO and  $\text{PPh}_3$  bond respectively or alternatively stabilizing the 16-electron intermediate.<sup>245</sup> This, with the observed dissociative mechanism negates the presence of a ring slip mechanism, as advocated for in other indenyl complexes.

The rates of carbonyl substitution on  $\text{IndRu}(\text{CO})_2\text{I}$  were measured in order to investigate a possible ring slippage mechanism in the dibenzoyl complexes.

At 135.5°C the rate of reaction was too fast to monitor. The reactions were then carried out with both a 10 and 20M excess of ligand at 60, 70 and 80°C and the rate calculated for 134.5°C using the Eyring equation.

Temp. (°C)	[PPh <sub>3</sub> ]	10 <sup>3</sup> k <sub>obs</sub> (sec <sup>-1</sup> )
60	2.00 x 10 <sup>-2</sup>	1.26 ± 0.2
70		1.8 ± 0.3
80		2.4 ± 0.6
60	4.01 x 10 <sup>-2</sup>	1.2 ± 0.2
70		2.0 ± 0.4
80		2.8 ± 0.2

**Table 6.25:** Rates of CO substitution on [Ru(indenyl)(CO)<sub>2</sub>I] with PPh<sub>3</sub>

Complex	ΔH <sup>‡</sup>	ΔS <sup>‡</sup>
[Ru(indenyl)(CO) <sub>2</sub> I]	28.7 ± 1.4	-215 ± 51

**Table 6.26:** Activation parameters for the CO substitution reaction of [Ru(indenyl)(CO)<sub>2</sub>I]

Although the reaction appears dissociative with respect to the independence of rate on the concentration of the incoming ligand, a large negative entropy of activation was recorded.

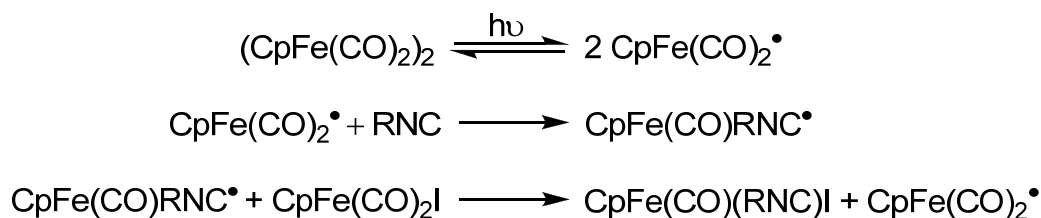
The predicted rate of reaction for [Ru(indenyl)(CO)<sub>2</sub>I] at 134.5°C is 10.5 s<sup>-1</sup>.

The relative rates of reaction for the Cp:dbzCp:Ind complexes are 1:37:700,000. The rapid rate of CO substitution recorded for the indenyl complex with respect to the dbzCp complex would imply a ring slip mechanism is not in operation in the dbzCpRu(CO)<sub>2</sub>X complexes.

## 6.7 The Radical Mechanism

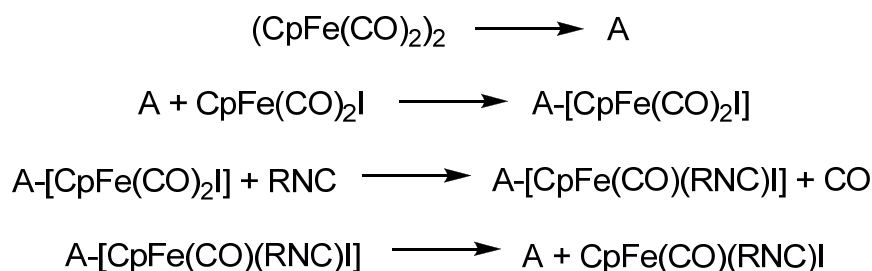
In their reinvestigation of the CO substitution reactions of  $\text{CpRu}(\text{CO})_2\text{Br}$ , White *et al.* found the reaction to undergo a radical pathway. They had found the reaction of the bromide complex with  $\text{PPh}_3$  to be irreproducible in diglyme.<sup>148</sup> The activation parameters recorded in diglyme were also markedly different to those reported by Brown *et al.*<sup>146</sup> The reaction of  $[\text{RuCp}(\text{CO})_2\text{Br}]$  with  $\text{P}(\text{OPh})_3$  in di-*n*-butyl ether was then repeated. The authors noticed an initial slow reaction followed by a rapid one, which usually declined after 60-80% reaction. Again they found the rate constants to be irreproducible. Such behaviour is characteristic of a radical mechanism.<sup>156,246</sup> The reactions were again repeated but with the addition of duroquinone (19.7mg, 12mM), a known radical inhibitor. These reactions resulted in linear, reproducible rate plots resembling the slow initial rates observed in di-*n*-butyl ether without the duroquinone. The rates recorded were also comparable to those obtained upon reaction in diglyme.

The dimeric complexes  $[\text{MCp}(\text{CO})_2]_2$  ( $\text{M} = \text{Fe}, \text{Ru}$ ) are known catalysts for substitution reactions.<sup>247</sup> The monomeric radical  $\text{CpFe}(\text{CO})_2^\bullet$  is readily generated from the dimer both thermally or photochemically.<sup>164,248</sup> The radicals are highly reactive and aid CO substitution. Substitution reactions catalysed by these dimers proceed *via* a radical-chain or non-chain mechanism.<sup>164</sup> An example of a chain-transfer process is the reaction of  $\text{CpFe}(\text{CO})_2\text{I}$  with RNC in the presence of  $(\text{CpFe}(\text{CO})_2)_2$  to yield the mono- or di-substituted products at 80°C, (*Scheme 6.5*).<sup>249</sup>



*Scheme 6.5: Radical chain mechanism*

However, at a lower temperature (40°C), an electron transfer process was in operation.



A = activated iron dimer

**Scheme 6.6:** *The electron transfer process*

These reaction mechanisms would imply that the dimer should catalyse ligand substitution on substrates that do not contain the  $[\text{FeCp}(\text{CO})_2]$  moiety. This has been proven to be the case for the reaction of  $[\text{RuCp}'(\text{CO})_2\text{I}]$  ( $\text{Cp}' = \text{Cp}, \text{C}_5\text{H}_4\text{Me}$ ) with tertiary phosphines in the presence of  $[\text{FeCp}(\text{CO})_2]_2$ . The reaction goes to completion after an hour upon the addition of  $[\text{FeCp}(\text{CO})_2]_2$ .<sup>250</sup> The reaction mechanisms (**Scheme 6.5, 6.6**) also suggest that the interaction between substrate and catalyst should lead to general ligand activation of the substrate.<sup>249</sup>

In their investigations into the catalysed reactions of  $[\text{FeCp}(\text{CO})_2\text{I}]$  with RNC, Coville and co-workers repeated the reactions with the catalyst and in the presence of hydroquinone or galvinoxyl, known radical inhibitors. This resulted in a substantial decrease in the rate of reaction.<sup>165</sup>

Both 17-electron radicals  $\text{CpFe}(\text{CO})_2\cdot$  and  $\text{CpRu}(\text{CO})_2\cdot$  are generated photochemically from the corresponding dimers.<sup>205</sup> These radicals have been shown to abstract halogen atoms from alkyl halides<sup>176</sup> and irradiation of  $[\text{FeCp}(\text{CO})_2]_2$  in a 0.1M solution of  $\text{PPh}_3$  in benzene results in the formation of  $[\text{FeCp}(\text{CO})_2\text{PPh}_3]$ . The radicals dimerise to their corresponding dimer  $[\text{MCp}(\text{CO})_2]_2$  at near-diffusion-controlled rates.<sup>179</sup> In the absence of suitable radical traps reactions of cyclopentadienyl metal hydrides with  $\text{Ar}_3\text{C}\cdot$  lead to the formation of the relevant dimer, (**Equation 6.1**).



**Equation 6.1:** *The reaction of Cp metal hydrides with the trityl radical*

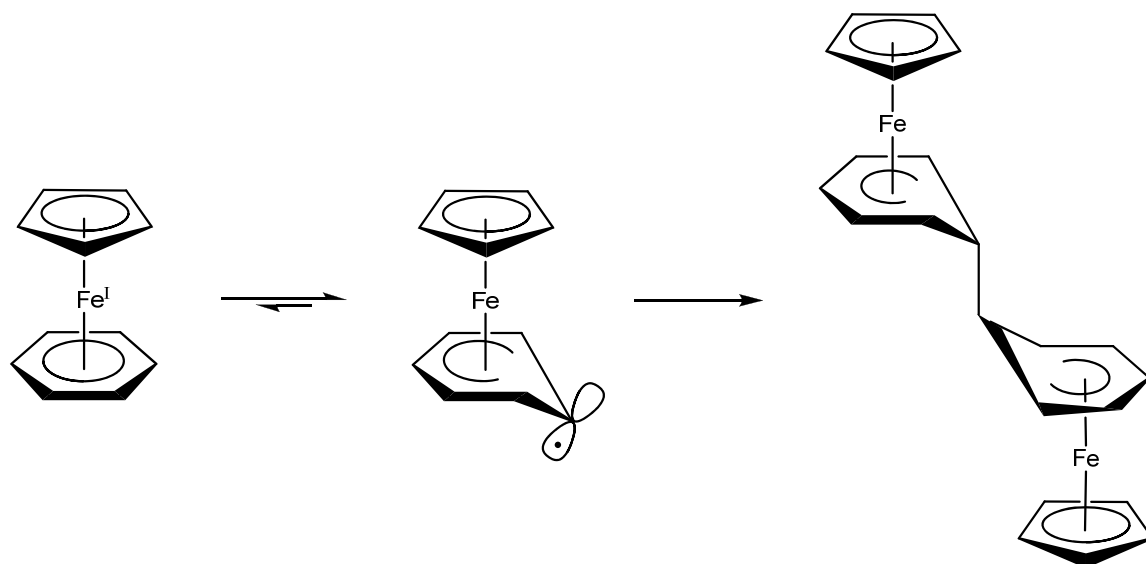
Treatment of  $[\text{FeCp}(\text{CO})_2\text{H}]$  with  $\text{Ph}_3\text{C}^\bullet$  leads to the immediate formation of  $[\text{FeCp}(\text{CO})_2]_2$  and treatment of  $[\text{FeCp}(\text{CO})\text{H}(\text{PPh}_3)]$  resulted in the formation of  $[\text{Fe}_2\text{Cp}_2(\text{CO})_3\text{PPh}_3]$ .

The 17-electron radicals  $(\text{C}_5\text{Ph}_4\text{Ar})\text{Fe}(\text{CO})_2^\bullet$  (Ar = Ph, *p*-tol) were synthesised by Baird *et al.* by the treatment of the relative metal hydride complex with the trityl radical  $\text{Ph}_3\text{C}^\bullet$ . These radicals were found to exist in solution in facile equilibrium with the corresponding 18-electron dimers.<sup>182</sup> These radicals undergo reactions with alkyl halides to form both the halide and alkyl complexes.<sup>188</sup>

19-electron radicals may be formed from the monoelectric reduction of their 18-electron parent complexes.<sup>191</sup> These complexes may be stabilized by the use of ligands that can delocalise the 19<sup>th</sup> electron onto  $\pi$  systems and/or provide steric crowding.<sup>193</sup> The use of peralkylated cyclopentadienyl or benzene ligands enhances the stability of the 19-electron radicals.<sup>251</sup> Dimerisation of 19-electron radicals is known to occur by metal-metal coupling proceeding *via* a 17-electron intermediate.<sup>191</sup>

The 19-electron radical must decoordinate a ligand before dimerisation or the resulting dimer would be 20-electron. The 19-electron species  $[\text{FeCp}(\text{CO})_2\text{L}]$  and  $[\text{FeCp}(\text{CO})\text{L}_2]$ , (L = phosphine), lose an L before dimerising.<sup>252</sup> Another mode of dimerisation of 19-electron radicals is ligand–ligand coupling, (**Scheme 6.7**).<sup>253</sup>

Dimerisation occurs through the decoordination of a carbon atom from the benzene ligand, upon which the radical centre is situated. The complex  $[\text{FeCp}(\text{C}_6\text{Me}_5\text{H})]$  dimerises readily<sup>254</sup> whereas  $[\text{FeCp}(\text{C}_6\text{Me}_6)]$  and  $[\text{FeCp}^*(\text{C}_6\text{H}_6)]$  do not.<sup>194</sup> The presence of five or more methyl groups on the Cp or benzene ligands aid dimerisation, however, this is more marked when the substituents are on the Cp ring.<sup>191</sup>



**Scheme 6.7:** Ligand–ligand coupling in 19-electron complexes

The reactions of 17-electron metal centred radicals generally proceed *via* an associative mechanism<sup>180</sup> whereas 19-electron metal centred radicals *via* a dissociative mechanism.<sup>191</sup>

In order to discount the possibility of a radical mechanism being employed in the substitution reactions of  $[\text{Ru}(\text{dbzCp})(\text{CO})_2\text{I}]$  with  $\text{PPh}_3$  the reaction was repeated in the presence of duroquinone and again in the presence of both the iron and ruthenium dimers,  $[\text{MCp}(\text{CO})_2]_2$ . The reaction of  $[\text{Ru}(\text{dbzCp})(\text{CO})_2\text{I}]$  with  $\text{PPh}_3$  upon the introduction of both dimers (2mg) went to completion in 5 minutes, as opposed to 60 minutes for the uncatalysed reaction. In the presence of duroquinone (49.3mg, 12mM) no decrease in rate was recorded for either the  $[\text{RuCp}(\text{CO})_2\text{I}]$  or dibenzoylcyclopentadienyl analogue. No  $[\text{RuCp}(\text{CO})_2]_2$  or  $[\text{Ru}(\text{dbzCp})(\text{CO})_2]_2$  were isolated from the final reaction products upon purification. This would imply that the complexes were adequately purified of the presence of dimer before reaction and the substitution reactions of  $[\text{RuCp}(\text{CO})_2\text{I}]$  and  $[\text{Ru}(\text{dbzCp})(\text{CO})_2\text{I}]$  do not proceed *via* a radical mechanism.

## Conclusion

A range of diacylcyclopentadienyl ligands have been used to synthesise the first ruthenium complexes of the general formula  $[\text{Ru}(\text{C}_5\text{H}_3\text{R}_2)(\text{CO})_2\text{X}]$ .

The rates of carbonyl substitution by tertiary phosphines have been measured for the  $[\text{Ru}(\text{dbzCp})(\text{CO})_2\text{X}]$  complexes ( $\text{X} = \text{Br}, \text{I}$ ) in xylene solution. There is a marked increase in the rates of substitution when compared to the parent cyclopentadienyl complexes. In the case of the iodo complexes, the dibenzoylcyclopentadienyl complex was found to undergo substitution at a relative rate that is 38 times faster than the parent cyclopentadienyl complex and the dibenzoylcyclopentadienyl bromide complex was 17 times faster than the parent complex. Both of the dibenzoylcyclopentadienyl complexes were found to react *via* a dissociative mechanism. Extrapolating the reaction rate for  $[\text{Ru}(\text{C}_5\text{Me}_4\text{Et})(\text{CO})_2\text{Br}]^{148}$  using the Eyring equation (the reaction was conducted in diglyme) showed that the electron inducing effect of the alkyl groups had accelerated the reaction relative to the parent complex by a factor of 10, however, relative to the dibenzoyl complex the rate is slower by a factor of 2.

Electron-withdrawing ring substituents clearly have the effect of activating the cyclopentadienyl ruthenium complexes studied in this work and thus make the complexes more synthetically useful. It is reasonable to suggest that this principle can be applied to cyclopentadienyl complexes of other metals.

- (1) Kealy, T. J.; Pauson, P. L.; *Nature*, 1951; Vol. 168.
- (2) Diana, E.; Rossetti, R.; Stanghellini, P. L.; Kettle, S. F. A. *Inorganic Chemistry* **1997**, *36*, 382-391.
- (3) Janiak, C.; Schumann, H.; West, F. G. A. S. a. R. In *Advances in Organometallic Chemistry*; Academic Press, 1991; Vol. Volume 33.
- (4) Jacobson, D. B.; Freiser, B. S.; American Chemical Society, 1985; Vol. 107.
- (5) O'Connor, J. M.; Casey, C. P.; American Chemical Society, 1987; Vol. 87.
- (6) Xu, S.; Yuan, F.; Zhuang, Y.; Wang, B.; Li, Y.; Zhou, X. *Inorganic Chemistry Communications* **2002**, *5*, 102-104.
- (7) Costa, M.; Dalcanale, E.; Dias, F. S.; Graiff, C.; Tiripicchio, A.; Bigliardi, L.; Elsevier, 2001; Vol. 619.
- (8) Overby, J. S.; Brady, E. D.; Slate, S. C.; Hanusa, T. P. *Journal of Molecular Structure* **1999**, *478*, 163-168.
- (9) Kang, J. W.; Maitlis, P. M. *Journal of the American Chemical Society* **1968**, *90*, 3259-3261.
- (10) Maitlis, P. M. *Journal of Organometallic Chemistry* **1995**, *500*, 239-249.
- (11) Schore, N. E.; LaBelle, B. E. *The Journal of Organic Chemistry* **2002**, *46*, 2306-2310.
- (12) Donovalova, J.; Jackson, C. R.; Mintz, E. A. *Journal of Organometallic Chemistry* **1996**, *512*, 85-89.
- (13) deVries, L. *The Journal of Organic Chemistry* **1960**, *25*, 1838-1838.
- (14) Kohl, F. X.; Jutzi, P. *Journal of Organometallic Chemistry* **1983**, *243*, 119-121.
- (15) King, R. B.; Bisnette, M. B. *Journal of Organometallic Chemistry* **1967**, *8*, 287-297.
- (16) Garner, C. M.; Prince, M. E. *Tetrahedron Letters* **1994**, *35*, 2463-2464.
- (17) McArdle, P.; Ryder, A. G.; Cunningham, D. *Organometallics* **1997**, *16*, 2638-2645.
- (18) Lindner, H. H.; Fischer, E. O. *Journal of Organometallic Chemistry* **1968**, *12*, P18-P20.
- (19) Tabatabaiean, K.; White, C. *Journal of Organometallic Chemistry* **1996**, *510*, 135-142.
- (20) Pauson, P. L. *Journal of the American Chemical Society* **1954**, *76*, 2187-2191.
- (21) Mehr, L.; Becker, E. I.; Spoerri, P. E. *Journal of the American Chemical Society* **1955**, *77*, 984-989.
- (22) Tsai, W.-M.; Rausch, M. D.; Rogers, R. D. *Organometallics* **1996**, *15*, 2591-2594.
- (23) Castellani, M. P.; Wright, J. M.; Geib, S. J.; Rheingold, A. L.; Trogler, W. C. *Organometallics* **1986**, *5*, 1116-1122.
- (24) Hirsch, S. S.; Bailey, W. J. *The Journal of Organic Chemistry* **1978**, *43*, 4090-4094.
- (25) Gupta, H. K.; Rampersad, N.; Stradiotto, M.; McGlinchey, M. J. *Organometallics* **1999**, *19*, 184-191.
- (26) Garbisch, E. W.; Sprecher, R. F. *Journal of the American Chemical Society* **1969**, *91*, 6785-6800.
- (27) Humphries, A. P.; Knox, S. A. R.; Royal Society of Chemistry, 1975; Vol. 1975.
- (28) Kochhar, R. K.; Pettit, R. *Journal of Organometallic Chemistry* **1966**, *6*, 272-278.

- (29) Knox, S. A. R.; Macpherson, K. A.; Orpen, A. G.; Rendle, M. C.; Royal Society of Chemistry, 1989; Vol. 1989.
- (30) Colborn, R. E.; Dyke, A. F.; Knox, S. A. R.; Mead, K. A.; Woodward, P.; Royal Society of Chemistry, 1983; Vol. 1983.
- (31) Costa, M.; Dias, F. S.; Chiusoli, G. P.; Gazzola, G. L. *Journal of Organometallic Chemistry* **1995**, *488*, 47-53.
- (32) Costa, M.; Dalcanale, E.; Dias, F. S.; Graiff, C.; Tiripicchio, A.; Bigliardi, L. *Journal of Organometallic Chemistry* **2001**, *619*, 179-193.
- (33) Fischer, R. D.; Vogler, A.; Noack, K. *Journal of Organometallic Chemistry* **1967**, *7*, 135-149.
- (34) Hedberg, F. L.; Rosenberg, H. *Journal of the American Chemical Society* **1973**, *95*, 870-875.
- (35) Chinchilla, R.; Nájera, C.; Yus, M. *Tetrahedron* **2005**, *61*, 3139-3176.
- (36) Schlenk, W.; Johanna, H., 1917; Vol. 50.
- (37) Ziegler, K.; Colonius, H., 1930; Vol. 479.
- (38) Gilman, H.; Zoellner, E. A.; Selby, W. M. *Journal of the American Chemical Society* **1932**, *54*, 1957-1962.
- (39) Wittig, G.; Leo, M., 1931; Vol. 64.
- (40) Yus, M.; Gomis, J. *Tetrahedron* **2003**, *59*, 4967-4971.
- (41) Knochel, P.; Singer, R. D. *Chemical Reviews* **1993**, *93*, 2117-2188.
- (42) Clayden, J. *Organolithiums: Selectivity for Synthesis*, 2002.
- (43) Collum, D. B. *Accounts of Chemical Research* **1992**, *25*, 448-454.
- (44) Gilman, H.; Haubein, A. H.; Hartzfeld, H. *The Journal of Organic Chemistry* **1954**, *19*, 1034-1040.
- (45) Gilman, H.; Gaj, B. J. *The Journal of Organic Chemistry* **1957**, *22*, 1165-1168.
- (46) Honeycutt, S. C. *Journal of Organometallic Chemistry* **1971**, *29*, 1-5.
- (47) Gilman, H.; Bebb, R. L. *Journal of the American Chemical Society* **1939**, *61*, 109-112.
- (48) Georg, W.; Gerhard, F., 1940; Vol. 73.
- (49) Gschwend, H. W.; Rodriguez, H. R., 1979; Vol. 26.
- (50) Roberts, J. D.; Curtin, D. Y. *Journal of the American Chemical Society* **1946**, *68*, 1658-1660.
- (51) Wakefield, B. J. *The chemistry of organolithium compounds*; Pergamon, 1974.
- (52) Beak, P.; Brown, R. A. *The Journal of Organic Chemistry* **1979**, *44*, 4463-4464.
- (53) Slocum, D. W.; Jennings, C. A. *The Journal of Organic Chemistry* **1976**, *41*, 3653-3664.
- (54) Snieckus, V. *Chemical Reviews* **1990**, *90*, 879-933.
- (55) Dieter, R. K.; Sharma, R. R.; Yu, H.; Gore, V. K. *Tetrahedron* **2003**, *59*, 1083-1094.
- (56) Gilman, H. S., J.M. *Rec. Trav. Chim* **1936**, *55*, 821.
- (57) Whiteside, G. M.; Casey, J., San Filippo, Jr., Panek, E.J. *Trans. N.Y. Acad. Sci* **1967**, *29*, 572.
- (58) Dieter, R. K. *Tetrahedron* **1999**, *55*, 4177-4236.
- (59) Larock, R. C. *Comprehensive Organic Transformations: A Guide to Functional Group Preparations*; Wiley-VCH, 1999.
- (60) Shirley, D. A. *Org. Reactions* **1954**, *8*.
- (61) J. Lawrence, N. *Journal of the Chemical Society, Perkin Transactions 1* **1998**.

- (62) Brook, A. G.; Harris, J. W.; Lennon, J.; El Sheikh, M. *Journal of the American Chemical Society* **1979**, *101*, 83-95.
- (63) Brook, A. G.; Krishna, R.; Kallury, M. R.; Poon, Y. C. *Organometallics* **1982**, *1*, 987-994.
- (64) Baines, K. M.; Brook, A. G. *Organometallics* **1987**, *6*, 692-696.
- (65) Granander, J.; Sott, R.; Hilmersson, G. *Tetrahedron: Asymmetry* **2003**, *14*, 439-447.
- (66) Yuan, Y.; Desjardins, S.; Harrison-Marchand, A.; Oulyadi, H.; Fressigné, C.; Giessner-Prettre, C.; Maddaluno, J. *Tetrahedron* **2005**, *61*, 3325-3334.
- (67) Lecomte, V.; Stéphan, E.; Le Bideau, F.; Jaouen, G. *Tetrahedron* **2003**, *59*, 2169-2176.
- (68) Lecomte, V.; Stéphan, E.; Jaouen, G. *Tetrahedron Letters* **2002**, *43*, 3463-3465.
- (69) Linn, W. J.; Sharkey, W. H. *Journal of the American Chemical Society* **1957**, *79*, 4970-4972.
- (70) Calucci, L.; Englert, U.; Grigiotti, E.; Laschi, F.; Pampaloni, G.; Pinzino, C.; Volpe, M.; Zanello, P. *Journal of Organometallic Chemistry* **2006**, *691*, 829-836.
- (71) Calucci, L.; Cloke, F. G. N.; Englert, U.; Hitchcock, P. B.; Pampaloni, G.; Pinzino, C.; Puccini, F.; Volpe, M. *Dalton Transactions* **2006**.
- (72) Chad E. Wallace, J. P. S., and Alberto Carrillo *Organometallics* **1998**, *17(15)*, 3390-3393.
- (73) Snyder, C. A.; Selegue, J. P.; Tice, N. C.; Wallace, C. E.; Blankenbuehler, M. T.; Parkin, S.; Allen, K. D. E.; Beck, R. T. *Journal of the American Chemical Society* **2005**, *127*, 15010-15011.
- (74) Basta, R.; Wilson, D. R.; Ma, H.; Arif, A. M.; Herber, R. H.; Ernst, R. D. *Journal of Organometallic Chemistry* **2001**, *637-639*, 172-181.
- (75) Savage, D.; Malone, G.; Gallagher, J. F.; Ida, Y.; Kenny, P. T. M. *Journal of Organometallic Chemistry* **2005**, *690*, 383-393.
- (76) Rebiere, F.; Samuel, O.; Kagan, H. B. *Tetrahedron Letters* **1990**, *31*, 3121-3124.
- (77) Bildstein, B.; Hradsky, A.; Kopacka, H.; Malleier, R.; Ongania, K.-H. *Journal of Organometallic Chemistry* **1997**, *540*, 127-145.
- (78) Calabrese, J. C.; Cheng, L. T.; Green, J. C.; Marder, S. R.; Tam, W. *Journal of the American Chemical Society* **1991**, *113*, 7227-7232.
- (79) Hart, W. P.; Macomber, D. W.; Rausch, M. D. *Journal of the American Chemical Society* **1980**, *102*, 1196-1198.
- (80) Little, W. F.; Koestler, R. C. *The Journal of Organic Chemistry* **1961**, *26*, 3245-3247.
- (81) Schutzenberger, M. P. *Annales (Paris)* **1868**, *15*, 100.
- (82) Mond, L.; Langer, C.; Quincke, F. *Journal of the Chemical Society, Transactions* **1890**, *57*, 749-753.
- (83) Radius, U.; Bickelhaupt, F. M.; Ehlers, A. W.; Goldberg, N.; Hoffmann, R. *Inorganic Chemistry* **1998**, *37*, 1080-1090.
- (84) Crabtree, R. H. *The Organometallic Chemistry of the Transition Metals* **2009**, 132.
- (85) Nakamoto, K. In *Infrared and Raman Spectra of Inorganic and Coordination Compounds Part B*; John Wiley & Sons, 2009, 134.
- (86) Bodenbinder, M.; Balzer-Jollenbeck, G.; Willner, H.; Batchelor, R. J.; Einstein, F. W. B.; Wang, C.; Aubke, F. *Inorganic Chemistry* **1996**, *35*, 82-92.

- (87) Willner, H.; Schaebs, J.; Hwang, G.; Mistry, F.; Jones, R.; Trotter, J.; Aubke, F. *Journal of the American Chemical Society* **1992**, *114*, 8972-8980.
- (88) Nakamoto, K. *Infrared and Ramann Spectra of Inorganic and Coordination Compounds Part B* **2009**, 135.
- (89) Liang, B.; Zhou, M.; Andrews, L. *The Journal of Physical Chemistry A* **2000**, *104*, 3905-3914.
- (90) Fritz, H. P.; Stone, F. G. A.; Robert, W. In *Advances in Organometallic Chemistry*; Academic Press, 1964; Vol. Volume 1.
- (91) Tacke, M.; Oskam, A.; Stufkens, D. J.; Teuben, J. H.; Luinstra, G. A.; de Wolf, J. M.; Tacke, C. *Journal of Molecular Structure* **1997**, 408-409, 499-505.
- (92) George, M. W.; Haward, M. T.; Hamley, P. A.; Hughes, C.; Johnson, F. P. A.; Popov, V. K.; Poliakoff, M. *Journal of the American Chemical Society* **1993**, *115*, 2286-2299.
- (93) Connelly, N. G.; Kitchen, M. D. *Journal of the Chemical Society, Dalton Transactions* **1976**, 2165-2168.
- (94) Capps, K. B.; Bauer, A.; Kiss, G.; Hoff, C. D. *Journal of Organometallic Chemistry* **1999**, 586, 23-30.
- (95) Nolan, S. P.; Hoff, C. D.; Landrum, J. T. *Journal of Organometallic Chemistry* **1985**, 282, 357-362.
- (96) Leoni, P.; Grilli, E.; Pasquali, M.; Tomassini, M. *Journal of the Chemical Society, Dalton Transactions* **1986**, 1041-1043.
- (97) Alway, D. G.; Barnett, K. W. *Inorganic Chemistry* **1980**, *19*, 1533-1543.
- (98) Moss, J. R.; Niven, M. L.; Stretch, P. M. *Inorganica Chimica Acta* **1986**, *119*, 177-186.
- (99) Straub\*, T.; Haukka, M.; Pakkanen\*, T. A. *Journal of Organometallic Chemistry* **2000**, 612, 106-116.
- (100) King, R. B.; Iqbal, M. Z.; King, J. A. D. *Journal of Organometallic Chemistry* **1979**, *171*, 53-63.
- (101) Kubas, G. J.; Kiss, G.; Hoff, C. D. *Organometallics* **1991**, *10*, 2870-2876.
- (102) Parker, D. J. *Journal of the Chemical Society, Dalton Transactions* **1974**, 155-162.
- (103) Bencze, É.; Mink, J.; Németh, C.; Herrmann, W. A.; Lokshin, B. V.; Kühn, F. E. *Journal of Organometallic Chemistry* **2002**, 642, 246-258.
- (104) McGuire, D. G.; Khan, M. A.; Ashby, M. T. *Inorganic Chemistry* **2002**, *41*, 2202-2208.
- (105) Kuksis, I.; Baird, M. C. *Journal of Organometallic Chemistry* **1997**, 527, 137-143.
- (106) Jutzi, P.; Mix, A. *Chemische Berichte* **1990**, *123*, 1043-1045.
- (107) McArdle, P. *Tautomerism In Some Binuclear Metal Carbonyl Complexes* **1969**.
- (108) Parker, D. J.; Stiddard, M. H. B. *Journal of the Chemical Society A: Inorganic, Physical, Theoretical* **1970**, 1040-1049.
- (109) Johnston, P.; Loonat, M. S.; Ingham, W. L.; Carlton, L.; Coville, N. J. *Organometallics* **1987**, *6*, 2121-2127.
- (110) Coombs, D. L.; Aldridge, S.; Rossin, A.; Jones, C.; Willock, D. J. *Organometallics* **2004**, *23*, 2911-2926.
- (111) Joseph, M. F.; Page, J. A.; Baird, M. C. *Organometallics* **1984**, *3*, 1749-1754.
- (112) Coville, N. J.; Darling, E. A. *Journal of Organometallic Chemistry* **1984**, 277, 105-111.

- (113) Nelson, G. O.; Sumner, C. E. *Organometallics* **1986**, *5*, 1983-1990.
- (114) Hallam, B. F.; Mills, O. S.; Pauson, P. L. *Journal of Inorganic and Nuclear Chemistry* **1955**, *1*, 313-316.
- (115) Piper, T. S.; Wilkinson, G. *Journal of Inorganic and Nuclear Chemistry* **1956**, *3*, 104-124.
- (116) Bennett, M. J.; Cotton, F. A.; Davison, A.; Faller, J. W.; Lippard, S. J.; Morehouse, S. M. *Journal of the American Chemical Society* **1966**, *88*, 4371-4376.
- (117) Cotton, F. A.; Stammreich, H.; Wilkinson, G. *Journal of Inorganic and Nuclear Chemistry* **1959**, *9*, 3-7.
- (118) Bryan, R. F.; Greene, P. T. *Journal of the Chemical Society A: Inorganic, Physical, Theoretical* **1970**, 3064-3068.
- (119) Bryan, R. F.; Greene, P. T.; Newlands, M. J.; Field, D. S. *Journal of the Chemical Society A: Inorganic, Physical, Theoretical* **1970**, 3068-3074.
- (120) Cotton, F. A.; Yagupsky, G. *Inorganic Chemistry* **1967**, *6*, 15-20.
- (121) Manning, A. R. *Journal of the Chemical Society A: Inorganic, Physical, Theoretical* **1968**, 1319-1324.
- (122) McArdle, P.; Manning, A. R. *J. Chem. Soc. (A)* **1970**, 2128 - 2132.
- (123) Nelson, N. J.; Kime, N. E.; Shriver, D. F. *Journal of the American Chemical Society* **1969**, *91*, 5173-5174.
- (124) Bor, G. *Spectrochimica Acta* **1962**, *18*, 817-822.
- (125) Orpen, A. G.; Connelly, N. G. *Journal of the Chemical Society, Chemical Communications* **1985**, 1310-1311.
- (126) Dias, P. B.; de Piedade, M. E. M.; Simões, J. A. M. *Coordination Chemistry Reviews* **1994**, *135-136*, 737-807.
- (127) Tolman, C. A. *Chemical Reviews* **1977**, *77*, 313-348.
- (128) Tolman, C. A. *Chemical Society Reviews* **1972**, *1*, 337-353.
- (129) Halpern, J. *Accounts of Chemical Research* **1970**, *3*, 386-392.
- (130) Day, J. P.; Basolo, F.; Pearson, R. G. *Journal of the American Chemical Society* **1968**, *90*, 6927-6933.
- (131) Cramer, R. *Journal of the American Chemical Society* **1967**, *89*, 4621-4626.
- (132) Crabtree, R. H. *The Organometallic Chemistry of the Transition Metals* **1987**, *1st edition*, 74.
- (133) Howell, J. A. S.; Burkinshaw, P. M. *Chemical Reviews* **1983**, *83*, 557-599.
- (134) Crabtree, R. H. *The Organometallic Chemistry of the Transition Metals* **1987**, *1st Edition*, 75.
- (135) Graham, J. R.; Angelici, R. J. *Inorganic Chemistry* **1967**, *6*, 2082-2085.
- (136) Meier, M.; Basolo, F.; Pearson, R. G. *Inorganic Chemistry* **1969**, *8*, 795-801.
- (137) Cross, R. J. *Chemical Society Reviews* **1985**, *14*, 197-223.
- (138) Crabtree, R. H. *The Organometallic Chemistry of the Transition Metals* **1987**, *1st Edition*, 78.
- (139) Thorsteinson, E. M.; Basolo, F. *Journal of the American Chemical Society* **1966**, *88*, 3929-3936.
- (140) Darensbourg, D. J.; Stone, F. G. A.; Robert, W. In *Advances in Organometallic Chemistry*; Academic Press, 1982; Vol. Volume 21.
- (141) Basolo, F. *Inorganica Chimica Acta* **1981**, *50*, 65-70.
- (142) Jensen, F. R.; Kiskis, R. C. *Journal of the American Chemical Society* **1975**, *97*, 5820-5825.
- (143) Wax, M. J.; Bergman, R. G. *Journal of the American Chemical Society* **1981**, *103*, 7028-7030.

- (144) Brown, D. A.; Lyons, H. J.; Manning, A. R.; Rowley, J. M. *Inorganica Chimica Acta* **1969**, *3*, 346-350.
- (145) Angelici, R. J. *Organometal. Chem. Rev.* **1968**, *3*, 173.
- (146) Brown, D. A.; Lyons, H. J.; Sane, R. T. *Inorganica Chimica Acta* **1970**, *4*, 621-625.
- (147) Schuster-Woldan, H. G.; Basolo, F. *Journal of the American Chemical Society* **1966**, *88*, 1657-1663.
- (148) Tabatabaian, K.; White, C. *Inorganic Chemistry* **1981**, *20*, 2020-2022.
- (149) Adams, H.; Bailey, N. A.; Browning, A. F.; Ramsden, J. A.; White, C. *Journal of Organometallic Chemistry* **1990**, *387*, 305-314.
- (150) King, R. B. *Inorganic Chemistry* **1968**, *7*, 90-94.
- (151) Cotton, F. A.; Rusholme, G. A. *Journal of the American Chemical Society* **1972**, *94*, 402-406.
- (152) Huttner, G.; Brintzinger, H. H.; Bell, L. G.; Friedrich, P.; Bejenke, V.; Neugebauer, D. *Journal of Organometallic Chemistry* **1978**, *145*, 329-333.
- (153) Casey, C. P.; Jones, W. D. *Journal of the American Chemical Society* **1980**, *102*, 6154-6156.
- (154) Casey, C. P.; O'Connor, J. M.; Jones, W. D.; Haller, K. J. *Organometallics* **1983**, *2*, 535-538.
- (155) Hart-Davis, A. J.; Mawby, R. J. *Journal of the Chemical Society A: Inorganic, Physical, Theoretical* **1969**, 2403.
- (156) C. White, R. J. M., A.J. Hart-Davis *Inorganica Chimica Acta* **1970**, *4*, 261-266
- (157) Rerek, M. E.; Ji, L.-N.; Basolo, F. *Journal of the Chemical Society, Chemical Communications* **1983**, 1208-1209.
- (158) Basolo, F. *Polyhedron* **1990**, *9*, 1503-1535.
- (159) Rerek, M. E.; Basolo, F. *Organometallics* **1983**, *2*, 372-376.
- (160) Rerek, M. E.; Basolo, F. *Journal of the American Chemical Society* **1984**, *106*, 5908-5912.
- (161) Cheong, M.; Basolo, F. *Organometallics* **1988**, *7*, 2041-2044.
- (162) Angelici, R. J.; Loewen, W. *Inorganic Chemistry* **1967**, *6*, 682-686.
- (163) Ji, L. N.; Rerek, M. E.; Basolo, F. *Organometallics* **1984**, *3*, 740-745.
- (164) Fabian, B. D.; Labinger, J. A. *Journal of the American Chemical Society* **1979**, *101*, 2239-2240.
- (165) Coville, N. J.; Albers, M. O.; Singleton, E. *Journal of the Chemical Society, Dalton Transactions* **1983**, 947-953.
- (166) Joshi, K. K.; Pauson, P. L.; Stubbs, W. H. *Journal of Organometallic Chemistry* **1963**, *1*, 51-57.
- (167) Brunner, H.; Vogel, M. *Journal of Organometallic Chemistry* **1972**, *35*, 169-177.
- (168) Byers, B. H.; Brown, T. L. *Journal of the American Chemical Society* **1977**, *99*, 2527-2532.
- (169) Hoffman, N. W.; Brown, T. L. *Inorganic Chemistry* **1978**, *17*, 613-617.
- (170) Rosenblum, M.; S. Waterman, P. *Journal of Organometallic Chemistry* **1980**, *187*, 267-275.
- (171) Alway, D. G.; Barnett, K. W. *Inorganic Chemistry* **1978**, *17*, 2826-2831.
- (172) Albers, M. O.; Coville, N. J.; Singleton, E. *Journal of Organometallic Chemistry* **1982**, *232*, 261-266.
- (173) Hepp, A. F.; Wrighton, M. S. *Journal of the American Chemical Society* **1981**, *103*, 1258-1261.

- (174) Tyler, D. R.; Schmidt, M. A.; Gray, H. B. *Journal of the American Chemical Society* **1979**, *101*, 2753-2755.
- (175) Caspar, J. V.; Meyer, T. J. *Journal of the American Chemical Society* **1980**, *102*, 7794-7795.
- (176) Baird, M. C. *Chemical Reviews* **1988**, *88*, 1217-1227.
- (177) Connelly, N. G.; Geiger, W. E.; Stone, F. G. A.; Robert, W. In *Advances in Organometallic Chemistry*; Academic Press, 1984; Vol. Volume 23.
- (178) Meyer, T. J.; Caspar, J. V. *Chemical Reviews* **1985**, *85*, 187-218.
- (179) Moore, B. D.; Poliakoff, M.; Turner, J. J. *Journal of the American Chemical Society* **1986**, *108*, 1819-1822.
- (180) Fabian, B. D.; Labinger, J. A. *Organometallics* **1983**, *2*, 659-664.
- (181) Huang, Y.; Carpenter, G. B.; Sweigart, D. A.; Chung, Y. K.; Lee, B. Y. *Organometallics* **1995**, *14*, 1423-1428.
- (182) Kuksis, I.; Baird, M. C. *Organometallics* **1994**, *13*, 1551-1553.
- (183) McLain, S. J. *Journal of the American Chemical Society* **1988**, *110*, 643-644.
- (184) Watkins, W. C.; Jaeger, T.; Kidd, C. E.; Fortier, S.; Baird, M. C.; Kiss, G.; Roper, G. C.; Hoff, C. D. *Journal of the American Chemical Society* **1992**, *114*, 907-914.
- (185) Cooley, N. A.; Watson, K. A.; Fortier, S.; Baird, M. C. *Organometallics* **1986**, *5*, 2563-2565.
- (186) Fortier, S.; Baird, M. C.; Preston, K. F.; Morton, J. R.; Ziegler, T.; Jaeger, T. J.; Watkins, W. C.; MacNeil, J. H.; Watson, K. A. *Journal of the American Chemical Society* **1991**, *113*, 542-551.
- (187) Hoobler, R. J.; Hutton, M. A.; Dillard, M. M.; Castellani, M. P.; Rheingold, A. L.; Rieger, A. L.; Rieger, P. H.; Richards, T. C.; Geiger, W. E. *Organometallics* **1993**, *12*, 116-123.
- (188) Kuksis, I.; Kovacs, I.; Baird, M. C.; Preston, K. F. *Organometallics* **1996**, *15*, 4991-5002.
- (189) Zhang, S.; Brown, T. L. *Journal of the American Chemical Society* **1993**, *115*, 1779-1789.
- (190) Brill, T. B.; Landon, S. J. *Chemical Reviews* **1984**, *84*, 577-585.
- (191) Astruc, D. *Chemical Reviews* **1988**, *88*, 1189-1216.
- (192) Wilkinson, G.; Pauson, P. L.; Cotton, F. A. *Journal of the American Chemical Society* **1954**, *76*, 1970-1974.
- (193) Lankamp, H.; Nauta, W. T.; MacLean, C. *Tetrahedron Letters* **1968**, *9*, 249-254.
- (194) Astruc, D. *Accounts of Chemical Research* **1986**, *19*, 377-383.
- (195) Astruc, D.; Hamon, J. R.; Althoff, G.; Roman, E.; Batail, P.; Michaud, P.; Mariot, J. P.; Varret, F.; Cozak, D. *Journal of the American Chemical Society* **1979**, *101*, 5445-5447.
- (196) Buet, A.; Darchen, A.; Moinet, C. *Journal of the Chemical Society, Chemical Communications* **1979**, 447-448.
- (197) Astruc, D. *Tetrahedron* **1983**, *39*, 4027-4095.
- (198) Nesmeyanov, A. N.; Vol'kenau, N. A.; Shilovtseva, L. S.; Petrakova, V. A. *Journal of Organometallic Chemistry* **1973**, *61*, 329-335.
- (199) Ruiz, J.; Lacoste, M.; Astruc, D. *Journal of the American Chemical Society* **1990**, *112*, 5471-5483.
- (200) Pevear, K. A.; Holl, M. M. B.; Carpenter, G. B.; Rieger, A. L.; Rieger, P. H.; Sweigart, D. A. *Organometallics* **1995**, *14*, 512-523.

- (201) Neto, C. C.; Kim, S.; Meng, Q.; Sweigart, D. A.; Chung, Y. K. *Journal of the American Chemical Society* **1993**, *115*, 2077-2078.
- (202) Huang, Y.; Neto, C. C.; Pevear, K. A.; Banaszak Holl, M. M.; Sweigart, D. A.; Chung, Y. K. *Inorganica Chimica Acta* **1994**, *226*, 53-60.
- (203) Hunt, I.; Johnson, C. D. *Journal of the Chemical Society, Perkin Transactions 2* **1991**, 1051-1056.
- (204) Hoch, M.; Duch, A.; Rehder, D. *Inorganic Chemistry* **1986**, *25*, 2907-2909.
- (205) Abrahamson, H. B.; Palazzotto, M. C.; Reichel, C. L.; Wrighton, M. S. *Journal of the American Chemical Society* **1979**, *101*, 4123-4127.
- (206) Haines, R. J.; Du Preez, A. L. *Journal of the Chemical Society, Dalton Transactions* **1972**, 944-948.
- (207) Sridevi, V. S.; Leong, W. K. *Journal of Organometallic Chemistry* **2007**, *692*, 4909-4916.
- (208) Heitler, W.; London, F. *Zeitschrift für Physik A Hadrons and Nuclei* **1927**, *44*, 455-472.
- (209) Leach, A. R. *Molecular Modelling Principles and Applications* **1998**, *1st edition*, 131.
- (210) Strohmeier, W., Muller, R. Z. *Phys. Chem.* **1964**, *40*, 85.
- (211) Allinger, N. L.; Yuh, Y. H.; Lii, J. H. *Journal of the American Chemical Society* **1989**, *111*, 8551-8566.
- (212) Ponder, J. W.; Richards, F. M. *Journal of Computational Chemistry* **1987**, *8*, 1016-1024.
- (213) Hückel, E. *Zeitschrift für Physik A Hadrons and Nuclei* **1931**, *70*, 204-286.
- (214) Elian, M.; Hoffmann, R. *Inorganic Chemistry* **1975**, *14*, 1058-1076.
- (215) Hoffmann, R. *The Journal of Chemical Physics* **1963**, *39*, 1397-1412.
- (216) Hoffmann, R.; Lipscomb, W. N. *The Journal of Chemical Physics* **1962**, *36*, 3489-3493.
- (217) Parr, R. G. *Annual Review of Physical Chemistry* **1983**, *34*, 631-656.
- (218) Wimmer, E. *Density Functional Methods in Chemistry* **1991**, 7.
- (219) Hohenberg, P.; Kohn, W. *Physical Review* **1964**, *136*, B864.
- (220) Thomas, L. H. *Mathematical Proceedings of the Cambridge Philosophical Society* **1927**, *23*, 542.
- (221) Ziegler, T. *Chemical Reviews* **1991**, *91*, 651-667.
- (222) Lundqvist, S., March, N.H., *Theory of the Inhomogenous Electron Gas* **1984**, Plenum Publishing, 79-147.
- (223) Baushlicher, C. W., Ricca, A., Partridge, H., Langhoff, S.R., *Recent Advances in Density Functional Methods. Part II* **1995**.
- (224) Frenking, G.; Pidun, U. *Journal of the Chemical Society, Dalton Transactions* **1997**, 1653-1662.
- (225) Ohlinger, W. S.; Klunzinger, P. E.; Deppmeier, B. J.; Hehre, W. J. *The Journal of Physical Chemistry A* **2009**, *113*, 2165-2175.
- (226) Hehre, W. J. *A Guide to Molecular Mechanics and Quantum Chemical Calculations* **2003**, 43.
- (227) Mulliken, R. S. *The Journal of Chemical Physics* **1955**, *23*, 1833-1840.
- (228) Breneman, C. M.; Wiberg, K. B. *Journal of Computational Chemistry* **1990**, *11*, 361-373.
- (229) Fitzgerald, C. *Cyclopentadienyl Complexes of Iron and Ruthenium with Electron-Withdrawing Substituents* **2005**.
- (230) Eyring, H. *Journal of Chemical Physics* **1935**, *3*, 107.
- (231) Sheldrick, G. *Acta Crystallographica Section A* **2008**, *64*, 112-122.

- (232) Butler, I. R. *Organometallic Chemistry* **2000**, 28, 455.
- (233) Etter, M. C. *Accounts of Chemical Research* **1990**, 23, 120-126.
- (234) Graham, J. R., Angelici, R. J. *Inorganic Chemistry* **1967**, 6, 2082.
- (235) Angelici, R. J.; Leach, B. E. *Journal of Organometallic Chemistry* **1968**, 11, 203-206.
- (236) Graziani, M.; Zingales, F.; Belluco, U. *Inorganic Chemistry* **1967**, 6, 1582-1586.
- (237) Basolo, F. *Coordination Chemistry Reviews* **1982**, 43, 7-15.
- (238) Basolo, F.; Wojcicki, A. *Journal of the American Chemical Society* **1961**, 83, 520-525.
- (239) Morris, D. E.; Basolo, F. *Journal of the American Chemical Society* **1968**, 90, 2531-2535.
- (240) Wawersik, H.; Basolo, F. *Journal of the American Chemical Society* **1967**, 89, 4626-4630.
- (241) Rerek, M. E.; Ji, L.-N.; Basolo, F. *Journal of the Chemical Society, Chemical Communications* **1983**, 1208-1209.
- (242) Badger, R. C.; Acchioli, J. S.; Gamoke, B. C.; Kim, S. B.; Oudenhoven, T. A.; Sweigart, D. A.; Tanke, R. S. *Organometallics* **2008**, 28, 418-424.
- (243) Jones, D. J.; Mawby, R. J. *Inorganica Chimica Acta* **1972**, 6, 157-160.
- (244) Gamasa, M. P.; Gimeno, J.; Gonzalez-Bernardo, C.; Martín-Vaca, B. M.; Monti, D.; Bassetti, M. *Organometallics* **1996**, 15, 302-308.
- (245) Cadierno, V.; Deza, J.; Pilar Gamasa, M.; Gimeno, J.; Lastra, E. **1999**, 193, 147-205.
- (246) Cohen, I. A.; Basolo, F. *Journal of Inorganic and Nuclear Chemistry* **1966**, 28, 511-520.
- (247) Coville, N. J.; Albers, M. O.; Ashworth, T. V.; Singleton, E. *Journal of the Chemical Society, Chemical Communications* **1981**, 408-409.
- (248) Cutler, A. R.; Rosenblum, M. *Journal of Organometallic Chemistry* **1976**, 120, 87-96.
- (249) Albers, M. O.; Coville, N. J. *Coordination Chemistry Reviews* **1984**, 53, 227-259.
- (250) Loonat, M. S.; Carlton, L.; Boeyens, J. C. A.; Coville, N. J. *Journal of the Chemical Society, Dalton Transactions* **1989**, 2407-2414.
- (251) Koelle, U.; Fuss, B.; Rajasekharan, M. V.; Ramakrishna, B. L.; Ammeter, J. H.; Boehm, M. C. *Journal of the American Chemical Society* **1984**, 106, 4152-4160.
- (252) Stiegman, A. E.; Tyler, D. R. *Comments on Inorganic Chemistry* **1986**, 5, 215-245.
- (253) Hamon, J. R.; Astruc, D.; Michaud, P. *Journal of the American Chemical Society* **1981**, 103, 758-766.
- (254) Moinet, C.; Roman, E.; Astruc, D. *Journal of Organometallic Chemistry* **1977**, 128, C45-C48.